FACULTY OF SCIENCES

Contourite depositional systems in the Le Danois Bank region, southern Bay of Biscay

Sedimentary, tectonic and paleoceanographic implications

Shan Liu

Supervisor: Prof. dr. David Van Rooij

Academic year 2019-2020

Submitted to the Faculty of Science of Ghent University
in fulfilment of the requirements for the degree of
Doctor of Science: Geology

GHENT UNIVERSITY

FACULTY OF SCIENCES

rcmg

Contourite depositional systems in the Le Danois Bank region, southern Bay of Biscay

Sedimentary, tectonic and paleoceanographic implications

Shan Liu

Supervisor:
Prof. dr. David Van Rooij

Submitted to the Faculty of Science of Ghent University in fulfillment of the requirements for the degree of Doctor of Science: Geology

Academic year: 2019-2020
Ghent University

GHENT UNIVERSITY

Members of the examination committee:

Prof. dr. S. Louwye (Ghent University, Belgium): chair
Prof. dr. M. De Batist (Ghent University, Belgium): secretary
Prof. dr. D. Stow (Heriot-Watt University, United Kingdom)
Prof. dr. F. J. Hernández-Molina (Royal Holloway University London, United Kingdom)
Prof. dr. J. De Grave (Ghent University, Belgium)
Dr. I. Meyer (Ghent University, Belgium)
Prof. dr. D. Van Rooij (Ghent University, Belgium): supervisor

This research was carried out by Shan Liu with financial support of a Chinese Scholarship Council "CSC Grant" (n° 201506410062). To refer to this thesis:

Liu, S., 2019. Contourite depositional system in the Le Danois Bank region, southern Bay of Biscay: Sedimentary, tectonic and paleoceanographic implications. PhD thesis, Ghent University, Ghent, Belgium.

Contents

Chapter 4

Chapter 5

Chapter 6

Chapter 7

Chapter 8

Research Highlights

- **Multi-resolution seismic imaging is a recommended geophysical method to study contourite depositional systems from large to small scales.** The multi-channel "low-resolution/low frequency" seismic data are suitable to document the external mounded geometry and the overall seismic stratigraphy of contourite drifts. The single-channel "medium-resolution/medium frequency" seismic profiles are preferable for the recognition of stratigraphic details, progradation/aggradation patterns and reflection terminations. The "high-resolution/high frequency" hull-mounted (parametric) echosounder seismic data better document the surficial morphology of contourite depositional systems.

- **The morphological constraint of topographic obstacles strongly enhances bottom currents (estimated acceleration up to 25 cm/s).** Consequently, changes in velocities of bottom currents result in variations in types, shapes and distributions of contourite drifts in the Le Danois Bank region. **The related sedimentary features of the Le Danois contourite depositional systems have more frequent lateral variations, a feature typical for small basins.**

- **The full domination of the Mediterranean Outflow Water and the Atlantic Mediterranean Water along the entire SW European continental margins is addressed at ~3.5-3.0 Ma.** During the early Quaternary (2.5-0.9 Ma), internal waves resulted from turbulent mixing of water masses induced the occurrence of sediment waves along the Cantabrian margin. The Le Danois contourite depositional systems were widely generated and built after the Middle-Pleistocene Transition (0.9-07 Ma).

- **Contourite features of the same contourite depositional system can be formed during different time intervals under the control of salt tectonics.** The different growth phases of salt diapirs created bathymetric highs on the paleo-seafloor. These topographic obstacles, in turn, significantly changed the pathway of bottom currents. The built-up of different contourite drifts was occurred during different periods, which has a profound effect on the geometry and the evolution of sedimentary basins.

- **During the late Miocene (Tortonian stage), a proto-Mediterranean overflow moved along the continental slopes in the NE Atlantic and reached the southern Bay of Biscay.** Sediments that were transported by this water mass show semi-transparent acoustic features. **The circulation of the late Miocene Mediterranean overflow in the NE Atlantic may influence the global CO_2 cycle and contribute to the late Miocene global cooling.**

List of Abbreviations

Abbreviation	Paraphrase
ADCP	Acoustic Doppler Current Profiler
AMW	Atlantic Mediterranean Water
BQD	Base of the Quaternary Discontinuity
CDS	Contourite Depositional System
CHIRP	Compressed High Intensity Radar Pulse
CTD	Conductivity, Temperature, Depth
CWC	Cold-water Coral
ENACW	Eastern North Atlantic Central Water
EPD	Early Pliocene Discontinuity
EQD	Early Quaternary Discontinuity
IGCP	International Geological Correlation Project
IODP	Integrated Ocean Drilling Program
IPC	Iberian Poleward Current
IPD	Intra Pliocene Discontinuity
LGM	Last Glacial Maximum
LPD	Late Pliocene Discontinuity
LQD	Late Quaternary Discontinuity
LSW	Labrador Sea Water
MIS	Marine Isotope Stage
MOW	Mediterranean Outflow Water
MPD	Mid Pleistocene Discontinuity
MPT	Mid-Pleistocene Transition
MSC	Messinian Salinity Crisis

(continued)

Abbreviation	**Paraphrase**
NADP	North Atlantic Deep Water
NHG	Northern Hemisphere Glacial
SST	Sea Surface Temperature
TWT	Two-way Travel Time
WOD	World Ocean Database

List of Figures

List of Tables

Acknowledgements

First and foremost I want to thank my supervisor, **David Van Rooij**, for providing me an opportunity to study the deep ocean. I appreciate his support and guidance during these past 4 years. I am grateful for all his contributions of advice and funding to my PhD. I am also very thankful for his patience in revising my manuscripts.

Secondly my special thanks go to **F. Javier Hernández-Molina**, **Gemma Ercilla** and **César González-Pola** for those brilliant ideas, comments and discussions, which inspire me to work on this project. The amazing times I spent in Royal Holloway (London), CSIC (Barcelona) and IEO (Gijón) are unforgettable. I am also grateful to all the crew members of the RV Belgica for the wonderful times during the research campaign in 2018.

I would like to acknowledge all the great colleagues of the RCMG. I very much appreciate to **Thomas V.**, **Thomas M.**, **Zak**, **Philipp**, **Carmen**, **An**, **Elke** and **Evelien** for sharing the office with me. I am indebted to work with you all: **Marc**, **Seb**, **Dawei**, **Tim**, **Stan**, **Nore**, **Koen**, **Inka**, **Maarten**, **Oscar**, **Vasilis**, **Maikel**, **David**, **Agostina**, **Katleen**, **Loic**, **Benjamin**, **Mathias, Alice, Lotte, Kurt**, **Wim**, and **Marc Faure.** I am grateful for their help in different ways and will never forget the BBQ, New Year dinners and croquet moments.

Also many thanks to the members of the DRIFTERS Research Group: **Sara**, **Debora**, **Sandra**, **Wouter**, **Oswaldo**, **Adam**, **Lin**, **Alex**, **Javier D.**. The group has been a source of friendships as well as good collaboration. I am grateful for the fun times we had in the seismic lab and in Drifters' house. I wish you all the best luck.

My time at UGent was made enjoyable in large part due to my friends. My appreciation goes to **Dawei**, with whom I have shared moments of anxiety but also big excitement. I want to express my gratitude to **Rema**, **Xin**, **Xia**, **Mariz**, **Dewina**, **Ruben**, **Doris**, **Yolanda** and **Helen** for their kindness and help. **Jing**, **Liyun**, **Maosong, Zhiyuan** and **Siying**, thank you all for the wonderful times we have shared in the place far away from home. I also wish to acknowledge the band members: **Sophie**, **Lydia**, **Alex**, **Sarah** and **Johannes**. I will always remember the great moments we spent playing music together.

Shuang, I do not know how to begin with saying thanks to you. This PhD was not possible without your support, understanding and love. Thank you very much for always standing by my side. 爸爸妈妈，感谢你们对我的支持和爱。这四年很多辛苦难熬的时刻，因为你们存在，我收获了更多的力量。我永远深深地，爱着你们。

Summary

Bottom currents, which are generated by the movement of the water masses, are able to primarily transport and deposit sediments in the deep sea. This type of sediments that show distinctive characteristics by comparing with turbidites and pelagites are defined as contourites. The action of bottom currents has the capability to build up small (1-10 km^2) to large (100-1000 km^2) scaled sedimentary bodies, which are known as contourite drifts. The lateral and temporal variations of contourite drifts and erosional features in the same region lead to the definition of the Contourite Depositional System (CDS). Contourite drifts and the CDS exhibit a global distribution but have been particularly well-studied in the NE Atlantic Ocean where the Mediterranean Outflow Water (MOW) profoundly interacts with the continental margin. These contourite examples are considered crucial for paleoclimate, palaeoceanographic, tectonic and slope-stability/geological hazard studies during the last two decades. They currently receive more attention for their economic significance in the context of hydrocarbon exploration.

In the NE Atlantic, the MOW shows different physical properties and dynamics after exiting the Gulf of Cádiz. This intermediate water mass is referred to as the Atlantic Mediterranean Water (AMW) in the rest NE Atlantic to distinguish with the pure MOW near the source. In the Le Danois Bank region (southern Bay of Biscay), the Le Danois contourite depositional systems are identified. These systems are respectively associated with the Eastern North Atlantic Central Water (ENACW; 350-600 m), the AMW (750-1550 m) and the Labrador Sea Water (LSW; 1750-2000 m), offering great potential to investigate the connection between contourite features, their temporal and spatial evolution, the related oceanic circulation and tectonics. Moreover, the Le Danois CDS lie in a key position to document regional paleocirculation and the associated influences on the continental margins at the intermediate site of the AMW. The contourite study at this specific location allows to shed more light on the paleo- MOW and AMW variations between their proximal and distal sites.

A combination of geophysical (multibeam bathymetry, seismic reflection profiling) and oceanographic (CTD) were used to investigate the geomorphological features and the associated oceanographic processes of the Le Danois CDS. Different reflection seismic data, containing nearly overlapping NNE-SSW to N-S orientated profiles, embrace different vertical resolutions from low to ultra-high. Based on the unique datasets, multi-resolution seismic imaging is used as the strategy to identify morphological and internal features of the Le Danois CDS. The multi-channel "low-resolution/low frequency" seismic data are suitable to document the external mounded geometry and the overall seismic stratigraphy of contourite drifts. The single-channel "medium-resolution/medium frequency" seismic profiles are preferable for the recognition of stratigraphic details, progradation/aggradation patterns and reflection terminations. Whereas the "high-resolution/high frequency" hull-mounted (parametric) echosounder seismic data better document the wavy-like surficial morphology of contourite drifts. These different-scaled features are linked to different Earth-system processes, such as long-term tectonic activities, short-term paleo- climate/oceanographic variations and sub-recent sedimentary processes. Additionally,

cyclic features, consisting of an acoustically transparent lower part and a moderate amplitude upper part, are shown in some seismic sub-units of the drift. Sediments deposited during related cycles have different thickness namely in single-channel sparker and ParaSound seismic profiles, indicating their different-scaled seismic expressions.

The present-day morphology and oceanography of the Le Danois Bank region have been investigated by using single-channel seismic data, hull-mounted (parametric) echosounder seismic profiles and multibeam bathymetry. The involved bottom-current processes are respectively associated with the ENACW, the AMW and the LSW. Bottom currents are locally accelerated (up to 25 cm/s) due to the presence of the Le Danois Bank and the Vizco High. Sediments originating from various canyon systems along the Cantabrian Margin are transported by downslope and alongslope processes towards the Le Danois intraslope basin. Consequently, six plastered drifts, three elongated mounded and separated drifts, a furrow and three moats are displayed. The extension and distribution of the drifts are controlled by slope morphology and/or bottom current velocities. Besides contourite drifts, internal waves may have induced the formation of sediment waves. Scouring of active bottom currents and rapid sedimentation rate of contourite drifts could be at the origin of slope instability events. In the Le Danois intraslope basin, multiple sedimentary processes work together and shape the present-day seafloor. Bottom currents are focused due to deflection on complex topographical obstacles within a relatively small basin setting and the resulted sedimentary features have more frequent lateral variations.

In order to explore the evolution of the Le Danois CDS, single-channel and multi-channel seismic data are used to establish a detailed seismic stratigraphy. Six seismic units (U1 to U6), bounded by major discontinuities (H1 to H6) have been identified from old to young. Regarding variations of the bottom-current circulation, four evolution stages, including precursor (~5.3 to 3.5-3.0 Ma), initiation (3.5-3.0 to 2.5-2.1 Ma), intermediate (2.5-2.1 to 0.9-0.7 Ma) and drift-growth (0.9-0.7 Ma to present day) stages, of the Le Danois CDS are identified. The CDS associated with the AMW initiated at ~3.5-3.0 Ma and had a full drift-growth after the Middle-Pleistocene Transition (MPT; 0.9-07 Ma). From the late Quaternary (~0.47 Ma) onwards, the CDS associated with the ENACW started to develop in the Le Danois Bank region. The LSW was not involved in the built-up of contourite drifts. The Le Danois Drift was generated by the AMW both in glacial and interglacial climatic conditions. Repeated acoustic cyclicities of the Le Danois Drift in unit 5, consisting of acoustically transparent lower parts, moderate amplitude upper parts and high amplitude erosional surfaces at the top, are compared with glacial/interglacial cycles between Marine Isotope Stage (MIS) 18 to 12. These cyclic features suggest coarsening-upward sequences of the Le Danois Drift, indicating enhanced AMW processes during glacial intervals. The estimated average sedimentation rate of the Le Danois CDS reached a maximum during the MPT (at least ~27 cm/ky) and then decreased until the present-day (~5 cm/ky). The evolution of the Le Danois CDS implies a significant influence of the intermediate water mass along the SW European continental margins from the late Pliocene (~3.5-3.0 Ma) onwards.

On the basis of the seismic stratigraphy of the Le Danois CDS, deeper seismic units are identified from new multi-channel seismic data. The interaction between basin-scale salt tectonics and past circulation of the AMW, thus, was investigated. Four tectonic-oceanographic stages of the Le Danois intraslope basin, including extension, compression, interaction and contourite stages, were divided. During the compression stage, the basin was significantly narrowed. The related salt movements and regional tectonics created various bathymetric highs on the paleo-seafloor.

These past topographic obstacles distributed along the northern and southern parts of the intraslope basin. They further interacted with AMW and efficiently accelerate the associated bottom currents. When the intraslope basin was dominated by alongslope processes, the Le Danois CDS was developed. Due to different period salt movements, the Le Danois and the Gijón Drifts, which belong to one CDS, are respectively generated since the late Pliocene and the middle Pleistocene. The time gap between the built-up of these drifts is related to the growth phase of different salt diapirs. This feature indicates that contourite features of a CDS can be formed during different time intervals under the control of salt tectonics.

Besides salt diapirs, buried contourite drifts, which have a Tortonian age, are identified in the new multi-channel seismic profiles. The evidence of the buried contourite features implies the presence of a proto-Mediterranean overflow in the NE Atlantic before the MSC during the late Miocene. Associated bottom currents were estimated as >0.3 m/s along the flank of the Le Danois Bank due to the presence of contourite erosional features. By comparing with other similar contourite examples, this old Mediterranean overflow moved along the past continental slopes after exiting the Betic and Rifian corridors. It at least had reached the southern Bay of Biscay. Sediments that transported and deposited by the proto Mediterranean overflow shows semi-transparent acoustic feature along the SW European margins. The settling depth of the proto Mediterranean overflow is suggested at 1100-1500 m, which could be one possibility to cause the absence of late Miocene contourite features in the Gulf of Cadiz. The circulation of the late Miocene Mediterranean overflow in the NE Atlantic may influence the global CO_2 cycle and contribute to the late Miocene global cooling.

Overall, by using the unique datasets of seismic reflection data, the study on the Le Danois CDS improves the acoustically diagnostic criteria of contourite drifts and contributes to the conceptual model of the CDS. Some sedimentary features of the Le Danois CDS are rarely known in any other contourite examples in the world's ocean. A comprehensive comparison between the MOW/AMW related products is provided, in turn unravelling the present-day to the past circulation pattern of the MOW/AMW in the NE Atlantic. Furthermore, in order to extend and verify some of the conclusions resulting from this thesis, several possible future research topics are proposed. The implications of paleo-oceanic gateways on the ocean circulation in the southern Bay of Biscay should be considered. The sediment source and sedimentary facies of contourite drifts, as well as and the chronostratigraphy of the Le Danois CDS, can be implied by acquiring sediment cores. New oceanographic observation and numerical modelling are urged to quantify present-day bottom-current and oceanographic processes associated with the Le Danois CDS.

Samenvatting

Bodemstromingen, die worden gegenereerd door de beweging van watermassa's, kunnen sedimenten in de diepzee transporteren en afzetten. Dit type sedimenten, die duidelijk onderscheiden kunnen worden van turbidieten en pelagieten, worden gedefinieerd als contourieten. Door de werking van bodemstromingen kunnen kleine (1-10 km^2) tot grote (100-1000 km^2) sedimentaire lichamen worden opgebouwd, die bekend staan als contourietdriften. De laterale en tijdelijke variaties in dergelijke contourietdriften, samen met de erosieve elementen in hetzelfde gebied, leiden tot de vorming van een 'Contourite Depositional System' (CDS). Contourietdriften en CDS vertonen een wereldwijde distributie, maar zijn bijzonder goed bestudeerd in de noordoostelijke Atlantische Oceaan, waar het 'Mediterranean Outflow Water' (MOW) een sterke interactie vertoont met de continentale randen. Gedurende de laatste twee decennia is het belang van contourieten duidelijk geworden in paleoklimaat- en paleoceanografische studies en in het onderzoek naar tektoniek, hellingsstabiliteit en geologische risico's. Ze krijgen momenteel ook meer en meer aandacht door hun economische potentieel in het kader van de exploratie van koolwaterstoffen.

In het noordoostelijke deel van de Atlantische Oceaan wordt het MOW, om het onderscheid te maken met het MOW sensu stricto in zijn meest bron-nabije omgeving (i.e. de Golf van Cádiz), aangeduid als 'Atlantic Mediterranean Water' (AMW), dat bovendien verschillende fysische eigenschappen en een eigen dynamiek heeft. In de regio van de 'Le Danois Bank' (zuidelijke Golf van Biskaje) werden de Le Danois CDS geïdentificeerd. Deze systemen worden respectievelijk geassocieerd met het 'Eastern North Atlantic Central Water' (ENACW; 350-600 m), het AMW (750-1550 m) en het 'Labrador Sea Water' (LSW; 1750-2000 m), en bieden een uitstekende kans om de verhouding te onderzoeken tussen contourieten, hun temporele en ruimtelijke evolutie, de bijbehorende oceanische circulatie en tektoniek. Bovendien liggen de Le Danois CDS in een sleutelpositie om regionale paleocirculatie en de bijbehorende invloeden op de continentale randen op een intermediaire site van het AMW te documenteren. De studie van contourieten op deze specifieke locatie maakt het mogelijk meer licht te werpen op de paleo-MOW en –AMW variaties tussen hun proximale en distale invloedssferen.

Een combinatie van geofysische (multibeam bathymetrie, seismische profilering) en oceanografische (CTD) technieken werden gebruikt om de geomorfologische kenmerken en de bijbehorende oceanografische processen van de Le Danois CDS te onderzoeken. Verschillende seismische datasets, die bijna overlappende NNE-SSW tot N-S georiënteerde profielen bevatten, omvatten verschillende verticale resoluties van laag tot ultrahoog. Gebaseerd op deze unieke datasets, wordt seismische beeldvorming met uiteenlopende resoluties gebruikt om morfologische en interne kenmerken van de Le Danois CDS te identificeren. De meerkanaals seismische profielen met lage resolutie/lage frequentie zijn geschikt om de externe opwaarts gebogen geometrie en de algemene seismische stratigrafie van contourietdriften te documenteren. De éénkanaals seismische profielen met medium resolutie en frequentie zijn het meest geschikt voor de herkenning van stratigrafische details, progradatie-/aggradatiepatronen en

reflectieterminaties. De seismische data van de op de romp gemonteerde (parametrische) echosounder met een hoge resolutie/hoge frequentie kunnen tenslotte gebruikt worden om de golvende oppervlaktemorfologie van contourietdriften beter te documenteren. Deze kenmerken met uiteenlopende schaalgroottes zijn gekoppeld aan processen van het aardsysteem met verschillende termijnen, zoals tektonische activiteit op lange termijn, paleoklimaat/oceanografische variaties op korte termijn, en sub-recente sedimentaire processen. Bovendien komen cyclische patronen, bestaande uit een akoestisch transparant onderste deel en een bovenste deel met gemiddelde amplitude, voor in sommige seismische sub-eenheden van de drift. Deze depositiecycli komen voor op verschillende schalen, namelijk in de éénkanaals sparker en ParaSound seismische profielen, wat hun seismische uitdrukking op verschillende schaal aantoont.

De huidige morfologie en oceanografie van de Le Danois Bank regio zijn onderzocht met behulp van éénkanaals seismische data, seismische profielen van een (op de romp gemonteerde) parametrische echosounder en multibeam bathymetrie. De betrokken bodemstromingsprocessen worden respectievelijk geassocieerd met het ENACW, het AMW en het LSW. Bodemstromingen worden lokaal versneld (tot 25 cm/sec) door de aanwezigheid van de Le Danois Bank en het 'Vizco High'. Sedimenten afkomstig van verschillende canyon-systemen langs de Cantabrische rand worden getransporteerd door helling-afwaartse en helling-parallele processen naar het 'Le Danois intraslopebekken'. Hierdoor worden zes 'plastered' en drie 'elongated mounded & separated' contourietdriften afgezet, en een 'furrow' en drie 'moats' geërodeerd. De positie van de contourietdriften wordt bepaald door de morfologie van de helling en/of de snelheid van de bodemstromingen. Naast contourietdriften kunnen interne golven de vorming van sedimentgolven hebben veroorzaakt. Erosie door actieve bodemstromingen en hoge sedimentatiesnelheden in contourietdriften kunnen de oorzaak zijn voor destabilisatie van de continentale helling. In het Le Danois intraslope bekken werken meerdere sedimentaire processen samen in het vormen van de huidige zeebodem. Bodemstromingen worden gefocust vanwege afbuiging op complexe topografische obstakels binnen het relatief kleine bekken, en de resulterende sedimentaire producten vertonen meer frequente laterale variaties.

Om de evolutie van de Le Danois CDS te verkennen, worden één- en meerkanaals seismische profielen gebruikt om een gedetailleerde seismische stratigrafie uit te werken. Zes seismische eenheden (U1 tot U6), begrensd door belangrijke discontinuïteiten (H1 tot H6) zijn geïdentificeerd van oud naar jong. Wat betreft variaties in de bodemstromingscirculatie werden vier evolutiestadia geïdentificeerd, met een precursor-fase (~ 5.3 tot 3.5-3.0 Ma), initiatiefase (3.5-3.0 tot 2.5-2.1 Ma), intermediaire fase (2.5-2.1 tot 0.9-0.7 Ma) en drift-groeifase (0,9-0,7 Ma tot heden). De CDS geassocieerd met het AMW werd geïnitieerd rond ~ 3.5-3.0 Ma en bouwde volledig uit na de 'Middle-Pleistocene Transition' (MPT; 0.9-07 Ma). Vanaf het laat Kwartair (~ 0,47 Ma) begon de CDS geassocieerd met het ENACW zich te ontwikkelen in de regio van de Le Danois Bank. Het LSW was niet betrokken bij de opbouw van contourietdriften. De Le Danois Drift werd gevormd door het AMW, zowel in glaciale als interglaciale klimatologische omstandigheden. Akoestische cycliciteiten binnen de Le Danois Drift in eenheid 5, bestaande uit akoestisch transparante onderste delen, medium-amplitude bovenste delen en hoge-amplitude erosieoppervlakken aan de top, worden gelinkt aan glaciale/interglaciale cycli tussen 'Marine Isotope Stage' (MIS) 18 tot 12. Deze cyclische elementen stellen sequenties voor van opwaarts grofkorreliger wordende sedimenten binnen de Le Danois Drift, wat duidt op sterker wordende AMW-processen tijdens glaciale intervallen. De geschatte gemiddelde sedimentatiesnelheid binnen de Le Danois CDS

bereikte een maximum tijdens de MPT (minstens ~ 27 cm/ky) en daalde daarna tot de tegenwoordige waarde (~ 5 cm/ky). De evolutie van de Le Danois CDS wijst op een significante invloed van intermediaire watermassa's langsheen de ZW-Europese continentale rand vanaf het late Plioceen (~ 3.5-3.0 Ma).

Op basis van de seismische stratigrafie van de Le Danois CDS worden diepere seismische eenheden geïdentificeerd op basis van nieuwe meerkanaals seismische data. Dit laat toe de interactie tussen grootschalige zouttektoniek (op bekken-niveau) en de vroegere circulatie van het AMW te onderzoeken. Vier tektonisch-oceanografische stadia van het Le Danois intraslope bekken werden onderscheiden, waaronder een extensie-, compressie-, interactie- en contouriet-stadium. Tijdens de compressiefase was het bekken aanzienlijk versmald. De bijbehorende zoutbewegingen en regionale tektoniek creëerden verschillende bathymetrische hoogtes op de paleo-zeebodem. Deze vroegere topografische obstakels waren verspreid langs de noordelijke en zuidelijke delen van het intraslope bekken. Ze interageerden verder met het AMW en versnelden op efficiënte wijze de bijbehorende bodemstromingen. Toen het intraslope-bekken werd gedomineerd door helling-parallelle processen, werd de Le Danois CDS ontwikkeld. Vanwege verschillende zoutbewegingen worden de Le Danois en de Gijón contourietdriften, die behoren tot één CDS, respectievelijk gegenereerd sinds het late Plioceen en het midden Pleistoceen. Het tijdsverschil tussen de opbouw van deze contourietdriften is gerelateerd aan de groeifase van verschillende zoutdiapieren. Dit toont aan dat contouriet-gerelateerde elementen binnen een en dezelfde CDS kunnen gevormd worden tijdens verschillende tijdsintervallen door de invloed van zouttektoniek.

Naast zoutdiapieren worden begraven contourietdriften, die een Tortoniaan ouderdom hebben, geïdentificeerd in de nieuwe meerkanaals seismische profielen. De aanwezigheid van deze begraven contourietdriften impliceert de aanwezigheid van een proto-'Mediterranean Overflow' in de Atlantische Oceaan vóór de 'Messinian Salinity Crisis' (MSC) tijdens het late Mioceen. De bijbehorende bodemstromingen werden geschat op > 0,3 m/s langs de flank van de Le Danois bank op basis van de aanwezigheid van contouriet-gerelateerde erosieve elementen. Door te vergelijken met andere contourietvoorbeelden kon afgeleid worden dat deze oude Mediterranean Overflow bewoog langsheen de vroegere continentale hellingen na het verlaten van de 'Betic & Rifian corridors', minstens tot in de zuidelijke Golf van Biskaje. Sedimenten die werden getransporteerd en afgezet door de proto-Mediterranean Overflow vertonen semi-transparante akoestische kenmerken langs de ZW-Europese continentale randen. De stromingsdiepte van de proto-Mediterranean Overflow wordt geschat op 1100-1500 m, wat mogelijks de afwezigheid van laat Miocene contourietelementen in de Golf van Cadiz zou kunnen verklaren. De circulatie van de laat Miocene Mediterranean Overflow in het noordoostelijke deel van de Atlantische Oceaan zou de wereldwijde CO_2-cyclus kunnen hebben beïnvloed, en zo bijgedragen hebben tot de wereldwijde afkoeling tijdens het late Mioceen.

Tot slot, door het gebruik van unieke seismische datasets helpt de studie van de Le Danois CDS de akoestische diagnostische kenmerken van contourietdriften te verbeteren, en draagt deze ook bij tot het conceptuele model van de CDS. Sommige sedimentaire kenmerken van de Le Danois CDS zijn nauwelijks bekend in andere contourietvoorbeelden elders ter wereld. Er wordt een uitgebreide vergelijking tussen de MOW/AMW-gerelateerde producten gegeven, die op hun beurt het vroegere tot huidige circulatiepatroon van het MOW/AMW in het noordoostelijke deel van de Atlantische Oceaan helpen te ontrafelen. Verder worden enkele mogelijke toekomstige

onderzoeksonderwerpen voorgesteld om de conclusies uit dit proefschrift uit te kunnen breiden en te verifiëren. De implicaties van vroegere zeeëngten voor de oceaancirculatie in de zuidelijke Golf van Biskaje moeten verder worden nagegaan. De sedimentbron en sedimentaire facies van contourietdriften, evenals de chronostratigrafie van de Le Danois CDS, kunnen gevalideerd worden door het verwerven van sedimentkernen. Nieuwe oceanografische observaties en numerieke modellering zijn nodig om de huidige bodemstromingen en oceanografische processen binnen de Le Danois CDS beter te kwantificeren.

There is the sea, vast and spacious,
teeming with creatures beyond number,
living things both large and small.

[Psalm 104:25]

Chapter 1

Introduction

1.1 Bottom currents and contourites

Oceans cover more than two-thirds of our blue planet. The global circulation of the ocean, driven by different forces from the deep sea to the surface, transports huge amounts of heat and significantly contributes to the Earth's climate (Rahmstorf, 2002). In the upper layers of the ocean, wind-driven circulation directly controls surface currents and mass fluxes (Tansley and Marshall, 2001; Toggweiler and Russell, 2008). The thermohaline circulation (Figure 1.1), which is defined as the circulation driven by differences in temperature and salinity, induces the stratification and distribution of water masses in the deep ocean (below 300 m) (Wunsch, 2002; Kuhlbrodt et al., 2007). The movement of the water masses generates semi-permanent alongslope currents, also known as bottom currents, near the bottom of the ocean (Faugères et al., 1993; Rebesco et al., 2014).

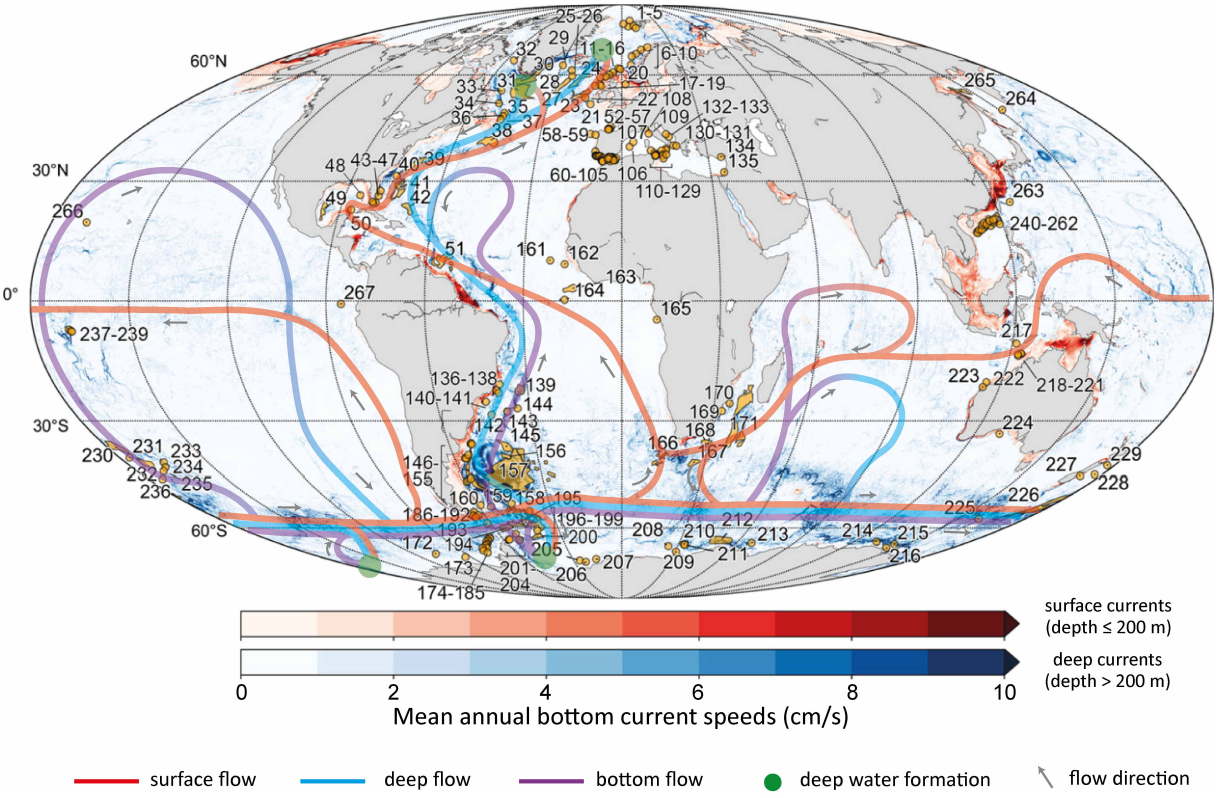

Figure 1.1: Overview map with the indication of the global thermohaline circulation pathways (Rahmstorf, 2002), the global distribution of modern contourite drifts (yellow boxes and points) and simulated mean annual bottom current speeds (Thran et al., 2018). Number labels correspond to contourite examples described by Thran et al. (2018).

Bottom currents were initially considered being able to influence sediment fluxes in the deep ocean by the German physical oceanographer George Wüst in 1936 (Stow et al., 2002). It was only until the 1960s, Wüst's conclusion was confirmed and extended based on the observation of bottom currents (with a velocity of 4-60 cm/s) and bottom photographs of ripples (Heezen and Hollister, 1964; Heezen et al., 1966). A more accurate view was developed during the 1980s, when the strength of bottom currents was linked with the sedimentary facies (Stow and Lovell, 1979; Gonthier et al., 1984; Stow and Holbrook, 1984). Since then, several international projects on bottom currents and the associated sedimentations, such as International Geological Correlation Project (IGCP) 432, 619 and Integrated Ocean Drilling Program (IODP) Expeditions 303, 317, 339, 342, were carried out (Rebesco et al., 2014). The concept of bottom currents was loudly heard with irrefutable geological and oceanographic evidence (Llave et al., 2001, 2007; Rebesco et al., 2008; Hernández-Molina et al., 2014).

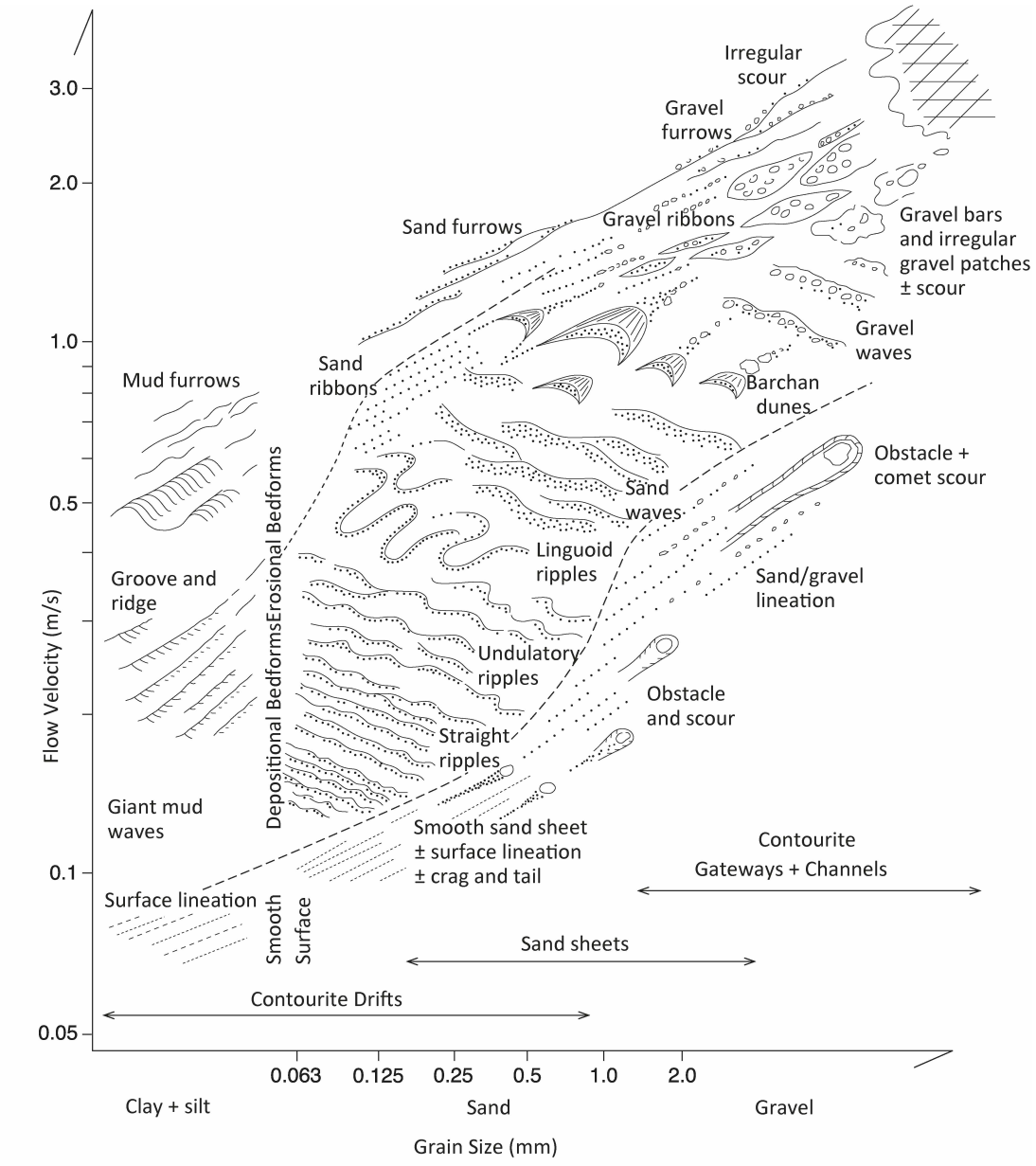

Figure 1.2: A schematic of bedform-velocity matrix for deep-water bottom current systems. The relationship between mean grain size of sediments and bottom-current velocity is shown (Stow et al., 2009).

In fact, measured velocities of bottom currents usually vary from 1 to 20 cm/s (Heezen et al., 1966). Exceptionally vigorous bottom currents, controlled by sea gateway restriction, can reach a velocity of up to about 120 cm/s (Gonthier et al., 1984; Sánchez-Leal et al., 2017). These bottom currents, having high velocities and sufficient energy, are capable of suspending, transporting and controlling the deposition of sediments at the seafloor (Figure 1.2) (Stow et al., 2009). Sediments deposited or significantly affected by bottom currents are known as contourites, while the sedimentary bodies they create are called contourite drifts (Faugères et al., 1993; Stow et al., 2002).

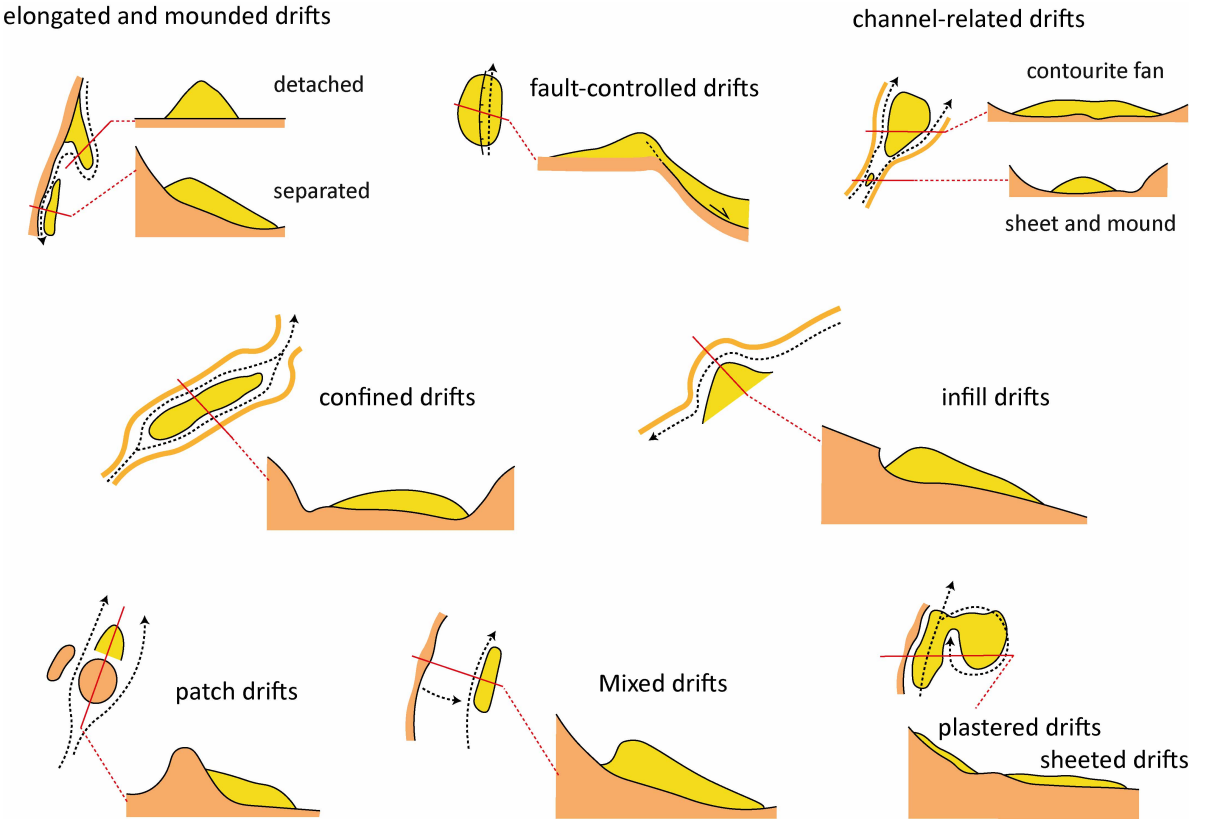

Figure 1.3: Classification of contourite drifts based on the morphology observed in seismic profiles. Modified from Rebesco et al. (2014).

The type and the morphology of contourite drifts is largely determined by bottom current properties, slope gradient, topographic features and sediment supply (Hernández-Molina et al., 2008; Rebesco et al., 2014). The most recent classification scheme for contourite drifts defines nine different depositional types (Figure 1.3) (Rebesco et al., 2014). *Elongated and mounded drifts*, characterized by a degree of mounding and evident elongation, are generally developed on the continental slopes (Hernández-Molina et al., 2008; Van Rooij et al., 2010). *Sheeted drifts*, displaying a broad and faintly mounded geometry, are commonly observed on abyssal plains (Masson et al., 2002; Gruetzner and Uenzelmann-Neben, 2016). *Plastered drifts*, which have a relatively small size, are generated by weak bottom currents on the gentle slopes (Rebesco et al., 2013; Miramontes et al., 2019). *Channel-related drifts* lie in gateways and the related bottom currents have higher velocity due to topographic restriction (Maldonado et al., 2005). Several other types of contourite drifts, including *patch drifts, confined drifts, infill drifts, fault-controlled drifts*, and *mixed drifts*, are significantly influenced by the regional topographic and geological settings (Ceramicola et al., 2001; Michels et al., 2001; Laberg et al., 2005; Soares et al., 2014; Pepe et al., 2018).

Bottom currents are also capable of creating erosional/non-depositional features (Figure 1.4) (Rebesco et al., 2014; García et al., 2016; Hernández-Molina et al., 2016). *Contourite channels*, resulting from the over-excavation by bottom currents, display asymmetric incisions within the channel (Hernández-Molina et al., 2003). *Subcircular scours* can either be influenced by the bottom-current promoted scouring effects or be eroded by powerful eddies (Rebesco et al., 2014; García et al., 2016). *Depositional hiatuses*, defined as erosional unconformities, occur by the winnowing of strong bottom currents and can reach thousands of square kilometre in the deep sea (Lofi et al., 2016). *Moats*, generally associated with elongated and mounded drifts, originate by non-depositional or localised erosional processes beneath the core of bottom currents (Rebesco et al., 2014). *Marginal valleys* are generated by flow instabilities resulting from the interaction between bottom currents and topographic ridges (García et al., 2009). *Contourite terraces*, resulting from the combined depositional and erosional processes, show scoured surfaces and occur at the interface between different water masses (Hernández-Molina et al., 2017).

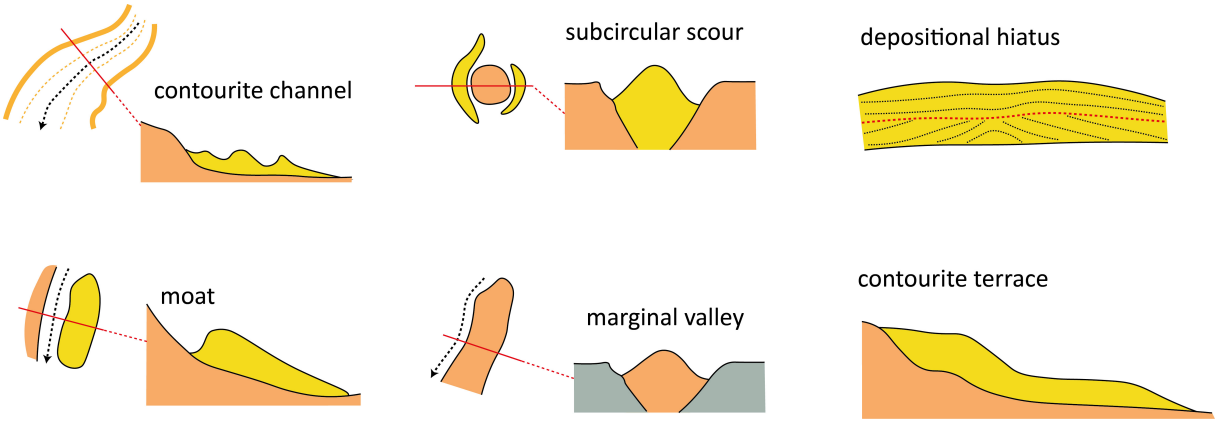

Figure 1.4: Classification of contourite erosional elements based on the morphology observed in seismic profiles. Modified from García et al. (2009).

1.2 Contourite depositional systems

In the same region, the lateral and temporal variations of contourite depositional features associated with a variety of erosional features lead to the definition of the Contourite Depositional System (CDS) (Hernández-Molina et al., 2008). A CDS is associated with one water mass and is generally located at the same water depth (Hernández-Molina et al., 2008). The CDS are identified in abyssal plains (Maldonado et al., 2003, 2005; Juan et al., 2018), along continental slopes (Laberg et al., 2005; Preu et al., 2013; Campbell and Mosher, 2016) and in shallow marine settings (Vandorpe et al., 2011; Collart et al., 2018;). Among these CDS examples, large-scale CDS, such as the well-studied Cádiz CDS along the SW Iberian continental margin (Llave et al., 2001, 2007), the Lofoten and Vesterålen Drifts along the NW European Atlantic margin (Laberg et al., 2005; Stoker et al., 2005) and the giant CDS along the Argentine continental margin (Preu et al., 2012, 2013), are being widely investigated. The giant size (>10^3 km^2) and the broad distribution of contourite features are the typical characteristics for these large-scale CDS (Rebesco et al., 2014). Some giant contourite drifts (e.g. the Zapiola Drift, the Eirik Drift, the Faro Drift) could reach a few hundreds of metres in thickness and a few hundreds of kilometres in length (Llave et al., 2001; von Lom-Keil et al., 2002; Maldonado et al., 2003; Müller-Michaelis et al., 2013). Bottom currents generating these large-scale CDS are associated with the circulation of the intermediate or deep-water masses,

which occur on broad and low slope gradient areas (Figure 1.5) (Maldonado et al., 2005; Hernández-Molina et al., 2010). However, small-scale CDS, which are positioned in smaller basins and around topographical obstacles, received far less attention and their mechanisms are not yet fully understood (Turnewitsch et al., 2004; Rebesco et al., 2014; Van Rooij et al., 2016; Zhang et al., 2016).

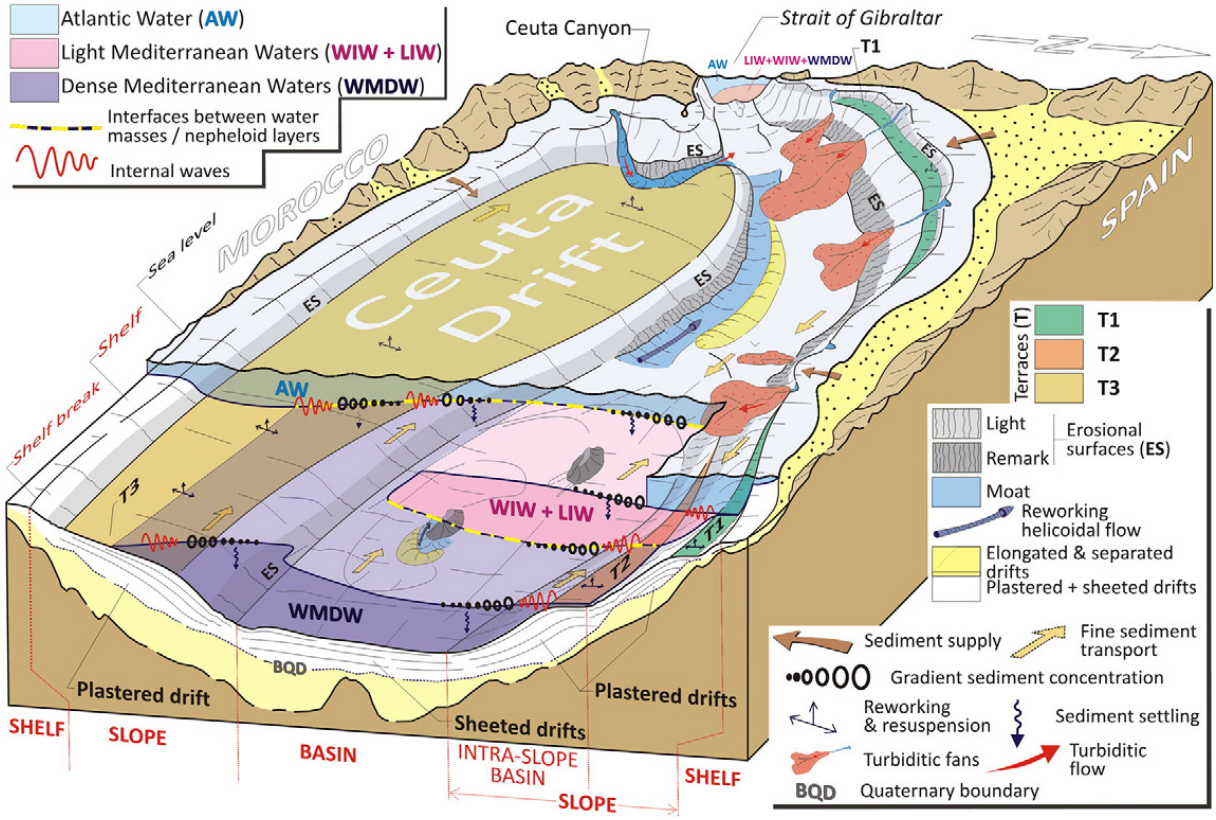

Figure 1.5: Sketch of large-scale contourite depositional systems and associated bottom-current processes in the Alboran Sea. The relevant water masses and other oceanographic processes are indicated. Image courtesy of Ercilla et al. (2016).

Small-scale contourite drifts have been documented at different continental margins (Tournadour et al., 2015; Juan et al., 2016). They are reported around the mud volcanoes of the Moroccan Atlantic margin (Vandorpe et al., 2016) and the Gulf of Cádiz (Palomino et al., 2016), around the Pontevedra obstacle in the Galicia Bank region (Ercilla et al., 2011; Zhang et al., 2016), associated with cold-water coral mounds in the Porcupine Seabight, SW of Ireland (Van Rooij et al., 2007), around a seamount in the South China Sea (Chen et al., 2014) and also associated with the Le Danois Bank along the northern Iberian continental margin (Van Rooij et al., 2010). The presence of topographic obstacles or irregularities can cause locally intensification of bottom currents (Rebesco et al., 2008, 2014). Based on numerical modelling, bottom currents could gain velocities that ranges from 7 cm/s up to 35 cm/s in those conditions (Chen et al., 2016; Zhang et al., 2016). Eventually, more focused bottom currents erode or deposit sediments on the seafloor, allowing the formation of specific morphological features associated with the small-scale CDS.

In addition, other oceanographic processes (e.g. internal waves/tides, eddies) can be involved in the generation of the CDS (Rebesco et al., 2014; Chen et al., 2019). An example is the oceanographic process at the interface between two overlying water masses (Figure 1.5). Downward and upward shifts of the interfaces, induced by paleoclimatic variation, could generate large-scale contourite

terraces (Hernández-Molina et al., 2017). Such contourite terraces can be found along the Argentinian margin (Preu et al., 2013) and in the Alboran Sea (Ercilla et al., 2016). At these interfaces, small-scale bedforms, such as sediment waves, can be shaped by internal waves, which propagate along a density pycnocline between different water masses as well (Pomar et al., 2012; Delivet et al., 2016; Ribó et al., 2016). When encountering the continental slope, internal waves can resuspend and transport sediments and efficiently shape the morphology of the continental slope (Cacchione et al., 2002; Klymak et al., 2010). Depending on the slope gradient, internal waves can have different reflection conditions and carry sediments in downslope or upslope directions (Cacchione et al., 2002; Cacchione and Wunsch, 2006; Lamb 2014) (Figure 1.6). When the reflection conditions are subcritical (transmissive), the waves with shorter wavelength and smaller velocity reflect upslope and the resulted sediment waves show upslope progradation (Cacchione et al., 2002; Ribó et al., 2016). In contrast, the waves reflect down and back towards deeper water when reflection conditions are supercritical (reflective) (Lamb, 2014). Up to now, only few sediment waves have been related with internal waves, which occur at the interface between different water masses, and they display small wavelengths and upslope migration (Delivet et al., 2016; Ribó et al., 2016).

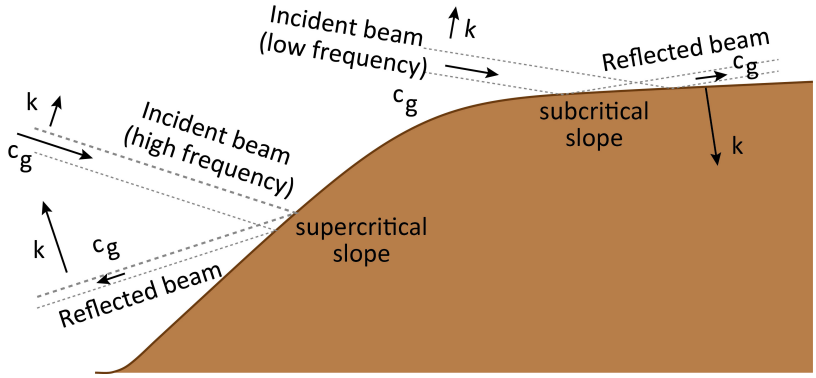

Figure 1.6: Sketch of internal wave reflection conditions. Subcritical and supercritical conditions are indicated. C_g is the group velocity. K is the wave vector pointing in the direction of phase propagation. Modified from Lamb (2014).

Besides the importance of the CDS in the ocean circulation studies, the evolution of the CDS provides valuable sedimentary records on the regional or global paleoclimate and paleocirculation (Van Rooij et al., 2007; Ercilla et al., 2011; García et al., 2016; Hernández-Molina et al., 2016). The onset of Northern Hemisphere Glaciation (NHG) during the late Pliocene strongly intensified the circulation of the intermediate water masses, which created large depositional hiatuses in the CDS along the North Atlantic margins (Flesche Kleiven et al., 2002; Becker et al., 2006; Rogerson et al., 2012; Hernández-Molina et al., 2014; Khélifi et al., 2014). Whereas the deep-water masses were largely influenced by the onset of the permanent East Antarctic Ice Sheet, in turn controlling the growth patterns of CDS in Antarctic (Martos et al., 2013).

Margin-scale plate tectonics and regional tectonic activities are documented by the CDS as well (Pérez-Asensio et al., 2012; Hernández-Molina et al., 2016). The closure and reopening of oceanic gateways, such as the Strait of Gibraltar and the Indonesian Straits, caused a morphological restriction, which favoured the formation of bottom currents (Rodgers et al., 2000; Roveri et al., 2014; Capella et al., 2018). Profound changes on the distribution and sedimentary stacking patterns of contourite drifts could be induced by the regional uplifts (García et al., 2016; Vandorpe et al., 2016). Interactions between strike-slip fault systems and bottom currents may significantly influence the type of erosional features of the CDS (Lobo et al., 2011). However, cause-and-effect

relationships between basin-scale tectonics (i.e. salt movements) and the circulation of water masses, as well as their impacts on temporal changes of basin geometry, remains challenging.

1.3 Intermediate water mass along the SW European margin

In the North Atlantic Ocean, the formation of the Mediterranean Outflow Water (MOW) in the Gulf of Cadiz, serves one of the most appealing natural laboratories in the world to study the interactions between the ocean circulation, sedimentary processes, plate tectonics and the basin evolution (Van Rooij et al., 2007; Llave et al., 2011; Roque et al., 2012; Hernández-Molina et al., 2016; Collart et al. 2018). The formation of the MOW is largely linked with the closure and the opening of respectively the Betic/Rifian and Gibraltar gateways (Hernández-Molina et al., 2016). The source area of the MOW, the Mediterranean Sea, experienced an extreme evaporation stage, also known as the Messinian Salinity Crisis (MSC), during the Miocene (Roveri et al., 2014). The resulted salt and warm water of the Mediterranean Sea started to exchange with the one from the Atlantic Ocean after the opening of the Strait of Gibraltar (at ~5.33 Ma) (Hernández-Molina et al., 2014; Roveri et al., 2014).

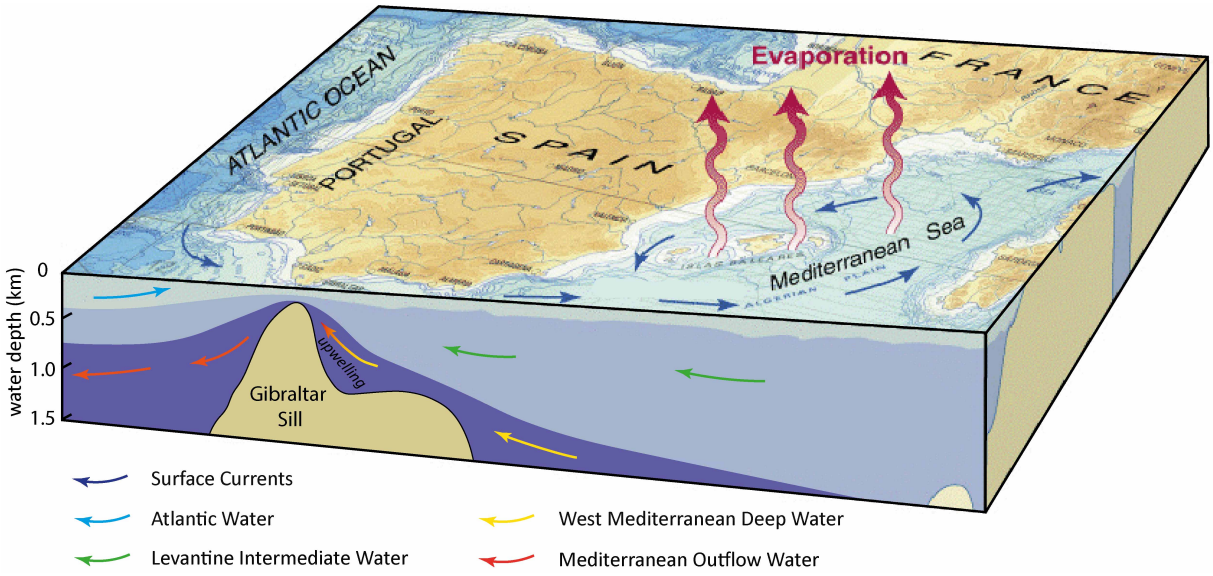

Figure 1.7: A scheme of the Atlantic-Mediterranean water exchange. The Mediterranean Outflow Water (MOW), which is sourced from the warm and salt Mediterranean Sea, sinks to a great depth after passing through the Strait of Gibraltar sill. The circulation pattern of different water masses or currents is adapted from Schroeder et al. (2016). The background basemap is from http://retosterricolas.blogspot.com/.

When the Mediterranean waters encountered the Strait of Gibraltar sill, some of them upwelled as secondary flows at 300–400 m water depth (Dietrich et al., 2008). The rest sinks at the west of the sill and mixed with the surrounding waters, creating the warm and saline MOW at the intermediated depth (Figure 1.7) (Millot et al., 2006; Schroeder et al., 2016). During the early Pliocene (~4.5 Ma), the MOW effectively interacted with the continental slope and shaped the seafloor morphology in the Gulf of Cádiz (Hernández-Molina et al., 2016). While at more distal sites, such as Goban Spur and Porcupine Seabight, the earliest evidence of the MOW is dated at ~3.5-3.3 Ma (Khélifi et al., 2009) (Figure 1.8). During the late Pliocene (3.2-3.0 Ma) and the early Quaternary (2.4-2.0 Ma), the MOW had enhanced circulation regimes and extended further (Hayward et al., 2009; Raddatz et al., 2011; Khélifi et al., 2014). When the periodicity of climate cycles of the Earth dramatically changed from 41 ky to 100 ky during the Mid-Pleistocene

Transition (MPT, ~1.25-0.7 Ma), the climate fluctuations started to significantly influence the MOW (Maslin and Ridgwell, 2005; Friocourt et al., 2007; Elderfield et al., 2012; Kaboth et al., 2016; Bahr et al., 2018). During interglacial periods, the circulation pattern of the MOW is similar to modern conditions (Kaboth et al., 2016). In contrast, the width of the core of MOW was increased and the velocity was accelerated during glacial periods. The MOW settled at a greater depth by comparing with the present-day oceanographic condition (Rogerson et al., 2005). From the late Quaternary onwards the MOW started to resemble the present day one. (Schönfeld and Zahn, 2000).

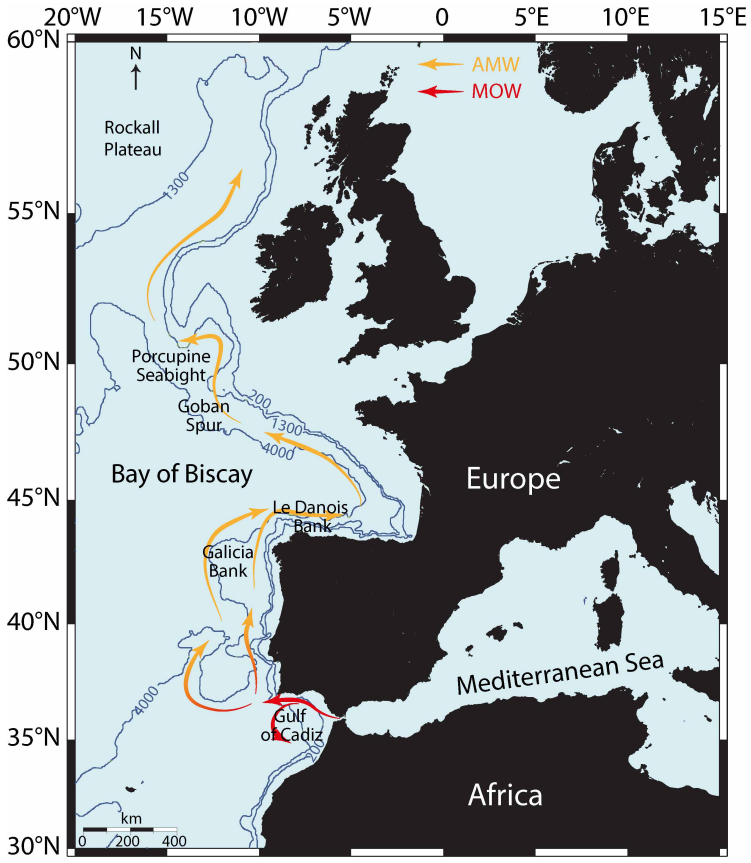

Figure 1.8: Map of the southwest European continental margin. The pathway of the Mediterranean Outflow Water (MOW) and the Atlantic Mediterranean Water (AMW) (red and orange arrows) is indicated. Modified from Khélifi et al., (2009). MOW=Mediterranean Outflow Water; AMW=Atlantic Mediterranean Water.

The circulation of the MOW leads to the generation of persistent bottom currents along the southwest European continental margins (van Aken, 2000; Rogerson et al., 2012) (Figure 1.8). The MOW refers to the pure thermohaline outflow in the Gulf of Cádiz (Hernández-Molina et al., 2014). To distinguish this thermohaline outflow in the most proximal site (the Gulf of Cádiz) near the source, the rest with different physical properties and dynamics is thus referred to as the Atlantic Mediterranean Water (AMW) (Rogerson et al., 2012; Flecker et al., 2015) (Figure 1.8). Bottom currents and the related oceanographic processes transported sediments along the MOW/AMW pathways, generating various contourite drifts and CDS (Llave et al., 2007; Van Rooij et al., 2007, 2010; Hernández-Molina et al., 2011; Mena et al., 2018; Collart et al., 2018). Along the pathways, the MOW/AMW -induced morphological features are observed in the Gulf of Cádiz (Roque et al., 2012; Brackenridge et al., 2013), the Galicia Bank region (Mena et al., 2018), Ortegal Spur (Hernández-Molina, 2009; Collart 2018), the Le Danois Bank region (Van Rooij et al., 2010), Goban Spur (Delivet et al., 2016) and Porcupine Seabight (Van Rooij et al., 2007). The resulted

contourite features display large variations in size, shape and vertical position, providing valuable sedimentary records of the margin evolution and paleoceanographic implications (Ercilla et al., 2011; García et al., 2016; Hernández-Molina et al., 2016).

Among them, the Cádiz CDS, one of the most well-studied contourite examples, indicates the variation of the MOW paleoceanography at its most proximal site (Hernández-Molina et al., 2014). Widespread depositional hiatuses, marked by variable geological durations, are interpreted as a signal of the intensification of the MOW (Figure 1.9) (Llave et al., 2001, 2007, 2011; Marchès et al., 2007, 2010; Roque et al., 2012). As a result, bottom currents associated with the MOW varied in flowing patterns and strength at 3.2-3.0 Ma, 2.4-2 Ma and 0.9-0.7 Ma, in turn profoundly changing the sedimentary stacking pattern of contourite drifts in the Gulf of Cádiz (Lofi et al., 2016). Consequently, three evolution stages of the Cádiz CDS, including an initial-drift stage (Pliocene, from 5.3–3.2 Ma), a transitional-drift stage (late Pliocene and early Quaternary, 3.2–2 Ma) and a growth-drift stage (Quaternary, from 2 Ma to present), are identified, regarding the variation of the MOW (Hernández-Molina et al., 2016).

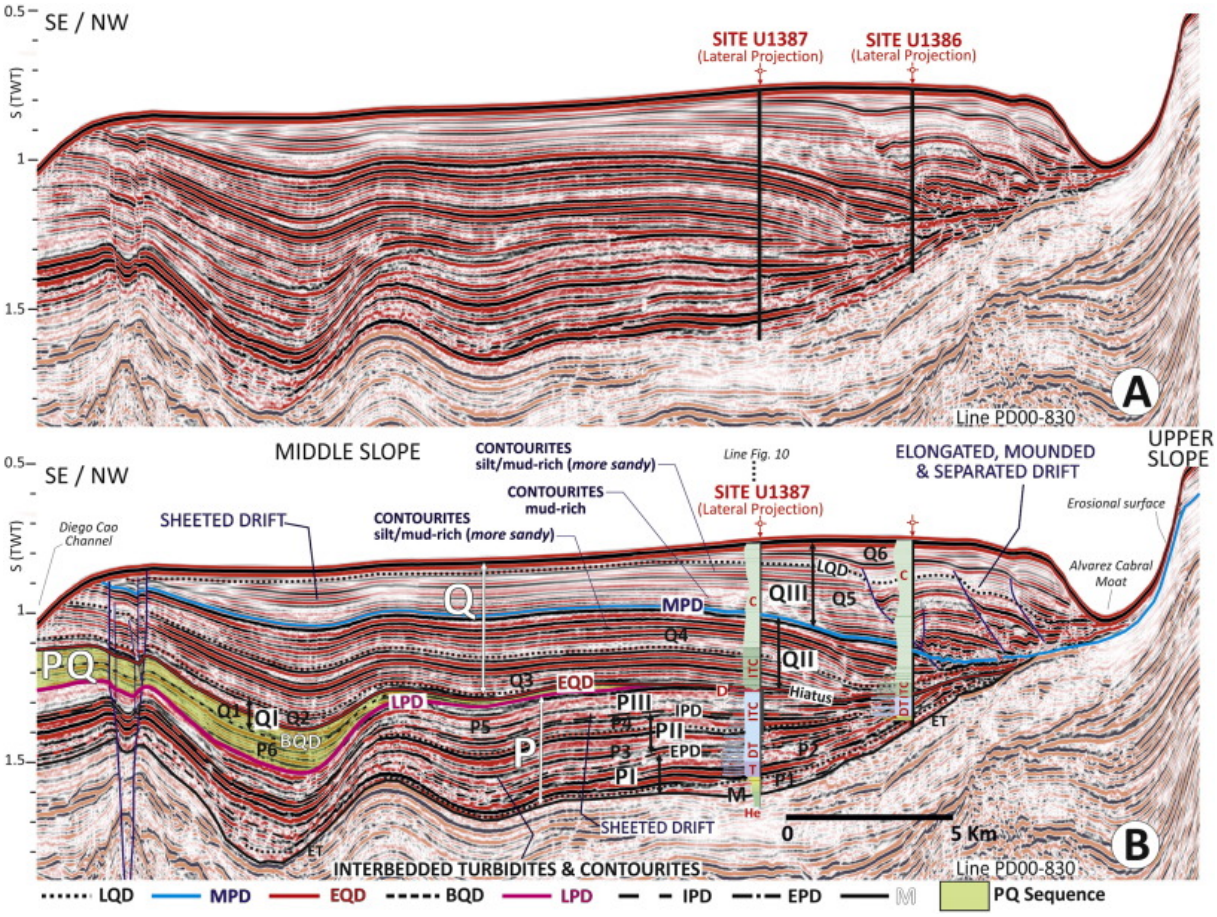

Figure 1.9: Seismic stratigraphy of a contourite drift in the Gulf of Cádiz. Abbreviations for major discontinuities (from bottom to top): M = Miocene–Pliocene boundary; EPD = early Pliocene discontinuity; IPD = intra Pliocene discontinuity; LPD = late Pliocene discontinuity; BQD = base of the Quaternary discontinuity; EQD = early Quaternary discontinuity, MPD = mid Pleistocene discontinuity; LQD = late Quaternary discontinuity. Image courtesy of Hernández-Molina et al. (2016).

At the distal site of the AMW, sediment records of Goban Spur and Porcupine Seabight document extreme erosive events resulted from the AMW since the late Pliocene (Figure 1.10) (Van Rooij et al., 2007; Huvenne et al., 2009; Thierens et al., 2013; Delivet et al., 2016). Thickness and stacking

patterns of the eroded sediments, as well as time series of the erosional activities, are hard to reconstruct (Raddatz et al., 2011). Fast accumulation rates of the Porcupine CDS have only been recorded after the middle Pleistocene (0.725–0.65 Ma), which is more than ~1 My later compared with the Cádiz CDS (Huvenne et al., 2009; Hebbeln et al., 2016). There are still temporal gaps of the MOW/AMW variability from the proximal to the distal site. As such, a linkage between the Gulf of Cádiz and Porcupine Seabight is needed to document regional paleocirculation and the associated influences on the continental margins.

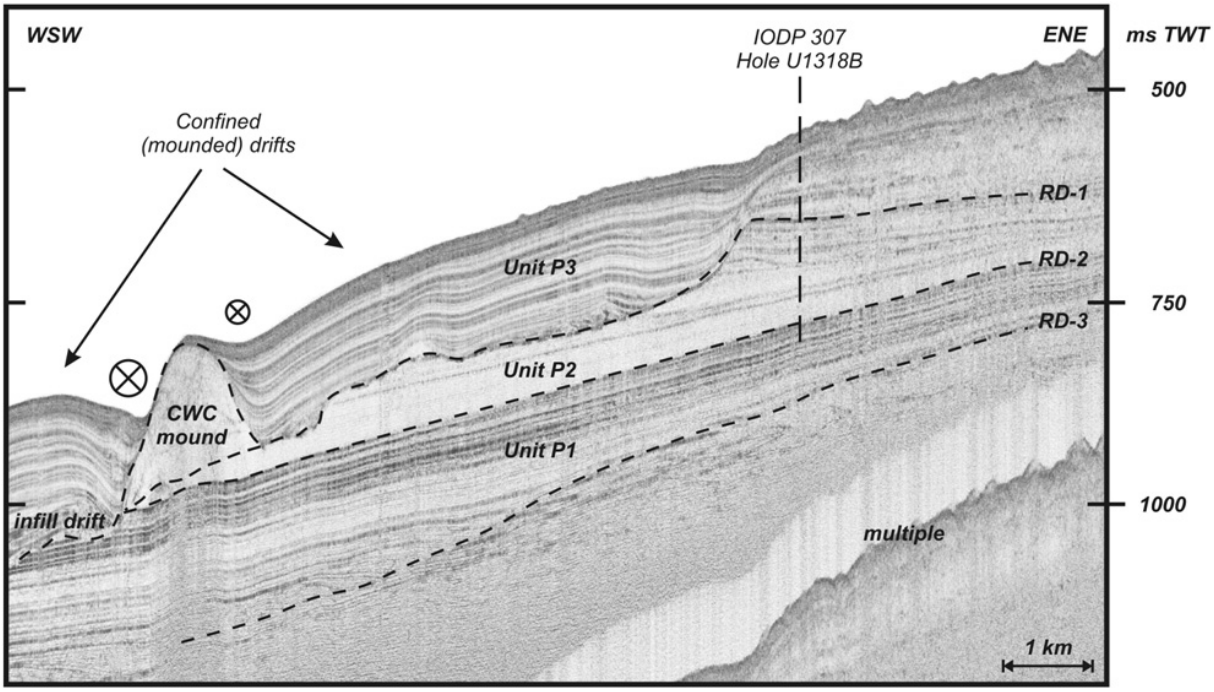

Figure 1.10: Single channel sparker reflection seismic profile (Ghent University) showing seismic characters and the stratigraphy of small mounded contourite drifts and cold-water coral (CWC) mound along the eastern slope of the Porcupine Seabight (Van Rooij et al., 2007; Hebbeln et al. 2016). Labels RD-1, RD-2, RD-3 represent major erosional unconformities. Among them the RD-1 discontinuity has a middle Pleistocene age (Kano et al., 2007).

The southern Biscay continental margin, positioned between the Gulf of Cádiz and Porcupine Seabight (Figure 1.8), lies in a most understudied region regarding the AMW paleoceanography. Intensively distributed submarine canyon systems interrupt alongslope transportation of sediments, suggesting the domination of downslope processes (Weaver et al., 2000; Toucanne et al., 2008; Mulder et al., 2012). However, the Le Danois CDS is identified among these canyon systems (Ercilla et al., 2008); Van Rooij et al., 2010). Present-day morphology and bottom-current dynamics have been studied previously (Ercilla et al., 2008; Iglesias, 2009; Van Rooij et al., 2010). The Le Danois CDS is respectively associated with three water masses, being the Eastern North Atlantic Central Water (ENACW), the AMW and the Labrador Sea Water (LSW) (González-Pola et al., 2012). The seismic stratigraphy of the Le Danois CDS has been addressed as well (Van Rooij et al., 2010), albeit on a relatively small set of seismic profiles. However, detailed Pliocene-Quaternary sedimentary processes and stacking patterns of the Le Danois CDS, as well as the past circulation patterns of the AMW, are still poorly understood.

In addition, the Le Danois Bank region was influenced by both tectonic and bottom-current processes during the Neogene and Quaternary (Gallastegui et al., 2002; Van Rooij et al., 2010). Previous studies addressed the Cretaceous-Neogene tectonic evolution and Quaternary sedimentary processes of the intraslope basin (Van Rooij et al., 2010; Fernández-Viejo et al., 2011;

Cadenas and Fernández-Viejo, 2017). Salt movements and the associated salt-roof thrust deformed the overlying strata during the Paleogene and the Neogene (Zamora et al., 2017). Whereas the Neogene and Quaternary sedimentary sections, mainly consisting of contourite drifts, indicate the domination of the MOW-related bottom currents. However, little is known about the responses of the AMW to salt tectonics in the Le Danois Bank region during the Neogene.

1.4 Late Miocene Mediterranean overflow

Most of the present-day studies have focused on modern contourite drifts or CDS resulted from the MOW/AMW (Llave et al., 2019). The observation of some buried/ancient contourite drifts in the NE Atlantic have highlighted the past global ocean circulation and their profound impact on global climate change (Soares et al., 2014; Capella et al., 2019). The late Miocene Atlantic-Mediterranean gateways are good examples to learn about the processes associated with the ancient intermediated water masses (Flecker et al., 2015).

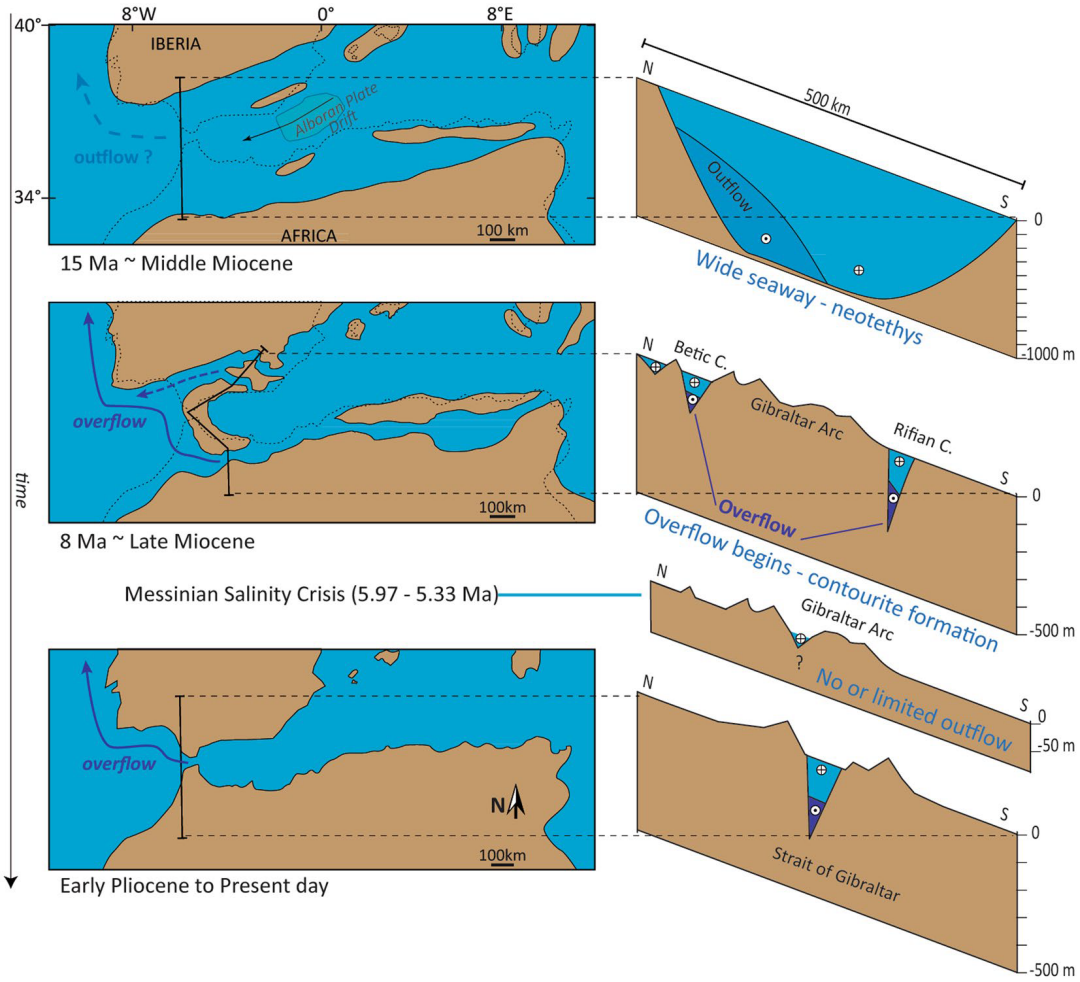

Figure 1.11: A sketch showing the tectonically-controlled reconfiguration of the Atlantic-Mediterranean seaways from the middle Miocene to the present-day. The relationship between the morphology of the seaways and the paleoceanographic conditions are indicated. Image courtesy of Capella et al. (2019).

During the middle Miocene at 16.8-14.7 Ma, the Middle Miocene Climate Optimum represents a global warming event that provides useful analogue for projections of a future warmer Earth (Holbourn et al., 2014). A pronounced phase of deep-sea water cooling occurred around 12–15 Ma, after the Middle Miocene Climatic Optimum (Zachos et al., 2001). During the late Miocene, up

to 6 °C of sea surface temperature (SST) cooling that affected the mid- and high-latitude of both hemispheres occurred between ~7.5 and 5.5 Ma (Herbert et al., 2016). This cooling trend further induced ocean-atmospheric CO_2 decoupling (Capella et al., 2019). Thermohaline circulation can significantly contribute to the ocean-atmospheric carbon changes by the opening and closing of oceanic gateways (Flecker et al., 2015; Capella et al., 2019). However, their effects on climate changes are still poorly understood.

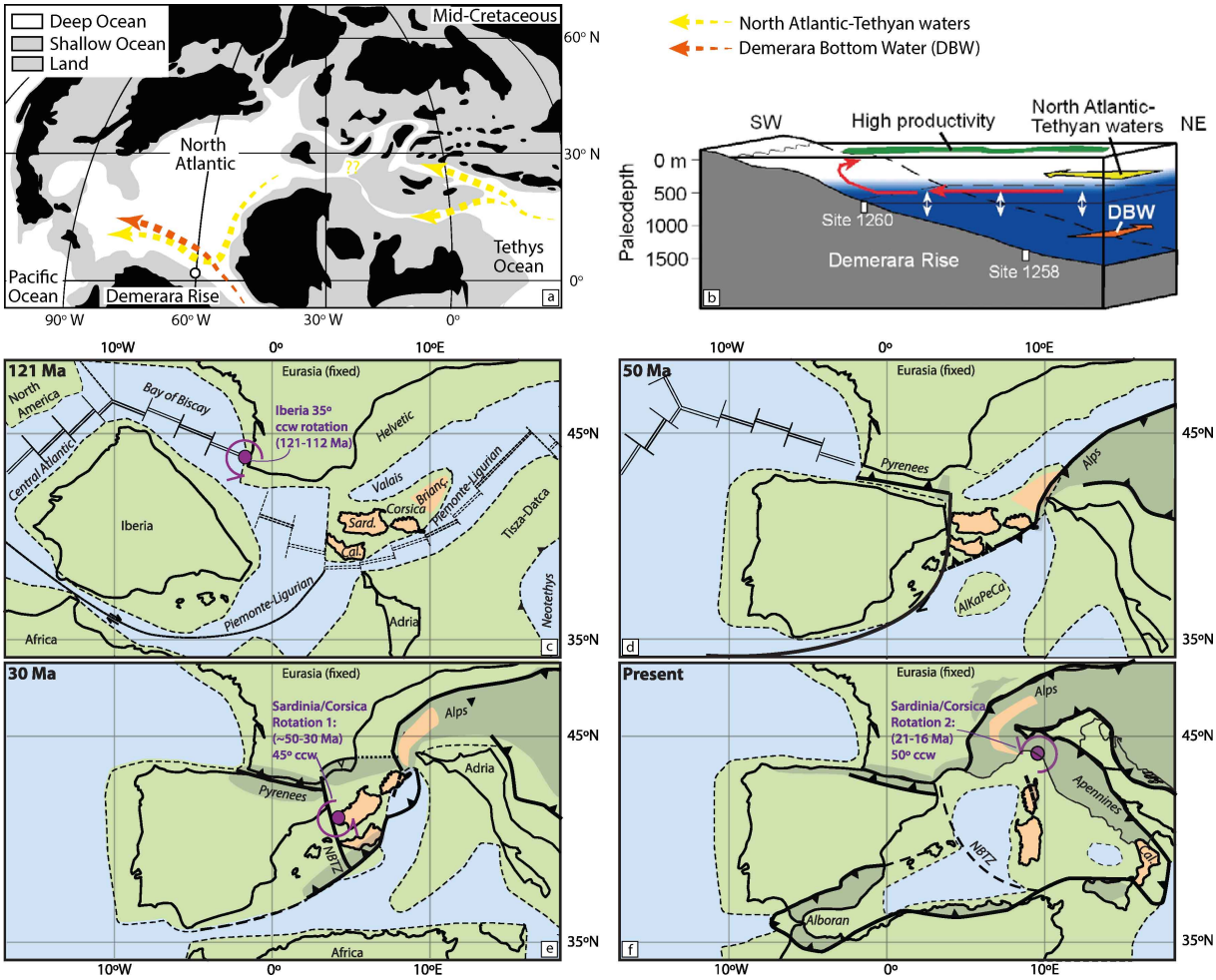

Figure 1.12: (a) The mid-Cretaceous paleogeographic map showing the general ocean circulation pattern (yellow and red arrows) (Zheng et al., 2016); (b) Diagram with Demerara Bottom Water (DBW), North Atlantic–Tethyan waters and their circulation patterns over Demerara Rise. The settling depth and flowing directions are indicated as well (Jiménez Berrocoso et al., 2010); (c, d, e, f) Tectonic reconstructions of the Iberian micro-plate from the mid-Cretaceous (121 Ma) to the present day (Advokaat et al., 2014).

Prior to the Messinian Salinity Crisis (MSC), Rifian and Betic corridors, created by the formation of the Gibraltar arc, replaced a wider gateway between the European and African plates (Capella et al., 2019) (Figure 1.12). The presence of such deep seaways allowed an ancient Atlantic-Mediterranean water exchange (Flecker et al., 2015). The restricted morphology of the deep seaways largely accelerated the water exchange, in turn creating overflows through the sills of the seaways (Capella et al., 2017). The resulted Mediterranean overflow was further promoted by tides and circulated into the NE Atlantic (Figure 1.11) (Capella et al., 2019). At the Rifian Corridor, contourite drifts, consisting of bigradational, sandy-muddy beds and cross-stratified sandstone, are linked to the circulation of the Mediterranean overflow (Capella et al, 2017). The associated bedforms and grain size indicate possible flow velocities (0.15–1.0 m/s) of the Mediterranean

overflow at the Rifian corridor (Capella et al., 2019). Currently, no evidence shows the pathways of the Mediterranean overflow after its exit from the Betic and Rifian corridors. Our understanding of this ancient intermediate water mass is poor. The Le Danois Bank region, located at the northern Iberian continental margin, could be in a key position to investigate the penetration of the late Miocene Mediterranean overflow in the NE Atlantic. The contribution of this water mass to the late Miocene global climate can be examined as well.

1.5 Research objectives

Future research on bottom currents and contourites still remains challenging, especially regarding the link between physical oceanography, sedimentary processes and regional geology (Van Rooij et al., 2016). More specifically, connections between contourite features, their temporal and spatial evolution, the related oceanic circulation and tectonics should be established (Rebesco et al., 2014). In addition, the comparison of seismic facies using different frequencies and resolutions of seismic profiles is needed to improve the seismic criteria of contourite features.

Along the SW European continental margin, the MOW/AMW has significant influence on the margin evolution, climate changes and ocean circulation. Numerous contourite studies have focused on the proximal site of the MOW near the source and the distal site of the AMW. However, the past variability of the MOW/AMW at the intermediate site is still poorly understood. The Le Danois CDS is located at a key position to link proximal and the distal sites of the MOW, providing a unique opportunity to examine the present-day/past oceanic circulation of the MOW and to tie it with basin-scale tectonics. This work aims to contribute to both fundamental and applied aspects and challenges of the contourite paradigm. In this study, we adopted a multidisciplinary approach in order to contribute to five overarching research questions:

1) What is the seismic appearance of contourite drifts in multi-resolution seismic reflection data?
2) How can present-day bottom currents and other oceanographic processes be linked to morphological features in small basin settings?
3) How does the past circulation of the MOW contribute to the temporal and spatial evolution of the basin-scale CDS?
4) How do basin-scale tectonics control on past dynamics of the MOW?
5) What was the pathway of the Mediterranean overflow in the NE Atlantic during the late Miocene? Could it circulate further and reach the Bay of Biscay?

In order to address these objectives, this work will use multi-resolution seismic data to identify contourite features and establish a seismic stratigraphy of the Le Danois CDS. The Le Danois CDS is located within the depth range of the Eastern North Atlantic Central Water (ENACW), the MOW and the Labrador Sea Water (LSW). This oceanographic setting not only offers the opportunity to explore bottom-current processes, but also oceanographic processes at the water mass interfaces. In addition, a combination of the bathymetry, oceanography, multi-resolution seismic reflection and borehole data allows a comprehensive description of the past basin geometry. As such, this work firstly describes the morphology and the distribution of the Le Danois CDS (Chapter 4) and then focuses on the evolution history of these contourite features (Chapter 5). Basin-scale tectonics and their effects on the Le Danois CDS are further discussed (Chapter 6). In older sedimentary sections, buried contourite drifts and the related paleocirculation pattern are explored (Chapter 7). In this order, this work aims to investigate the temporal and spatial

variation of contourite drift systems and the interaction between the paleo-seafloor and bottom currents.

In **chapter 3**, the first research objective is addressed by the seismic expression of the Le Danois CDS. We optimally make use of multiple types of reflection seismic profiling which have different penetration depths and vertical resolutions. The external geometry, the overall seismic stratigraphy, sedimentary stacking patterns, reflection terminations and surficial morphology of contourite drifts are displayed by the multi-channel "low-resolution/low frequency", single-channel "medium-resolution/medium frequency" and the "high-resolution/high frequency" hull-mounted (parametric) echosounder seismic data, respectively. These different-scaled features of contourite drifts are linked to different Earth-system processes, such as long-term tectonic activities, short-term paleo- climate/oceanographic variations and sub-recent sedimentary processes. An edited version of this chapter will be submitted to *Geo-Marine Letters*.

Chapter 4 focuses on the second research objective by a comprehensive description of the distribution and current morphology of various depositional and erosional features of the Le Danois CDS. By combining seismic reflection profiling and present-day oceanographic data, the recent interaction between topographic obstacles and bottom currents is addressed. A contourite model and associated processes are introduced for small-basin settings. This chapter has been published in *Deep-Sea Research Part I: Oceanographic Research Papers*.

Chapter 5 answers the third research objective by establishing a high-resolution seismic stratigraphy of the Le Danois CDS. Sedimentary stacking patterns and the temporal variability of contourite features of the Le Danois CDS are documented. Based on the analysis of sedimentary processes and the evolution of the drift systems, the understanding of past dynamics of intermediate water masses through the late Pliocene to the present day along the Cantabrian continental margin is improved. An edited version of this chapter will be submitted to *Marine Geology*.

In **chapter 6**, a basin-level analysis, derived from the interpretation on seismic reflection data, evaluates the effects of salt tectonics on the paleoceanography of the AMW and the margin evolution (research objective 4). The location of the salt diapirs is compared with the distribution of the Le Danois CDS. Based on basin-level analysis, derived from the interpretation on seismic reflection data, the paleo-seafloor morphology is reconstructed and the effects of salt tectonics on paleoceanography and margin evolution are evaluated. An edited version of this chapter will be submitted for publication in *Basin Research*.

The last research objective is addressed in **chapter 7** by the geophysical mapping of the Miocene contourite drifts in the Le Danois Bank region. Contourite drifts, which are generated by the Miocene Mediterranean overflow, are identified. The related contourite features are linked with the Miocene contourite deposits in the Rifian Corridor (Capella et al., 2017) and Miocene sediment waves in Porcupine Seabight (Van Rooij et al., 2007). The late Miocene circulation pattern of the Mediterranean overflow in the NE Atlantic is discussed. An edited version of this chapter will be submitted for publication in *Geology*.

References

Bahr, A., Kaboth, S., Hodell, D., Zeeden, C., Fiebig, J., Friedrich, O., 2018. Oceanic heat pulses fueling moisture transport towards continental Europe across the mid-Pleistocene transition. Quaternary Science Reviews 179, 48-58.

Becker, J., Lourens, L.J., Raymo, M.E., 2006. High-frequency climate linkages between the North Atlantic and the Mediterranean during marine oxygen isotope stage 100 (MIS100). Paleoceanography 21.

Brackenridge, R.E., Hernández-Molina, F.J., Stow, D.A.V., Llave, E., 2013. A Pliocene mixed contourite–turbidite system offshore the Algarve Margin, Gulf of Cadiz: Seismic response, margin evolution and reservoir implications (Cadiz). Marine and Petroleum Geology 46, 36-50.

Cacchione, D.A., Pratson, L.F., Ogston, A.S., 2002. The Shaping of Continental Slopes by Internal Tides. Science 296, 724-727.

Cacchione, D., Wunsch, C., 2006. Experimental study of internal waves over a slope. Journal of Fluid Mechanics 66, 223-239.

Cadenas, P., Fernández-Viejo, G., 2017. The Asturian Basin within the North Iberian margin (Bay of Biscay): seismic characterisation of its geometry and its Mesozoic and Cenozoic cover. Basin Research 29, 521-541.

Calvin Campbell, D., Mosher, D.C., 2016. Geophysical evidence for widespread Cenozoic bottom current activity from the continental margin of Nova Scotia, Canada. Marine Geology 378, 237-260.

Capella, W., Hernández-Molina, F.J., Flecker, R., Hilgen, F.J., Hssain, M., Kouwenhoven, T.J., van Oorschot, M., Sierro, F.J., Stow, D.A.V., Trabucho-Alexandre, J., Tulbure, M.A., de Weger, W., Yousfi, M.Z., Krijgsman, W., 2017. Sandy contourite drift in the late Miocene Rifian Corridor (Morocco): Reconstruction of depositional environments in a foreland-basin seaway. Sedimentary Geology 355, 31-57.

Capella, W., Barhoun, N., Flecker, R., Hilgen, F.J., Kouwenhoven, T., Matenco, L.C., Sierro, F.J., Tulbure, M.A., Yousfi, M.Z., Krijgsman, W., 2018. Palaeogeographic evolution of the late Miocene Rifian Corridor (Morocco): Reconstructions from surface and subsurface data. Earth-Science Reviews 180, 37-59.

Capella, W., Flecker, R., Hernández-Molina, F.J., Simon, D., Meijer, P.T., Rogerson, M., Sierro, F.J., Krijgsman, W., 2019. Mediterranean isolation preconditioning the Earth System for late Miocene climate cooling. Scientific Reports 9, 3795.

Ceramicola, S., Rebesco, M., De Batist, M., Khlystov, O., 2001. Seismic evidence of small-scale lacustrine drifts in Lake Baikal (Russia). Marine Geophysical Researches 22, 445-464.

Chen, H., Xie, X., Van Rooij, D., Vandorpe, T., Su, M., Wang, D., 2014. Depositional characteristics and processes of alongslope currents related to a seamount on the northwestern margin of the Northwest Sub-Basin, South China Sea. Marine Geology 355, 36-53.

Chen, H., Xie, X., Zhang, W., Shu, Y., Wang, D., Vandorpe, T., Van Rooij, D., 2016. Deep-water sedimentary systems and their relationship with bottom currents at the intersection of Xisha Trough and Northwest Sub-Basin, South China Sea. Marine Geology 378, 101-113.

Chen, H., Zhang, W., Xie, X., Ren, J., 2019. Sediment dynamics driven by contour currents and mesoscale eddies along continental slope: A case study of the northern South China Sea. Marine Geology 409, 48-66.

Collart, T., Verreydt, W., Hernandez-Molina, F.J., Llave, E., Leon, R., Gomez-Ballesteros, M., Pons-Branchu, E., Stewart, H., Van Rooij, D., 2018. Sedimentary processes and cold-water coral mini-mounds at the Ferrol canyon head, NW Iberian margin. Progress in Oceanography 169, 48-65.

Delivet, S., Van Eetvelt, B., Monteys, X., Ribó, M., Van Rooij, D., 2016. Seismic geomorphological reconstructions of Plio-Pleistocene bottom current variability at Goban Spur. Marine Geology 378, 261-275.

Dietrich, D.E., Tseng, Y.-H., Medina, R., Piacsek, S.A., Liste, M., Olabarrieta, M., Bowman, M.J., Mehra, A., 2008. Mediterranean Overflow Water (MOW) simulation using a coupled multiple-grid Mediterranean Sea/North Atlantic Ocean model. Journal of Geophysical Research: Oceans 113.

Elderfield, H., Ferretti, P., Greaves, M., Crowhurst, S., McCave, I.N., Hodell, D., Piotrowski, A.M., 2012. Evolution of Ocean Temperature and Ice Volume Through the Mid-Pleistocene Climate Transition. Science 337, 704-709.

Ercilla, G., Casas, D., Estrada, F., Vázquez, J.T., Iglesias, J., García, M., Gómez, M., Acosta, J., Gallart, J., Maestro-González, A., 2008. Morphosedimentary features and recent depositional architectural model of the Cantabrian continental margin. Marine Geology 247, 61-83.

Ercilla, G., Casas, D., Vázquez, J.T., Iglesias, J., Somoza, L., Juan, C., Medialdea, T., León, R., Estrada, F., García-Gil, S., Farran, M.l., Bohoyo, F., García, M., Maestro, A., 2011. Imaging the recent sediment dynamics of the Galicia Bank region (Atlantic, NW Iberian Peninsula). Marine Geophysical Research 32, 99-126.

Ercilla, G., Juan, C., Hernández-Molina, F.J., Bruno, M., Estrada, F., Alonso, B., Casas, D., Farran, M.l., Llave, E., García, M., Vázquez, J.T., D'Acremont, E., Gorini, C., Palomino, D., Valencia, J., El Moumni, B., Ammar, A., 2016. Significance of bottom currents in deep-sea morphodynamics: An example from the Alboran Sea. Marine Geology 378, 157-170.

Faugères, J.C., Mézerais, M.L., Stow, D.A.V., 1993. Contourite drift types and their distribution in the North and South Atlantic Ocean basins. Sedimentary Geology 82, 189-203.

Fernández-Viejo, G., Gallastegui, J., Pulgar, J.A., Gallart, J., 2011. The MARCONI reflection seismic data: A view into the eastern part of the Bay of Biscay. Tectonophysics 508, 34-41.

Flecker, R., Krijgsman, W., Capella, W., de Castro Martíns, C., Dmitrieva, E., Mayser, J.P., Marzocchi, A., Modestou, S., Ochoa, D., Simon, D., Tulbure, M., van den Berg, B., van der Schee, M., de Lange, G., Ellam, R., Govers, R., Gutjahr, M., Hilgen, F., Kouwenhoven, T., Lofi, J., Meijer, P., Sierro, F.J., Bachiri, N., Barhoun, N., Alami, A.C., Chacon, B., Flores, J.A., Gregory, J., Howard, J., Lunt, D., Ochoa, M., Pancost, R., Vincent, S., Yousfi, M.Z., 2015. Evolution of the Late Miocene Mediterranean–Atlantic gateways and their impact on regional and global environmental change. Earth-Science Reviews 150, 365-392.

Flesche Kleiven, H., Jansen, E., Fronval, T., Smith, T.M., 2002. Intensification of Northern Hemisphere glaciations in the circum Atlantic region (3.5–2.4 Ma) – ice-rafted detritus evidence. Palaeogeography, Palaeoclimatology, Palaeoecology 184, 213-223.

Friocourt, Y., Levier, B., Speich, S., Blanke, B., Drijfhout, S.S., 2007. A regional numerical ocean model of the circulation in the Bay of Biscay. Journal of Geophysical Research: Oceans 112, C09008.

Gallastegui, J., Pulgar, J.A., Gallart, J., 2002. Initiation of an active margin at the North Iberian continent-ocean transition. Tectonics 21, 15-11-15-14.

García, M., Hernández-Molina, F.J., Llave, E., Stow, D.A.V., León, R., Fernández-Puga, M.C., Diaz del Río, V., Somoza, L., 2009. Contourite erosive features caused by the Mediterranean Outflow Water in the Gulf of Cadiz: Quaternary tectonic and oceanographic implications. Marine Geology 257, 24-40.

García, M., Hernández-Molina, F.J., Alonso, B., Vázquez, J.T., Ercilla, G., Llave, E., Casas, D., 2016. Erosive sub-circular depressions on the Guadalquivir Bank (Gulf of Cadiz): Interaction between bottom current, mass-wasting and tectonic processes. Marine Geology 378, 5-19.

Gonthier, E., Faugères, J.-C., Stow, D.A.V., 1984. Contourite facies of the Faro Drift, Gulf of Cadiz, in: Stow, D.A.V., Piper, D.J.W. (Eds.), Fine Grained Sediments, Deep-Water Processes and Facies. Geological Society, London, pp. 275-291.

González-Pola, C., Díaz del Río, G., Ruiz-Villarreal, M., Sánchez, R.F., Mohn, C., 2012. Circulation patterns at Le Danois Bank, an elongated shelf-adjacent seamount in the Bay of Biscay. Deep Sea Research Part I: Oceanographic Research Papers 60, 7-21.

Gruetzner, J., Uenzelmann-Neben, G., 2016. Contourite drifts as indicators of Cenozoic bottom water intensity in the eastern Agulhas Ridge area, South Atlantic. Marine Geology 378, 350-360.

Hayward, B.W., Sabaa, A.T., Kawagata, S., Grenfell, H.R., 2009. The Early Pliocene re-colonisation of the deep Mediterranean Sea by benthic foraminifera and their pulsed Late Pliocene–Middle Pleistocene decline. Marine Micropaleontology 71, 97-112.

Hebbeln, D., Van Rooij, D., Wienberg, C., 2016. Good neighbours shaped by vigorous currents: Cold-water coral mounds and contourites in the North Atlantic. Marine Geology 378, 171-185.

Heezen, B.C., Hollister, C., 1964. Deep-sea current evidence from abyssal sediments. Marine Geology 1, 141-174.

Heezen, B.C., Hollister, C.D., Ruddiman, W.F., 1966. Shaping of the Continental Rise by Deep Geostrophic Contour Currents. Science 152, 502.

Herbert, T.D., Lawrence, K.T., Tzanova, A., Peterson, L.C., Caballero-Gill, R., Kelly, C.S., 2016. Late Miocene global cooling and the rise of modern ecosystems. Nature Geoscience 9, 843.

Hernández-Molina, J., Llave, E., Somoza, L., Fernández-Puga, M.C., Maestro, A., León, R., Medialdea, T., Barnolas, A., García, M., del Río, V.D., Fernández-Salas, L.M., Vázquez, J.T., Lobo, F., Dias, J.M.A., Rodero, J., Gardner, J., 2003. Looking for clues to paleoceanographic imprints: A diagnosis of the Gulf of Cadiz contourite depositional systems. Geology 31, 19-22.

Hernández-Molina, F.J., Llave, E., Stow, D.A.V., 2008. Chapter 19 Continental Slope Contourites, in: Rebesco, M., Camerlenghi, A. (Eds.), Developments in Sedimentology. Elsevier, pp. 379-408.

Hernández-Molina, F.J.N.M., Van Rooij D, Roson G, Ercilla G, Urgorri V, Llave E, Francés G, De Mol L, Estrada F, León R, Mena A, Pérez Arlucea M, Alejo I, Jane G, VanReusel A 2009. The Ortegal spur contourite depositional dystem (Bay of Biscay): the implications of the Mediterranean Outflow Waters in sedimentary processes and cold-water coral ecosystems. In: Ext Abstr Vol 6th Symp Atlantic Iberian Margin (MIA 09), Nuevas Contribuciones al Margen Ibérico Atlántico, 1–5 December 2009, University of Oviedo, pp 281–284.

Hernández-Molina, F.J., Paterlini, M., Somoza, L., Violante, R., Arecco, M.A., de Isasi, M., Rebesco, M., Uenzelmann-Neben, G., Neben, S., Marshall, P., 2010. Giant mounded drifts in the Argentine Continental Margin: Origins, and global implications for the history of thermohaline circulation. Marine and Petroleum Geology 27, 1508-1530.

Hernández-Molina, F.J., Serra, N., Stow, D.A.V., Llave, E., Ercilla, G., Van Rooij, D., 2011. Along-slope oceanographic processes and sedimentary products around the Iberian margin. Geo-Marine Letters 31, 315-341.

Hernández-Molina, F.J., Stow, D.A.V., Alvarez-Zarikian, C.A., Acton, G., Bahr, A., Balestra, B., Ducassou, E., Flood, R., Flores, J.-A., Furota, S., Grunert, P., Hodell, D., Jimenez-Espejo, F., Kim, J.K., Krissek, L., Kuroda, J., Li, B., Llave, E., Lofi, J., Lourens, L., Miller, M., Nanayama, F., Nishida, N., Richter, C., Roque, C., Pereira, H., Sanchez Goñi, M.F., Sierro, F.J., Singh, A.D., Sloss, C., Takashimizu, Y., Tzanova, A., Voelker, A., Williams, T., Xuan, C., 2014. Onset of Mediterranean outflow into the North Atlantic. Science 344, 1244-1250.

Hernández-Molina, F.J., Sierro, F.J., Llave, E., Roque, C., Stow, D.A.V., Williams, T., Lofi, J., Van der Schee, M., Arnáiz, A., Ledesma, S., Rosales, C., Rodríguez-Tovar, F.J., Pardo-Igúzquiza, E., Brackenridge, R.E., 2016. Evolution of the gulf of Cadiz margin and southwest Portugal contourite depositional system: Tectonic, sedimentary and paleoceanographic implications from IODP expedition 339. Marine Geology 377, 7-39.

Hernández-Molina, F.J., Campbell, S., Badalini, G., Thompson, P., Walker, R., Soto, M., Conti, B., Preu, B., Thieblemont, A., Hyslop, L., Miramontes, E., Morales, E., 2017. Large bedforms on contourite terraces: Sedimentary and conceptual implications. Geology 46, 27-30.

Holbourn, A., Kuhnt, W., Lyle, M., Schneider, L., Romero, O., Andersen, N., 2014. Middle Miocene climate cooling linked to intensification of eastern equatorial Pacific upwelling. Geology 42: 19-22.

Huvenne, V.A.I., Van Rooij, D., De Mol, B., Thierens, M., O'Donnell, R., Foubert, A., 2009. Sediment dynamics and palaeo-environmental context at key stages in the Challenger cold-water coral mound formation: Clues from sediment deposits at the mound base. Deep Sea Research Part I: Oceanographic Research Papers 56, 2263-2280.

Iglesias, J., 2009. Sedimentation on the cantabrian continental margin from late oligocene to quaternary. Universidade de Vigo, Vigo, p. 185.

Juan, C., Ercilla, G., Javier Hernández-Molina, F., Estrada, F., Alonso, B., Casas, D., García, M., Farran, M.l., Llave, E., Palomino, D., Vázquez, J.-T., Medialdea, T., Gorini, C., D'Acremont, E., El Moumni, B., Ammar, A., 2016. Seismic evidence of current-controlled sedimentation in the Alboran Sea during the Pliocene and Quaternary: Palaeoceanographic implications. Marine Geology 378, 292-311.

Juan, C., Van Rooij, D., De Bruycker, W., 2018. An assessment of bottom current controlled sedimentation in Pacific Ocean abyssal environments. Marine Geology 403, 20-33.

Kaboth, S., Bahr, A., Reichart, G.-J., Jacobs, B., Lourens, L.J., 2016. New insights into upper MOW variability over the last 150 kyr from IODP 339 Site U1386 in the Gulf of Cadiz. Marine Geology 377, 136-145.

Kano, A., Ferdelman, T.G., Williams, T., Henriet, J.-P., Ishikawa, T., Kawagoe, N., Takashima, C., Kakizaki, Y., Abe, K., Sakai, S., Browning, E.L., Li, X., 2007. Age constraints on the origin and growth history of a deep-water coral mound in the northeast Atlantic drilled during Integrated Ocean Drilling Program Expedition 307. Geology 35, 1051-1054.

Khélifi, N., Sarnthein, M., Andersen, N., Blanz, T., Frank, M., Garbe-Schönberg, D., Haley, B.A., Stumpf, R., Weinelt, M., 2009. A major and long-term Pliocene intensification of the Mediterranean outflow, 3.5–3.3 Ma ago. Geology 37, 811-814.

Khélifi, N., Sarnthein, M., Frank, M., Andersen, N., Garbe-Schönberg, D., 2014. Late Pliocene variations of the Mediterranean outflow. Marine Geology 357, 182-194.

Klymak, J.M., Legg, S., Pinkel, R., 2010. A Simple Parameterization of Turbulent Tidal Mixing near Supercritical Topography. Journal of Physical Oceanography 40, 2059-2074.

Kuhlbrodt, T., Griesel, A., Montoya, M., Levermann, A., Hofmann, M., Rahmstorf, S., 2007. On the driving processes of the Atlantic meridional overturning circulation. Reviews of Geophysics 45.

Laberg, J.S., Stoker, M.S., Dahlgren, K.I.T., Haas, H.d., Haflidason, H., Hjelstuen, B.O., Nielsen, T., Shannon, P.M., Vorren, T.O., van Weering, T.C.E., Ceramicola, S., 2005. Cenozoic alongslope processes and sedimentation on the NW European Atlantic margin. Marine and Petroleum Geology 22, 1069-1088.

Lamb, K.G., 2014. Internal Wave Breaking and Dissipation Mechanisms on the Continental Slope/Shelf. Annual Review of Fluid Mechanics 46, 231-254.

Llave, E., Hernandez-Molina, F.J., Somoza, L., Diaz-del Rio, V., Stow, D.A.V., Maestro, A., Alveirinho Dias, J.M., 2001. Seismic stacking pattern of the Faro-Albufeira contourite system (Gulf of Cadiz): a Quaternary record of paleoceanographic and tectonic influences. Marine Geophysical Researches 22, 487-508.

Llave, E., Hernandez-Molina, F.J., Somoza, L., Stow, D.A.V., Diaz del Rio, G., 2007. Quaternary evolution of the contourite depositional system in the Gulf of Cadiz, in: Viana, A.R., Rebesco, M. (Eds.), Economic and Palaeoceanographic Significance of Contourite Deposits. Geological Society, London, pp. 49-79.

Llave, E., Matias, H., Hernandez-Molina, F.J., Ercilla, G., Stow, D.A.V., Medialdea, T., 2011. Pliocene-Quaternary contourites along the northern Gulf of Cadiz margin: sedimentary stacking pattern and regional distribution. Geo-Marine Letters 31, 377-390.

Llave, E., Hernández-Molina, F.J., García, M., Ercilla, G., Roque, C., Juan, C., Mena, A., Preu, B., Van Rooij, D., Rebesco, M., Brackenridge, R., Jané, G., Gómez-Ballesteros, M., Stow, D., 2019. Contourites along the Iberian continental margins: conceptual and economic implications. Geological Society, London, Special Publications 476, SP476-2017-2046.

Lobo, F.J., Hernández-Molina, F.J., Bohoyo, F., Galindo-Zaldívar, J., Maldonado, A., Martos, Y., Rodríguez-Fernández, J., Somoza, L., Vázquez, J.T., 2011. Furrows in the southern Scan Basin, Antarctica: interplay between tectonic and oceanographic influences. Geo-Marine Letters 31, 451-464.

Lofi, J., Voelker, A.H.L., Ducassou, E., Hernández-Molina, F.J., Sierro, F.J., Bahr, A., Galvani, A., Lourens, L.J., Pardo-Igúzquiza, E., Pezard, P., Rodríguez-Tovar, F.J., Williams, T., 2016. Quaternary chronostratigraphic framework and sedimentary processes for the Gulf of Cadiz and Portuguese Contourite Depositional Systems derived from Natural Gamma Ray records. Marine Geology 377, 40-57.

Maldonado, A., Barnolas, A., Bohoyo, F., Galindo-Zaldívar, J., Hernández-Molina, J., Lobo, F., Rodríguez-Fernández, J., Somoza, L., Tomás Vázquez, J., 2003. Contourite deposits in the central Scotia Sea: the importance of the Antarctic Circumpolar Current and the Weddell Gyre flows. Palaeogeography, Palaeoclimatology, Palaeoecology 198, 187-221.

Maldonado, A., Barnolas, A., Bohoyo, F., Escutia, C., Galindo-Zaldívar, J., Hernández-Molina, J., Jabaloy, A., Lobo, F.J., Nelson, C.H., Rodríguez-Fernández, J., Somoza, L., Vázquez, J.-T., 2005. Miocene to Recent contourite drifts development in the northern Weddell Sea. Global and Planetary Change 45, 99-129.

Marchès, E., Mulder, T., Cremer, M., Bonnel, C., Hanquiez, V., Gonthier, E., Lecroart, P., 2007. Contourite drift construction influenced by capture of Mediterranean Outflow Water deep-sea current by the Portimão submarine canyon (Gulf of Cadiz, South Portugal). Marine Geology 242, 247-260.

Marchès, E., Mulder, T., Gonthier, E., Cremer, M., Hanquiez, V., Garlan, T., Lecroart, P., 2010. Perched lobe formation in the Gulf of Cadiz: Interactions between gravity processes and contour currents (Algarve Margin, Southern Portugal). Sedimentary Geology 229, 81-94.

Martos, Y.M., Maldonado, A., Lobo, F.J., Hernández-Molina, F.J., Pérez, L.F., 2013. Tectonics and palaeoceanographic evolution recorded by contourite features in southern Drake Passage (Antarctica). Marine Geology 343, 76-91.

Maslin, M.A., Ridgwell, A.J., 2005. Mid-Pleistocene revolution and the 'eccentricity myth'. Geological Society, London, Special Publications 247, 19-34.

Masson, D.G., Howe, J.A., Stoker, M.S., 2002. Bottom-current sediment waves, sediment drifts and contourites in the northern Rockall Trough. Marine Geology 192, 215-237.

Mena, A., Francés, G., Pérez-Arlucea, M., Hanebuth, T.J.J., Bender, V.B., Nombela, M.A., 2018. Evolution of the Galicia Interior Basin over the last 60 ka: sedimentary processes and palaeoceanographic implications. Journal of Quaternary Science 33, 536-549.

Michels, K.H., Rogenhagen, J., Kuhn, G., 2001. Recognition of contour-current influence in mixed contourite-turbidite sequences of the western Weddell Sea, Antarctica. Marine Geophysical Researches 22, 465-485.

Millot, C., Candela, J., Fuda, J.-L., Tber, Y., 2006. Large warming and salinification of the Mediterranean outflow due to changes in its composition. Deep Sea Research Part I: Oceanographic Research Papers 53, 656-666.

Miramontes, E., Garreau, P., Caillaud, M., Jouet, G., Pellen, R., Hernández-Molina, F.J., Clare, M.A., Cattaneo, A., 2019. Contourite distribution and bottom currents in the NW Mediterranean Sea: Coupling seafloor geomorphology and hydrodynamic modelling. Geomorphology 333, 43-60.

Mulder, T., Zaragosi, S., Garlan, T., Mavel, J., Cremer, M., Sottolichio, A., Sénéchal, N., Schmidt, S., 2012. Present deep-submarine canyons activity in the Bay of Biscay (NE Atlantic). Marine Geology 295–298, 113-127.

Müller-Michaelis, A., Uenzelmann-Neben, G., Stein, R., 2013. A revised Early Miocene age for the instigation of the Eirik Drift, offshore southern Greenland: Evidence from high-resolution seismic reflection data. Marine Geology 340, 1-15.

Palomino, D., López-González, N., Vázquez, J.-T., Fernández-Salas, L.-M., Rueda, J.-L., Sánchez-Leal, R., Díaz-del-Río, V., 2016. Multidisciplinary study of mud volcanoes and diapirs and their relationship to seepages and bottom currents in the Gulf of Cádiz continental slope (northeastern sector). Marine Geology 378, 196-212.

Pepe, F., Di Donato, V., Insinga, D., Molisso, F., Faraci, C., Sacchi, M., Dera, R., Ferranti, L., Passaro, S., 2018. Seismic stratigraphy of upper Quaternary shallow-water contourite drifts in the Gulf of Taranto (Ionian Sea, southern Italy). Marine Geology 397, 79-92.

Pérez-Asensio, J.N., Aguirre, J., Schmiedl, G., Civis, J., 2012. Impact of restriction of the Atlantic-Mediterranean gateway on the Mediterranean Outflow Water and eastern Atlantic circulation during the Messinian. Paleoceanography 27.

Pomar, L., Morsilli, M., Hallock, P., Bádenas, B., 2012. Internal waves, an under-explored source of turbulence events in the sedimentary record. Earth-Science Reviews 111, 56-81.

Preu, B., Schwenk, T., Hernández-Molina, F.J., Violante, R., Paterlini, M., Krastel, S., Tomasini, J., Spieß, V., 2012. Sedimentary growth pattern on the northern Argentine slope: The impact of North Atlantic Deep Water on southern hemisphere slope architecture. Marine Geology 329-331, 113-125.

Preu, B., Hernández-Molina, F.J., Violante, R., Piola, A.R., Paterlini, C.M., Schwenk, T., Voigt, I., Krastel, S., Spiess, V., 2013. Morphosedimentary and hydrographic features of the northern Argentine margin: The interplay between erosive, depositional and gravitational processes and its conceptual implications. Deep Sea Research Part I: Oceanographic Research Papers 75, 157-174.

Raddatz, J., Rüggeberg, A., Margreth, S., Dullo, W.-C., 2011. Paleoenvironmental reconstruction of Challenger Mound initiation in the Porcupine Seabight, NE Atlantic. Marine Geology 282, 79-90.

Rahmstorf, S., 2002. Ocean circulation and climate during the past 120,000 years. Nature 419, 207-214.

Rebesco, M., Camerlenghi, A., Van Loon, A.J., 2008. Chapter 1 Contourite Research: A Field in Full Development, in: Rebesco, M., Camerlenghi, A. (Eds.), Developments in Sedimentology. Elsevier, pp. 1-10.

Rebesco, M., Wåhlin, A., Laberg, J.S., Schauer, U., Beszczynska-Möller, A., Lucchi, R.G., Noormets, R., Accettella, D., Zarayskaya, Y., Diviacco, P., 2013. Quaternary contourite drifts of the Western Spitsbergen margin. Deep Sea Research Part I: Oceanographic Research Papers 79, 156-168.

Rebesco, M., Hernández-Molina, F.J., Van Rooij, D., Wåhlin, A., 2014. Contourites and associated sediments controlled by deep-water circulation processes: State-of-the-art and future considerations. Marine Geology 352, 111-154.

Ribó, M., Puig, P., Muñoz, A., Lo Iacono, C., Masqué, P., Palanques, A., Acosta, J., Guillén, J., Gómez Ballesteros, M., 2016. Morphobathymetric analysis of the large fine-grained sediment waves over the Gulf of Valencia continental slope (NW Mediterranean). Geomorphology 253, 22-37.

Rodgers, K.B., Latif, M., Legutke, S., 2000. Sensitivity of equatorial Pacific and Indian Ocean watermasses to the position of the Indonesian Throughflow. Geophysical Research Letters 27, 2941-2944.

Rogerson, M., Rohling, E.J., Bigg, G.R., Ramirez, J., 2012. Paleoceanography of the Atlantic-Mediterranean exchange: Overview and first quantitative assessment of climatic forcing. Reviews of Geophysics 50.

Roque, C., Duarte, H., Terrinha, P., Valadares, V., Noiva, J., Cachão, M., Ferreira, J., Legoinha, P., Zitellini, N., 2012. Pliocene and Quaternary depositional model of the Algarve margin contourite drifts (Gulf of Cadiz, SW Iberia): Seismic architecture, tectonic control and paleoceanographic insights. Marine Geology 303–306, 42-62.

Roveri, M., Flecker, R., Krijgsman, W., Lofi, J., Lugli, S., Manzi, V., Sierro, F.J., Bertini, A., Camerlenghi, A., De Lange, G., Govers, R., Hilgen, F.J., Hübscher, C., Meijer, P.T., Stoica, M., 2014. The Messinian Salinity Crisis: Past and future of a great challenge for marine sciences. Marine Geology 352, 25-58.

Sánchez-Leal, R.F., Bellanco, M.J., Fernández-Salas, L.M., García-Lafuente, J., Gasser-Rubinat, M., González-Pola, C., Hernández-Molina, F.J., Pelegrí, J.L., Peliz, A., Relvas, P., Roque, D., Ruiz-Villarreal, M., Sammartino, S., Sánchez-Garrido, J.C., 2017. The Mediterranean Overflow in the Gulf of Cadiz: A rugged journey. Science Advances 3, eaao0609.

Schönfeld, J., Zahn, R., 2000. Late Glacial to Holocene history of the Mediterranean Outflow. Evidence from benthic foraminiferal assemblages and stable isotopes at the Portuguese margin. Palaeogeography, Palaeoclimatology, Palaeoecology 159, 85-111.

Schroeder, K., Chiggiato, J., Bryden, H.L., Borghini, M., Ben Ismail, S., 2016. Abrupt climate shift in the Western Mediterranean Sea. Scientific Reports 6, 23009.

Soares, D.M., Alves, T.M., Terrinha, P., 2014. Contourite drifts on early passive margins as an indicator of established lithospheric breakup. Earth and Planetary Science Letters 401, 116-131.

Stoker, M.S., Hoult, R.J., Nielsen, T., Hjelstuen, B.O., Laberg, J.S., Shannon, P.M., Praeg, D., Mathiesen, A., van Weering, T.C.E., McDonnell, A., 2005. Sedimentary and oceanographic responses to early Neogene compression on the NW European margin. Marine and Petroleum Geology 22, 1031-1044.

Stow, D.A.V., Lovell, J.P.B., 1979. Contourites: Their recognition in modern and ancient sediments. Earth-Science Reviews 14, 251-291.

Stow, D.A.V., Holbrook, J.A., 1984. North Atlantic contourites: an overview. Geological Society, London, Special Publications 15, 245-256.

Stow, D.A.V., Faugères, J.-C., Howe, J.A., Pudsey, C.J., Viana, A.R., 2002. Bottom currents, contourites and deep-sea sediment drifts: current state-of-the-art. Geological Society, London, Memoirs 22, 7-20.

Stow, D.A.V., Javier Hernández-Molina, F., Llave, E., Sayago, M., 2009. Bedform-velocity matrix: The estimation of bottom current velocity from bedform observations. Geology 37, 327-330.

Tansley, C.E., Marshall, D.P., 2001. On the Dynamics of Wind-Driven Circumpolar Currents. Journal of Physical Oceanography 31, 3258-3273.

Thierens, M., Browning, E., Pirlet, H., Loutre, M.F., Dorschel, B., Huvenne, V.A.I., Titschack, J., Colin, C., Foubert, A., Wheeler, A.J., 2013. Cold-water coral carbonate mounds as unique palaeo-archives: the Plio-Pleistocene Challenger Mound record (NE Atlantic). Quaternary Science Reviews 73, 14-30.

Thran, A.C., Dutkiewicz, A., Spence, P., Müller, R.D., 2018. Controls on the global distribution of contourite drifts: Insights from an eddy-resolving ocean model. Earth and Planetary Science Letters 489, 228-240.

Toggweiler, J.R., Russell, J., 2008. Ocean circulation in a warming climate. Nature 451, 286.

Toucanne, S., Zaragosi, S., Bourillet, J.F., Naughton, F., Cremer, M., Eynaud, F., Dennielou, B., 2008. Activity of the turbidite levees of the Celtic-Armorican margin (Bay of Biscay) during the last 30,000 years: Imprints of the last European deglaciation and Heinrich events. Marine Geology 247, 84-103.

Tournadour, E., Mulder, T., Borgomano, J., Hanquiez, V., Ducassou, E., Gillet, H., 2015. Origin and architecture of a Mass Transport Complex on the northwest slope of Little Bahama Bank (Bahamas): Relations

between off-bank transport, bottom current sedimentation and submarine landslides. Sedimentary Geology 317, 9-26.

Turnewitsch, R., Reyss, J.-L., Chapman, D.C., Thomson, J., Lampitt, R.S., 2004. Evidence for a sedimentary fingerprint of an asymmetric flow field surrounding a short seamount. Earth and Planetary Science Letters 222, 1023-1036.

van Aken, H.M., 2000. The hydrography of the mid-latitude Northeast Atlantic Ocean: II: The intermediate water masses. Deep Sea Research Part I: Oceanographic Research Papers 47, 789-824.

Van Rooij, D., Blamart, D., Kozachenko, M., Henriet, J.-P., 2007. Small mounded contourite drifts associated with deep-water coral banks, Porcupine Seabight, NE Atlantic Ocean. Geological Society, London, Special Publications 276, 225-244.

Van Rooij, D., De Mol, L., Le Guilloux, E., Wisshak, M., Huvenne, V.A.I., Moeremans, R., Henriet, J.P., 2010. Environmental setting of deep-water oysters in the Bay of Biscay. Deep Sea Research Part I: Oceanographic Research Papers 57, 1561-1572.

Van Rooij, D., Campbell, C., Rueggeberg, A., Wahlin, A., 2016. The contourite log-book: significance for palaeoceanography, ecosystems and slope instability. Marine Geology 378, 1-4.

Vandorpe, T.P., Van Rooij, D., Stow, D.A.V., Henriet, J.-P., 2011. Pliocene to Recent shallow-water contourite deposits on the shelf and shelf edge off south-western Mallorca, Spain. Geo-Marine Letters 31, 391-403.

Vandorpe, T., Martins, I., Vitorino, J., Hebbeln, D., García, M., Van Rooij, D., 2016. Bottom currents and their influence on the sedimentation pattern in the El Arraiche mud volcano province, southern Gulf of Cadiz. Marine Geology 378, 114-126.

von Lom-Keil, H., Spieß, V., Hopfauf, V., 2002. Fine-grained sediment waves on the western flank of the Zapiola Drift, Argentine Basin: evidence for variations in Late Quaternary bottom flow activity. Marine Geology 192, 239-258.

Weaver, P.P.E., Wynn, R.B., Kenyon, N.H., Evans, J., 2000. Continental margin sedimentation, with special reference to the north-east Atlantic margin. Sedimentology 47, 239-256.

Wunsch, C., 2002. What Is the Thermohaline Circulation? Science 298, 1179.

Zachos, J., Pagani, H., Sloan, L., Thomas, E., Billups, K., 2001. Trends, rhythms, and aberrations in global climate 65 Ma to present. Science 292, 686–693.

Zamora, G., Fleming, M., Gallastegui, J., 2017. Chapter 16 - Salt Tectonics Within the Offshore Asturian Basin: North Iberian Margin, in: Soto, J.I., Flinch, J.F., Tari, G. (Eds.), Permo-Triassic Salt Provinces of Europe, North Africa and the Atlantic Margins. Elsevier, pp. 353-368.

Zhang, W., Hanebuth, T.J.J., Stöber, U., 2016. Short-term sediment dynamics on a meso-scale contourite drift (off NW Iberia): Impacts of multi-scale oceanographic processes deduced from the analysis of mooring data and numerical modelling. Marine Geology 378, 81-100.

Chapter 2

Setting

2.1 Geology

The Le Danois Bank, an E-W narrow topographic high, is located at the northern Iberian continental margin in the southern Bay of Biscay (Figure 2.1a). The northern flank of the Le Danois Bank steeply drops into the Biscay abyssal plain. The slope gradient varies between 18° and 20° and can locally reach 34°. The southern flank is connected to the upper continental slope and has mean slope values varying from 0.8° to 15°. The presence of the Le Danois Bank creates an intraslope basin (about 65 km long and 15-25 km wide) between the bank and the Asturias continental shelf. This intraslope basin is bounded to the west by the Vizco High and to the southeast by the Lastres Canyon (Figure 2.1b). The basin becomes shallower from the centre (1070 m) towards the Le Danois Bank (855 m) and the Asturias continental shelf (443 m).

The Le Danois Bank is originated from the Iberian rift and extensional events during the Late Permian (Ries, 1978; Catalán et al., 2007). During the Triassic and the Jurassic, the extension continued, resulting in N-S crustal thrusts (Costa and Rey, 1995). During the Cretaceous, the northward displacement of the African Plate changed plate kinematics and led to the uplift of the Cantabrian Mountains (Gallastegui et al., 2002). After a tectonic stable stage in the Paleocene, the Le Danois Bank and the intraslope basin started to deform due to the shortening of the Northern Iberian margin during the Eocene (Alvarez-Marrón et al., 1996; Cadenas and Fernández-Viejo, 2017). During the Oligocene, crustal shortening of the former continental slope resulted in E-W orientated faults within the intraslope basin (Boillot et al., 1979; Gallastegui et al., 2002; Vissers and Meijer, 2012). From the late Eocene to the early Miocene, former faults and thrust were inverted (Zamora et al., 2017).

The sedimentary infill within the Le Danois intraslope basin is relatively thin and its maximum thickness is estimated at about 10 km (Boillot et al., 1979; Cadenas and Fernández-Viejo, 2017). Early oil exploration wells confirmed the presence of Triassic evaporites which were formed during the comparison stage between the Cantabrian and the Armorican margin. A carbonate platform, containing limestones, was created associating with the onset of seafloor spreading during the Cretaceous (Boillot and Malod, 1988; Riaza Molina, 1996). The Eocene and Oligocene sediments originate from shallow marine settings, but an important presence of neritic limestones and calcareous sandstones has been observed (Cadenas and Fernández-Viejo, 2017). In the Miocene units, slumps and mass-wasting deposits have been recognized, suggesting downslope processes (Cadenas and Fernández-Viejo, 2017; Zamora et al., 2017). The observation of contourite drifts in the Pliocene unit suggests a shift from downslope to alongslope processes (Van Rooij et al., 2010). Two mounded and elongated drifts, being the Le Danois and the Gijón Drifts, primarily make up the uppermost succession of the Le Danois intraslope basin (Liu et al., 2019).

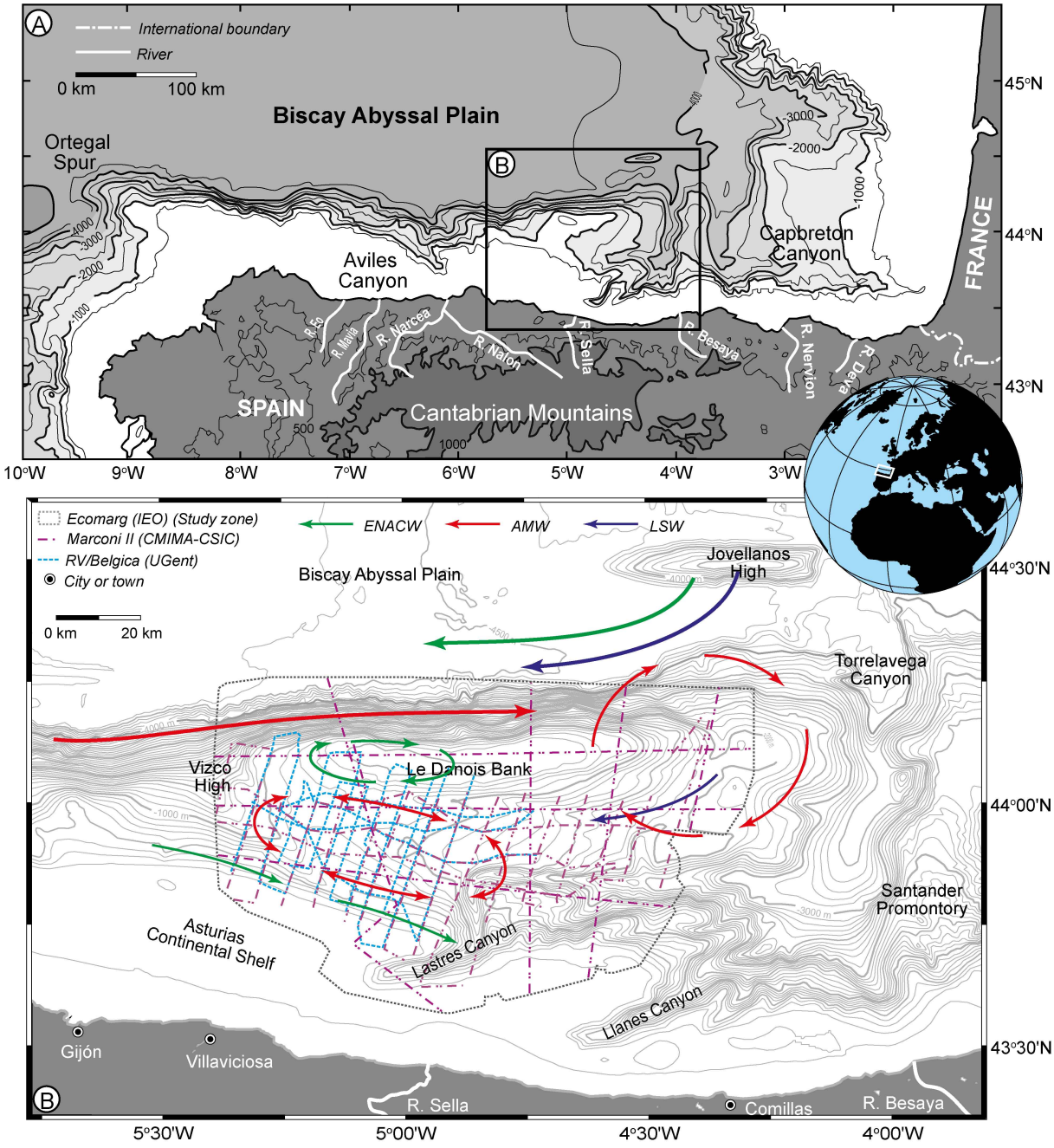

Figure 2.1: Location of the study area: A) Position with respect to the Northern Iberian continental margin (Ercilla et al., 2008), contour lines every 500 m. Location of the rivers is based on Prego et al. (2008); B) Available geophysical datasets for this study. The present-day oceanographic circulation pattern is modified from González-Pola et al. (2012). The main morphological expressions are shown (contour lines every 100 m). ENACW = Eastern North Atlantic Central Water; AMW = Atlantic Mediterranean Water; LSW = Labrador Sea Water.

Contourite drifts and associated moats are observed in the intraslope basin (Van Rooij et al., 2010). The geometry, size and morphology of the intraslope basin are described in **chapter 4.2.1** in considerable detail. The Le Danois Bank originates from the Iberian rift and extensional events during the Late Permian (Ries 1978; Catalán et al., 2007). The intraslope basin, however, started to deform due to the shortening of the northern Iberian margin during the Eocene (Alvarez-Marrón et al., 1996; Cadenas and Fernández-Viejo, 2017). No major deformation or tectonic activities have been observed since the early Miocene (Figure 2.2) (Zamora et al., 2017). The detailed tectonic history of the Le Danois Bank region is discussed in **chapters 5.2.1** and **6.2.1**.

2.2 Oceanography

The present-day circulation of the Le Danois Bank region is dominated by the ENACW between 350 and 600 m water depth (McCartney and Mauritzen, 2001), the AMW between 750 and 1550 m water depth (Iorga and Lozier, 1999a, b), and the LSW between 1750 and 2000 m water depth (van Aken, 2000a) (Figures 2.1b, 2.2a, 2.3). Two interfaces between these water masses are respectively located at 600-750 m and 1550-1750 m water depth (van Aken, 2000a, b). The core of the ENACW is centred at 400 m with a minimum salinity of about 35.5[1] (van Aken, 2000b; Lavín et al., 2006). The warm (9°-10.5° C) and saline (35.7-35.9) AMW is centred at 1000 m water depth (Lavín et al., 2006). Below the MOW, the core of the LSW is recognized at 1800 m water depth with a salinity minimum at about 35.05 (Pingree and Le Cann, 1990; van Aken, 2000a). Due to the topographic constraint of the Le Danois Bank, these water masses display distinctive circulation patterns (Figure 2.3) (González-Pola et al., 2012).

Before the establishment of the present-day oceanographic conditions, the past ENACW, AMW and LSW varied in physical structure, circulation regime and settling depth (Hillaire-Marcel et al., 2001; Voelker et al., 2006; Rogerson et al., 2010; Bahr et al., 2015). At the latest Miocene < 5.33 Ma), the initiation of the present-day Atlantic-Mediterranean exchange resulted in the formation of the MOW (Hernández-Molina et al., 2014). At ~4.5 Ma, the MOW circulated into the Gulf of Cádiz (Hernández-Molina et al., 2014), resulting in the stratification of the ENACW and the MOW/AMW (Jia et al., 2007; Volkov and Fu, 2010). During the late Pliocene (3.2-3.0 Ma) and the early Quaternary (2.4-2.0 Ma), the MOW had enhanced circulation regimes and extended further (Hayward et al., 2009; Raddatz et al., 2011; Khélifi et al., 2014). At ~1.8 Ma, the LSW was stratified from the North Atlantic Deep Water (NADW) and flowed below the MOW/AMW (Burton et al., 1997). The pathways of these water masses started to resemble modern ones (Raymo et al., 2004; Rogerson et al., 2012).

During the Middle-Pleistocene Transition (MPT, ~1.25-0.7 Ma), the periodicity of climate cycles of the Earth dramatically changed from 41 ky to 100 ky (Maslin and Ridgwell, 2005; Elderfield et al., 2012). The resulting glacial/interglacial fluctuations started to significantly influence the properties and dynamics of these water masses (Friocourt et al., 2007; Kaboth et al., 2016; Bahr et al., 2018). The MOW/AMW was 300-700 m deeper and resulted bottom currents were more vigorous during glacial periods (Rogerson et al., 2005; Voelker et al., 2006; Kaboth et al., 2016). During interglacial periods, the AMW was weaker and was located between 600 and 1000 m water depths (Schönfeld and Zahn, 2000; Rogerson et al., 2005). Increased MOW production promoted the ENACW, in turn resulting in strong ENACW currents (Bahr et al., 2018).

[1] When describing the physical oceanography, the no unit convention of the salinity is used in this work. According to UNESCO (1985), the practical salinity scale, defined as conductivity ratio, has no units. During the last two decades of the last century, oceanographic studies commonly used the 'Practical Salinity Unit' (psu) to describe the salinity of the ocean (Haynes and Barton, 1990; Baringer et al., 1997). However, "psu" is currently discouraged and more and more papers published in oceanographic and marine science journals use the no unit convention (Rebesco et al., 2013; Somoza et al., 2014). As such, the salinity of the water masses, which is a dimensionless parameter, is represented by a number in this work.

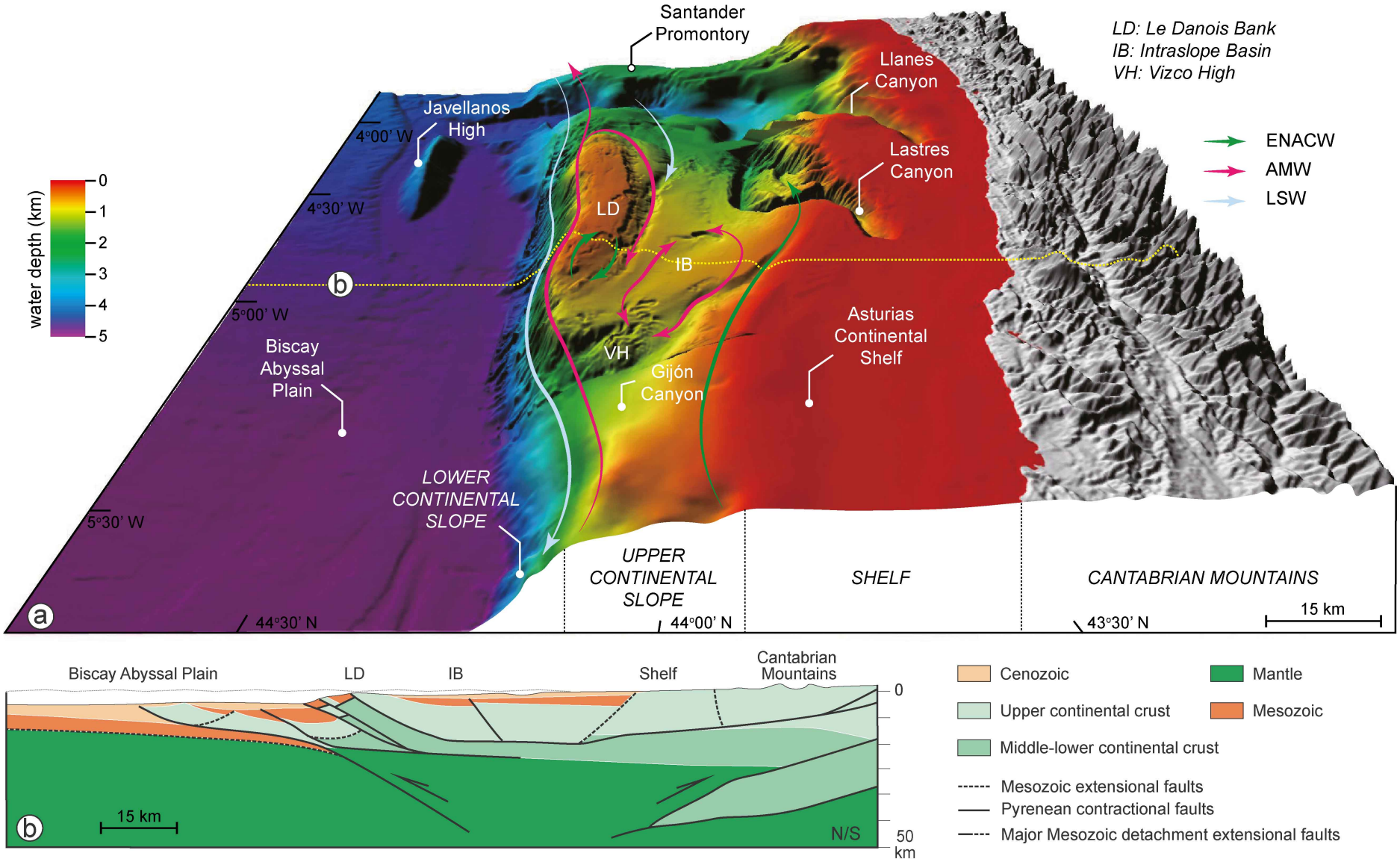
Santander Promontory
Llanes Canyon
Javellanos High
Lastres Canyon
LD: Le Danois Bank
IB: Intraslope Basin
VH: Vizco High
ENACW
AMW
LSW
water depth (km)
0
1
2
3
4
5
4°00' W
4°30' W
5°00' W
5°30' W
LD
IB
VH
Gijón Canyon
Asturias Continental Shelf
Biscay Abyssal Plain
LOWER CONTINENTAL SLOPE
UPPER CONTINENTAL SLOPE
SHELF
CANTABRIAN MOUNTAINS
44°30' N
44°00' N
43°30' N
15 km
a
b
Biscay Abyssal Plain
LD
IB
Shelf
Cantabrian Mountains
0
15 km
N/S
50 km
Cenozoic
Mantle
Upper continental crust
Mesozoic
Middle-lower continental crust
Mesozoic extensional faults
Pyrenean contractional faults
Major Mesozoic detachment extensional faults

Figure 2.2: (a) Map of the Le Danois Bank area with the indication of: the morphological domains and pathways of the Eastern North Atlantic Central Water (ENACW), the Atlantic Mediterranean Water (AMW) and the Labrador Sea Water (LSW); (b) Tectonic structure modified from Roca et al. (2011). The location of this cross-section is shown in the morphological map (a).

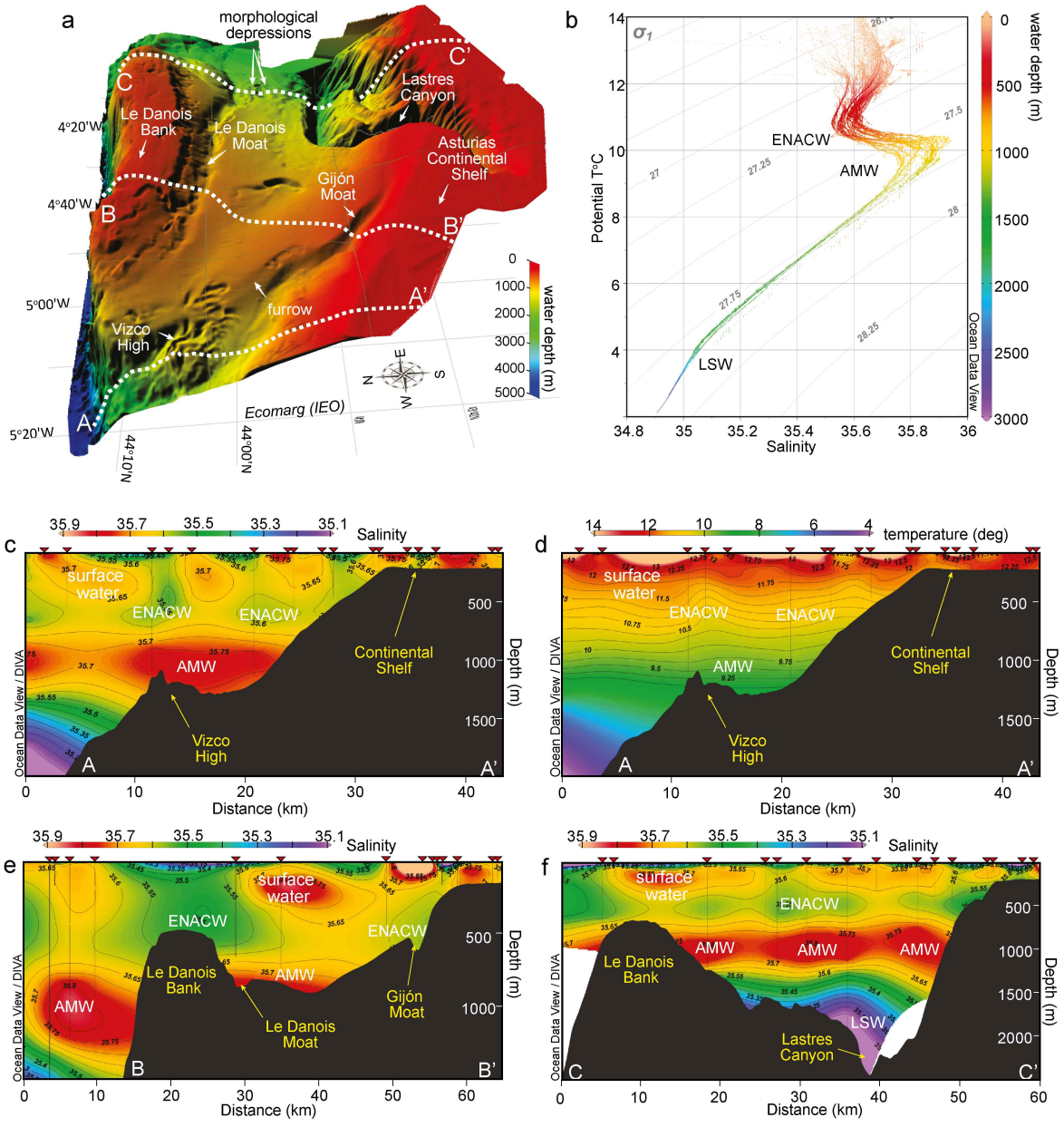

Figure 2.3: (a) 3D colour shaded relief multibeam high-resolution bathymetric map of the study area (ECOMARG project, IEO), with the location of oceanographic cross-sections A-A', B-B' and C-C (World Ocean Database, 2013); (b) Potential temperature versus salinity diagram from the water masses in the study area (World Ocean Database, 2013). CTD stations (red triangles) and their respective locations are indicated in cross-section profiles; (c, d, e, f) Oceanographic cross-sections from the Le Danois Bank towards the Cantabrian continental margin. The water column colour ranges indicate salinity (c, e, f) and temperature (d).

During the middle Pleistocene (~420-396 ka), the ENACW was continuously enhanced during glacial intervals, due to the domination of the Iberian Poleward Current (IPC) (Voelker et al., 2010). However, the MOW/AMW was largely unaffected by glacial-interglacial cycles between ~0.47 Ma and ~0.13 Ma (Kaboth et al., 2017). Whereas the LSW was instable during climate cycles, due to the reduced production of the NADW (Hillaire-Marcel and Bilodeau, 2000). During the Last Glacial Maximum (LGM), the ENACW extended further towards the Bay of Biscay (Bender et al., 2012; Mena et al., 2018). Below the ENACW, the core of the AMW prevailed at a deeper depth (2000 m) due to increased density (Schönfeld and Zahn, 2000). Between 7.5 and 6 ka, the core of the AMW retreated to 1000 m (Schönfeld and Zahn, 2000). Finally, the modern circulation of the ENAWC, the MOW/AMW and the LSW was respectively established at ~15.5 ka, ~7.5-6 ka, ~7 ka (Schönfeld and Zahn, 2000; Hillaire-Marcel et al., 2001; Bender et al., 2012; Mena et al., 2018). A detailed description of the relevant regional paleoceanography is represented in **chapter 5.2.3**.

References

Alvarez-Marrón, J., Pérez-Estaún, A., Danñobeitia, J.J., Pulgar, J.A., Martínez, Catalán, J.R., Marcos, A., Bastida, F., Ayarza, Arribas, P., Aller, J., Gallart, A., Gonzalez-Lodeiro, F., Banda, E., Comas, M.C., Córdoba, D., 1996. Seismic structure of the northern continental margin of Spain from ESCIN deep seismic profiles. Tectonophysics 264, 153-174.

Bahr, A., Kaboth, S., Jiménez-Espejo, F.J., Sierro, F.J., Voelker, A.H.L., Lourens, L., Röhl, U., Reichart, G.J., Escutia, C., Hernández-Molina, F.J., Pross, J., Friedrich, O., 2015. Persistent monsoonal forcing of Mediterranean Outflow Water dynamics during the late Pleistocene. Geology 43, 951-954.

Baringer, M.O.N., Price, J.F., 1997. Mixing and Spreading of the Mediterranean Outflow. Journal of Physical Oceanography 27, 1654-1677.

Bender, V.B., Hanebuth, T.J.J., Mena, A., Baumann, K.-H., Francés, G., von Dobeneck, T., 2012. Control of sediment supply, palaeoceanography and morphology on late Quaternary sediment dynamics at the Galician continental slope. Geo-Marine Letters 32, 313-335.

Boillot, G., Dupeuble, P.A., Malod, J., 1979. Subduction and tectonics on the continental margin off northern Spain. Marine Geology 32, 53-70.

Boillot, G., Malod, J., 1988. The north and north-west Spanish continental margin: a review. Rev. Soc. Geol. España 1, 295-316.

Burton, K.W., Ling, H.-F., O'Nions, R.K., 1997. Closure of the Central American Isthmus and its effect on deep-water formation in the North Atlantic. Nature 386, 382.

Cadenas, P., Fernández-Viejo, G., 2017. The Asturian Basin within the North Iberian margin (Bay of Biscay): seismic characterisation of its geometry and its Mesozoic and Cenozoic cover. Basin Research 29, 521-541.

Catalán, J.R.M., Arenas, R., García, F.D., Cuadra, P.G., Gómez-Barreiro, J., Abati, J., Castiñeiras, P., Fernández-Suárez, J., Martínez, S.S., Andonaegui, P., Clavijo, E.G., Montes, A.D., Pascual, F.J.R., Aguado, B.V., 2007. Space and time in the tectonic evolution of the northwestern Iberian Massif: Implications for the Variscan belt. Geological Society of America Memoirs 200, 403-423.

Elderfield, H., Ferretti, P., Greaves, M., Crowhurst, S., McCave, I.N., Hodell, D., Piotrowski, A.M., 2012. Evolution of Ocean Temperature and Ice Volume Through the Mid-Pleistocene Climate Transition. Science 337, 704-709.

Friocourt, Y., Levier, B., Speich, S., Blanke, B., Drijfhout, S.S., 2007. A regional numerical ocean model of the circulation in the Bay of Biscay. Journal of Geophysical Research: Oceans 112, C09008.

Gallastegui, J., Pulgar, J.A., Gallart, J., 2002. Initiation of an active margin at the North Iberian continent-ocean transition. Tectonics 21, 15-11-15-14.

González-Pola, C., Díaz del Río, G., Ruiz-Villarreal, M., Sánchez, R.F., Mohn, C., 2012. Circulation patterns at Le Danois Bank, an elongated shelf-adjacent seamount in the Bay of Biscay. Deep Sea Research Part I: Oceanographic Research Papers 60, 7-21.

Haynes, R., Barton, E.D., 1990. A poleward flow along the Atlantic coast of the Iberian peninsula. Journal of Geophysical Research: Oceans 95, 11425-11441.

Hernández-Molina, F.J., Llave, E., Preu, B., Ercilla, G., Fontan, A., Bruno, M., Serra, N., Gomiz, J.J., Brackenridge, R.E., Sierro, F.J., Stow, D.A. V, García, M., Juan, C., Sandoval, N., Arnaiz, A., 2014. Contourite processes associated with the Mediterranean Outflow Water after its exit from the Strait of Gibraltar: Global and conceptual implications. Geology 42, 227–230.

Hillaire-Marcel, C., Bilodeau, G., 2000. Instabilities in the Labrador Sea water mass structure during the last climatic cycle. Canadian Journal of Earth Sciences 37, 795-809.

Hillaire-Marcel, C., de Vernal, A., Bilodeau, G., Weaver, A.J., 2001. Absence of deep-water formation in the Labrador Sea during the last interglacial period. Nature 410, 1073.

Iorga, M.C., Lozier, M.S., 1999a. Signatures of the Mediterranean outflow from a North Atlantic climatology 1. Salinity and density fields. Journal of Geophysical Research-Oceans 104, 25985-26009.

Iorga, M.C., Lozier, M.S., 1999b. Signatures of the Mediterranean outflow from a North Atlantic climatology 2. Diagnostic velocity fields. Journal of Geophysical Research-Oceans 104, 26011-26029.

Jia, Y., Coward, A.C., de Cuevas, B.A., Webb, D.J., Drijfhout, S.S., 2007. A Model Analysis of the Behavior of the Mediterranean Water in the North Atlantic. Journal of Physical Oceanography 37, 764-786.

Kaboth, S., Bahr, A., Reichart, G.-J., Jacobs, B., Lourens, L.J., 2016. New insights into upper MOW variability over the last 150 kyr from IODP 339 Site U1386 in the Gulf of Cadiz. Marine Geology 377, 136-145.

Khélifi, N., Sarnthein, M., Frank, M., Andersen, N., Garbe-Schönberg, D., 2014. Late Pliocene variations of the Mediterranean outflow. Marine Geology 357, 182-194.

Lavín, A., Valdés, L., Sánchez, F., Abaunza, P., Forest, A., Boucher, J., Lazure, P., Jegou, A.M., 2006. The Bay of Biscay: the encountering of the ocean and the shelf, in: Brink, A.R.R.K.H. (Ed.), The Sea. the President and Fellows of Harvard College, pp. 933-999.

Liu, S., Van Rooij, D., Vandorpe, T., González-Pola, C., Ercilla, G., Hernández-Molina, F.J., 2019. Morphological features and associated bottom-current dynamics in the Le Danois Bank region (southern Bay of Biscay, NE Atlantic): A model in a topographically constrained small basin. Deep Sea Research Part I: Oceanographic Research Papers, 149, 103054.

Maslin, M.A., Ridgwell, A.J., 2005. Mid-Pleistocene revolution and the 'eccentricity myth'. Geological Society, London, Special Publications 247, 19-34.

McCartney, M.S., Mauritzen, C., 2001. On the origin of the warm inflow to the Nordic Seas. Progress in Oceanography 51, 125-214.

Mena, A., Francés, G., Pérez-Arlucea, M., Hanebuth, T.J.J., Bender, V.B., Nombela, M.A., 2018. Evolution of the Galicia Interior Basin over the last 60 ka: sedimentary processes and palaeoceanographic implications. Journal of Quaternary Science 33, 536-549.

Pingree, R.D., Le Cann, B., 1990. Structure, strength and seasonality of the slope currents in the Bay of Biscay region. Journal of the Marine Biological Association of the United Kingdom 70, 857-885.

Raddatz, J., Rüggeberg, A., Margreth, S., Dullo, W.-C., 2011. Paleoenvironmental reconstruction of Challenger Mound initiation in the Porcupine Seabight, NE Atlantic. Marine Geology 282, 79-90.

Raymo, M.E., Oppo, D.W., Flower, B.P., Hodell, D.A., McManus, J.F., Venz, K.A., Kleiven, K.F., McIntyre, K., 2004. Stability of North Atlantic water masses in face of pronounced climate variability during the Pleistocene. Paleoceanography 19, PA2008.

Rebesco, M., Wåhlin, A., Laberg, J.S., Schauer, U., Beszczynska-Möller, A., Lucchi, R.G., Noormets, R., Accettella, D., Zarayskaya, Y., Diviacco, P., 2013. Quaternary contourite drifts of the Western Spitsbergen margin. Deep Sea Research Part I: Oceanographic Research Papers 79, 156-168.

Riaza Molina, C., 1996. Inversión estructural en la cuenca mesozoica del off-shore asturiano. Revisión de un modelo exploratorio Geogaceta. Geogaceta 20, 169–171.

Ries, A.C., 1978. The opening of the Bay of Biscay - a review. Earth-Science Reviews 14, 35-63.

Roca, E., Muñoz, J.A., Ferrer, O., Ellouz, N., 2011. The role of the Bay of Biscay Mesozoic extensional structure in the configuration of the Pyrenean orogen: Constraints from the MARCONI deep seismic reflection survey. Tectonics 30, TC2001.

Rogerson, M., Rohling, E.J., Weaver, P.P.E., Murray, J.W., 2005. Glacial to interglacial changes in the settling depth of the Mediterranean Outflow plume. Paleoceanography 20, PA3007.

Rogerson, M., Colmenero-Hidalgo, E., Levine, R.C., Rohling, E.J., Voelker, A.H.L., Bigg, G.R., Schönfeld, J., Cacho, I., Sierro, F.J., Löwemark, L., Reguera, M.I., de Abreu, L., Garrick, K., 2010. Enhanced Mediterranean-Atlantic exchange during Atlantic freshening phases. Geochemistry, Geophysics, Geosystems 11, Q08013.

Rogerson, M., Rohling, E.J., Bigg, G.R., Ramirez, J., 2012. Paleoceanography of the Atlantic-Mediterranean exchange: Overview and first quantitative assessment of climatic forcing. Reviews of Geophysics 50, RG2003.

Schönfeld, J., Zahn, R., 2000. Late Glacial to Holocene history of the Mediterranean Outflow. Evidence from benthic foraminiferal assemblages and stable isotopes at the Portuguese margin. Palaeogeography, Palaeoclimatology, Palaeoecology 159, 85-111.

Somoza, L., Ercilla, G., Urgorri, V., León, R., Medialdea, T., Paredes, M., Gonzalez, F.J., Nombela, M.A., 2014. Detection and mapping of cold-water coral mounds and living Lophelia reefs in the Galicia Bank, Atlantic NW Iberia margin. Marine Geology 349, 73-90.

Unesco, 1985. The International System of Units (SI) in Oceanography. Unesco Technical Papers in Marine Science 45.

van Aken, H.M., 2000a. The hydrography of the mid-latitude northeast Atlantic Ocean: I: The deep water masses. Deep Sea Research Part I: Oceanographic Research Papers 47, 757-788.

van Aken, H.M., 2000b. The hydrography of the mid-latitude Northeast Atlantic Ocean: II: The intermediate water masses. Deep Sea Research Part I: Oceanographic Research Papers 47, 789-824.

Van Rooij, D., Iglesias, J., Hernández-Molina, F.J., Ercilla, G., Gomez-Ballesteros, M., Casas, D., Llave, E., De Hauwere, A., Garcia-Gil, S., Acosta, J., Henriet, J.P., 2010. The Le Danois Contourite Depositional System: Interactions between the Mediterranean Outflow Water and the upper Cantabrian slope (North Iberian margin). Marine Geology 274, 1-20.

Vissers, R.L.M., Meijer, P.T., 2012. Iberian plate kinematics and Alpine collision in the Pyrenees. Earth-Science Reviews 114, 61-83.

Voelker, A.H.L., Salgueiro, E., Rodrigues, T., Jimenez-Espejo, F.J., Bahr, A., Alberto, A., Loureiro, I., Padilha, M., Rebotim, A., Röhl, U., 2015. Mediterranean Outflow and surface water variability off southern

Portugal during the early Pleistocene: A snapshot at Marine Isotope Stages 29 to 34 (1020–1135ka). Global and Planetary Change 133, 223-237.

Volkov, D.L., Fu, L.-L., 2010. On the Reasons for the Formation and Variability of the Azores Current. Journal of Physical Oceanography 40, 2197-2220.

Zamora, G., Fleming, M., Gallastegui, J., 2017. Chapter 16 - Salt Tectonics Within the Offshore Asturian Basin: North Iberian Margin, in: Soto, J.I., Flinch, J.F., Tari, G. (Eds.), Permo-Triassic Salt Provinces of Europe, North Africa and the Atlantic Margins. Elsevier, pp. 353-368.

Chapter 3

Methods: Multi-resolution seismic imaging of contourite drifts

An edited version of this chapter will be submitted as:

Liu, S., Van Rooij, D., Ercilla, G., Hernández-Molina, F.J., in prep. Multi-resolution seismic imaging of contourite drifts. *Geo-Marine Letters*.

Abstract: Different types of contourite drifts are identified in the Le Danois Bank region, southern Bay of Biscay. Nearly overlapping reflection seismic datasets, including multi-channel airgun, single-channel sparker and ParaSound seismic profiles, are used to image multi-scaled seismic features of contourite drifts. The multi-channel airgun seismic profiles are used to explore the external geometry, pre-drift units and major depositional units of contourite drifts. These large scale seismic features are related to long-term tectonic/oceanographic influences. The single-channel sparker seismic data are applied for a higher-resolution seismic stratigraphy of contourite drifts. The internal features of seismic sub-units are linked to climatic and eustatic changes based on the medium-scaled seismic imaging. Ultra-high resolution sub-bottom profilers are used to identify the surficial morphology of contourite drifts. The small scale seismic imaging of contourite drifts are indicate sub-recent sedimentary processes associated with contourite drifts. Cyclic features, which consist of an acoustically transparent lower part and a moderate amplitude upper part, are shown in some seismic sub-units of the elongated and mounded drift in single-channel sparker and ParaSound seismic profiles. These depositional cycles have different thickness and indicate different durations. Longer frequency depositional cycles of contourite drifts, which are uniquely related to tectonic variations, can be displayed by the low resolution, high penetration seismic systems. The moderate-high resolution, low-moderate penetration deep data show shorter frequency depositional cycles of contourite drifts, which generally are linked to climatic or Milankovitch/sea-level cycles.

Keywords: multi-resolution seismic profiles; seismic interpretation; contourite drifts; seismic facies.

Author contributions: Seismic processing on single channel reflection seismic data was performed by Liu, S.. Seismic interpretation was performed by Liu, S. and Hernández-Molina, F.J.

Processed ParaSound and airgun seismic data was provided by Ercilla, G.. Writing was performed by Liu, S. and under supervision of Van Rooij, D.

3.1 Introduction

Contourite drifts are sedimentary bodies deposited or substantially reworked by bottom currents (Heezen et al., 1966; Rebesco et al., 2014). During last two decades, contourite drifts have been identified from shallow to deep marine settings in the world's ocean through seismic imaging (Faugères et al., 1998; Howe et al., 2002; Maldonado et al., 2005; Hernández-Molina et al., 2006; Preu et al., 2013; Miramontes et al., 2016). Sand-rich sedimentary facies of contourite drifts can hold the potential for the good reservoir for the hydrocarbon exploration (Viana et al., 2007; Brackenridge et al., 2013). Contourite drifts also play a crucial role in slope instability (Laberg et al., 2005). Slope failures and mass movements can be triggered due to high sedimentation rates of contourite drifts and active scouring of bottom currents, in turn resulting in profound changes of the (paleo-) seafloor morphology (Sultan et al., 2004; Laberg and Camerlenghi, 2008). In geological records, contourite drifts can document Earth-system processes that range from millions of years (the opening and closure of the oceanic gateways) to thousands of years (glacial/interglacial climate cycles) (Llave et al., 2001; Schlüter and Uenzelmann-Neben, 2008; Khélifi et al., 2014; Capella et al., 2017). As such, contourite studies have far-reaching implications for petroleum exploration and deep-sea basin analysis (Viana, 2008; Rebesco et al., 2014).

In the deep ocean, the identification and interpretation of contourite drifts is commonly based on seismic reflection data (Faugères et al., 1999; Nielsen et al., 2008). In some regions, only one type of seismic data was used (Nielsen et al., 2008). External geometry, internal architecture, erosional unconformities and reflector terminations are considerable seismic elements to distinguish contourite drifts from other deep-sea deposits (turbidite levees and fans) (Stow et al., 2002). However, seismic data with different resolutions, which depend on the type of the seismic source, contain different levels of interpretation (Reynolds, 2011). Stratified-wavy seismic reflections can be interpreted as a series of small contourite drifts (through 60 Hz airgun seismic profiles in the South China Sea; Chen et al., 2014), slope failures (through 3.5 kHz uniboom seismic profiles on the Adriatic shelf; Correggiari et al., 2001) or sediment waves (through 16-20 kHz TOPAS seismic profiles in the Gulf of Valencia; Ribó et al., 2016). Different types of seismic profiles also contain multi-scaled geological information due to the penetration of the seismic signal (Nielsen et al., 2008). An example is the mounded drift in the Corsica Trough (Northern Tyrrhenian Sea), where sub-recent pockmarks and the basal discontinuity of the drift are respectively documented by the 1.8-5.3 kHz CHIRP (Compressed High Intensity Radar Pulse) and the 50-250 Hz mini-gun seismic profiles (Miramontes et al., 2016). Therefore, the full-scale seismic interpretation of contourite drifts and better seismic diagnostic criteria of contourite drifts are needed for contourite studies.

In the Le Danois Bank region, different types of contourite drifts were widely distributed in the intraslope basin (Van Rooij et al., 2010; Liu et al., 2019). Here, three sets of reflection seismic data, embracing different vertical resolutions from low to ultra-high, have been used (Figure 3.2) in order to illustrate the seismic expression of contourite drifts. These different datasets contain

nearly overlapping NNE-SSW to N-S orientated profiles, allowing a more detailed seismic interpretation of contourite drifts in all its aspects. This study specifically focuses on the multi-scaled seismic expression of contourite drifts, aiming to 1) illustrate the variable seismic elements of contourite drifts from large to small scales; 2) discuss the expression of cyclic variations of contourite drifts in multi-resolution seismic profiles; 3) assist improving the diagnostic criteria of contourite drifts through the use for a multi-resolution exploration strategy.

3.2 Material and methods

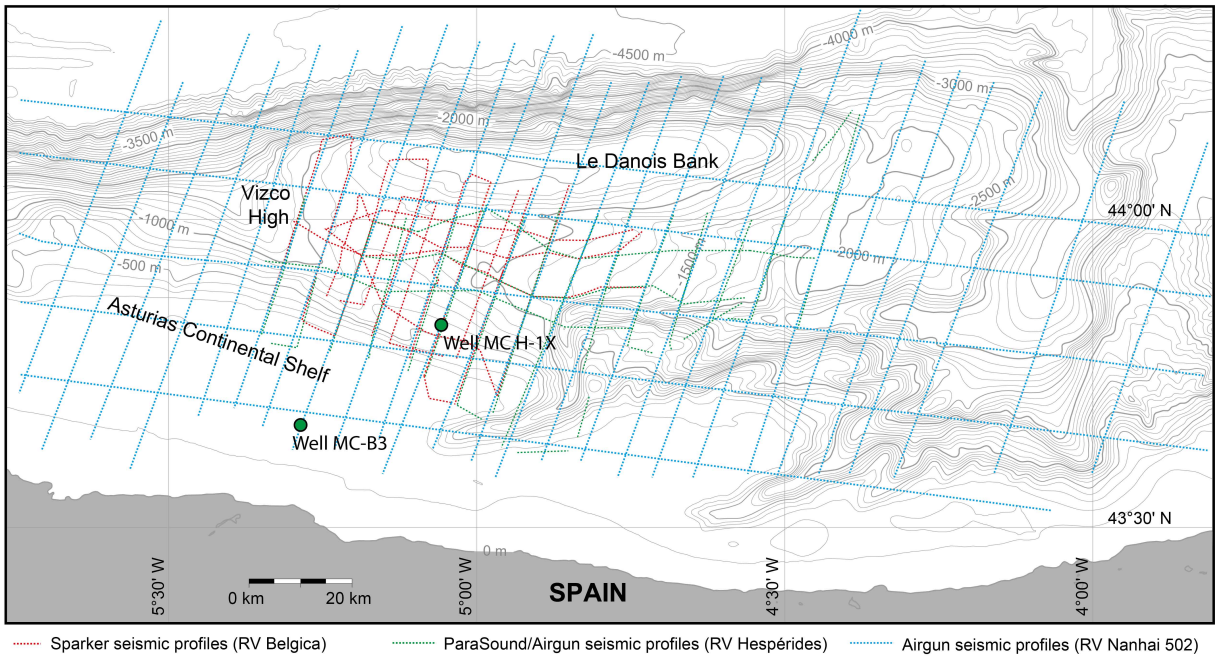

Figure 3.1: Study area, indicating the location of borehole data (Cadenas and Fernández-Viejo, 2017) and different sets of seismic data.

	ParaSound	Single-channel	Multi-channel
scientific cruise	RV Hespérides MARCONI II	RV Belgica 11/18a	RV Hespérides MARCONI II
seismic source	ParaSound P-35	SIG sparker	Sercel G-GUN II
transmission energy	35 kW		
operating energy		500 J	
source volume			530 cu.in
main frequency	18 kHz	800 Hz	80 Hz
penetration	0.2 s TWT	0.5 s TWT	1.5 s TWT
vertical resolution	0.15 m	1.5 m	4.5 m
shot interval	0.4 s	2.5 s	6 s
distance between shot points	1.8 m	5 m	12.7 m

Table 3.1: Summary of the seismic data used in this chapter. Locations of seismic lines are indicated in Figure 3.1.

Four sets of reflection seismic data, which were obtained during different projects and cruises, were used for this work (Figure 3.1, Table 3.1). Ultra-high resolution ParaSound (topographic parametric sonar) and multi-channel airgun profiles were obtained during the RV Hespérides campaign MARCONI II in 2003. High-resolution single-channel sparker seismic profiles were obtained during the RV Belgica cruise ST1118a in June 2011. Another set of multi-channel airgun profiles were acquired during the RV Nanhai 502 cruise in 2001 within the framework of TGS-NOPEC seismic experiment CS-01 (not used in this chapter). Details on the seismic source, acquisition and processing of these data are respectively indicated in methods sections of **chapters 4, 5, 6** and **7**.

3.3.1 Elongated and mounded drifts

Along the southern flank of the Le Danois Bank and the upper continental slope, two mounded sedimentary bodies are displayed in the airgun seismic profiles (Figures 3.2, 3.3, 3.4), They are identified as elongated and mounded drifts, namely defined as the Le Danois and Gijon Drifts, based on their mounded geometry, internal structure and bounding reflectors (Figures 3.3, 3.4).

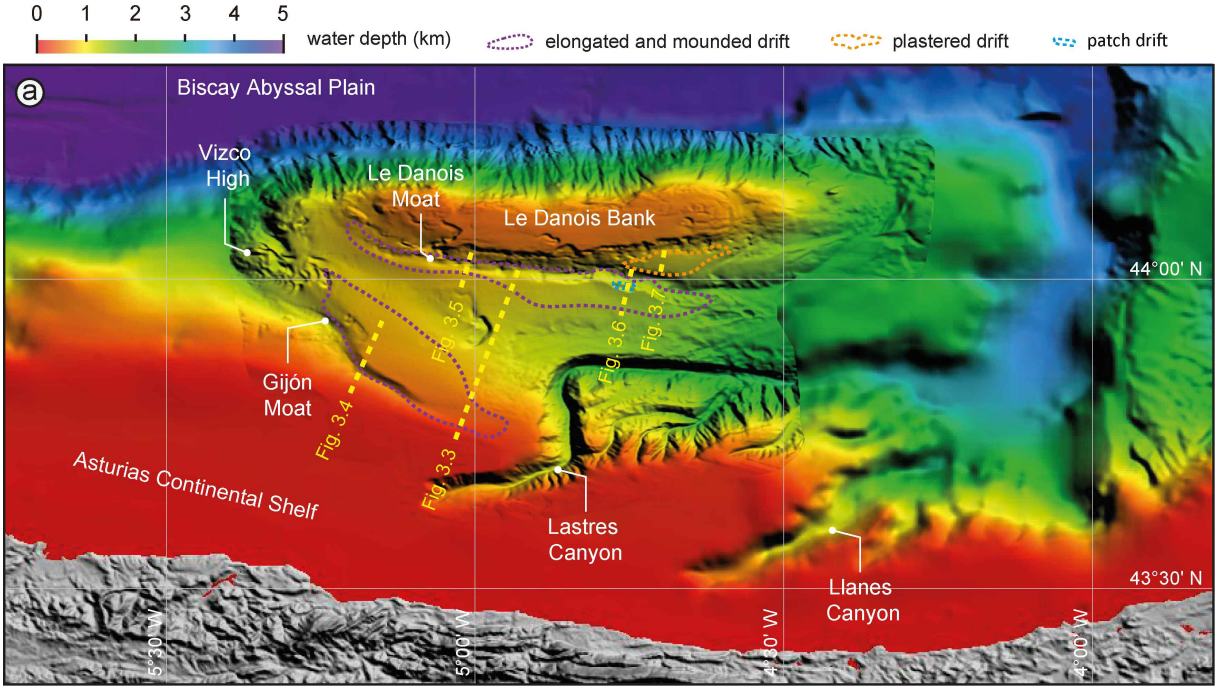

Figure 3.2: Map of the Le Danois Bank region with the indication of the morphological domains and identified contourite drifts (purple, orange and blue boxes). Locations of overlapping ParaSound, single-channel sparker and multi-channel airgun seismic profiles are shown.

Figure 3.3: Interpreted ParaSound (a), sparker (b) and airgun (c) seismic profiles showing the morphological and internal features of the Le Danois and Gijon Drifts. Variations in vertical resolution of seismic data are indicated by the scale of red boxes. The location of the overlapping seismic lines is indicated on the morphological map (Figure 3.2)

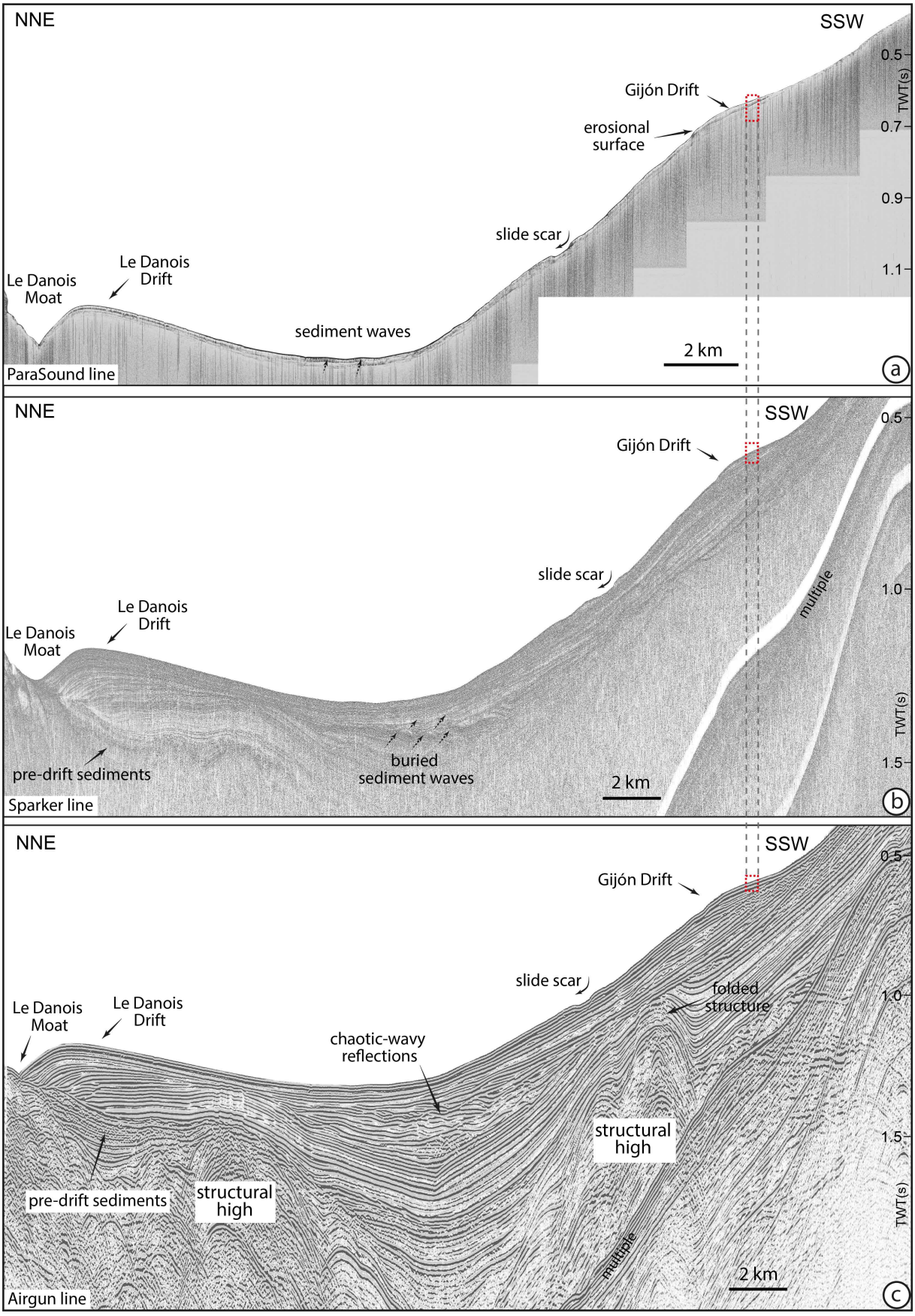
NNE
SSW
0.5
0.7
0.9
1.1
TWT(s)
Gijón Drift
erosional surface
slide scar
Le Danois Moat
Le Danois Drift
sediment waves
2 km
ParaSound line
a
NNE
SSW
0.5
1.0
1.5
TWT(s)
Gijón Drift
slide scar
multiple
Le Danois Moat
Le Danois Drift
pre-drift sediments
buried sediment waves
2 km
Sparker line
b
NNE
SSW
0.5
1.0
1.5
TWT(s)
Gijón Drift
slide scar
folded structure
Le Danois Moat
Le Danois Drift
chaotic-wavy reflections
structural high
pre-drift sediments
structural high
multiple
2 km
Airgun line
c

In the airgun seismic profiles, these contourite drifts migrate laterally in a downcurrent direction (Figure 3.2). Internally, widespread erosional unconformities, which show continuous high amplitude reflections, are presented at the base of and within contourite drifts (Figure 3.3). Major depositional units are separated by these discontinuities. Oblique onlap and downlap reflection configurations are displayed at the top and base of major units (Figures 3.4c, 3.5c, 3.6c, 3.7a). The major depositional units are characterized by moderate-high amplitude parallel reflectors and show a lenticular shape (Figure 3.4c). They display an upward convex geometry and an oblique stacking pattern, which reveals the sigmoidal progradation of contourite drifts (Figures 3.5c, 3.6c). Pre-drift sediments, which show high amplitude, chaotic-subparallel reflections and a sheeted geometry, are identified beneath the basal discontinuity of the Le Danois Drift (Figure 3.3c). They display a concave geometry (Figure 3.4c). Towards the north, pre-drift sediments are bounded by buried structural highs, which are characterized by high amplitude chaotic reflectors (Figures 3.3c, 3.4c).

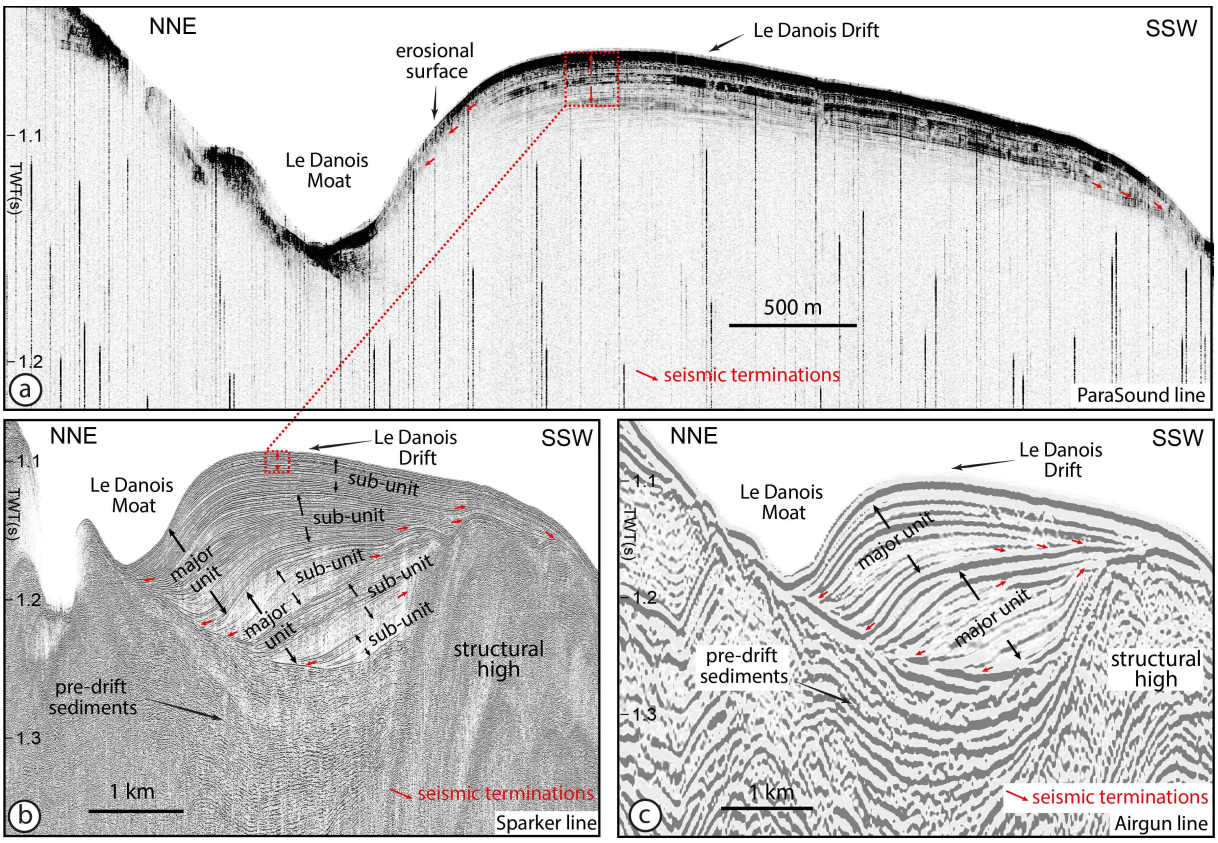

Figure 3.4: Interpreted ParaSound (a), sparker (b) and airgun (c) seismic profiles showing the morphological and internal features of the Le Danois Drift. Variations in vertical resolution of seismic data are indicated by the scale of red boxes. Onlap and downlap terminations (red arrows), major depositional units and sub-units are displayed. The location of the overlapping seismic lines is indicated on the morphological map (Figure 3.1).

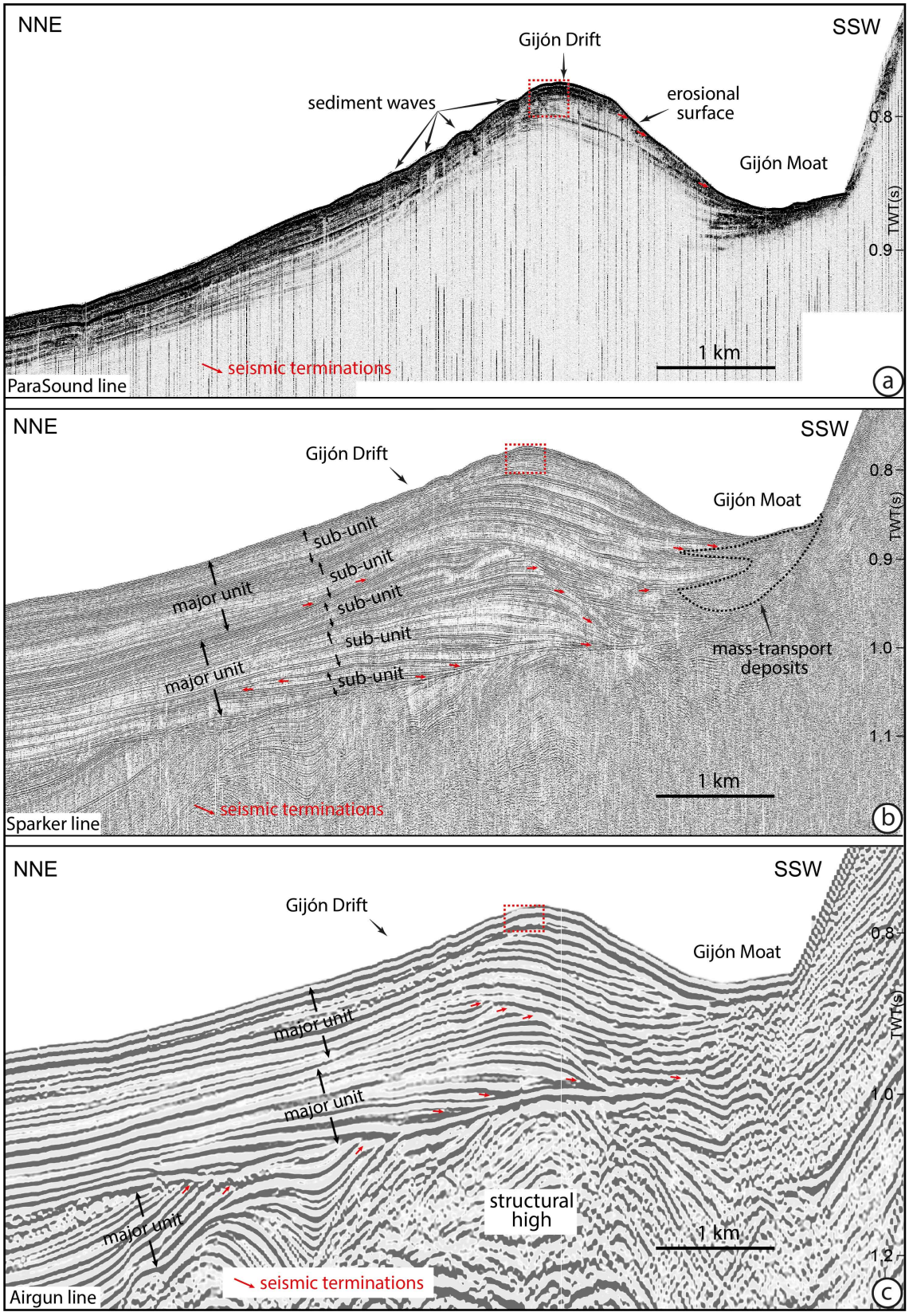

Figure 3.5: Interpreted ParaSound (a), sparker (b) and airgun (c) seismic profiles showing the morphological and internal features of the Gijon Drift. Variations in vertical resolution of seismic data are indicated by the scale of red boxes. Onlap and downlap terminations (red arrows), major depositional units and sub-units are displayed. The location of the overlapping seismic lines is indicated on the morphological map (Figure 3.2).

Broad lenticular and convex-upward sub-units are observed within the Le Danois and the Gijon Drifts in the single-channel sparker seismic profiles (Figures 3.4b, 3.5b). These sub-units are separated by moderate amplitude erosional discontinuities and show a sigmoidal progradation architecture (Figures 3.4b, 3.5b). Moderate-high amplitude, continuous subparallel reflections are presented within sub-units, while onlap and downlap reflections are observed toward their top and basal discontinuities (Figures 3.5b, 3.6b). In some sub-units of the Gijon Drift, stratified layers of continuous sigmoidal reflections interbed with discontinuous low-amplitude chaotic reflections (Figure 3.5b). Pre-drift sediments beneath the Le Danois Drift display high amplitude chaotic reflections (Figure 3.4b), which differs from the seismic facies shown in the multi-channel airgun seismic profiles (Figure 3.4c).

The Le Danois and the Gijon Drifts display moderate-high amplitude, horizontal to low-inclination reflections in the ParaSound seismic profiles (Figures 3.3a, 3.4a, 3.5a). At the seafloor of these elongated and mounded drifts, greater details, such as sediment waves with well-stratified wavy reflectors, slide scars with truncations, are displayed in the ParaSound seismic profiles (Figures 3.4a, 3.5a). At the flanks of the Le Danois and the Gijon Drifts, erosional surfaces with low-angle downlap reflection configurations are displayed (Figures 3.3a, 3.4a, 3.5a). Sigmoidal progradation patterns could only be observed in some ParaSound seismic profiles (Figure 3.5a). Whereas aggradation patterns are widely identified within the elongated and mounded drifts (Figures 3.3a, 3.4a).

Therefore, the identification of the seismic stratigraphy, pre-drift sediments and the external geometry of elongated and mounded drifts is suggested to use the multi-channel and single channel seismic lines. Whereas the ultra-high resolution ParaSound seismic data are preferable to study the associated surficial morphology of elongated and mounded drifts (Figures 3.3, 3.4. 3.5).

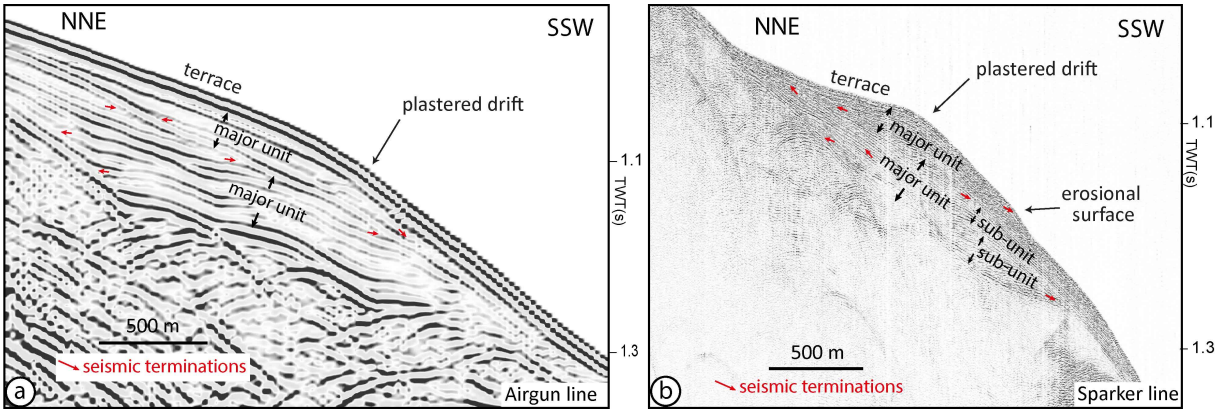

Figure 3.6: Interpreted airgun (a) and sparker (b) seismic profiles showing the morphological and internal features of a plastered drift. Onlap and downlap terminations (red arrows), major depositional units and sub-units are displayed. The location of the overlapping seismic lines is indicated on the morphological map (Figure 3.2).

3.3.2 Plastered drifts

Along the upper continental slope, a slight-mounded sedimentary body, plastered against the slope, is identified as a plastered drift (Figure 3.6). In the airgun seismic lines, the major depositional units show low-moderate amplitude parallel reflections. Low-angle onlap and downlap reflections are shown in major units, indicating slightly downcurrent progradation (Figure 3.6a). In the sparker seismic profiles, the plastered drift shows similar seismic

characteristics (Figure 3.6b). However, the drift displays a more clear terrace-like morphology, while convex-shaped sub-units with onlap and downlap reflections are shown within the drifts (Figure 3.6b). At the lower part of the plastered drift, an erosional surface is presented, which cannot be observed in the airgun seismic data. Hence, the single-channel sparker seismic data not only contain the stratigraphic details and internal structures, but also display the surficial morphology of the plastered drift (Figure 3.6b). This type of seismic reflection data is more suitable for the identification of the plastered drift.

3.3.3 Patch drift

At the southeast foot of the Le Danois Bank, a slide scar is identified (Figure 3.7). The associated slide deposits display a patch geometry and an internal structure with high-angle onlap and downlap terminations in the sparker seismic profiles (Figure 3.7b). The type of these sedimentary deposits is hardly to distinguish due to the limit resolution of seismic data. One possibility is that these features are related to mass-transport deposits. However, on the basis of the geometry and reflection terminations of these sedimentary deposits, the mounded sedimentary body is most likely a patch drift. The patch drift is relatively small and elongate in an alongslope (E-W trending) direction (Figures 3.2, 3,7b). It displays low-moderate amplitude, chaotic-subparallel seismic reflections (Figure 3.7b). The patch drift overlies on an acoustically chaotic-transparent part (Figure 3.7b). Sigmodal progradation patterns are observed within the patch drift in the single-channel sparker seismic profile (Figure 3.7b).

The patch drift shows low amplitude, semi-transparent to subparallel seismic reflections and a slightly mounded geometry in ParaSound seismic profiles (Figure 3.7a). It overlies on acoustically chaotic section and only low-angle onlap seismic reflections are presented (Figure 3.7a). The basal discontinuity of the drift could hardly be identified in the ParaSound seismic profiles (Figure 3.7a). As such, the single-channel sparker seismic data are suited better than others on the identification and a more comprehensive description of the patch drift.

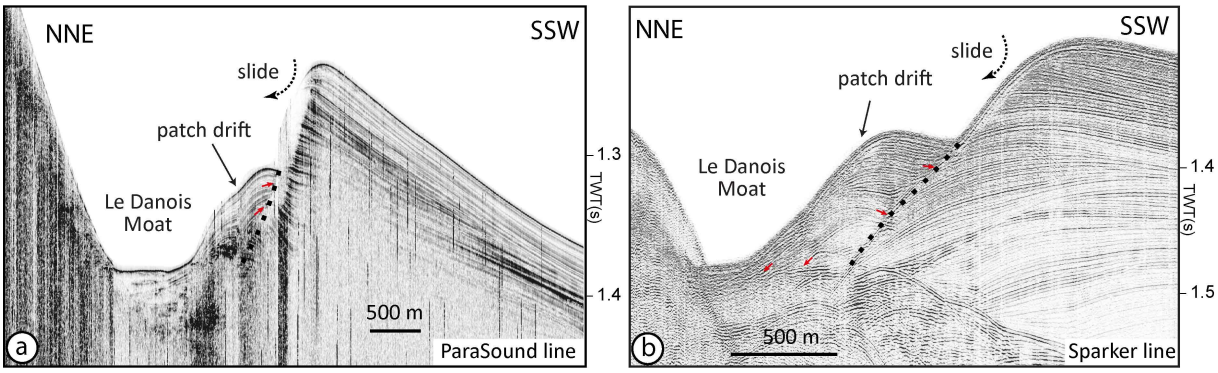

Figure 3.7: Interpreted ParaSound (a) and sparker (b) seismic profiles showing the morphological and internal features of a plastered drift. Onlap and downlap terminations (red arrows), major depositional units and sub-units are displayed. The location of the overlapping seismic lines is indicated on the morphological map (Figure 3.2).

3.3.4 Seismic expression of contourite-related features

In the single-channel sparker seismic profiles, a buried sediment wave field is identified between the Le Danois and the Gijon Drifts (Figure 3.3b). The key elements for the identification of these sediment waves are well-stratified wavy reflections (Figure 3.3b). However, these sediment

waves, showing less-stratified chaotic-wavy reflections, can hardly be identified in the multi-channel airgun seismic profiles (Figure 3.3c).

Depositional cycles, consisting of acoustically transparent lower parts and moderate-high amplitude stratified upper parts, are displayed in some sub-units of the Le Danois Drift in the single-channel sparker seismic lines (Figure 3.8). These depositional cycles are bounded by erosional discontinuities at the top and the base (Figure 3.8). The scale of depositional cycles is about 20 ms TWT in thickness in the sparker seismic data. However, no clear cyclic seismic features are to be observed in comparable units in the multi-channel airgun seismic profiles (Figure 3.8). Similar cyclic features are shown in the ParaSound seismic profiles (Figure 3.8). By comparing with the ones displayed in the single-channel sparker seismic profiles, cyclic features have a relatively smaller scale in the ParaSound seismic profiles. The average thickness of a single deposition cycle is about 10 ms TWT (Figure 3.8).

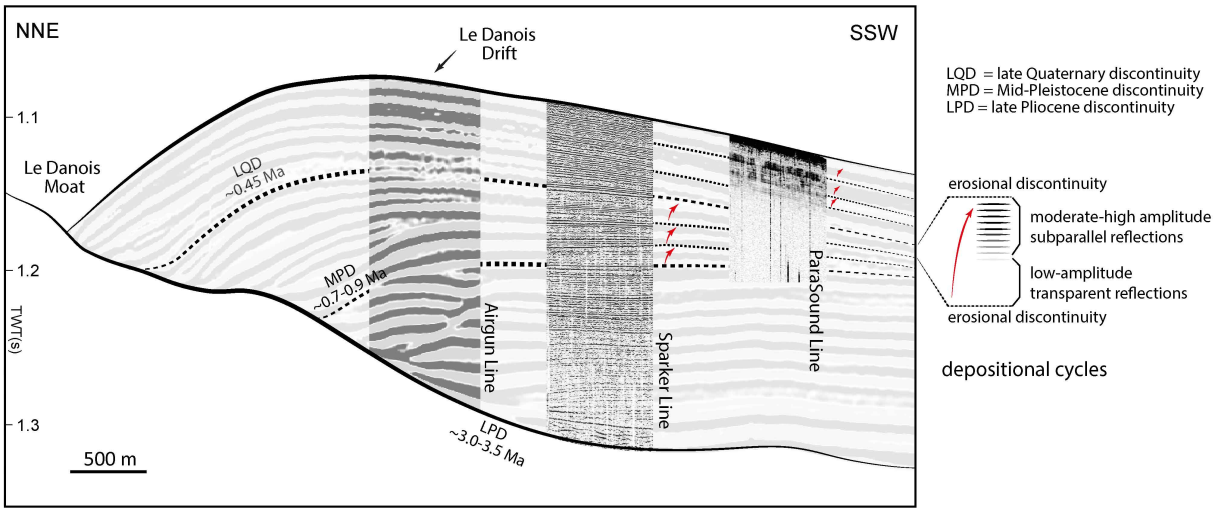

Figure 3.8: Cyclic variation in seismic facies of contourite drifts in the ParaSound, sparker and airgun seismic profiles. A depositional cycle contains a low-amplitude to transparent lower part, a moderate-high amplitude upper part and a top discontinuity. The seismic data are extracted from Figure 3.2 and the location is indicated on the morphological map (Figure 3.2).

3.4 Discussion

3.4.1 Seismic imaging of contourite drifts

The seismic imaging and the interpretation of large scale contourite features are commonly based on low resolution, high penetration seismic systems within a multichannel (MC) configuration (Michels et al., 2001; Chen et al., 2014; García et al., 2016). These systems use airguns, sleeve guns and water guns as seismic sources (frequency ranging from 10 to 100 Hz) and the penetration of the seismic signal are several kilometres (Faugères et al., 1999; Nielsen et al., 2008). In the study area, the 80 Hz airgun seismic profiles are used to examine large-scale seismic features of contourite drifts. High-mounded geometry, sigmoidal progradation patterns, downcurrent elongation and major depositional units with moderate-high amplitude reflections are the key large-scale elements to recognize elongated and mounded drifts (Figure 3.9). Whereas low-mounded geometry, slightly downcurrent progradation and major depositional units with low-moderate amplitude reflections are the large scale seismic features to identify plastered drifts.

Well-stratified layers of the major units indicate long-term stable depositional processes associated with bottom currents, which laterally and temporally favours the accumulation of the drifts (Stow et al., 2002). At the boundary of the depositional units, erosional discontinuities and the associated onlap and downlap reflectors (Figures 3.4c, 3.6a) point out an abrupt change in the strength of bottom currents (Llave et al., 2001, 2007). Contourite deposition ceases and is replaced by non-depositional/erosional processes, which are resulted from faster bottom currents (Nielsen et al., 2008). As such, large-scaled contourite features are generally linked to the enhancement or reduction of bottom currents.

Notably, beneath the elongated and mounded drifts, buried structural highs are presented in the airgun seismic profiles, indicating possible tectonic influences in the study area (Figures 3.3b, 3.9). Regional tectonics, such as uplift events and compressional restrictions can profoundly change the circulation pattern of bottom currents, in turn affecting the distribution and stacking patterns of contourite drifts (García et al., 2016; Gruetzner and Uenzelmann-Neben, 2016; Vandorpe et al., 2016; Capella et al., 2017). Therefore, large scale seismic features, such as acoustic variation of major depositional units and erosional discontinuities, can be used to examine the interaction between tectonic activities and bottom-current processes (Figure 3.9).

The moderate resolution, moderate penetration single-channel sparker (or boomer) seismic data, which have a frequency of about 0.1 to 3 kHz, are used to interpreted medium scale seismic features of contourite drifts (Nielsen et al., 2008). The penetration of the seismic signal commonly ranges from 100 m to 1 km (Faugères et al., 1999). Medium scale seismic features of contourite drifts are displayed on the 800 Hz sparker seismic profiles in the study area (Figures 3.2, 3.3, 3.4, 3.5). Sigmoidal progradation patterns and convex-upward sub-units with moderate-high amplitude parallel reflections are typical medium scale features for the seismic identification of elongated and mounded drifts (Figure 3.9). Whereas the plastered drift has progradation to aggradation patterns and the patch drift is characterized by a patch geometry and low-moderate amplitude, chaotic-subparallel seismic reflections (Figures 3.6b, 3.7b).

Seismic sub-units and the bounding discontinuities of contourite drifts indicate smaller and more frequent fluctuations in contourite depositional and erosional conditions (Figures 3.3a, 3.9). These variations can be related to short-term oceanographic conditions resulted from paleoclimatic changes (Laberg et al., 2005; Llave et al., 2007) (Figure 3.9). During glacial and interglacial climate intervals, variations of the freshwater input into the deep sea can result in vigorous or weak bottom currents (Rogerson et al., 2005; Voelker et al., 2006; Kaboth et al., 2016). Consequently, shifts between depositional and non-depositional/erosional processes can be displayed by medium scale seismic features of contourite drifts (Llave et al., 2007). Eustatic sealevel changes can significantly influence the properties of water masses, as well as the stacking pattern of contourite drifts (Brackenridge et al., 2011). During sea-level lowstand/highstand conditions, changes in the sediment supply and the regime of bottom currents can result in erosional unconformities, which separate seismic sub-units of contourite drifts (Brackenridge et al., 2011). As such, moderate seismic features can display the influence of paleoclimatic and eustatic changes on the evolution of contourite drifts (Figure 3.9).

Small scale seismic features of contourite drifts can be better revealed by the (ultra-) high resolution, low penetration echosounder seismic systems, using hull-mounted sub-bottom profilers or parametric echosounders (such as TOPAS and ParaSound) (Faugères et al., 1999; Nielsen et al., 2008). The frequency of these seismic systems is about 3.5-24 k kHz and the penetration of the seismic signal ranges from a few metres to tens of metres (Faugères et al., 1999).

In the study area, the surficial morphology of contourite drifts is presented by different-resolution seismic data (Figure 3.3). However, the scale and the shape of these features are better addressed by the 18 kHz ParaSound seismic profiles (Figures 3.3a, 3.4a, 3.5a). The slide scar at the surface of the Gijon Drift show sub-recent slope instability in the southern part of the Le Danois Bank intraslope basin (Figure 3.3a). Sediment waves associated with the Le Danois and the Gijon Drifts are related to bottom currents or internal waves (Figure 3.3a). Erosion surfaces of contourite drifts are resulted from sub-recent erosion of bottom currents (Figures 3.4a, 3.5a). As such, small scale features of contourite drifts can be related to sub-recent downslope, alongslope, oceanographic processes and their interactions (Figure 3.9).

Interestingly, pre-drift sediments beneath the Le Danois Drift display subparallel reflections and have a sheeted geometry in the airgun seismic profiles (Figures 3.3c, 3.4c), which can be interpreted as a sheeted drift (Stow et al., 2002; Rebesco et al., 2014). Whereas in the sparker seismic profiles, these sedimentation patterns display discontinuous chaotic reflections (Figures 3.3b, 3.4b), which resemble seismic features of the gravitational deposits (Mulder and Cochonat, 1996). Buried sediment waves between the Le Danois and the Gijon Drifts namely show well-stratified wavy and less-stratified chaotic-wavy reflections in the sparker (Figure 3.3b) and the airgun (Figure 3.3c) seismic profiles. As such, the seismic interpretation of contourite-related features should be cautious and multi-scaled seismic imaging of contourite drifts are suggested to exam their external geometry, internal and surficial features.

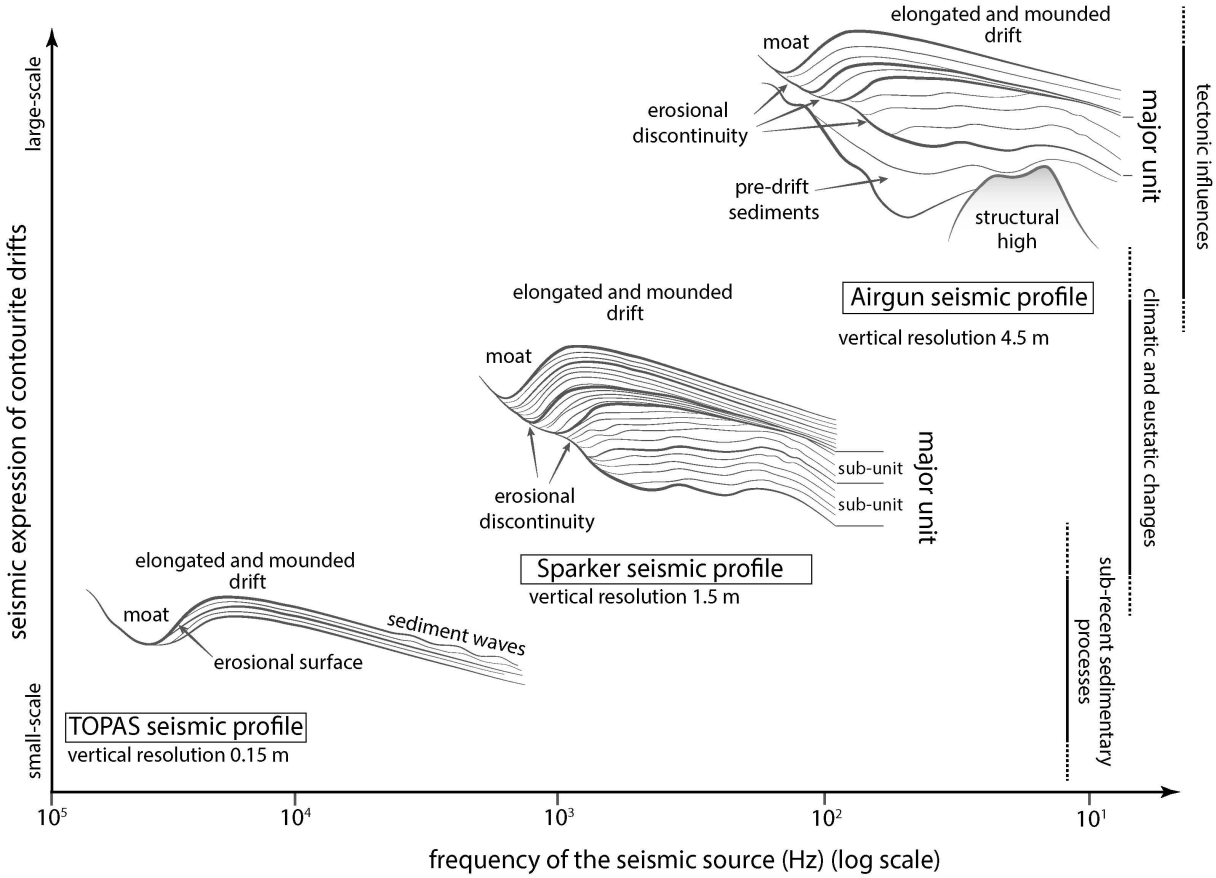

Figure 3.9: A sketch showing the relationship between seismic data, seismic expression of contourite drifts and long-/short- term tectonic, climatic, eustatic, sedimentary variations.

3.4.2 Cyclic variation of contourite drifts

Cyclic patterns within the Le Danois Drift, although registered at different scales, all display similar depositional patterns in different seismic datasets (Figure 3.7). The transparent lower parts represent muddy contourite sections, whereas moderate-high amplitude stratified upper parts represent silt/sand contourite sections (Llave et al., 2001; 2007; Stow et al., 2002; Hernández-Molina et al., 2016). In the airgun seismic data, no depositional cycles are observed in major seismic units. I n the sparker seismic profiles, depositional cycles are identified in the seismic sub-units (Figure 3.7). Whereas in the ParaSound seismic data, two depositional cycles belonging to the same sub-unit which is shown in the sparker seismic profile, indicating different durations of the cyclicity in multi-resolution seismic data (Figure 3.7).

The cyclic variation of sedimentary sequences is generally linked to short-/long- Earth-system processes (Catuneanu et al., 2009). In some contourite drifts, longer frequency cyclicities (2.5 - 0.4Ma), resulted from tectonic compressive-flexural stress, can be displayed by multi-channel seismic profiles (Hernández-Molina et al., 2016). Whereas moderate-high resolution seismic data show smaller-scaled cyclicities, which are related to climatic (orbital) or Milankovitch/sea-level cycles (Llave et al., 2001; Mestdagh et al., 2019). Therefore, longer frequency cycles of contourite drifts can be indicated by the low resolution, high penetration seismic systems. The moderate-high resolution, low-moderate penetration seismic data can be used to display shorter frequency cycles of contourite drifts.

3.5 Conclusion

The multi-resolution seismic imaging is used as the strategy to identify contourite drifts in different scales. These different datasets enable a more detailed seismic interpretation of the encountered morphological features. Multi-channel “low-resolution/low frequency” seismic data are suitable to document the external mounded geometry and the overall seismic stratigraphy of contourite drifts. Single-channel “medium-resolution/medium frequency” seismic profiles are preferable for the recognition of stratigraphic details, progradation/aggradation patterns and reflection terminations of contourite drifts. “High-resolution/high frequency” hull-mounted (parametric) echosounder seismic data better document the wavy-like surficial morphology of contourite drifts. These different-scaled features of contourite drifts are linked to different-term Earth-system processes, such as long-term tectonic activities, short-term paleo-climate/oceanographic variations and sub-recent sedimentary processes.

The multi-scale seismic imaging records the cyclic variation of contourite drifts. These depositional cycles, although have different scales in the different seismic data, display similar seismic patterns. Longer frequency depositional cycles, which may be documented by the airgun seismic profiles, can be resulted from tectonic compressive-flexural stress. Shorter frequency depositional cycles, which are well recorded by the sparker and the ParaSound seismic profiles may be linked to climatic or Milankovitch/sea-level cycles.

Different types of seismic profiles contain multi-scaled geological information due to the penetration of the seismic signal. The geometry of buried structural highs is better documented by multi-channel seismic data, indicating long-term basin-scale tectonic activities. Instead of deeper tectonic structures, cyclic depositional features are well illustrated by single-channel seismic profiles. These features can be linked to short-term oceanographic and climate variations.

Sub-bottom profiler documents detailed morphological features, which are generally related to present-day sedimentary processes. As such, multi-channel seismic data are suggested for the first stage of the interpretation of contourite features. The resulted tectonic background of the basin or the margin can further help for next interpretation stages which use seismic data with higher resolutions. This strategy can provide a better understanding of the evolution of contourite depositional systems. Therefore, future contourite studies can take the advantage of different types of the seismic reflection data to investigate the seismic expression of contourite drifts. In order to correlate related sedimentary processes from the past to the present day, full-scaled seismic imaging of contourite drifts is recommended as well.

Acknowledgements

This study was carried out within the framework of a Chinese Scholarship Council "CSC Grant" (201506410062). This study built on achievements of project ESF Euromargins MOUNDFORCE, EC FP5 RTN EURODOM and EC FP6 HERMES 626 (GOCE-CT-2005-511234-1). The research cruises namely framed within the ECOMARG (REN2002-624 00916/MAR) and MARCONI (REN2001-1734 C03-01/M) projects. Shiptime RV Belgica was provided by BELSPO and RBINS–OD Nature. This study was conducted in collaboration with "The Drifters Research Group" of the Royal Holloway University of London (UK) and it is related to the projects CTM 2012-39599-C03, CGL2016-80445-R, and CTM2016-75129-C3-1-R (REN2001-1734 C03-01/M). It was also carried out in collaboration with the Continental Margins Group-GMC from ICM-CSIC (Spain) and its related Spanish projects (CTM2008-06399-C04-04/MAR; CTM2012-39599-CO3-O3; CMT2015-65461-C2-R (MINEICO/FEDER).

References

Brackenridge, R., Stow, D.A.V., Hernández-Molina, F.J., 2011. Contourites within a deep-water sequence stratigraphic framework. Geo-Marine Letters 31, 343-360.

Brackenridge, R.E., Hernández-Molina, F.J., Stow, D.A.V., Llave, E., 2013. A Pliocene mixed contourite–turbidite system offshore the Algarve Margin, Gulf of Cadiz: Seismic response, margin evolution and reservoir implications (Cadiz). Marine and Petroleum Geology 46, 36-50.

Cadenas, P., Fernández-Viejo, G., 2017. The Asturian Basin within the North Iberian margin (Bay of Biscay): seismic characterisation of its geometry and its Mesozoic and Cenozoic cover. Basin Research 29, 521-541.

Capella, W., Hernández-Molina, F.J., Flecker, R., Hilgen, F.J., Hssain, M., Kouwenhoven, T.J., van Oorschot, M., Sierro, F.J., Stow, D.A.V., Trabucho-Alexandre, J., Tulbure, M.A., de Weger, W., Yousfi, M.Z., Krijgsman, W., 2017. Sandy contourite drift in the late Miocene Rifian Corridor (Morocco): Reconstruction of depositional environments in a foreland-basin seaway. Sedimentary Geology 355, 31-57.

Catuneanu, O., Abreu, V., Bhattacharya, J.P., Blum, M.D., Dalrymple, R.W., Eriksson, P.G., Fielding, C.R., Fisher, W.L., Galloway, W.E., Gibling, M.R., Giles, K.A., Holbrook, J.M., Jordan, R., Kendall, C.G.S.C., Macurda, B., Martinsen, O.J., Miall, A.D., Neal, J.E., Nummedal, D., Pomar, L., Posamentier, H.W., Pratt, B.R., Sarg, J.F., Shanley, K.W., Steel, R.J., Strasser, A., Tucker, M.E., Winker, C., 2009. Towards the standardization of sequence stratigraphy. Earth-Science Reviews 92, 1-33.

Chen, H., Xie, X., Van Rooij, D., Vandorpe, T., Su, M., Wang, D., 2014. Depositional characteristics and processes of alongslope currents related to a seamount on the northwestern margin of the Northwest Sub-Basin, South China Sea. Marine Geology 355, 36-53.

Correggiari, A., Trincardi, F., Langone, L., Roveri, M., 2001. Styles of Failure in Late Holocene Highstand Prodelta Wedges on the Adriatic Shelf. Journal of Sedimentary research 71, 218-236.

Faugères, J.-C., Imbert, P., Mézerais, M.L., Cremer, M., 1998. Seismic patterns of a muddy contourite fan (Vema Channel, South Brazilian Basin) and a sandy distal turbidite deep-sea fan (Cap Ferret system, Bay of Biscay): a comparison. Sedimentary Geology 115, 81-110.

Faugères, J.-C., Stow, D.A.V., Imbert, P., Viana, A., 1999. Seismic features diagnostic of contourite drifts. Marine Geology 162, 1-38.

García, M., Hernández-Molina, F.J., Alonso, B., Vázquez, J.T., Ercilla, G., Llave, E., Casas, D., 2016. Erosive sub-circular depressions on the Guadalquivir Bank (Gulf of Cadiz): Interaction between bottom current, mass-wasting and tectonic processes. Marine Geology 378, 5-19.

Gruetzner, J., Uenzelmann-Neben, G., 2016. Contourite drifts as indicators of Cenozoic bottom water intensity in the eastern Agulhas Ridge area, South Atlantic. Marine Geology 378, 350-360.

Heezen, B.C., Hollister, C.D., Ruddiman, W.F., 1966. Shaping of the Continental Rise by Deep Geostrophic Contour Currents. Science 152, 502.

Hernández-Molina, F.J., Llave, E., Stow, D.A.V., García, M., Somoza, L., Vázquez, J.T., Lobo, F.J., Maestro, A., Díaz del Río, V., León, R., Medialdea, T., Gardner, J., 2006. The contourite depositional system of the Gulf of Cádiz: A sedimentary model related to the bottom current activity of the Mediterranean outflow water and its interaction with the continental margin. Deep Sea Research Part II: Topical Studies in Oceanography 53, 1420-1463.

Hernández-Molina, F.J., Sierro, F.J., Llave, E., Roque, C., Stow, D.A.V., Williams, T., Lofi, J., Van der Schee, M., Arnáiz, A., Ledesma, S., Rosales, C., Rodríguez-Tovar, F.J., Pardo-Igúzquiza, E., Brackenridge, R.E., 2016. Evolution of the gulf of Cadiz margin and southwest Portugal contourite depositional system: Tectonic, sedimentary and paleoceanographic implications from IODP expedition 339. Marine Geology 377, 7-39.

Howe, J.A., Stoker, M.S., Stow, D.A.V., Akhurst, M.C., 2002. Sediment drifts and contourite sedimentation in the northeastern Rockall Trough and Faroe-Shetland Channel, North Atlantic Ocean. Geological Society, London, Memoirs 22, 65-72.

Kaboth, S., Bahr, A., Reichart, G.-J., Jacobs, B., Lourens, L.J., 2016. New insights into upper MOW variability over the last 150 kyr from IODP 339 Site U1386 in the Gulf of Cadiz. Marine Geology 377, 136-145.

Khélifi, N., Sarnthein, M., Frank, M., Andersen, N., Garbe-Schönberg, D., 2014. Late Pliocene variations of the Mediterranean outflow. Marine Geology 357, 182-194.

Laberg, J.S., Camerlenghi, A., 2008. Chapter 25 The Significance of Contourites for Submarine Slope Stability, in: Rebesco, M., Camerlenghi, A. (Eds.), Developments in Sedimentology. Elsevier, pp. 537-556.

Laberg, J.S., Stoker, M.S., Dahlgren, K.I.T., Haas, H.d., Haflidason, H., Hjelstuen, B.O., Nielsen, T., Shannon, P.M., Vorren, T.O., van Weering, T.C.E., Ceramicola, S., 2005. Cenozoic alongslope processes and sedimentation on the NW European Atlantic margin. Marine and Petroleum Geology 22, 1069-1088.

Llave, E., Hernandez-Molina, F.J., Somoza, L., Diaz-del Rio, V., Stow, D.A.V., Maestro, A., Alveirinho Dias, J.M., 2001. Seismic stacking pattern of the Faro-Albufeira contourite system (Gulf of Cadiz): a Quaternary record of paleoceanographic and tectonic influences. Marine Geophysical Researches 22, 487-508.

Llave, E., Hernández-Molina, F.J., Stow, D.A.V., Fernández-Puga, M.C., García, M., Vázquez, J.T., Maestro, A., Somoza, L., Díaz del Río, V., 2007. Reconstructions of the Mediterranean Outflow Water during the quaternary based on the study of changes in buried mounded drift stacking pattern in the Gulf of Cadiz. Marine Geophysical Researches 28, 379-394.

Maldonado, A., Barnolas, A., Bohoyo, F., Escutia, C., Galindo-Zaldívar, J., Hernández-Molina, J., Jabaloy, A., Lobo, F.J., Nelson, C.H., Rodríguez-Fernández, J., Somoza, L., Vázquez, J.-T., 2005. Miocene to Recent

contourite drifts development in the northern Weddell Sea. Global and Planetary Change 45, 99-129.

Mestdagh, T., Lobo, F.J., Llave, E., Hernández-Molina, F.J., Van Rooij, D., 2019. Review of the late Quaternary stratigraphy of the northern Gulf of Cadiz continental margin: New insights into controlling factors and global implications. Earth-Science Reviews 198, 102944.

Michels, K.H., Rogenhagen, J., Kuhn, G., 2001. Recognition of contour-current influence in mixed contourite-turbidite sequences of the western Weddell Sea, Antarctica. Marine Geophysical Researches 22, 465-485.

Miramontes, E., Cattaneo, A., Jouet, G., Théreau, E., Thomas, Y., Rovere, M., Cauquil, E., Trincardi, F., 2016. The Pianosa Contourite Depositional System (Northern Tyrrhenian Sea): Drift morphology and Plio-Quaternary stratigraphic evolution. Marine Geology 378, 20-42.

Mulder, T., Cochonat, P., 1996. Classification of offshore mass movements. Journal of Sedimentary research 66, 43-57.

Nielsen, T., Knutz, P.C., Kuijpers, A., 2008. Chapter 16 Seismic Expression of Contourite Depositional Systems, in: Rebesco, M., Camerlenghi, A. (Eds.), Developments in Sedimentology. Elsevier, pp. 301-321.

Preu, B., Hernández-Molina, F.J., Violante, R., Piola, A.R., Paterlini, C.M., Schwenk, T., Voigt, I., Krastel, S., Spiess, V., 2013. Morphosedimentary and hydrographic features of the northern Argentine margin: The interplay between erosive, depositional and gravitational processes and its conceptual implications. Deep Sea Research Part I: Oceanographic Research Papers 75, 157-174.

Rebesco, M., Hernández-Molina, F.J., Van Rooij, D., Wåhlin, A., 2014. Contourites and associated sediments controlled by deep-water circulation processes: State-of-the-art and future considerations. Marine Geology 352, 111-154.

Reynolds, J.M., 2011. An introduction to applied and environmental geophysics, 2nd edition. Wiley-Blackwell, West Sussex.

Ribó, M., Puig, P., Muñoz, A., Lo Iacono, C., Masqué, P., Palanques, A., Acosta, J., Guillén, J., Gómez Ballesteros, M., 2016. Morphobathymetric analysis of the large fine-grained sediment waves over the Gulf of Valencia continental slope (NW Mediterranean). Geomorphology 253, 22-37.

Rogerson, M., Rohling, E.J., Weaver, P.P.E., Murray, J.W., 2005. Glacial to interglacial changes in the settling depth of the Mediterranean Outflow plume. Paleoceanography 20, PA3007.

Schlüter, P., Uenzelmann-Neben, G., 2008. Indications for bottom current activity since Eocene times: The climate and ocean gateway archive of the Transkei Basin, South Africa. Global and Planetary Change 60, 416-428.

Stow, D.A.V., Faugères, J.-C., Howe, J.A., Pudsey, C.J., Viana, A.R., 2002. Bottom currents, contourites and deep-sea sediment drifts: current state-of-the-art. Geological Society, London, Memoirs 22, 7-20.

Sultan, N., Cochonat, P., Canals, M., Cattaneo, A., Dennielou, B., Haflidason, H., Laberg, J.S., Long, D., Mienert, J., Trincardi, F., Urgeles, R., Vorren, T.O., Wilson, C., 2004. Triggering mechanisms of slope instability processes and sediment failures on continental margins: a geotechnical approach. Marine Geology 213, 291-321.

Vandorpe, T., Martins, I., Vitorino, J., Hebbeln, D., García, M., Van Rooij, D., 2016. Bottom currents and their influence on the sedimentation pattern in the El Arraiche mud volcano province, southern Gulf of Cadiz. Marine Geology 378, 114-126.

Viana, A.R., 2008. Chapter 23 Economic Relevance of Contourites, in: Rebesco, M., Camerlenghi, A. (Eds.), Developments in Sedimentology. Elsevier, pp. 491-510.

Viana, A.R., Almeida, W., Jr., Nunes, M.C.V., Bulhões, E.M., 2007. The economic importance of contourites, in: Viana, A.R., Rebesco, M. (Eds.), Economic and Palaeoceanographic Significance of Contourite Deposits. Geological Society of London, p. 0.

Voelker, A.H.L., Lebreiro, S.M., Schönfeld, J., Cacho, I., Erlenkeuser, H., Abrantes, F., 2006. Mediterranean outflow strengthening during northern hemisphere coolings: A salt source for the glacial Atlantic? Earth and Planetary Science Letters 245, 39-55.

Chapter 4

Morphological features and associated bottom-current dynamics in the Le Danois Bank region (southern Bay of Biscay, NE Atlantic): a model in a topographically constrained small basin

---

The chapter has been slightly modified from the published version:

Liu, S., Van Rooij, D., Vandorpe, T., González-Pola, C., Ercilla, G., Hernández-Molina, F.J., 2019. Morphological features and associated bottom-current dynamics in the Le Danois Bank region (southern Bay of Biscay, NE Atlantic): A model in a topographically constrained small basin. *Deep Sea Research Part I: Oceanographic Research Papers*, 149, 103054.

Abstract: The present-day morphology of the Le Danois Bank region has been investigated based on bathymetric and high to ultra-high resolution seismic reflection data. The involved bottom-current processes are associated with the Eastern North Atlantic Central Water, the Atlantic Mediterranean Water and the Labrador Sea Water. Sediments originating from various canyon systems along the Cantabrian Margin and the Asturias continental shelf are transported by downslope and alongslope processes towards the Le Danois intraslope basin. The background flow velocities of bottom currents are all below the threshold (8-10 cm/s) of generating plastered and mounded geometries of contourite drifts. However, bottom currents are locally accelerated (up to 25 cm/s) due to the presence of the Le Danois Bank and the Vizco High, creating six plastered drifts, three elongated mounded and separated drifts, a furrow and three moats at different depth intervals. The extension and distribution of the drifts are controlled by slope morphology and/or bottom current velocities. Unlike contourite drifts along other continental slopes, a single contourite drift (the Gijón Drift) with a lateral variation in drift geometry and internal structure indicates the interaction of bottom currents with different flow dynamics. Additionally, scouring of active bottom currents and rapid sedimentation rate of contourite drifts may be at the origin of slope instability events. Besides contourite drifts, internal waves may have induced the formation of sediment waves. In the Le Danois intraslope basin, multiple sedimentary processes work together and shape the present-day seafloor. Bottom currents are focused due to

deflection on complex topographical obstacles within a relatively small basin setting, and create a wide variety of sedimentary features, including contourite drifts. The resulting sedimentary features thus have more frequent lateral variations, a feature typical for topographically constrained small basins.

Keywords: bottom currents; contourites; southern Bay of Biscay; small basin.

Author contributions: All the authors are involved in writing this article. The seismic reflection data was processed and interpreted by Liu S.. Van Rooij, D., Vandorpe, T. and Ercilla, G. took part in the acquisition of the seismic reflection data. Vandorpe, T. and Ercilla, G.. was involved in the processing of the data as well. The physical oceanographic data were provided and explained by González-Pola, C..

4.1 Introduction

In the NE Atlantic, at the intermediate site of the AMW (Atlantic Mediterranean Water), contourite features are observed in the Le Danois Bank region (Van Rooij et al., 2010). Its location is key for better understanding the local interaction of the AMW with the continental slope. Due to the presence of the Le Danois Bank, the study area is also ideal for investigating the relationship between topographic obstacles, bottom current dynamics, and different contourite features.

This study aims to provide a comprehensive description of the distribution and current morphology of various depositional and erosional features of the Le Danois Bank region. By combining previous observations with additional ones derived from more recent seismic datasets and improved insights regarding the present-day oceanographic setting, this study aims to improve the understanding of the recent interaction between topographic obstacles and bottom currents. As such, this study introduces a unique model related to the responsible bottom-current dynamics in a topographically constrained small basin.

4.2 Regional setting

4.2.1 Geology and morphology

The Le Danois Bank, an E-W narrow topographic high, is located at the Cantabrian continental slope, in the southern Bay of Biscay (Figure 2.1). The northern flank (mean slope values between 18° and 20°, reaching 34° locally) of the Le Danois Bank steeply drops into the Biscay abyssal plain, whereas the southern flank (slope gradient varying from 0.8° to 15°) is connected to the upper continental slope (Figures 4.1, 4.2). The presence of the Le Danois Bank creates an intraslope basin (about 65 km long and 15-25 km wide) between the bank and the Asturias continental shelf. This basin is bounded to the west by the Vizco High and to the southeast by the Lastres Canyon (Figure 2.1b). The basin becomes shallower from the centre (1070 m) towards the bank (855 m) and the continental shelf (443 m).

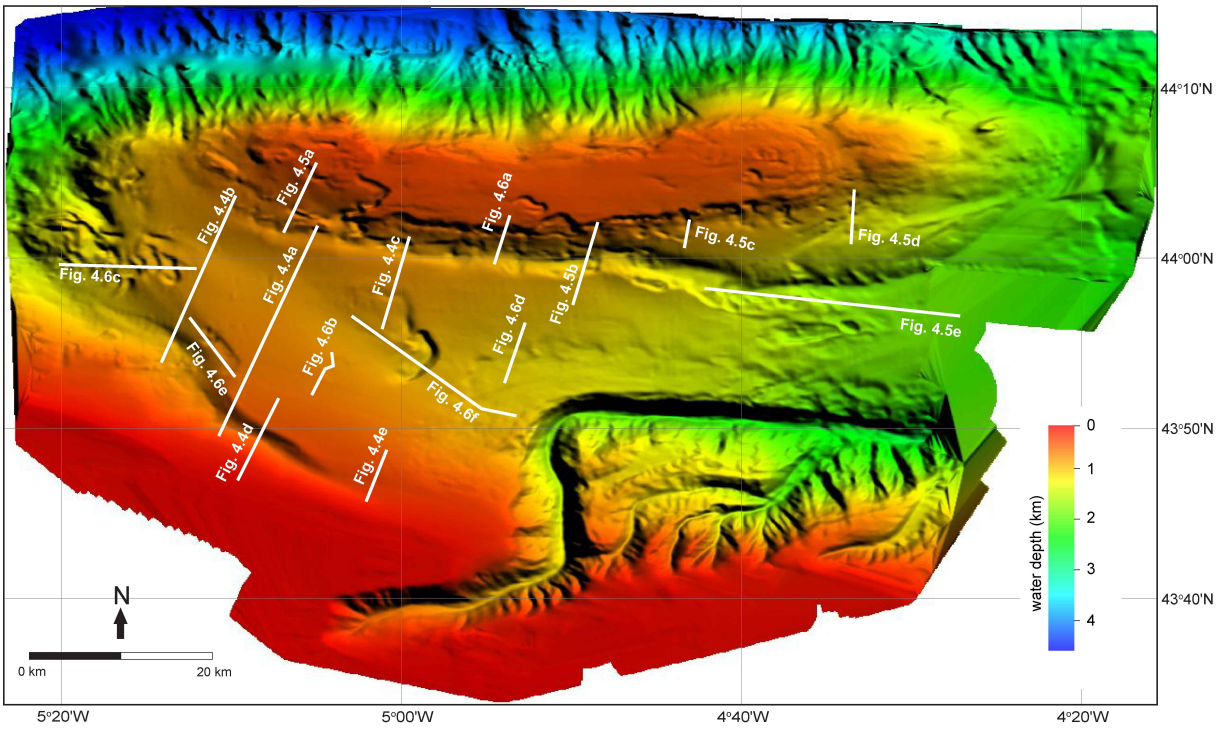

Figure 4.1: Multibeam bathymetry map of the study area, with the location of displayed seismic profiles.

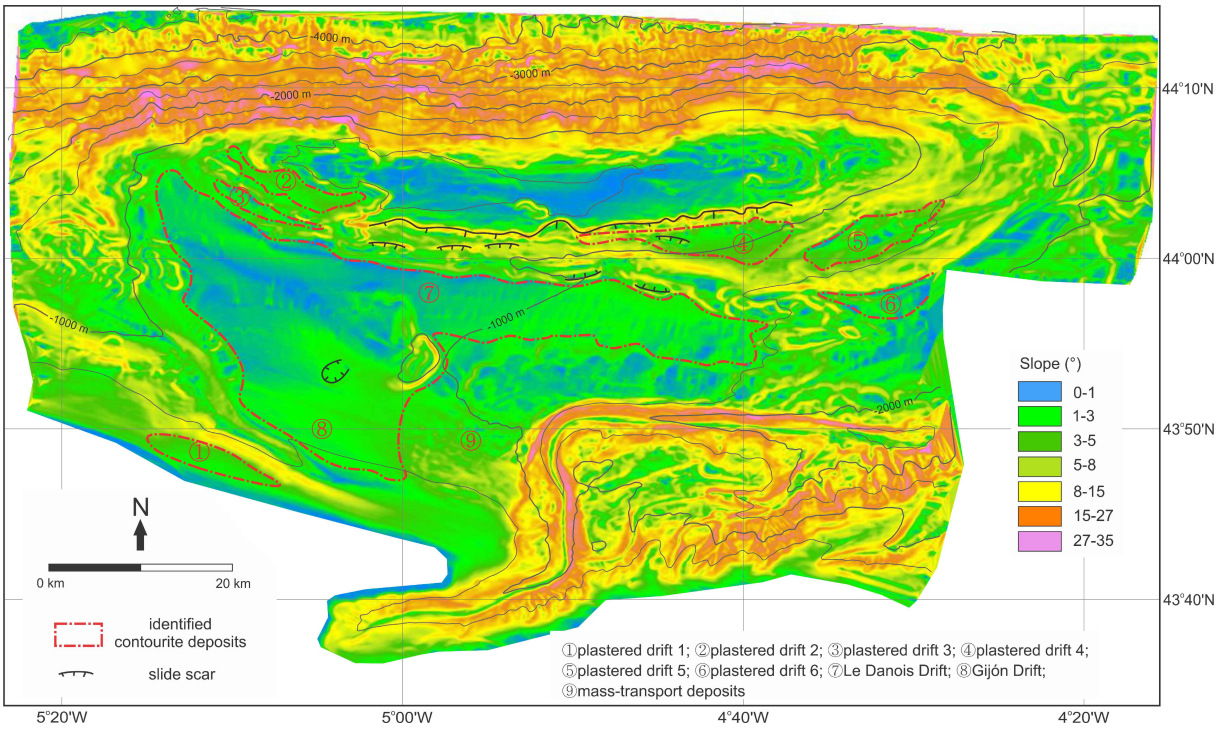

Figure 4.2: Slope map (in degrees) of the study area. The identified contourite deposits (outlined in red) and slide scars are indicated.

The Cantabrian margin was deformed by compression during the Early Paleocene to the Eocene when the northward displacement of the African plate led to the Iberian-European collision, resulting in the Cantabrian-Pyrenean chain along the northern border of the Iberian plate (Boillot

et al., 1979; Alvarez-Marrón et al., 1996). In the Early Oligocene, the subduction of the Iberian plate beneath the European plate, as well as shortening of the northern Iberia plate, resulted in regional compression in the Bay of Biscay (Fernández-Lozano et al., 2011). The subsequent mantle exhumation and crustal thinning beneath the Cantabrian continental margin induced the formation of the Le Danois Bank and the intraslope basin (Vissers and Meijer, 2012; Cadenas and Fernandez-Viejo, 2016). At the end of the Oligocene, the collision of the Iberian and European plates halted and there is no evidence of large-scale tectonic activity in the Le Danois Bank region from the Miocene onwards (Muñoz, 2002; Vergés et al., 2002; Roca et al., 2011; Tugend et al., 2014; Cadenas and Fernandez-Viejo, 2016).

The contourite deposits (drifts) are observed in the Pliocene unit (Van Rooij et al., 2010). Confined contourite drifts have been identified in the Upper Pliocene unit and the elongated mounded and separated drifts are generated in the Middle Pleistocene unit (Van Rooij et al., 2010). The sediment supply consists of fine-grained material eroded from the Cantabrian Mountain range (Gaudin et al., 2006; Ercilla et al., 2008). Gómez-Ballesteros et al. (2014) suggested that the sediments are transported into the ocean through the Narcea and Nalón rivers (Figure 2.1a) and move along the Cantabrian continental slope eastwards by means of alongslope currents.

4.2.2 Oceanography

At present, three water masses are found below the surface mixed layer in the Le Danois Bank region: (1) The Eastern North Atlantic Central Water (ENACW) between 350 and 600 m water depth (McCartney and Mauritzen, 2001), (2) the Atlantic Mediterranean Water (AMW) between 750 and 1550 m water depth (Iorga and Lozier, 1999a, b), and (3) the Labrador Sea Water (LSW) between 1750 and 2000 m water depth (van Aken, 2000a). Between these water masses, two interfaces are located respectively at 600 to 750 m and 1550 to 1750 m water depth (van Aken, 2000a, b) (Figure 2.3).

The ENACW originates at the northeast of the Azores (Pollard et al., 1996). Its subpolar branch penetrates southwards into the Bay of Biscay following an anticyclonic circulation (Pingree, 1993; Pollard et al., 1996; McCartney and Mauritzen, 2001). Its subtropical branch constitutes an eastward slope current along the northern Iberian continental slope and flows polewards (Pingree and Le Cann, 1990; van Aken, 2000b). The ENACW contains relatively small variations in temperature and salinity in the Bay of Biscay, ranging respectively between 11.8° to 12.2 °C and 35.53 to 35.58 (Haynes and Barton, 1990; Ríos et al., 1992; Pingree, 1993). The mean velocity is around 1 cm/s in the southern Bay of Biscay (Frouin et al., 1990; Lavín et al., 2006). In the Le Danois Bank region, the ENACW has a higher velocity (10-30 cm/s) and flows eastwards along the Asturias continental upper slope (Lavín et al., 2006; González-Pola et al., 2012). Along the rim of the eastern summit of the Le Danois Bank, an anticyclonic circulation with a velocity of about 15 cm/s has been observed at the ENACW depth range (González-Pola et al., 2012) (Figure 2.1b). This circulation cell is most likely induced by a steady background flow impinging on the topographical barrier or interaction between periodically enhanced currents and the Le Danois Bank (González-Pola et al., 2012). Its core is located at 400 m water depth with a minimum salinity of 35.5 (Figure 2.3).

At a depth of about 1000 m, a core of eastward-flowing AMW is observed hugging the northern Iberian continental slope with a mean velocity of 1-5 cm/s (Iorga and Lozier, 1999a). In the Le Danois Bank region, its maximum salinity reaches 35.8 while the temperature remains about 10°C

(Figure 2.4b). Most of the AMW flow penetrates along the northern flank of the Le Danois Bank and there is no dominant flow within the intraslope basin at present day (González-Pola, personal communication). The intraslope basin has the capability to develop its own recirculation pattern, due to the topographic constraints of the Le Danois Bank and the continental shelf (González-Pola et al., 2012). Anticyclonic recirculation during upwelling conditions and cyclonic recirculation during downwelling conditions have been observed at the AMW level between the bank and the continental shelf (González-Pola, personal communication) (Figure 2.1b). At the eastern edge of the Le Danois Bank, a pronounced anticyclonic circulation, potentially caused by eddy shedding from the shelf, is also observed at the AMW level (González-Pola et al., 2012) (Figure 2.1b). It symmetrically distributes over the bank and has a mean velocity of 10 cm/s (González-Pola et al., 2012).

Below the AMW, the LSW penetrates along the northern Iberian continental margin from east to west (Lazier, 1973; Gascard and Clarke, 1983; van Aken, 2000a). In the study area, the core of the LSW is recognized at 1800 m water depth with a minimum salinity of 35.05 (Figures 2.3b, f). Due to the depth of the intraslope basin (max. 1720 m), the LSW is hindered and fails to penetrate the basin towards the west. Intense diapycnal mixing, resulting from the highly energetic internal tidal waves, has been observed between the LSW and the AMW over the Cantabrian continental slope (Pingree, 1993; van Aken, 2000a, b). This mixing action makes the Le Danois Bank region a focal point for the occurrence of the high-energetic turbulent events at the interface between the AMW and the LSW (van Aken, 2000b; Lavín et al., 2006).

4.3 Material and methods

Three sets of reflection seismic data have been used for this study (Figure 4.1). These datasets embrace different vertical resolutions, ranging from high to ultra-high. These different datasets contain nearly overlapping NNE-SSW to N-S orientated profiles, enabling a more detailed seismic interpretation of the morphological features. The ultra-high resolution TOPAS (topographic parametric sonar) PS18 profiles were obtained during the BIO Hespérides campaign MARCONI II in 2003 (Ercilla et al., 2008; Iglesias, 2009) and penetrates down to 200 ms two-way travel time (TWT) at full oceanic depth. The primary frequency was 15 kHz (secondary 0.5-6 kHz), while the maximum vertical resolution was about 0.2 m. Four S-N trending and three E-W trending TOPAS lines were acquired in the study area with a mean spacing of 25 km. The high-resolution single-channel sparker seismic profiles were obtained during the R/V Belgica cruise ST1118a in June 2011. A 500 J energy SIG sparker (800 Hz frequency) has been used, with a shot interval of 2.5 s. The penetration depth of the acoustic signal varies around 500 ms TWT and the vertical resolution varies around 1.5 m. Twelve NNE-SSW and fifteen W-E to WNW-ESE orientated sparker seismic lines with a spacing of 3-5 km have been acquired. The three-channel airgun seismic records have been acquired during the MARCONI II campaign. The seismic source, a 5-metre-long airgun array of 6 Sercel G-GUN II (140 bars, 80 Hz frequency), was located at 2.5 m depth with a shot interval of 6 s. The receiver system was a 150 m SIG streamer with 3 sections of 40 hydrophones each. The penetration of the acoustic signal is about 1.5 s TWT. The standard vertical resolution was about 4.5 m. Seventeen NNE-SSW and nine WNW-ESE orientated airgun seismic lines with a spacing of 10-15 km were surveyed.

The TOPAS and sparker seismic data have been processed using the DECO Geophysical RadexPro Software. They were corrected for spherical divergence, amplitude loss and burst noise. The sparker seismic data was further processed using a swell filter and an Ormsby bandpass filter

(160 to 250 Hz and 1400 to 1500 Hz). The airgun seismic data was processed on board using the Delph Seismic Plus Software and included a bandpass filter (2.5 kHz high pass and 80 kHz low pass). Afterwards, the data were processed by applying a spherical divergence correction, an interactive velocity analysis, and a burst noise removal.

The multibeam data had been acquired with the RV Vizconde de Eza in 2003 within the framework of the ECOMARG project (http://www.ecomarg.com/). The positioning data was provided by Seapath 204, while the SIMRAD EM 300 provided the bathymetric data. This system operated at a water depth ranging between 200 and 3000 m and had a vertical error of less than 1 %. The sampling frequency was set at 30 kHz. The footprint is 15 x 15 m at 500-600 m and 25 x 25 m at about 1000 m. The data covered an area of 5530 km2. It encompasses the entire study area including the Le Danois Bank, the intraslope basin, the Vizco High, the Lastres Canyon and the adjacent continental shelf (Figures 4.1, 4.2). Vertical CTD profiles were extracted from the World Ocean Database (2013) (https://www.nodc.noaa.gov/OC5/WOD13/). The salinity and temperature cross sections (Figure 4.7) were made using Ocean Data View (ODV) software.

4.4 Results

In the Le Danois Bank region, the most pronounced physiographic features were already reported by Ercilla et al. (2008) and Van Rooij et al. (2010). Based on these previous results, the combination of three currently available seismic datasets, the multibeam data and the updated classification of contourite drifts presented in Rebesco et al. (2014), new insights have been provided on morphosedimentary characteristics of alongslope, downslope and mixed features and their distribution.

4.4.1 Alongslope features

4.4.1.1 Elongated mounded and separated drifts

The SW-NE oriented Le Danois Drift is located between 790 and 1080 m water depth (Figures 4.3, 4.4a, b, c). The drift encompasses an area of 242 km^2 and is about 42 km long and 4-11 km wide and 50 m high. The main element characterizing this drift is the high mounded geometry (slope gradient of 0.5° to 2.8°) (Figure 4.2). Internally, it comprises continuous parallel-stratified reflections, onlapping upslope with a sigmoidal-oblique progradational pattern towards the Le Danois Bank (Figure 4.4c). Towards the south, the mean thickness laterally decreases from 280 to 130 ms TWT. At the western limit of the Le Danois Drift, the thickness reaches its minimum (10-20 ms TWT).

The NW-SE oriented Gijón Drift is located at the southernmost part of the intraslope basin between 320 m and 1060 m water depth (Figures 4.3, 4.4a, b, d). The drift is 34 km long and 2 to 13 km wide. It displays a broad mounded geometry (slope gradient of 1° to 3°) and a basal unconformity with onlap terminations (Figure 4.4d). The mounded part rises 80 m above the surrounding seafloor. The seismic facies of the Gijón Drift is characterized by stratified layers of continuous sigmoidal reflections interbedded with discontinuous low-amplitude chaotic reflections (Figures 4.4a, d). Towards the north, the sedimentary bodies of the Gijón and the Le Danois Drifts overlapped, where the seismic reflections are continuous parallel-even configurations (Figure 4.4a). The thickness of the Gijón Drift gradually decreases from 320 to 30

ms TWT towards the southeast. The southeast extension of the Gijón Drift is limited by the presence of the Lastres Canyon (Figure 4.3). Towards the northwest, the geometry of the Gijón Drift evolves from elongated and mounded (Figures 4.4a, d) to confined and mounded (Figure 4.4b). The change of the geometry is associated with a reduction in thickness (from 220 to 110 ms TWT). The internal structure of this part of the Gijón Drift is characterized by convex-upward seismic patterns with high- to medium-amplitude sigmoidal reflections thinning towards the edges (Figure 4.4b).

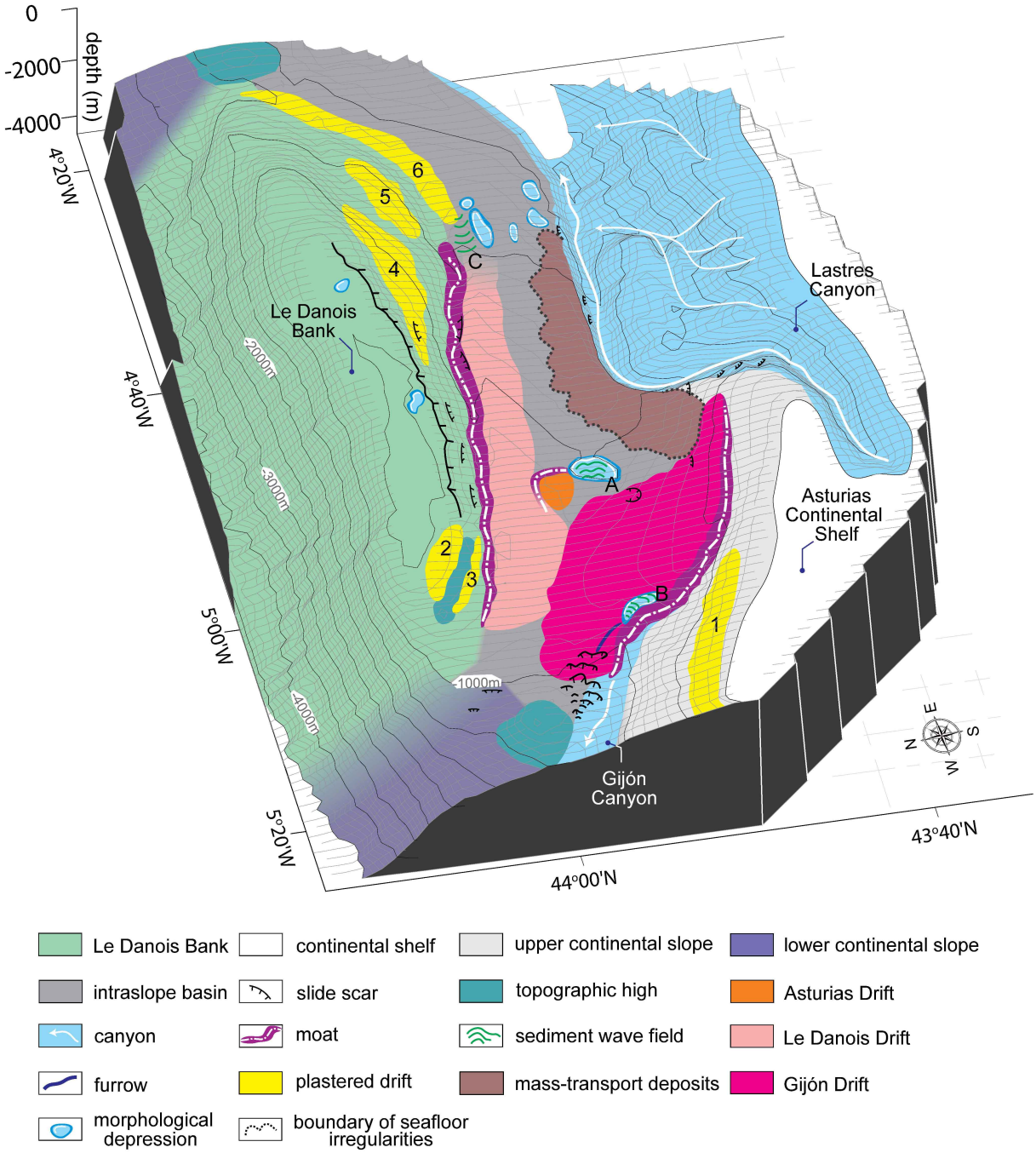

Figure 4.3: Morphosedimentary map of the Le Danois Bank region, based on the interpretation of multibeam bathymetry and seismic profiles. Numbers (1-6) and letters (A, B, C) respectively denote plastered drifts and sediment wave fields.

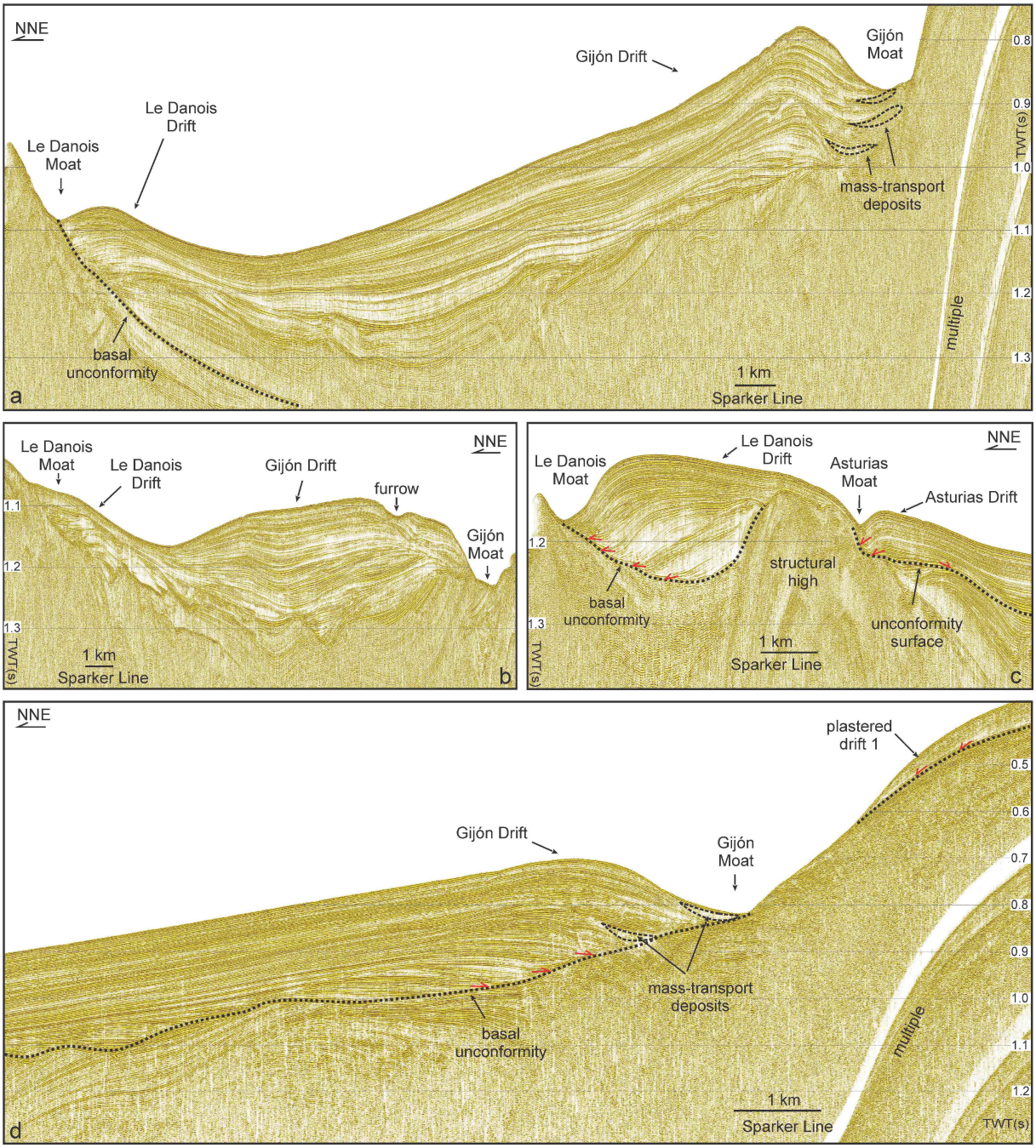

Figure 4.4: Interpreted sparker seismic profiles showing the morphological features of elongated mounded and separated drifts and a plastered drift. Onlap and downlap terminations (red arrows) are indicated. The location the seismic lines is indicated on the multibeam bathymetry map (Figure 4.1).

At the centre of the intraslope basin, a small elongated mounded and separated drift is identified (Figure 4.4c). Based on the proximal physiographic feature, the Asturias continental shelf, this drift is referred to as the Asturias Drift (Figure 4.3). The Asturias Drift covers an area of 21 km2 at water depths between 900 and 1080 m. It is characterized by an unconformity surface with onlap and downlap terminations and mounded geometry (slope gradient of about 1°) (Figures 4.2, 4.4c). The drift displays a sigmoidal-oblique seismic stacking pattern (Figure 4.4c). The maximum thickness is 90 ms TWT, decreasing towards the southwest.

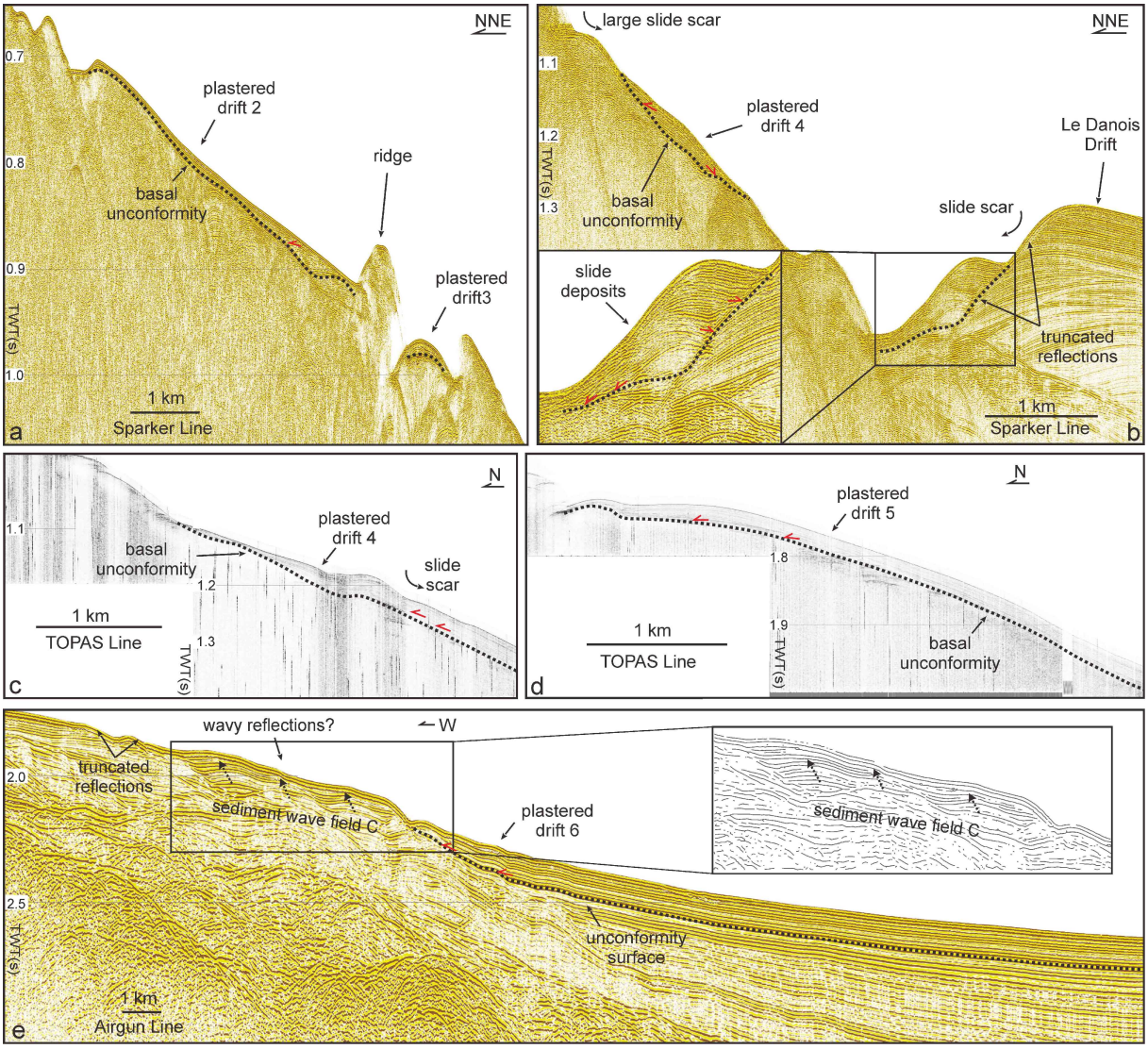

Figure 4.5: Interpreted sparker (a, b), TOPAS (c, d) and airgun (e) seismic profiles showing the morphological features of plastered drifts and slide scars. Onlap and downlap terminations (red arrows) are indicated. The location of the seismic lines is indicated on the multibeam bathymetry map (Figure 4.1).

4.4.1.2 Plastered drifts

Along the upper continental slope, WNW-ESE trending plastered drift 1 is identified between 200 and 500 m. It encompasses an area of about 48 km2 and has a length of about 7.5 km and a width of 1.5-2.5 km (Figures 4.2, 4.3, 4.4d). The drifts are characterized by sigmoidal reflections draped over the upper continental slope and is about 10 to 90 ms TWT thick. At the southern flank of the Le Danois Bank, four E-W trending narrow plastered drifts are recognized at different water depths. Plastered drifts 2 (9 km long and 2.4 km wide, from 528 to 642 m) and 3 (9.3 km long and 0.8 km wide, from 715 to 782 m) are located at the western edge of the Le Danois Bank and are separated by a ridge (Figures 4.3, 4.5a). The ridge (10 km long, 600 m wide) rises 20 m above the surrounding seafloor with a WNW-ESE orientation. Plastered drift 4 (from 870 to 1100 m) is positioned at the upper southeast flank of the bank and has a length of 10 km and a width of 0.8 to 1.1 km (Figures 4.2, 4.5b, c). Plastered drift 5 (from 1350 to 1780 m), located at the lower southeast flank of the bank, is 7 km long and 1.8-3.8 km wide (Figures 4.2, 4.3, 4.5d). Along the southeast foot of the Le Danois Bank, the SW-NE oriented plastered drift 6 is located at water depths between 1760 and 1920 m (Figures 4.2, 4.3, 4.5e). This plastered drift covers an area of 56

km2 and is about 18 km long and 1.8 km wide. The thickness ranges from 20 to 60 ms TWT. The internal structure is characterized by sigmoid reflection configurations and an unconformity surface with onlap and downlap terminations.

4.4.1.3 Moats and furrows

The Le Danois Moat parallels the southern foot of the Le Danois Bank between 866 and 1530 m water depth (Figures 4.4a, b, c). It separates the Le Danois Drift from the bank along a WNW-ESE linear trend (Figure 4.3). The Le Danois Moat is about 42 km long. It has a U-shaped profile with widths ranging from 1.9 to 2.2 km and depths from 20 to 80 m (Figures 4.4a, c). Towards the west, the moat narrows to a minimum width of 400 m.

The NW-SE oriented Gijón Moat separates the Gijón Drift from the upper continental slope (Figure 4.3). This moat (from 320 to 1090 m) starts at the southern foot of the Vizco High and extends towards the Lastres Canyon. It deflects to the southeast and loses expression to the east. The northwest part of the moat shows an asymmetric U-shape profile (Figures 4.4a, b, d) and has a depth ranging from 25 to 110 m, a width of about 2.3 km. Towards the southeast, the moat narrows to a minimum width of 800 m and the depth reduces to 10 to 20 m.

The Asturias Moat is associated with the Asturias Drift (Figure 4.3). It is oriented in a W-E direction in the western part and becomes NNW-SSE towards its NE limit. The moat is about 6 km long, 400 m wide, 80 m deep and displays a V-shape profile (Figure 4.4c).

A NW-SE oriented furrow occurs at the southwest edge of the Gijón Drift (Figure 4.3). It can be identified on the multibeam bathymetry (Figures 4.1a) and seismic reflection profiles (Figure 4.4b) by its vertical incision, ranging from 10 to 20 m. The length is 4.1 km and the width is 0.8 km. It gradually loses its expression towards the southeast, as well as towards the Vizco High.

4.4.2 Downslope features

Four isolated small slide scars are identified along the southern flank of the Le Danois Bank (Figure 4.3). They possess relatively steep slopes (values between 6° and 18°) compared to the surrounding seafloor (values between 1° and 4°) (Figure 4.2). They are characterized by crescent shapes, lengths varying between 1.3 and 4.1 km, depths ranging between 20 and 80 m and south-dipping orientations. All of the slide scars are present between 544 and 1020 m water depth (Figure 4.2). The slide scars located at plastered drift 4 (from 840 to 877 m, slope gradient of 12°) and central part of the southern flank of the bank (from 803 to 854 m, slope gradient of 15°) are namely documented by Figures 4.4c and 4.5a.

Along the southern rim of the top of the Le Danois Bank, one large isolated slide scar with a steep slope gradient of 15° to 20° has been identified (Figures 4.2, 4.3, 4.5b, 4.6a). The headwall, between 565 and 681 m, is characterized by a linear geometry (Figure 4.3). This W-E orientated slide scar is about 33 km long and has a mean depth of 90 m.

Along the southern flank of the Le Danois Moat, between 990 and 1120 m water depth, two slide scars are identified based on their arcuate morphology (Figures 4.2, 4.3, 4.5b). Compared to the entire southern flank (mean slope gradient of 2.5°) of the Le Danois Moat, both slide scars are located on the steepest slopes (7° to 9.5° slope). The eastern scar (2.2 km long and 60 m deep) has a north-dipping trend and an average slope gradient of 8.2°. The western one (3.4 km long and 30 m deep) displays a lower slope gradient of 7.8° with a northeast-dipping trend. Their associated

slide deposits are characterized by onlap and downlap terminations overlying an unconformity surface (Figure 4.5b).

At the centre of the intraslope basin, a 2.7 km2 isolated ellipse-shaped slide scar is shown on the bathymetric and seismic data (Figures 4.2, 4.3, 4.6b). This well-developed seafloor scarp shows a higher slope gradient (4.3°) compared to the surrounding slopes (1.5°). It has a northeast-dipping trend and gradually loses its expression from southwest to northeast (Figures 4.2, 4.3). The headwall, located between 750 to 777 m water depth, is about 2.5 km long and displays truncated seismic reflection configurations in the seismic records. At the bottom of this slide scar, chaotic-transparent seismic reflections are present (Figure 4.6b).

A series of isolated slide scars have been identified southeast of the Vizco High between 870 and 1280 m water depth (Figures 4.3, 4.6c). They are positioned on an erosive unconformity surface and display a step-like pattern with at least 5 levels (at 1070, 1010, 960, 940 and 920 m) (Figure 4.6c). These slide scars have an east-dipping trend and gradually lose their expressions from the west to the east. The seismic facies of these features are truncated reflections at their headwalls and chaotic-transparent reflections at the bottom. They have small variations in shape (arcuate), size (2.8 to 4.1 km in diametre, 20 to 60 m deep) and orientation (N-S) (Figure 4.3). The slope gradient of the headwalls ranges from 7° to 13° (Figure 4.2).

A large area (233 km2) of mass-transport deposit is located between the Le Danois Drift, the Gijón Drift and the Lastres Canyon (Figure 4.3). The identification is based on a distinctive seafloor irregularity and discontinuous low-amplitude chaotic and transparent reflections in the seismic records (Figure 4.6d). The boundary of these mass-transport deposits has a relatively sharp slope gradient (about 4.5°) compared to the surrounding area (about 0.8°) (Figure 4.2).

4.4.3 Topographic irregularities and morphological depressions

At the northeast edge of the Gijón Moat, an ellipse-shaped morphological depression (about 20 m deep) is identified between 680 and 770 m water depth (Figure 4.6e). It is 5.5 km in diameter and 30 to 80 m deep with a NW-SE orientation. The scarp is characterized by an erosive unconformity surface and truncated reflections. Undulating wavy-oblique reflections make up the succession between the seafloor and the unconformity surface in the seismic records. The wave-crest features are about 1-2 km long, 200 m wide and rise 10 m above the surrounding areas with a trend of upslope migration. The wave ridges have a NE-SW orientation.

At the centre of the intraslope basin, a remarkable asymmetric ear-shaped depression is identified between 990 and 1080 m water depth (Figures 4.3, 4.6f). It is 6 km in diameter and has a northwest-dipping trend. The upslope facing flank is 20 to 90 m deep with a slope gradient of about 18° (Figure 4.2). It is characterized by truncation of parallel-stratified reflections (Figure 4.6f). This depression delimits an oblique terrace (2.3° slope) with wavy morphology along the downslope facing flank. The related terrace displays high-amplitude chaotic reflections overlain by continuous wavy-stratified reflections (Figure 4.6f). These wave-like features are about 2.5-4.3 km long, 400 m wide and rise 30 m above the surrounding seafloor. The wave ridges have a N-S orientation.

Several topographic irregularities and morphological depressions (from 1540 to 2100 m) occur between the Le Danois Drift, plastered drift 6 and the Lastres Canyon. The identification is based on their irregular shapes (circular, crescent and ellipse-shaped), sizes (0.8 to 4.5 km in diameter,

40 to 80 m deep), slope gradients (values between 15° and 22°) and orientations (WSW-ENE to NW-SW trending) (Figures 4.2, 4.3). Only a few seismic profiles document these depressions. They are characterized by truncated, chaotic, semi-transparent or wavy-stratified reflections (Figure 4.5e).

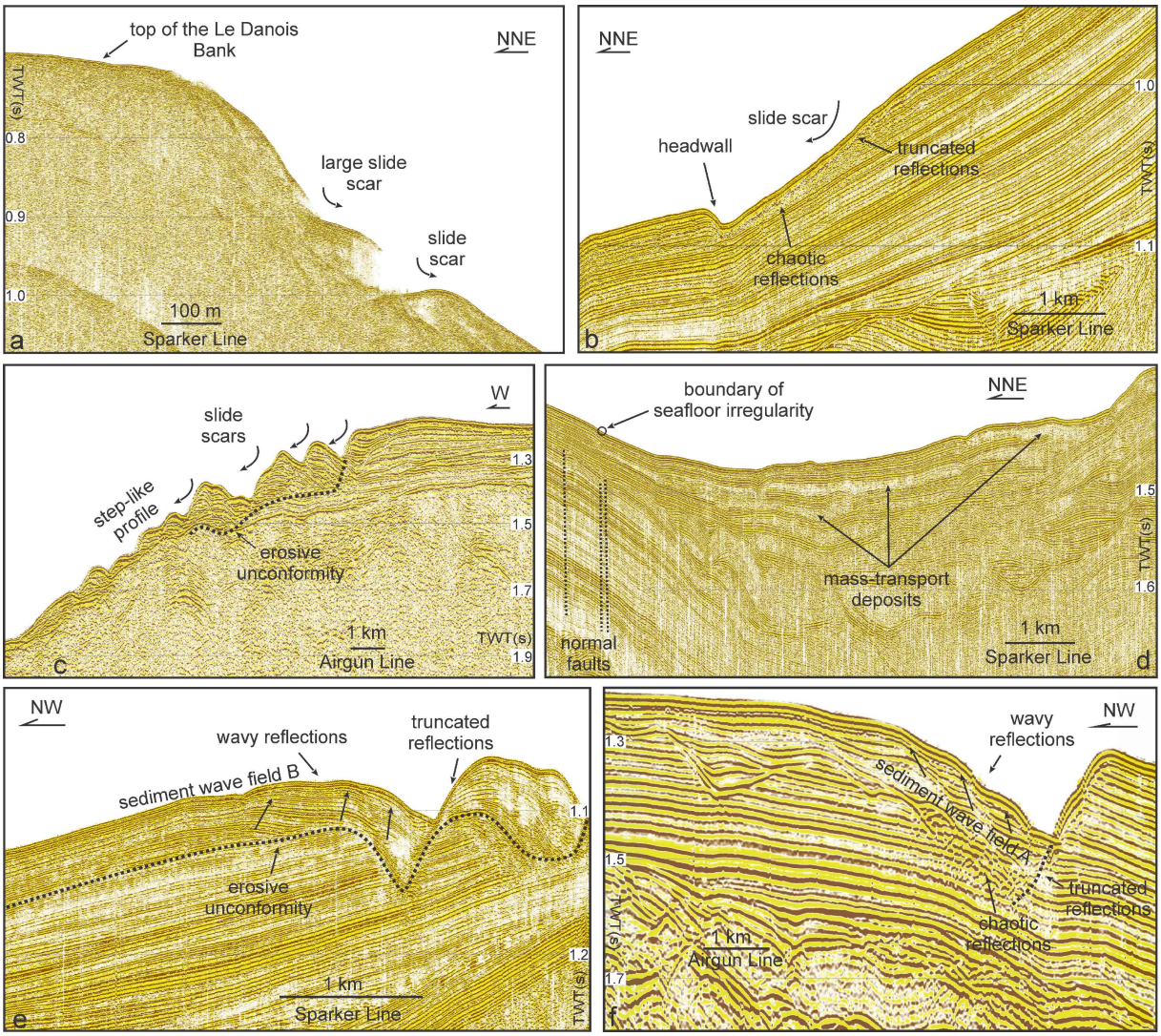

Figure 4.6: Interpreted sparker (a, b, d, e) and airgun (c, f) seismic profiles showing the morphological features of slide scars, mass-transport deposits and sediment waves. The location of the seismic lines is indicated on the multibeam bathymetry map (Figure 4.1).

4.5 Discussion

4.5.1 Present-day bottom-current implications on contourite features

The present-day bottom-current circulation within the Le Danois intraslope basin is dominated by three water masses: the ENACW, the AMW and the LSW. Due to their different physical characteristics and circulation patterns, they may play a significant role in shaping the present-day depositional and erosional contourite features. The combination of the CTD data (World Ocean Database, 2013) and the interpreted seismic profiles (Figures 4.4, 4.5, 4.6) allow gaining

more insights regarding the interaction between each water mass and its impact on the local seabed (contouritic) processes.

4.5.1.1 ENACW related processes

The ENACW (flowing between 200 and 570 metre water depth) mainly interacts with the upper continental slope and the upper southern flank of the Le Danois Bank, where plastered drifts 1 and 2, 3 are respectively located (Figures 4.7a, b, c). Present-day bottom currents along the southern flank of the bank in that depth interval are approximately 15 cm/s (González-Pola et al., 2012). Along the Asturias continental slope, the ENACW generally has a mean velocity of 10-30 cm/s (González-Pola et al., 2012). All of these values meet the conditions (Stow et al., 2002, 10-30 cm/s) for generating plastered geometry of contourite drifts 1, 2, 3, and related bottom currents are most likely resulted from the ENACW circulation documented by González-Pola et al. (2012) (Figure 4.8). Additionally, plastered drifts 2 and 3 are distributed along the northern and southern foot of a ridge (Figure 4.5a) with similar orientations, shapes and lengths. These features illustrate similar bottom-current processes resulting from interactions between small flow filaments and the adjacent topographic obstacle. The related bottom-current dynamics could be compared with the present-day anticyclonic circulation cell along the western rim of the Le Danois Bank (González-Pola et al., 2012) (Figure 4.8).

Gentle slope morphology is one of the main elements responsible for the formation of plastered drifts as well (Laberg and Camerlenghi, 2008). At the eastern edge of plastered drifts 2 and 3, the slope gradient abruptly increases to 8.5°. This steep slope is maintained to the southeast flank of the bank (Figure 4.2). Higher slope gradients could accelerate bottom currents, in turn shifting sedimentary processes from deposition to non-deposition/erosion (Rebesco et al., 2014). These higher slope angles could inhibit the generation of plastered drifts along this part of the Le Danois Bank. Towards the eastern boundary of plastered drift 1, the slope gradient maintains but the space between the lower continental slope and the Asturias continental shelf is widened (Figure 4.2). The wide morphology will decelerate bottom currents (Faugères and Stow, 2008). Slower flows could limit the lateral extension of plastered drift 1 towards the east.

4.5.1.2 AMW related processes

The AMW mainly interacts with the southern flank of the Le Danois Bank and the intraslope basin between 750 and 1500 m water depth (Figure 4.7). Plastered drift 4 (from 870 to 1100 m) is positioned along the upper southeast flank of the Le Danois Bank (Figures 4.5b, 4.7d), where bottom currents are estimated at 10-15 cm/s (González-Pola et al., 2012). This drift covers a gentle slope (mean slope gradient of about 3.5°) (Figure 4.2) and is shaped by the AMW (Figure 4.8). Along the entire boundary of plastered drift 4, the slope gradients abruptly increase to 8-15° (Figure 4.2), delineating its extent. Considering all, slope morphology is the main controlling factor for the spatial distribution of plastered drift 4.

The Le Danois Drift (from 790 to 1080 m) is suggested to be generated by the AMW as well. The associated Le Danois moat indicates a focused flow pathway of bottom currents all along the southern foot of the Le Danois Bank. This feature matches with the present-day oceanographic data documented by González-Pola et al., (2012). A 12-month long mooring record (at 44°02.33', N 4°49.33' W) indicates a persistent westward near-bottom flow along the southern foot of the bank at the AMW level (González-Pola et al., 2012). Direct current measurements at this level, consisting of few snapshots made by landers, fit with the velocity in the range of 10-25 cm/s

(González-Pola et al., 2012). This velocity is sufficient to generate associated contourite drifts (Stow et al., 2002, 2009). Towards its western limit, the Le Danois Drift extends to an open area between the lower continental slope and the intraslope basin (Figure 4.3). In this area, the Le Danois bank is absent and bottom currents most likely will drop to the reported background values, which are less than 5 cm/s (Iorga and Lozier, 1999a). Towards the eastern limit of this drift, the presence of a group of morphological depressions limits the distribution of the Le Danois Drift (Figure 4.3). Consequently, slower bottom currents and seabed morphology limit the distribution of the Le Danois Drift. The Le Danois Drift and plastered drift 4 have similar orientations and are located at the same water depths (Figures 4.3, 4.8). The distribution suggests that the associated bottom-current processes of both drifts are related to the same current (Figure 4.8). The presence of two types of contourite drifts along the AMW pathway can be explained by changes in current velocities (Faugères and Stow, 2008). This implies accelerated and then decelerated processes from the southeast towards the southwest flank of the Le Danois Bank.

The Gijón Drift and the Moat extend from 320 to 1090 m water depth. A CDS is usually associated with one water mass (Rebesco et al., 2014). However, at the present day, the Gijón Drift is situated within the boundaries of two different water masses, being the ENACW and the AMW (Figures 4.7a, b, c). Along the Cantabrian continental upper slope, the ENACW does not reach to 1000 m for prolonged periods of time (McCartney and Mauritzen, 2001), while the AMW could only reach up to 400 m during interglacial climate cycles (Zhang et al., 2016; Kaboth et al., 2016, 2017). Additionally, shape and morphology of the Gijón Drift display different features in different depth intervals. Within the ENACW, the Gijón Drift has elongated and mounded geometry (Figures 4.7b, c), whereas the part within the AMW is confined and mounded (Figure 4.7a). Different shapes of contourite drifts are related to different bottom-current conditions (Faugères and Stow, 2008). As such, it is possible that the ENACW and the AMW interacted with the upper continental slope during different climate intervals and both are responsible for the Gijón Drift.

The spatial variation of the Gijón Drift could be controlled by the slope morphology as well. On the multibeam bathymetry, the Gijón Moat (NE-SW trending) does not fit the alongslope distribution compared to the Asturias continental slope (WNW-ESE trending) (Figures 4.3). The obliquity may be caused by the presence of the Gijón Canyon (NE-SW trending) (Figures 4.3, 4.7f). Interactions between canyon channels and bottom currents are possible to provoke streamline distortions and accelerate current flows (Holland, 1972). The related distortion and acceleration enable bottom currents flowing upwards along canyon channels (Jackson et al., 2006). When the AMW encounters the Gijón Canyon, bottom currents could follow the canyon morphology (Allen and De Madron, 2009; Muench et al., 2009) and arise towards the shallower continental slope (320 m water depth). The variation of the Gijón Drift could also link with the interaction between the Gijón Canyon and the AMW.

Figure 4.7: Seismic and oceanographic profiles in the Le Danois Bank region. The depth intervals of the water masses and contourite features show the dynamic interaction between water masses and the present-day sedimentary regime. The locations of airgun seismic profiles are indicated in the bathymetric map. The junctions of Line a, b and f; and Line e and g (dotted black lines) are indicated in the seismic profiles. The CTD stations (red triangles) and their respective locations are indicated in the seismic and oceanographic profiles.

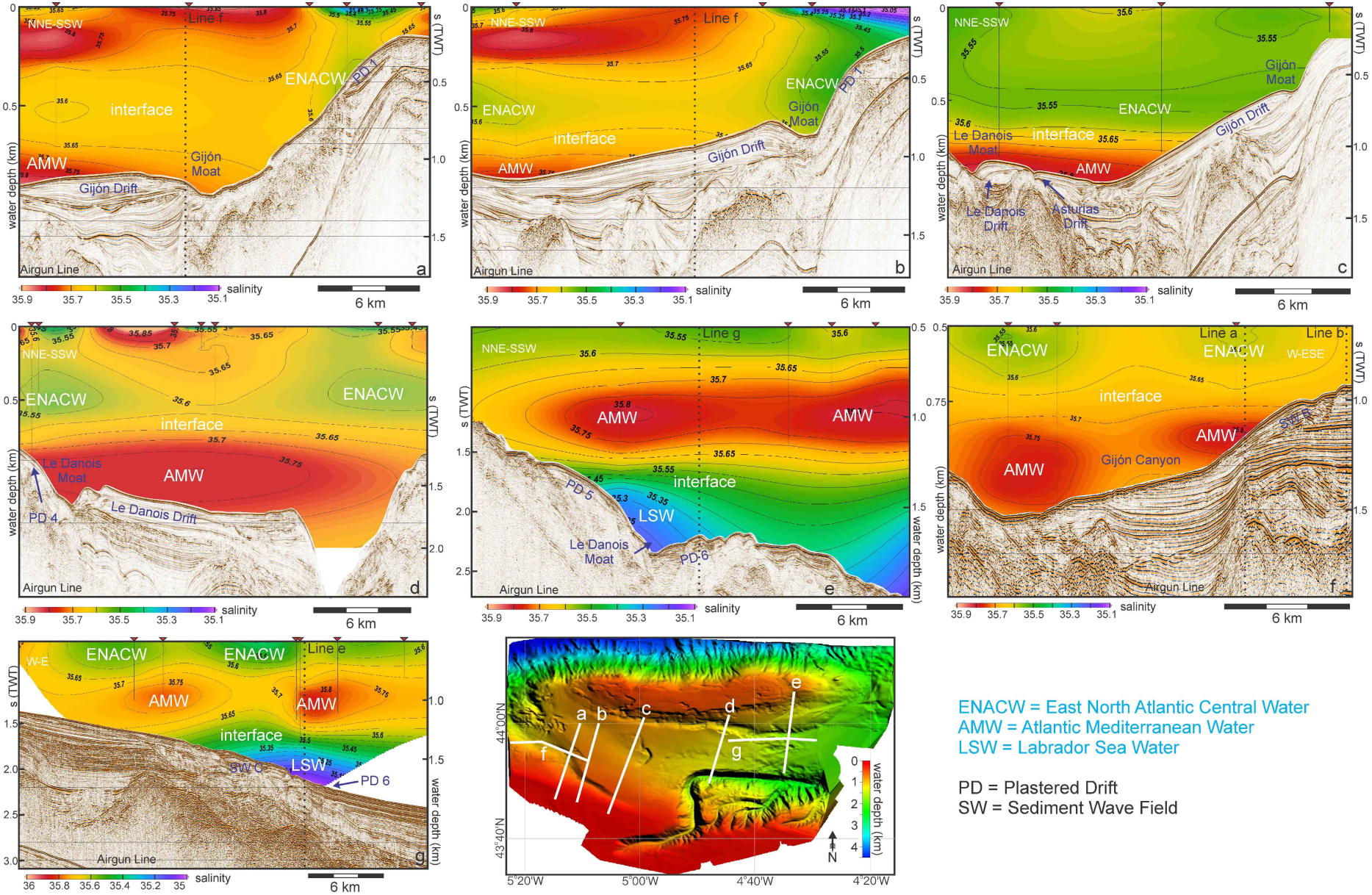

ENACW = East North Atlantic Central Water
AMW = Atlantic Mediterranean Water
LSW = Labrador Sea Water

PD = Plastered Drift
SW = Sediment Wave Field

The Asturias Drift lies around a buried structural high at the centre of the intraslope basin (Figures 4.3, 4.4c, 4.7c). The presence of a topographical obstacle can create faster currents, in turn generating contourite depositional and erosional features (Ercilla et al., 2016; García et al., 2016). The associated Asturias Moat indicates the pathway of bottom currents. The W-E to NNW-SSE deflection of the moat may result from the morphological control of the associated depression (Figure 4.8). As such, the Asturias Drift and Moat result from interactions of the AMW with a buried structural high and a morphological depression. Related bottom-current processes could be linked with the present-day AMW circulation cell (González-Pola et al., 2012) in the intraslope basin (Figure 4.8).

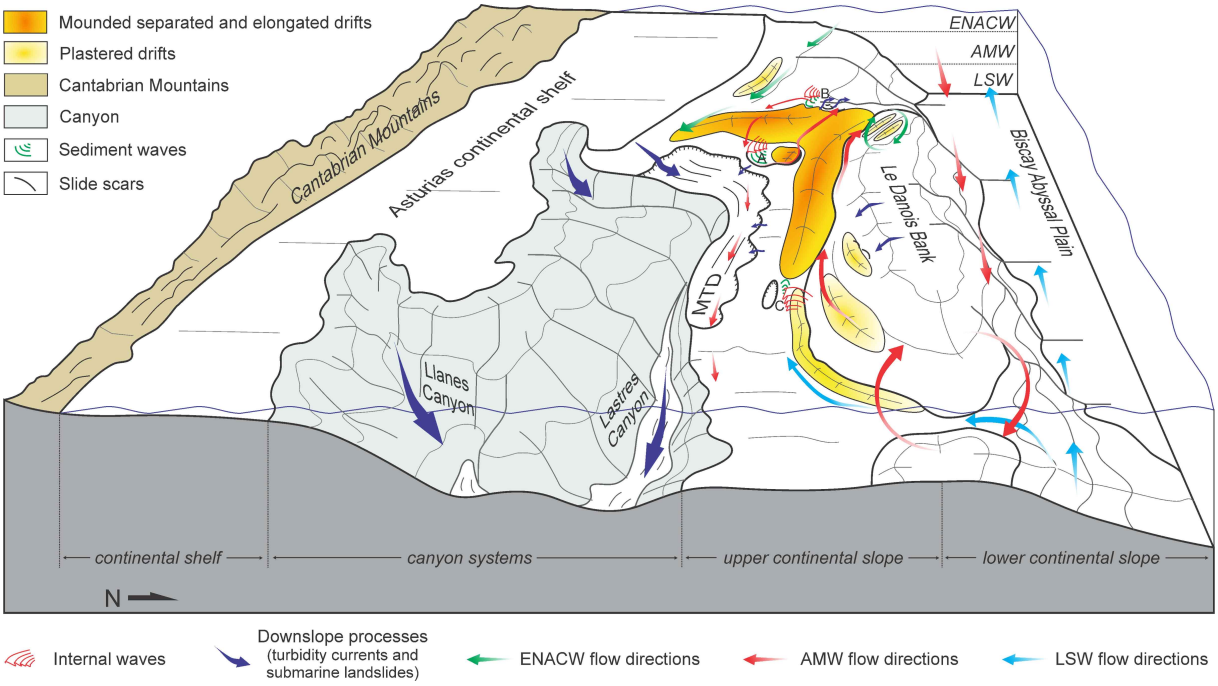

Figure 4.8: Sketch of the recent sedimentary processes within the Le Danois Bank region. This sketch has been produced based on the morphosedimentary features defined in the morphosedimentary map (Figure 4.3).

At the southeast edge of a group of slide scars, a furrow is located in the Gijón Drift at water depths of 844 to 870 m (Figures 4.3, 4.4b). Present-day bottom currents associated with the AMW in the intraslope basin (from 10 to 20 cm/s, González-Pola et al., 2012) do not have sufficient energy to create erosive furrows, which require at least 30 cm/s (Stow et al., 2009). However, it is well documented that the presence of topographic obstacles or irregularities can cause locally intensified bottom currents (Rebesco et al., 2008, 2014). Examples include the Galicia Bank region where (numerically modelled) intensifications from 7 cm/s up to 35 cm/s are recorded (Zhang et al., 2016), the Porcupine Abyssal Plain where accelerations reach 15 cm/s (Turnewitsch et al., 2004), and the Xisha Trough where (also numerically modelled) enhancements from 15 cm/s up to 30 cm/s are documented (Chen et al., 2016). Similarly, bottom currents can recirculate around the Vizco High, possibly speeding up from 10-20 cm/s to over 30 cm/s in this region. The presence of the furrow indicates faster bottom currents resulted from strong interactions with the Vizco High.

4.5.1.3 LSW related processes

The LSW is only present between the Lastres Canyon and the lower southern flank of the Le Danois Bank in the study area (below 1750 m water depth) (Figures 4.7). Plastered drifts 5 is located

along the lower southern flank (2.4° slope) while plastered drift 6 lies along the southeast foot (1.2° slope) of the bank (Figures 4.2, 4.3, 4.7e). Both lay within the depth windows of the LSW. Along the Cantabrian continental slope, the bottom current velocities (2-6 cm/s; Speer et al., 1999; Friocourt et al., 2007) are below the threshold for depositing plastered drifts (Stow et al., 2002, 2009). Consequently, the presence of these two plastered drifts indicates local intensification. Since there are no known measurements of current velocities at this depth interval in the study area, tentative bottom-current velocities generating these plastered drifts have to be estimated in order to better understand the acceleration of bottom currents in a topographically constrained basin. Since the average threshold for deposition of plastered drifts has been indicated at 10 cm/s (Stow et al., 2009), we thus estimate the local current velocities must exceed this value. Along the entire boundary of plastered drift 5, slope gradients increase to 6°-10° (Figures 4.2, 4.3). As such, steeper slope morphologies control and limit the distribution of plastered drift 5. The extension of plastered drift 6 is limited by seafloor depressions positioned between the bank and the Lastres Canyon (Figure 4.3). Towards the northeast boundary of plastered drift 6, the presence of a topographic high locally creates slopes from 1° to 11° (Figure 4.2). These slopes limit the distribution of plastered drift 6.

4.5.2 Interaction with slope instability processes

In the study area, plenty of slide scars occur at the surfaces of contourite drifts and along the southern flank of the Le Danois Bank (Figures 4.1, 4.2, 4.3). The main causal factors for submarine slides include high slope angles, seismic activity, volcanic activity, gas charging and rapid sediment accumulation (Locat and Lee, 2002; Sultan et al., 2004; Verdicchio and Trincardi, 2008; Miramontes et al., 2016; Rashid et al., 2017). Recent seismic activities along the Cantabrian continental margin is of low to moderate magnitude (Ruiz et al., 2006), which probably have not enough shaking intensity to trigger mass wasting. Since volcanic activity and gassy sediments have been observed in the study area, the triggering mechanisms for these slide scars are either rapid sediment accumulation or oversteeping.

4.5.2.1 Increased sediment accumulation

An isolated slide scar is positioned at the northeast part (3° slope) of the Gijón Drift (Figures 4.1, 4.2, 4.6b). The sedimentation rate of the Gijón Drift is unknown. However, mounded drifts are known to have relatively high sedimentation rates (5-60 cm/ka) compared to pelagic (<2 cm/ka) and hemipelagic (5-15 cm/ka) sediments (Stow et al., 2008). During the build-up of the Gijón Drift, high sedimentation rates are capable of decreasing shear strength of sediments, favouring the formation of mass-wasting events (Baeten et al., 2013). Since the slide scar lies between the Asturias Drift and the Gijón Drift (Figure 4.3), two drift systems can deliver sediments to this location and drastically increase the sedimentation rate. As such, the occurrence of a slope instability event at this location is more likely, compared to other areas of the Gijón Drift.

Opposed to the Gijón Drift, no slope instability processes occur at the surface of the Le Danois Drift (Figures 4.1, 4.2, 4.3). The difference between both drifts may be related to their internal depositional structures. Interbedded continuous sigmoidal reflections and discontinuous low-amplitude chaotic reflections within the Gijón Drift are interpreted as interbedded mass-transport and contourites deposits (Figures 4.4a, d), whereas only contourites are present within the Le Danois Drift (Figures 4.4a, c). These interbedded features are mainly located at the Gijón Moat, indicating multiple shifts between alongslope and downslope processes over the Gijón Drift.

Different degree of sedimentary sorting, resulting from distinct sedimentary processes, could lead to the deposition of different sedimentation layers (Wilson et al., 2004). These sedimentation layers generally have higher sensitivity, due to their distinct physical properties (Laberg and Camerlenghi, 2008). Higher sensitive layers can effectively reduce shear resistance strength of sedimentary bodies and thus a dynamic slide process can initiate (Kvalstad et al., 2005). Similar examples have been documented in the vicinity of the Storegga Slide region (glacigenic/contouritic deposits), offshore Norway (Bryn et al., 2005) and in the Afen Slide area (mud/sand contouritic deposits), offshore UK (Wilson et al., 2004). Within the Gijón Drift, multiple shifts between alongslope and downslope processes create high sensitive layers which could reduce the shear resistance strength and induce mass movements. Conversely, the shear strength of the Le Danois Drift is not low enough to trigger slope instability events.

Between the northwest end of the Gijón Drift and the Vizco High, a series of slide scars overlay a steep slope (10°) (Figures 4.1, 4.2, 4.6c). Thick contourite deposits of the Gijón Drift, as well as steep slope morphology could have a significant potential for producing mass movements.

4.5.2.2 Scouring of active bottom currents

Two slide scars occur at the southern flank of the Le Danois Moat (Figures 4.1, 3, 5). Both slide scars are distributed along the steepest (9°) parts of the moat (Figure 4.2). The focused flow within the Le Danois Moat could be held responsible for the formation of these slide scars. Similar to the Cape Basin, where a slide scar is induced by scouring of bottom currents (Weigelt and Uenzelmann-Neben, 2004), higher angles and active bottom currents can provide favourable conditions for slope instability processes in this part of the moat. The associated slide deposits display internal structures with onlap and downlap terminations and their geometry resemble patched drift features (Figure 4.5b), hinting towards reworking of bottom currents. The observed features in the study area are similar to recent discoveries in the Guadalquivir Bank, where reworking of bottom currents reshaped the slide deposits (García et al., 2016). In conclusion, focused bottom currents within the Le Danois Moat locally scour the steeper flank, this may lead to undercutting of the slope, triggering mass movements.

4.5.2.3 Mixed processes

In the Le Danois Bank region, a large area of mass-transport deposits lies between the Lastres Canyon, the Gijón and the Le Danois Drifts (Figure 4.3). The associated scarp is about 10 km away from the Lastres canyon channel (Figures 4.1, 4.2). The seafloor morphology of the mass-transport deposits shows an upslope trending from the canyon wall towards the scarp. As such, turbidity currents associated with the Lastres canyon are not possible to penetrate (10 km) upslope undercutting the scarp, and are most likely not responsible for the formation of these mass-transport deposits. The slope gradient (9.5°) of this location is much higher than the surrounding seafloor (2.8°) (Figure 4.3). High slope angles lead to downslope processes at this particular location. Towards the east, the orientation of this mass-transport deposits area gradually changes from downslope (N-S trending) to alongslope (W-E trending) directions (Figure 4.3). This deflection indicates the interaction between mass movements and AMW currents (Figure 4.8). Characteristics of these mass-transport deposits can be compared to those at the southeast Grand Banks (Rashid et al., 2017) and along the Mid-Norwegian Margin (Bryn et al., 2005), where the area of mass-transport deposits is elongated and enlarged and the related distribution and location are highly influenced by bottom currents. As such, a high slope gradient and bottom

currents resulting from the AMW could be predisposing factors for the formation of these mass-transport deposits.

4.5.3 A genetic model for the sediment waves of the Le Danois Bank region

Within the intraslope basin, wavy features are identified in the seismic records (Figures 4.5e, 4.6e, f). These features are interpreted as sediment wave fields (respectively A, B and C on Figure 4.3) based on the traceable and continuous seismic reflections, as opposed to slope failure deposits with sharp and acoustically incoherent reflections (Gardner et al., 1999; Lee et al., 2002; Mosher and Thomson, 2002; Wynn and Stow, 2002). The formation of sediment waves has three possible causes, being turbidity currents, bottom currents or internal waves (Ercilla et al., 2002; Ribó et al., 2016). Turbidity-current related sediment waves generally occur on the back-slopes of channel levees and in turbidity-current channels (Wynn and Masson, 2008). Since the study area with sediment waves lacks the presence of channel-levee systems and turbidity-current processes (Wynn and Masson, 2008). Unconfined turbidity currents can generate slope creeps with the wavy morphology. However, sediment wave fields of the study area display continuous reflectors and are lack of truncations, which does not fit the internal structure of slope creeps. As such, these sediment wave fields most likely result from bottom currents or internal waves.

Sediment wave field A is located within the AMW level and is induced by internal waves. Bottom currents can be ruled out as the moat in the vicinity of sediment wave field A suggests N-S oriented bottom currents (Figure 4.8), which is parallel to the wave crests. This orientation does not fit the bottom-current induced sediment waves (oblique or perpendicular orientations of the wave crests; Masson et al., 2002; Wynn and Masson, 2008).

Sediment waves created by internal waves are documented in several regions (Pomar et al., 2012; Delivet et al., 2016; Ribó et al., 2016). When internal waves propagate down a sloping bottom, three possible reflection conditions exist based on the propagation angle of the internal wave (c) and the bottom slope angle (γ) (Cacchione et al., 2002). The relationship was established by Cacchione and Wunsch (2006) and can be written as:

$$c = arctan\left[\left(\frac{\sigma^2 - f^2}{N^2 - \sigma^2}\right)^{\frac{1}{2}}\right]$$

where σ is the internal wave frequency, f is the local Coriolis (inertial) frequency, and N is the Brunt–Väisälä (buoyancy) frequency. Different values of γ/c correspond to subcritical (γ/c<1), critical (γ/c≈1) and supercritical (γ/c>1) reflection conditions (Lamb, 2014). In the study area, high-frequency internal waves have been observed near the centre of the intraslope basin at the level of the AMW (González-Pola et al., 2012). Based on the local flow properties, González-Pola et al. (2012) proposed the following parameters: f as 1.013 x 10-4 /s, σ as 0.09 cph and N as 1.5 to 2.5 x 10-3 s-1. Thus, internal wave reflection condition in sediment wave field A (1.6° slope) is subcritical. Subcritical conditions of internal waves are generally characterized by smaller wave heights and upslope migration (Lamb, 2014; Delivet et al., 2016; Ribó et al., 2016). And this is true for sediment wave field A, which migrates upslope and their wave heights is relatively small (10 m) compared to those in the Argentine Basin (30 m) (von Lom-Keil et al., 2002), the Gulf of Valencia (50 m) (Ribó et al., 2016) and the Bahama Outer Ridge (60 m) (Flood and Giosan, 2002).

Sediment wave fields B (Figure 4.7f) and C (Figure 4.7g) are respectively located at the ENACW/AMW and the AMW/LSW interfaces. No mooring measurements have been performed at these interfaces and the present-day oceanographic dynamics are unknown. However, the mean salinity values at the ENACW/AMW (35.6) and the AMW/LSW interfaces (35.2) (Figure 4.7) indicate mixing processes as the ENACW has a mean salinity of 35.5, the AMW 35.8 and the LSW 35.1 (Figure 2.3b). Turbulent mixing at the interface between water masses generally produces relatively high energetic currents associated with internal waves, which are capable of transporting and depositing sediments (Preu et al., 2013; Ercilla et al., 2016; Juan et al., 2016). The relatively small wave heights (7 and 10 m for wave fields B and C) and the observed upslope migration both indicate a subcritical reflection parameter (Lamb, 2014). As such, sediment wave fields B and C are most likely related to internal waves as well. Both sediment wave fields are located within morphological depressions (slopes of 8°-10°) (Figures 4.2, 4.3) and overlie irregular unconformity surfaces (Figures 4.5d, 4.6c), which are the prerequisites for the formation of sediment waves (Aghsaee et al., 2010).

4.5.4 Sediment sources

The sediments constituting the various drifts in the region are mainly transported by downslope processes to the continental slopes and caught by bottom currents from adjacent areas towards the Le Danois Bank region (Gómez-Ballesteros et al., 2014). One year long current meter data, obtained from the Avilés Canyon (west of the Le Danois area, Figure 2.1a) indicates direct delivery of river-sourced (the Narcea and Nalon Rivers) material into the canyon and its adjacent continental slope (Rumín-Caparrós et al., 2013). Frequent severe storms and repeated cycles of semidiurnal tides regionally enhanced the bottom currents, assuring a permanent amount of sediment in suspension in the canyon region (Rumín-Caparrós et al., 2016). Additionally, the Narcea and Nalon Rivers are generated before the formation period (the Neogene, Gómez-Ballesteros et al., 2014) of the Avilés canyon (Fernández-Viejo et al., 2014). The suspended material is possible to be picked up by eastward moving water masses towards the Le Danois Bank since the intensification of the AMW (during the late Pliocene, Hernández-Molina et al., 2014) and the establishment of the Iberian Poleward Current (during the late Pleistocene, Mena et al., 2018). Consequently, the Narcea and Nalon Rivers could provide sediments for identified contourite deposits for prolonged periods of time (Gómez-Ballesteros et al., 2014; Rumín-Caparrós et al., 2016).

The Avilés Canyon is not the only sediment source for the contourite deposits. Current meter data reveal a long-term (12-month) persistent westward flow within the Le Danois Moat (González-Pola et al., 2012), which has an opposite direction compared to the major branch of the AMW (Figure 4.8). Additionally, the LSW flows towards the intraslope basin in a westward direction as well (Figure 4.8). These observations suggest an additional eastern sediment source should be present. The Torrelavega Canyon is located in the vicinity of the study area and fed by sediments from the Besaya River (Figure 2.1a) (Caballero et al., 2014). Eddies extending from the surface down to 3500 m water depth have been observed above the Torrelavega canyon (Caballero et al., 2014), which remained stationary for a long time (locally up to 7 months) (Pingree and Le Cann, 1992; Caballero et al., 2014), creating the possibility for associated energetic current patterns to erode the seafloor and suspend sediments (Shanmugam, 2013). As such, suspended sediments can be transported towards the Le Danois Bank area by bottom currents associated with the AMW and the LSW.

The Gijón and the Lastres Canyons can be possible sediment sources as well. Few studies have documented these two canyon systems. Based on their locations, the Sella River is suggested to be the sediment supply for both canyons (Figure 2.1a). Erosive features at the canyon walls have been displayed in the seismic records (Figure 4.7f). Due to the consistent AMW flowing above the intraslope basin, eroded sediments can contribute to the sediment accumulation of the prevailing contourite drifts. Finally, mass-transport deposits are interbedded within the Gijón Drift (Figures 4.4a, d) and indicate the interaction between bottom currents and gravitational processes along the upper continental slope. These processes may add sediments from the Asturias continental shelf to the contourite drifts.

4.6 Conclusion

The spatial variability of contourite drifts, slope morphology and small-scale bottom-current processes are all tied together in this topographically constrained small basin. Bottom currents associated with the ENACW, the AMW and the LSW are more focused and strongly intensified (estimated acceleration up to 25 cm/s) due to the morphological constraint of the Le Danois Bank and the Vizco High. Changes in velocities of bottom currents and slope gradients result in variations in types, shapes and spatial distributions of contourite drifts, especially along the current pathways of the AMW. Unlike typical elongated and mounded drifts, the Gijón Drift exhibits a lateral variation (evolving from elongated to confined geometry) at different depth intervals, which evidently indicate different bottom-current dynamics associated with one contourite drift, suggesting specific geometries and shapes of contourite drifts in topographically constrained small basins. Despite the influence of large topographic obstacles, small steep (slopes of 8°-10°) morphologic irregularities may interact with internal waves, generating small-scale (wave heights 7-10 m) upslope-migrated sediment waves in the intraslope basin. Enhanced bottom-current processes interplay with internal waves and slope instability events, and determine the complex morphology of the present-day seafloor. The observation and the interpretation are based on the comparison with similar features in other studies. Detailed sedimentary processed which are related to wavy features and mass-transport deposits are still unkown. More work on these morpholohical features is suggested for future study. Compared with large contourite features resulted from deep water masses, small basin-scale contourite features of the Le Danois Bank region is an exquisite example of multiple processes interacting in a topographically constrained basin at an intermediate water depth. The spatial variability of the contourite features is more frequent than anticipated so far and can have far-reaching implications for comparable topographic and oceanographic settings all over the world.

Acknowledgements

This study was carried out within the framework of a Chinese Scholarship Council “CSC Grant” (201506410062). The research was conducted in collaboration with “The Drifters Research Group” of the Royal Holloway University of London (UK) and it is related to the projects CTM 2012-39599-C03, CGL2016-80445-R, and CTM2016-75129-C3-1-R. The authors wish to express our gratitude to the crews and scientific researchers of the MARCONI II, the ECOMARG and the R/V Belgica ST1118a campaigns. Shiptime RV Belgica was provided by BELSPO and RBINS–OD Nature. These research campaigns framed within the ECOMARG (REN2002-00916/MAR) and MARCONI (REN2001-1734 C03-01/M) projects. This study also builds upon achievements of

project ESF Euromargins MOUNDFORCE, EC FP5 RTN EURODOM and EC FP6 HERMES (GOCE-CT-2005-511234-1).

References

Aghsaee, P., Boegman, L., Lamb, K.G., 2010. Breaking of shoaling internal solitary waves. Journal of Fluid Mechanics 659, 289–317.

Allen, E.S., Durrieu de Madron, X., 2009. A review of the role of submarine canyons in deep-ocean exchange with the shelf. Ocean Science 5, 607–620.

Alvarez-Marrón, J., Pérez-Estaún, A., Danñobeitia, J.J., Pulgar, J.A., Martínez, Catalán, J.R., Marcos, A., Bastida, F., Ayarza, Arribas, P., Aller, J., Gallart, A., Gonzalez-Lodeiro, F., Banda, E., Comas, M.C., Córdoba, D., 1996. Seismic structure of the northern continental margin of Spain from ESCIN deep seismic profiles. Tectonophysics 264, 153–174.

Baeten, N.J., Laberg, J.S., Forwick, M., Vorren, T.O., Vanneste, M., Forsberg, C.F., Kvalstad, T.J., Ivanov, M., 2013. Morphology and origin of smaller-scale mass movements on the continental slope off northern Norway. Geomorphology 187, 122–134.

Boillot, G., Dupeuble, P.A., Malod, J., 1979. Subduction and tectonics on the continental margin off northern Spain. Marine Geology 32, 53–70.

Bryn, P., Berg, K., Stoker, M.S., Haflidason, H., Solheim, A., 2005. Contourites and their relevance for mass wasting along the Mid-Norwegian Margin, in: Ormen Lange–an Integrated Study for Safe Field Development in the Storegga Submarine Area. Elsevier, Oxford, pp. 85–96.

Caballero, A., Ferrer, L., Rubio, A., Charria, G., Taylor, B.H., Grima, N., 2014. Monitoring of a quasi-stationary eddy in the Bay of Biscay by means of satellite, in situ and model results. Deep Sea Research Part II: Topical Studies in Oceanography 106, 23–37.

Cacchione, D., Wunsch, C., 2006. Experimental study of internal waves over a slope. Journal of Fluid Mechanics 66, 223–239.

Cacchione, D.A., Pratson, L.F., Ogston, A.S., 2002. The Shaping of Continental Slopes by Internal Tides. Science 296, 724–727.

Cadenas, P., Fernández-Viejo, G., 2017. The Asturian Basin within the North Iberian margin (Bay of Biscay): seismic characterisation of its geometry and its Mesozoic and Cenozoic cover. Basin Research 29, 521-541.

Cartes, J.E., Huguet, C., Parra, S., Sanchez, F., 2007. Trophic relationships in deep-water decapods of Le Danois bank (Cantabrian Sea, NE Atlantic): Trends related with depth and seasonal changes in food quality and availability. Deep Sea Research Part I: Oceanographic Research Papers 54, 1091–1110.

Chen, H., Xie, X., Zhang, W., Shu, Y., Wang, D., Vandorpe, T., Van Rooij, D., 2016. Deep-water sedimentary systems and their relationship with bottom currents at the intersection of Xisha Trough and Northwest Sub-Basin, South China Sea. Marine Geology 378, 101–113.

Delivet, S., Van Eetvelt, B., Monteys, X., Ribó, M., Van Rooij, D., 2016. Seismic geomorphological reconstructions of Plio-Pleistocene bottom current variability at Goban Spur. Marine Geology 378, 261–275.

Ercilla, G., Alonso, B., Wynn, R.B., Baraza, J., 2002. Turbidity current sediment waves on irregular slopes: observations from the Orinoco sediment–wave field. Marine Geology 192, 171–187.

Ercilla, G., Casas, D., Estrada, F., Vázquez, J.T., Iglesias, J., García, M., Gómez, M., Acosta, J., Gallart, J., Maestro-González, A., 2008. Morphosedimentary features and recent depositional architectural model of the Cantabrian continental margin. Marine Geology 247, 61–83.

Ercilla, G., Casas, D., Vázquez, J.T., Iglesias, J., Somoza, L., Juan, C., Medialdea, T., León, R., Estrada, F., García-Gil, S., Farran, M. l., Bohoyo, F., García, M., Maestro, A., 2011. Imaging the recent sediment dynamics of the Galicia Bank region (Atlantic, NW Iberian Peninsula). Marine Geophysical Research 32, 99–126.

Ercilla, G., Juan, C., Hernández-Molina, F.J., Bruno, M., Estrada, F., Alonso, B., Casas, D., Farran, M. lí, Llave, E., García, M., Vázquez, J.T., D'Acremont, E., Gorini, C., Palomino, D., Valencia, J., El Moumni, B., Ammar, A., 2016. Significance of bottom currents in deep-sea morphodynamics: An example from the Alboran Sea. Marine Geology 378, 157–170.

Faugères, J.-C., Stow, D.A. V, 1993. Bottom-current-controlled sedimentation: a synthesis of the contourite problem. Sedimentary Geology 82, 287–297.

Faugères, J.-C., Stow, D.A. V, Imbert, P., Viana, A., 1999. Seismic features diagnostic of contourite drifts. Marine Geology 162, 1–38.

Faugères, J.C., Stow, D.A. V, 2008. Chapter 14 Contourite Drifts: Nature, Evolution and Controls, in: Rebesco, M., Camerlenghi, A. (Eds.), Developments in Sedimentology. Elsevier, pp. 257–288.

Fernández-Lozano, J., Sokoutis, D., Willingshofer, E., Cloetingh, S., De Vicente, G., 2011. Cenozoic deformation of Iberia: A model for intraplate mountain building and basin development based on analogue modeling. Tectonics 30, TC1001.

Flecker, R., Krijgsman, W., Capella, W., de Castro Martíns, C., Dmitrieva, E., Mayser, J.P., Marzocchi, A., Modestou, S., Ochoa, D., Simon, D., Tulbure, M., van den Berg, B., van der Schee, M., de Lange, G., Ellam, R., Govers, R., Gutjahr, M., Hilgen, F., Kouwenhoven, T., Lofi, J., Meijer, P., Sierro, F.J., Bachiri, N., Barhoun, N., Alami, A.C., Chacon, B., Flores, J.A., Gregory, J., Howard, J., Lunt, D., Ochoa, M., Pancost, R., Vincent, S., Yousfi, M.Z., 2015. Evolution of the Late Miocene Mediterranean–Atlantic gateways and their impact on regional and global environmental change. Earth-Science Reviews 150, 365–392.

Flood, R.D., Giosan, L., 2002. Migration history of a fine-grained abyssal sediment wave on the Bahama Outer Ridge. Marine Geology 192, 259–273.

Friocourt, Y., Levier, B., Speich, S., Blanke, B., Drijfhout, S.S., 2007. A regional numerical ocean model of the circulation in the Bay of Biscay. Journal of Geophysical Research: Oceans 112, C09008.

Frouin, R., Fiúza, A.F.G., Ambar, I., Boyd, T.J., 1990. Observations of a poleward surface current off the coasts of Portugal and Spain during winter. Journal of Geophysical Research: Oceans 95, 679–691.

García, M., Hernández-Molina, F.J., Alonso, B., Vázquez, J.T., Ercilla, G., Llave, E., Casas, D., 2016. Erosive sub-circular depressions on the Guadalquivir Bank (Gulf of Cadiz): Interaction between bottom current, mass-wasting and tectonic processes. Marine Geology 378, 5–19.

Gardner, J. V, Prior, D.B., Field, M.E., 1999. Humboldt Slide — a large shear-dominated retrogressive slope failure. Marine Geology 154, 323–338.

Gascard, J.-C., Clarke, R.A., 1983. The Formation of Labrador Sea Water. Part II. Mesoscale and Smaller-Scale Processes. Journal of Physical Oceanography 13, 1779–1797.

Gaudin, M., Mulder, T., Cirac, P., Berne, S., Imbert, P., 2006. Past and present sedimentary activity in the Capbreton Canyon, southern Bay of Biscay. Geo-Marine Letters 26, 331–345.

Gómez-Ballesteros, M., Druet, M., Muñoz, A., Arrese, B., Rivera, J., Sánchez, F., Cristobo, J., Parra, S., García-Alegre, A., González-Pola, C., Gallastegui, J., Acosta, J., 2014. Geomorphology of the Avilés Canyon System, Cantabrian Sea. Deep Sea Research Part II: Topical Studies in Oceanography 106, 99–117.

González-Pola, C., Díaz del Río, G., Ruiz-Villarreal, M., Sánchez, R.F., Mohn, C., 2012. Circulation patterns at Le Danois Bank, an elongated shelf-adjacent seamount in the Bay of Biscay. Deep Sea Research Part I: Oceanographic Research Papers 60, 7–21.

Haynes, R., Barton, E.D., 1990. A poleward flow along the Atlantic coast of the Iberian peninsula. Journal of Geophysical Research: Oceans 95, 11425–11441.

Hernández-Molina, F.J., Llave, E., Ercilla, G., Maestro, A., Medialdea, T., Ferrin, A., Somoza, L., Gràcia, E., Masson, D.G., García, M., Vizcaino, A., León, R., 2008. Recent sedimentary processes in the Prestige site area (Galicia Bank, NW Iberian Margin) evidenced by high-resolution marine geophysical methods. Marine Geology 249, 21–45.

Hernández-Molina, F.J., Llave, E., Preu, B., Ercilla, G., Fontan, A., Bruno, M., Serra, N., Gomiz, J.J., Brackenridge, R.E., Sierro, F.J., Stow, D.A. V, García, M., Juan, C., Sandoval, N., Arnaiz, A., 2014. Contourite processes associated with the Mediterranean Outflow Water after its exit from the Strait of Gibraltar: Global and conceptual implications. Geology 42, 227–230.

Hernández-Molina, F.J., Paterlini, M., Somoza, L., Violante, R., Arecco, M.A., de Isasi, M., Rebesco, M., Uenzelmann-Neben, G., Neben, S., Marshall, P., 2010. Giant mounded drifts in the Argentine Continental Margin: Origins, and global implications for the history of thermohaline circulation. Marine and Petroleum Geology 27, 1508–1530.

Hernández-Molina, F.J., Wåhlin, A., Bruno, M., Ercilla, G., Llave, E., Serra, N., Rosón, G., Puig, P., Rebesco, M., Van Rooij, D., Roque, D., González-Pola, C., Sánchez, F., Gómez, M., Preu, B., Schwenk, T., Hanebuth, T.J.J., Sánchez Leal, R.F., García-Lafuente, J., Brackenridge, R.E., Juan, C., Stow, D.A. V, Sánchez-González, J.M., 2016. Oceanographic processes and morphosedimentary products along the Iberian margins: A new multidisciplinary approach. Marine Geology 378, 127–156.

Holland, W.R., 1972. Baroclinic and topographic influences on the transport in western boundary currents. Geophysical Fluid Dynamics 4, 187–210.

Iglesias, J., 2009. Sedimentation on the cantabrian continental margin from late oligocene to quaternary. Unpublished PhD Thesis.

Iorga, M.C., Lozier, M.S., 1999a. Signatures of the Mediterranean outflow from a North Atlantic climatology 1. Salinity and density fields. Journal of Geophysical Research-Oceans 104, 25985–26009.

Iorga, M.C., Lozier, M.S., 1999b. Signatures of the Mediterranean outflow from a North Atlantic climatology 2. Diagnostic velocity fields. Journal of Geophysical Research-Oceans 104, 26011–26029.

Jackson, L., Hughes, C.W., Williams, R.G., 2006. Topographic Control of Basin and Channel Flows: The Role of Bottom Pressure Torques and Friction. Journal of Physical Oceanography 36, 1786–1805.

Juan, C., Ercilla, G., Javier Hernández-Molina, F., Estrada, F., Alonso, B., Casas, D., García, M., Farran, M., Llave, E., Palomino, D., Vázquez, J.-T., Medialdea, T., Gorini, C., D'Acremont, E., El Moumni, B., Ammar, A., 2016. Seismic evidence of current-controlled sedimentation in the Alboran Sea during the Pliocene and Quaternary: Palaeoceanographic implications. Marine Geology 378, 292–311.

Kaboth, S., Bahr, A., Reichart, G.-J., Jacobs, B., Lourens, L.J., 2016. New insights into upper MOW variability over the last 150 kyr from IODP 339 Site U1386 in the Gulf of Cadiz. Marine Geology 377, 136–145.

Kaboth, S., de Boer, B., Bahr, A., Zeeden, C., Lourens, L.J., 2017. Mediterranean Outflow Water dynamics during the past ~570 kyr: Regional and global implications. Paleoceanography 32, 634–647.

Kvalstad, T.J., Andresen, L., Forsberg, C.F., Berg, K., Bryn, P., Wangen, M., 2005. The Storegga slide: evaluation of triggering sources and slide mechanics. Marine and Petroleum Geology 22, 245–256.

Laberg, J.S., Camerlenghi, A., 2008. Chapter 25 The Significance of Contourites for Submarine Slope Stability, in: Rebesco, M., Camerlenghi, A. (Eds.), Developments in Sedimentology. Elsevier, pp. 537–556.

Laberg, J.S., Stoker, M.S., Dahlgren, K.I.T., Haas, H. de, Haflidason, H., Hjelstuen, B.O., Nielsen, T., Shannon, P.M., Vorren, T.O., van Weering, T.C.E., Ceramicola, S., 2005. Cenozoic alongslope processes and sedimentation on the NW European Atlantic margin. Marine and Petroleum Geology 22, 1069–1088.

Lamb, K.G., 2014. Internal Wave Breaking and Dissipation Mechanisms on the Continental Slope/Shelf. Annual Review of Fluid Mechanics 46, 231–254.

Lavín, A., Valdés, L., Sánchez, F., Abaunza, P., Forest, A., Boucher, J., Lazure, P., Jegou, A.M., 2006. The Bay of Biscay: the encountering of the ocean and the shelf, in: Brink, A.R.R.K.H. (Ed.), The Sea. the President and Fellows of Harvard College, pp. 933–999.

Lazier, J.R.N., 1973. The renewal of Labrador sea water. Deep Sea Research and Oceanographic Abstracts 20, 341–353.

Lee, H.J., Syvitski, J.P.M., Parker, G., Orange, D., Locat, J., Hutton, E.W.H., Imran, J., 2002. Distinguishing sediment waves from slope failure deposits: field examples, including the 'Humboldt slide', and modelling results. Marine Geology 192, 79–104.

Llave, E., Hernandez-Molina, F.J., Somoza, L., Diaz-del Rio, V., Stow, D.A. V, Maestro, A., Alveirinho Dias, J.M., 2001. Seismic stacking pattern of the Faro-Albufeira contourite system (Gulf of Cadiz): a Quaternary record of paleoceanographic and tectonic influences. Marine Geophysical Researches 22, 487–508.

Llave, E., Schönfeld, J., Hernandez-Molina, F.J., Mulder, T., Somoza, L., Diaz-del Rio, V., Sanchez-Almazo, I., 2006. High-resolution stratigraphy of the Mediterranean outflow contourite system in the Gulf of Cadiz during the late Pleistocene: The impact of Heinrich events. Marine Geology 277, 241–262.

Locat, J., Lee, H.J., 2002. Submarine landslides: advances and challenges. Canadian Geotechnical Journal 39, 193–212.

Maldonado, A., Barnolas, A., Bohoyo, F., Escutia, C., Galindo-Zaldívar, J., Hernández-Molina, J., Jabaloy, A., Lobo, F.J., Nelson, C.H., Rodríguez-Fernández, J., Somoza, L., Vázquez, J.-T., 2005. Miocene to Recent contourite drifts development in the northern Weddell Sea. Global and Planetary Change 45, 99–129.

Masson, D.G., Howe, J.A., Stoker, M.S., 2002. Bottom-current sediment waves, sediment drifts and contourites in the northern Rockall Trough. Marine Geology 192, 215–237.

McCartney, M.S., Mauritzen, C., 2001. On the origin of the warm inflow to the Nordic Seas. Progress in Oceanography 51, 125–214.

Mena, A., Francés, G., Pérez-Arlucea, M., Hanebuth, T.J.J., Bender, V.B., Nombela, M.A., 2018. Evolution of the Galicia Interior Basin over the last 60 ka: sedimentary processes and palaeoceanographic implications. Journal of Quaternary Science 33, 536–549.

Miramontes, E., Cattaneo, A., Jouet, G., Garziglia, S., 2016. Implications of Sediment Dynamics in Mass Transport along the Pianosa Ridge (Northern Tyrrhenian Sea), in: Lamarche, G., Mountjoy, J., Bull, S., Hubble, T., Krastel, S., Lane, E., Micallef, A., Moscardelli, L., Mueller, C., Pecher, I., Woelz, S. (Eds.),

Submarine Mass Movements and Their Consequences: 7th International Symposium. Springer International Publishing, Cham, pp. 301–309.

Mosher, D.C., Thomson, R.E., 2002. The Foreslope Hills: large-scale, fine-grained sediment waves in the Strait of Georgia, British Columbia. Marine Geology 192, 275–295.

Muench, R.D., Wåhlin, A.K., Özgökmen, T.M., Hallberg, R., Padman, L., 2009. Impacts of bottom corrugations on a dense Antarctic outflow: NW Ross Sea. Geophysical Research Letters 36.

Muñoz, J.A., 2002. The pyrenees. The geology of Spain 370–385.

Palomino, D., López-González, N., Vázquez, J.-T., Fernández-Salas, L.-M., Rueda, J.-L., Sánchez-Leal, R., Díaz-del-Río, V., 2016. Multidisciplinary study of mud volcanoes and diapirs and their relationship to seepages and bottom currents in the Gulf of Cádiz continental slope (northeastern sector). Marine Geology 378, 196–212.

Pingree, R.D., 1993. Flow of surface waters to the west of the British Isles and in the Bay of Biscay. Deep Sea Research Part II: Topical Studies in Oceanography 40, 369–388.

Pingree, R.D., Le Cann, B., 1992. Three anticyclonic slope water oceanic eDDIES (SWODDIES) in the Southern Bay of Biscay in 1990. Deep Sea Research Part A. Oceanographic Research Papers 39, 1147–1175.

Pingree, R.D., Le Cann, B., 1990. Structure, strength and seasonality of the slope currents in the Bay of Biscay region. Journal of the Marine Biological Association of the United Kingdom 70, 857–885.

Pollard, R.T., Griffttths, M.J., Cunningham, S.A., Read, J.F., Pérez, F.F., Ríos, A.F., 1996. Vivaldi 1991 - A study of the formation, circulation and ventilation of Eastern North Atlantic Central Water. Progress in Oceanography 37, 167–192.

Pomar, L., Morsilli, M., Hallock, P., Bádenas, B., 2012. Internal waves, an under-explored source of turbulence events in the sedimentary record. Earth-Science Reviews 111, 56–81.

Preu, B., Hernández-Molina, F.J., Violante, R., Piola, A.R., Paterlini, C.M., Schwenk, T., Voigt, I., Krastel, S., Spiess, V., 2013. Morphosedimentary and hydrographic features of the northern Argentine margin: The interplay between erosive, depositional and gravitational processes and its conceptual implications. Deep Sea Research Part I: Oceanographic Research Papers 75, 157–174.

Preu, B., Schwenk, T., Hernández-Molina, F.J., Violante, R., Paterlini, M., Krastel, S., Tomasini, J., Spieß, V., 2012. Sedimentary growth pattern on the northern Argentine slope: The impact of North Atlantic Deep Water on southern hemisphere slope architecture. Marine Geology 329–331, 113–125.

Rashid, H., MacKillop, K., Sherwin, J., Piper, D.J.W., Marche, B., Vermooten, M., 2017. Slope instability on a shallow contourite-dominated continental margin, southeastern Grand Banks, eastern Canada. Marine Geology 393, 203–215.

Rebesco, M., Camerlenghi, A., Van Loon, A.J., 2008. Chapter 1 Contourite Research: A Field in Full Development, in: Rebesco, M., Camerlenghi, A. (Eds.), Developments in Sedimentology. Elsevier, pp. 1–10.

Rebesco, M., Hernández-Molina, F.J., Van Rooij, D., Wåhlin, A., 2014. Contourites and associated sediments controlled by deep-water circulation processes: State-of-the-art and future considerations. Marine Geology 352, 111–154.

Ribó, M., Puig, P., Muñoz, A., Lo Iacono, C., Masqué, P., Palanques, A., Acosta, J., Guillén, J., Gómez Ballesteros, M., 2016. Morphobathymetric analysis of the large fine-grained sediment waves over the Gulf of Valencia continental slope (NW Mediterranean). Geomorphology 253, 22–37.

Ríos, A.F., Pérez, F.F., Fraga, F., 1992. Water masses in the upper and middle North Atlantic Ocean east of the Azores. Deep Sea Research Part A. Oceanographic Research Papers 39, 645–658.

Roca, E., Muñoz, J.A., Ferrer, O., Ellouz, N., 2011. The role of the Bay of Biscay Mesozoic extensional structure in the configuration of the Pyrenean orogen: Constraints from the MARCONI deep seismic reflection survey. Tectonics 30, TC2001.

Rogerson, M., Rohling, E.J., Bigg, G.R., Ramirez, J., 2012. Paleoceanography of the Atlantic-Mediterranean exchange: Overview and first quantitative assessment of climatic forcing. Reviews of Geophysics 50, RG2003.

Rumín-Caparrós, A., Sanchez-Vidal, A., Calafat, A., Canals, M., Martín, J., Puig, P., Pedrosa-Pàmies, R., 2013. External forcings, oceanographic processes and particle flux dynamics in Cap de Creus submarine canyon, NW Mediterranean Sea. Biogeosciences 10, 3493–3505

Rumín-Caparrós, A., Sanchez-Vidal, A., González-Pola, C., Lastras, G., Calafat, A., Canals, M., 2016. Particle fluxes and their drivers in the Avilés submarine canyon and adjacent slope, central Cantabrian margin, Bay of Biscay. Progress in Oceanography 144, 39–61.

Ruiz, M., Gallart J., Díaz J., Olivera C., Pedreira D., López C., González-Cortina J. M., Pulgar J. A., 2006., Seismic activity at the western Pyrenean edge. Tectonophysics 412, 3–4.

Shanmugam, G., 2013. New perspectives on deep-water sandstones: Implications. Petroleum Exploration and Development 40, 316–324.

Speer, K.G., Gould, J., LaCasce, J., 1999. Year-long float trajectories in the Labrador Sea Water of the eastern North Atlantic Ocean. Deep Sea Research Part II: Topical Studies in Oceanography 46, 165–179.

Stoker, M.S., Hoult, R.J., Nielsen, T., Hjelstuen, B.O., Laberg, J.S., Shannon, P.M., Praeg, D., Mathiesen, A., van Weering, T.C.E., McDonnell, A., 2005. Sedimentary and oceanographic responses to early Neogene compression on the NW European margin. Marine and Petroleum Geology 22, 1031–1044.

Stow, D.A. V, Faugères, J.-C., Howe, J.A., Pudsey, C.J., Viana, A.R., 2002. Bottom currents, contourites and deep-sea sediment drifts: current state-of-the-art. Geological Society, London, Memoirs 22, 7–20.

Stow, D.A. V, Hernández-Molina, F.J., Llave, E., Bruno, M., García, M., Díaz del Rio, V., Somoza, L., Brackenridge, R.E., 2013. The Cadiz Contourite Channel: Sandy contourites, bedforms and dynamic current interaction. Marine Geology 343, 99–114.

Stow, D.A. V, Hunter, S., Wilkinson, D., Hernández-Molina, F.J., 2008. Chapter 9 The Nature of Contourite Deposition, in: Rebesco, M., Camerlenghi, A. (Eds.), Developments in Sedimentology. Elsevier, pp. 143–156.

Stow, D.A. V, Javier Hernández-Molina, F., Llave, E., Sayago, M., 2009. Bedform-velocity matrix: The estimation of bottom current velocity from bedform observations. Geology 37, 327–330.

Sultan, N., Cochonat, P., Canals, M., Cattaneo, A., Dennielou, B., Haflidason, H., Laberg, J.S., Long, D., Mienert, J., Trincardi, F., Urgeles, R., Vorren, T.O., Wilson, C., 2004. Triggering mechanisms of slope instability processes and sediment failures on continental margins: a geotechnical approach. Marine Geology 213, 291–321.

Tugend, J., Manatschal, G., Kusznir, N.J., Masini, E., Mohn, G., Thinon, I., 2014. Formation and deformation of hyperextended rift systems: Insights from rift domain mapping in the Bay of Biscay-Pyrenees. TECTONICS 33, 1239–1276.

Turnewitsch, R., Reyss, J.-L., Chapman, D.C., Thomson, J., Lampitt, R.S., 2004. Evidence for a sedimentary fingerprint of an asymmetric flow field surrounding a short seamount. Earth and Planetary Science Letters 222, 1023–1036.

van Aken, H.M., 2000a. The hydrography of the mid-latitude northeast Atlantic Ocean: I: The deep water masses. Deep Sea Research Part I: Oceanographic Research Papers 47, 757–788.

van Aken, H.M., 2000b. The hydrography of the mid-latitude Northeast Atlantic Ocean: II: The intermediate water masses. Deep Sea Research Part I: Oceanographic Research Papers 47, 789–824.

Van Rooij, D., Blamart, D., Kozachenko, M., Henriet, J.-P., 2007. Small mounded contourite drifts associated with deep-water coral banks, Porcupine Seabight, NE Atlantic Ocean. Geological Society, London, Special Publications 276, 225–244.

Van Rooij, D., Campbell, C., Rueggeberg, A., Wahlin, A., 2016. The contourite log-book: significance for palaeoceanography, ecosystems and slope instability. Marine Geology 378, 1–4.

Van Rooij, D., Iglesias, J., Hernández-Molina, F.J., Ercilla, G., Gomez-Ballesteros, M., Casas, D., Llave, E., De Hauwere, A., Garcia-Gil, S., Acosta, J., Henriet, J.P., 2010. The Le Danois Contourite Depositional System: Interactions between the Mediterranean Outflow Water and the upper Cantabrian slope (North Iberian margin)(Bay of Biscay). Marine Geology 274, 1–20.

Vandorpe, T., Martins, I., Vitorino, J., Hebbeln, D., García, M., Van Rooij, D., 2016. Bottom currents and their influence on the sedimentation pattern in the El Arraiche mud volcano province, southern Gulf of Cadiz. Marine Geology 378, 114–126.

Verdicchio, G., Trincardi, F., 2008. Chapter 20 Shallow-Water Contourites, in: Rebesco, M., Camerlenghi, A. (Eds.), Developments in Sedimentology. Elsevier, pp. 409–433.

Vergés, J., Fernàndez, M., Martìnez, A., 2002. The Pyrenean orogen: pre-, syn-, and post-collisional evolution. Journal of the Virtual Explorer 8, 55–74.

Vissers, R.L.M., Meijer, P.T., 2012. Iberian plate kinematics and Alpine collision in the Pyrenees. Earth-Science Reviews 114, 61–83.

von Lom-Keil, H., Spieß, V., Hopfauf, V., 2002. Fine-grained sediment waves on the western flank of the Zapiola Drift, Argentine Basin: evidence for variations in Late Quaternary bottom flow activity. Marine Geology 192, 239–258.

Weigelt, E., Uenzelmann-Neben, G., 2004. Sediment deposits in the Cape Basin: Indications for shifting ocean currents? AAPG Bulletin 88, 765–780.

Wilson, C.K., Long, D., Bulat, J., 2004. The morphology, setting and processes of the Afen Slide. Marine Geology 213, 149–167.

Wynn, R.B., Masson, D.G., 2008. Chapter 15 Sediment Waves and Bedforms, in: Rebesco, M., Camerlenghi, A. (Eds.), Developments in Sedimentology. Elsevier, pp. 289–300.

Wynn, R.B., Stow, D.A. V, 2002. Classification and characterisation of deep-water sediment waves. Marine Geology 192, 7–22.

Zhang, W., Hanebuth, T.J.J., Stöber, U., 2016. Short-term sediment dynamics on a meso-scale contourite drift (off NW Iberia): Impacts of multi-scale oceanographic processes deduced from the analysis of mooring data and numerical modelling. Marine Geology 378, 81-100.

Chapter 5

Sedimentary evolution of the Le Danois contourite drift systems (southern Bay of Biscay, NE Atlantic): a reconstruction of the Atlantic Mediterranean Water circulation since the Pliocene

---

An edited version of this chapter will be submitted as:

Liu, S., Hernández-Molina, F.J., Ercilla, G., Van Rooij, D., ready to submit. Sedimentary evolution of the Le Danois contourite drift system (southern Bay of Biscay, NE Atlantic): a reconstruction of the Atlantic Mediterranean Water circulation since the Pliocene. *Marine Geology.*

Abstract: The Pliocene-Quaternary evolution of the Le Danois contourite depositional systems (CDS) has been investigated based on high-resolution seismic reflection data. From old to young, six seismic units (U1 to U6), bounded by major discontinuities (H1 to H6) have been identified. Regarding variations of the bottom-current circulation, four evolution stages, including precursor (~5.3 to 3.5-3.0 Ma), initiation (3.5-3.0 to 2.5-2.1 Ma), intermediate (2.5-2.1 to 0.9-0.7 Ma) and drift-growth (0.9-0.7 Ma to present day) stages, of the Le Danois CDS are identified. The CDS associated with the Atlantic Mediterranean Water (AMW) initiated at ~3.5-3.0 Ma and was widely generated and built after the Middle-Pleistocene Transition (MPT; 0.9-07 Ma). From the late Quaternary (~0.47 Ma) onwards, the CDS associated with the Eastern North Atlantic Central Water (ENACW) started to develop in the Le Danois Bank region. In the AMW-related drift system, the Le Danois Drift was generated both in glacial and interglacial climatic conditions. Repeated acoustic cyclicities of the Le Danois Drift in unit 5, consisting of acoustically transparent lower parts, moderate amplitude upper parts and high amplitude erosional surfaces at the top, are compared with glacial/interglacial cycles between Marine Isotope Stage (MIS) 18 to 12. These cyclic features suggest coarsening-upward sequences of the Le Danois Drift, indicating enhanced AMW processes during glacial intervals. The estimated average sedimentation rate of the Le Danois CDS reached a maximum during the MPT (at least ~27 cm/ky) and then decreased until the present-day (~5 cm/ky). The variations of sedimentary stacking pattern and processes of the Le Danois CDS imply a significant influence of the intermediate water mass along the southwest European continental margins from the late Pliocene (~3.5-3.0 Ma) onwards.

Keywords: contourite deposition system; seismic stratigraphy; continental margin evolution; southern Bay of Biscay.

Author contributions: Seismic processing on single channel seismic data was performed by Liu, S.. Seismic interpretation was performed by Liu, S. and Hernández-Molina, F.J. Processed ParaSound and airgun seismic data was provided by Ercilla, G.. Writing was performed by Liu, S. and under supervision of Van Rooij, D.

5.1 Introduction

The Le Danois contourite depositional systems (CDS) are identified in the southern Bay of Biscay (Ercilla et al., 2008; Iglesias, 2009; Van Rooij et al., 2010; Liu et al., 2019), providing a unique opportunity to exam the AMW paleoceanography at the intermediate site. Present-day morphology and bottom-current dynamics have been studied by previous studies (Ercilla et al., 2008; Iglesias, 2009; Liu et al., 2019). The Le Danois CDS are respectively associated with three water masses, being the Eastern North Atlantic Central Water (ENACW), the AMW and the Labrador Sea Water (LSW) (Liu et al., 2019). Topographically constrained morphologies strongly intensify bottom currents, resulting in more frequent spatial variations of the related contourite features (González-Pola et al., 2012; Liu et al., 2019). The seismic stratigraphy of the Le Danois CDS has been addressed as well (Van Rooij et al., 2010), albeit on a relatively small set of seismic profiles. The Le Danois CDS initiated during the early Pliocene and underwent the major growth stage from the late Pliocene onwards (Van Rooij et al., 2010). However, detailed Pliocene-Quaternary sedimentary processes and stacking patterns of the Le Danois CDS, as well as the past circulation patterns of the AMW, are still lack of knowledge.

The location of the Le Danois CDS key for the understanding of the past AMW variability between its proximal and distal sites. Newly acquired seismic data allows us to identify contourite features of the Le Danois CDS in a higher resolution. This work describes the seismic stratigraphy and sedimentary stacking patterns of the Le Danois CDS. The main objectives of this study are: (1) to document the temporal variability of contourite features; (2) to discuss sedimentary processes and evolution of the drift systems; (3) to improve the understanding of past dynamics of intermediate water masses through the late Pliocene to the present day along the Cantabrian continental margin.

5.2 Regional setting

5.2.1 Geological setting

The Le Danois Bank region, located at the Cantabrian continental margin, consists of the intraslope basin, the Le Danois Bank, the Lastres Canyon and the Asturias continental shelf (Figure 2.1). The present-day seafloor morphology of the intraslope basin is linked with the presence of contourite drifts and associated moats (Van Rooij et al., 2010; Liu et al., 2019). Among them, the Le Danois Drift is located between 790 and 1080 m water depth, while the Gijón Drift is located at the

southernmost part of the intraslope basin between 320 m and 1060 m water depth (Liu et al., 2019). Besides these two elongated and mounded drifts, six plastered drifts are respectively recognized along the southern flank of the bank and at the upper continental slope (Liu et al., 2019).

The Le Danois Bank is originated from the Iberian rift and extensional events during the Late Permian (Ries, 1978; Catalán et al., 2007). During the Triassic and the Jurassic, the extension continued, resulting in N-S crustal thrusts (Costa and Rey, 1995). During the Cretaceous, the northward displacement of the African Plate changed plate kinematics and led to the uplift of the Cantabrian Mountains (Gallastegui et al., 2002). After a tectonic stable stage in the Paleocene, the Le Danois Bank and the intraslope basin started to deform due to the shortening of the Northern Iberian margin during the Eocene (Alvarez-Marrón et al., 1996; Cadenas and Fernández-Viejo, 2017). During the Oligocene, crustal shortening of the former continental slope resulted in E-W orientated faults within the intraslope basin (Boillot et al., 1979; Gallastegui et al., 2002; Vissers and Meijer, 2012). From the late Eocene to the early Miocene, former faults and thrust were inverted (Zamora et al., 2017). No major deformation or tectonic activities have been observed since the early Miocene (Figure 2.1b) (Cadenas and Fernandez-Viejo, 2017; Zamora et al., 2017).

5.2.2 Present-day oceanography

The present-day circulation of the Le Danois Bank region is dominated by the ENACW, the AMW and the LSW (Figure 2.1a). The ENACW mainly penetrates eastwards along the Asturias continental slope between 350 to 600 m and forms an anticyclonic circulation along the rim of the eastern summit of the Le Danois Bank (González-Pola et al. 2012). The core of this water mass is centred at 400 m with a minimum salinity of about 35.5 (van Aken, 2000b; Lavín et al., 2006). Below the ENACW and the mixing layer, the warm (9°-10.5° C) and saline (35.7-35.9) AMW flows between 750 to 1550 m, while its core is positioned at 1000 m (Iorga and Lozier, 1999; van Aken, 2000b; Lavín et al., 2006). The AMW mainly penetrates eastwards along the outer (northern) flank of the Le Danois Bank (Lavín et al., 2006; González-Pola et al., 2012). Whereas along the southern flank of the bank, a branch of the AMW flows in a westward direction (González-Pola et al., 2012). Between 1750 and 2000 m water depth, the LSW penetrates westwards below the AMW and the mixing layer (van Aken, 2000a). The core is recognized at 1800 m with a salinity minimum at about 35.05 (Pingree and Le Cann, 1990; van Aken, 2000a). It mainly follows the outer flank of the Le Danois Bank (Lavín et al., 2006). Along the southern foot of the bank, a branch of the LSW flows westwards to the intraslope basin. Compared to the background flow velocities (1-5 cm/s; Iorga and Lozier, 1999), bottom currents from three water masses are strongly enhanced (estimated acceleration up to 25 cm/s) due to the topographic control of the Le Danois Bank (Liu et al., 2019).

5.2.3 AMW paleoceanography

Before the establishment of the present-day oceanographic conditions, the past ENACW, AMW and LSW varied in physical structure, circulation regime and settling depth (Hillaire-Marcel et al., 2001; Voelker et al., 2006; Rogerson et al., 2010; Bahr et al., 2015). At the latest Miocene < 5.33 Ma), the initiation of the present-day Atlantic-Mediterranean exchange resulted in the formation of the MOW (Hernández-Molina et al., 2014). At ~4.5 Ma, the MOW circulated into the Gulf of Cádiz (Hernández-Molina et al., 2014), resulting in the stratification of the ENACW and the MOW/AMW (Jia et al., 2007; Volkov and Fu, 2010). During the late Pliocene (3.2-3.0 Ma) and the early Quaternary (2.4-2.0 Ma), the MOW had enhanced circulation regimes and extended further

(Hayward et al., 2009; Raddatz et al., 2011; Khélifi et al., 2014). At ~1.8 Ma, the LSW was stratified from the North Atlantic Deep Water (NADW) and flowed below the MOW/AMW (Burton et al., 1997). The pathways of these water masses started to resemble modern ones (Raymo et al., 2004; Rogerson et al., 2012).

During the Middle-Pleistocene Transition (MPT, ~1.25-0.7 Ma), the periodicity of climate cycles of the Earth dramatically changed from 41 ky to 100 ky (Maslin and Ridgwell, 2005; Elderfield et al., 2012). The resulting glacial/interglacial fluctuations started to significantly influence the properties and dynamics of these water masses (Friocourt et al., 2007; Kaboth et al., 2016; Bahr et al., 2018). The MOW/AMW was 300-700 m deeper and resulted bottom currents were more vigorous during glacial periods (Rogerson et al., 2005; Voelker et al., 2006; Kaboth et al., 2016). During interglacial periods, the AMW was weaker and was located between 600 and 1000 m water depths (Schönfeld and Zahn, 2000; Rogerson et al., 2005). Increased MOW production promoted the ENACW, in turn resulting in strong ENACW currents (Bahr et al., 2018).

During the middle Pleistocene (~420-396 ka), the ENACW was continuously enhanced during glacial intervals, due to the domination of the Iberian Poleward Current (IPC) (Voelker et al., 2010). However, the MOW/AMW was largely unaffected by glacial-interglacial cycles between ~0.47 Ma and ~0.13 Ma (Kaboth et al., 2017). Whereas the LSW was instable during climate cycles, due to the reduced production of the NADW (Hillaire-Marcel and Bilodeau, 2000). During the Last Glacial Maximum (LGM), the ENACW extended further towards the Bay of Biscay (Bender et al., 2012; Mena et al., 2018). Below the ENACW, the core of the AMW prevailed at a deeper depth (2000 m) due to increased density (Schönfeld and Zahn, 2000). Between 7.5 and 6 ka, the core of the AMW retreated to 1000 m (Schönfeld and Zahn, 2000). Finally, the modern circulation of the ENAWC, the MOW/AMW and the LSW was respectively established at ~15.5 ka, ~7.5-6 ka, ~7 ka (Schönfeld and Zahn, 2000; Hillaire-Marcel et al., 2001; Bender et al., 2012; Mena et al., 2018).

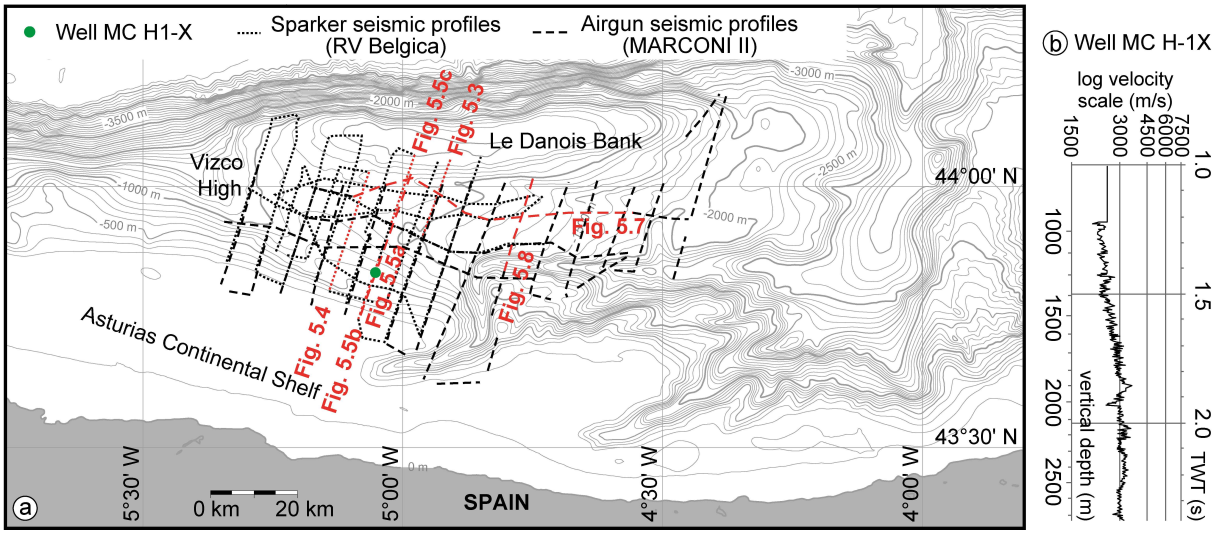

Figure 5.1: (a) Map of the Le Danois Bank area with the indication of: the morphological domains and pathways of the Eastern North Atlantic Central Water (ENACW), the Atlantic Mediterranean Water (AMW) and the Labrador Sea Water (LSW); (b) Tectonic structure modified from Roca et al. (2011). The location of this cross-section is shown in the morphological map (a).

5.3 Methodology

This study is based on single channel sparker and multi-channel airgun reflection seismic data, which were obtained during different projects and cruises (Figure 5.1a). High-resolution single channel seismic data were acquired using a 500 J energy SIG sparker (120 electrodes) during the R/V Belgica cruise ST1118a in 2011. The penetration of the acoustic signal is around 500 ms TWT. The dominant frequency is around 800 Hz and the vertical resolution is about 1.5 m. A total of 27 sparker seismic lines, with a NNE-SSW (12 lines) and W-E to WNW-ESE (15 lines) orientation and with a 3-5 km spacing have been acquired (Figure 2a). Multi-channel airgun seismic data was obtained by a 150 m SIG streamer during the BIO HESPERIDES campaign MARCONI II in 2003. The penetration depth of the acoustic signal varies around 1.5 s TWT. The dominant frequency is around 80 Hz and the vertical resolution is about 4.5 m. A total of 26 airgun seismic lines have been acquired with NNE-SSW (17 lines) and WNW-ESE (9 lines) orientation and a 10-15 km line spacing (Figure 5.1a).

Processing of the seismic data was conducted by the Delph Seismic Plus and the DECO Geophysical RadexPro software. Seismic interpretations are applied using the IHS Kingdom Suite™ package. Seismic reflection travel time between each horizon and the seafloor is gridded to produce thickness isopach maps. A minimum curvature is used as the gridding method to avoid sharp boundaries of sediment bodies resulting from the spacing (3-15 km) of the seismic profiles. Depths have been converted from seconds two-way-travel time to metres by using a velocity model (Figure 5.1b) derived from borehole data (Cadenas and Fernandez-Viejo, 2017). Different depth, namely corresponded to different value of seconds two-way-travel time, are used for the calculation of sedimentation rates.

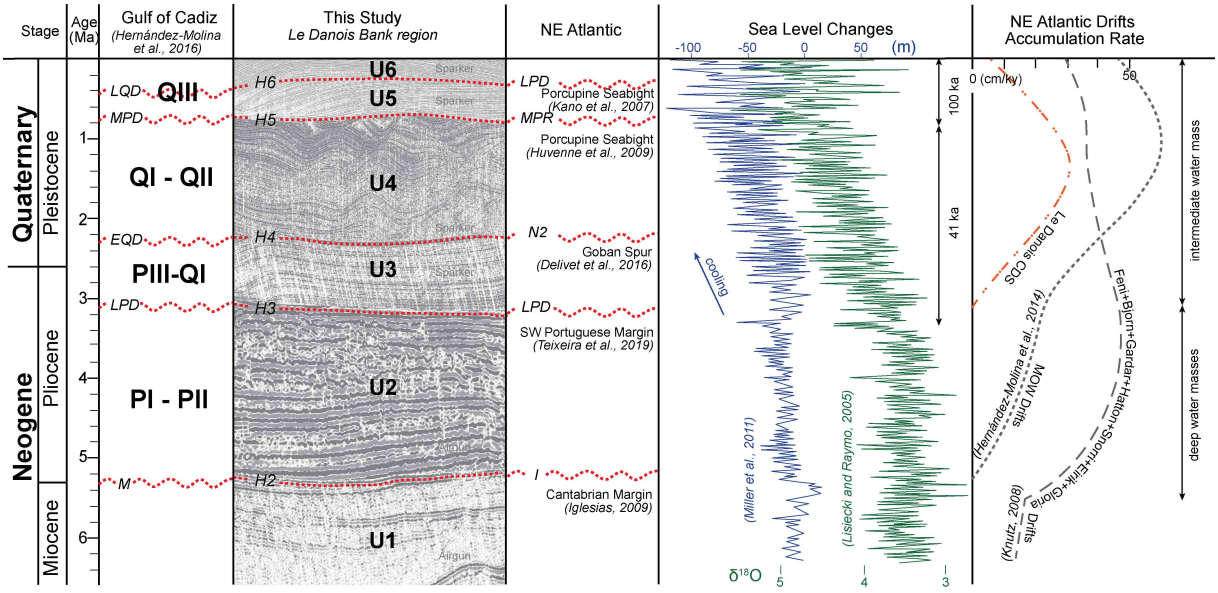

Figure 5.2: Seismic stratigraphic framework of the Le Danois Bank region. Timings of major unconformities are compared with significant hiatuses of the NE Atlantic. Sea-level changes and accumulation rates of the NE Atlantic drifts are indicated as well. Abbreviations for discontinuities (from bottom to top): M=Miocene–Pliocene boundary; LPD=late Pliocene discontinuity; EQD=early Quaternary discontinuity; MPD=Middle Pleistocene discontinuity; LQD=late Quaternary discontinuity.

5.4 Results

5.4.1 Seismic stratigraphic framework

Based on the seismic interpretation of the sparker and airgun seismic profiles, six seismic units (U1 to U6) bounded by major discontinuities (H1 to H6) have been identified from old to young, respectively (Figure 5.2). The penetration of the sparker source (~500 ms TWT, while ~1500 ms TWT for airgun source) inhibits the observation of unit 1 (Figures 5.3, 5.4). Unit 2 could only be recognized within the northern part of the intraslope basin (Figures 5.3, 5.4), whereas both units could be identified in airgun seismic profiles (Figures 5.5a, 5.6, 5.7, 5.8). Below unit 1, several buried structural highs have been observed, characterized by medium-high amplitude chaotic and discontinuous reflections (Figure 5.6). Subunits could hardly be identified in the airgun seismic data due to the reduced vertical resolution (4.5 m) with respect to the sparker seismic profiles (vertical resolution of about 1.5 m).

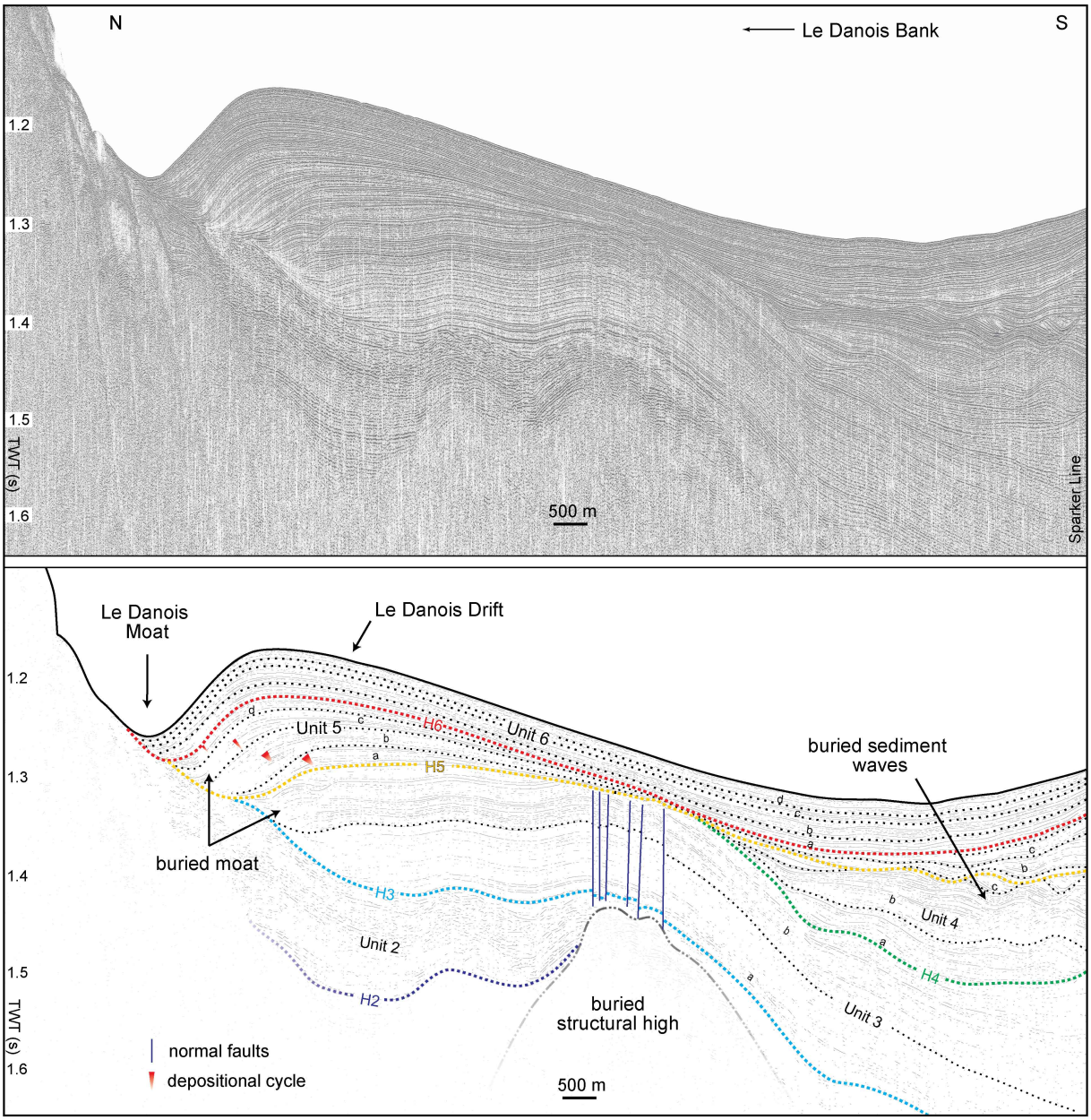

Figure 5.3: Single channel sparker seismic profile and the interpretation, showing 5 units (U2-U6) and associated subunits from the bottom to the top. Relative scales of depositional cycles are indicated by the size of red triangles. The location of this seismic line is displayed in Figure 5.1a. H2=the Miocene top (~5.33 M; dark blue dotted line); H3=late Pliocene discontinuity (~3.5-3.0 Ma; light blue dotted line); H4=early Quaternary discontinuity (~2.5-2.1 Ma; green dotted line); H5=mid Pleistocene discontinuity (~0.9-0.7 Ma; orange dotted line); H6=late Quaternary discontinuity (~0.47 Ma; red dotted line).

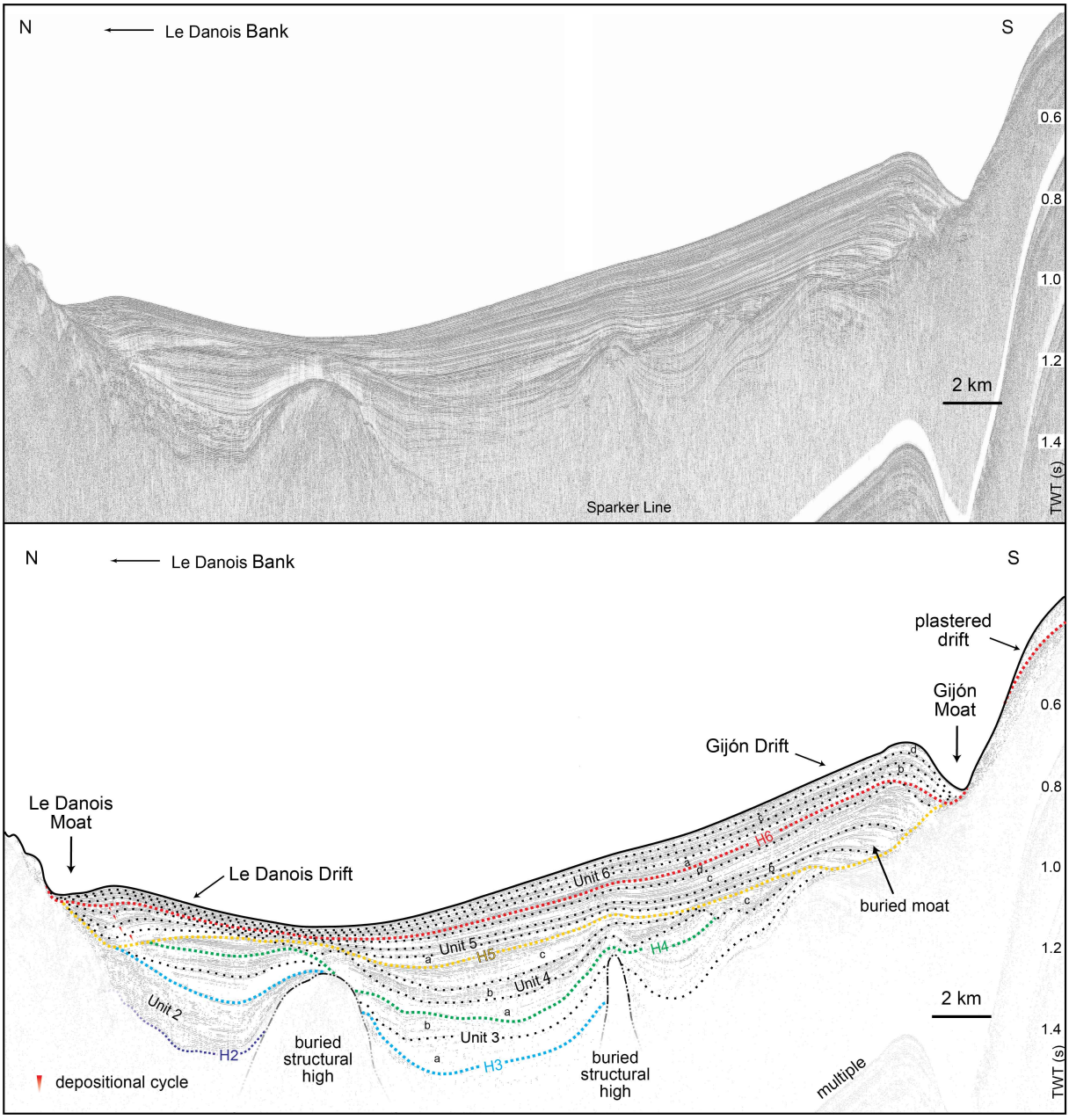

Figure 5.4: Single channel sparker seismic profile and the interpretation, showing 5 units (U2-U6) and associated subunits from the bottom to the top. Relative scales of depositional cycles are indicated by the size of red triangles. The location of this seismic line is displayed in Figure 5.1a. H2=the Miocene top (~5.33 M; dark blue dotted line); H3=late Pliocene discontinuity (~3.5-3.0 Ma; light blue dotted line); H4=early Quaternary discontinuity (~2.5-2.1 Ma; green dotted line); H5=mid Pleistocene discontinuity (~0.9-0.7 Ma; orange dotted line); H6=late Quaternary discontinuity (~0.47 Ma; red dotted line).

5.4.1.1 Unit 1

Unit 1 is bound by H1 at the base. H1 is the unconformity with strong high-amplitude reflections (Figure 5.7). Onlap terminations have been observed onto the basement (H1) of unit 1 (Figure 5.6). The seismic facies of unit 1 consists of low-moderate amplitude, semi-continuous transparent-subparallel reflection configurations (Figure 5.6). This unit mainly distributes in the mini-basins between buried structural highs. The thickness of unit 1 ranges from 250 ms to 350 ms TWT at the intraslope basin centre (Figure 5.7). Towards the Le Danois Bank and the continental shelf, the thickness gradually declines to 20-80 ms TWT.

The depth and the width of the mini-basins vary between 50 to 350 ms TWT and 3.5 to 12.5 km, respectively. Most of these mini-basins are located along the northern and southern boundaries of the Le Danois intraslope basin (Figure 5.6). The largest mini-basin is positioned at the central part of the intraslope basin with a depth of about 350 ms TWT and a width of 12.5 km (Figure 5.4). Additionally, various buried structural highs are located along the southern and northern boundaries of the intraslope basin (Figures 5.3, 5.4, 5.5, 5.8). They have an average length of 10-20 km and a width of 5-6 km (Figure 5.6).

5.4.1.2 Unit 2

Unit 2, characterized by high amplitude, disrupted/semi-continuous chaotic-subparallel reflections, is separated from unit 1 by H2 (Figures 5.3, 5.7). H2 displays strong high-amplitude reflections. At the base of unit 2, onlap terminations towards the Le Danois Bank and buried structural highs are shown (Figure 5.5c), whereas onlap and downlap terminations are shown at the central part of the intraslope basin (Figure 5.5a). Towards the top of unit 2, toplap and truncations have been recognized (Figures 5.4, 5.6). The distribution of this unit is mainly in the mini-basins (Figures 5.5c, 5.6). At the southern and northern parts of the intraslope basin, unit 2 overlies on two buried structural highs (Figures 5.5a, 5.8). The thickness reaches a maximum value of 310 ms TWT at the centre of the Le Danois intraslope basin (Figure 5.5a). Towards the Le Danois Bank, unit 2 gradually loses its expression and the thickness reduces to 10 ms TWT (Figure 5.7).

Figure 5.5: Multi-channel airgun (a) with higher-resolution sections obtained through a single channel sparker (b, c) seismic profile and the interpretation. The boundary of the Miocene-Quaternary and the Eocene-Oligocene units, which is derived from the borehole data (Well MC H1-X), is tentatively correlated with horizon 1. Relative scales of depositional cycles are indicated by the size of red triangles. The location of this seismic line is displayed in Figure 5.1a. H1= the Miocene base (black dotted line); H2=the Miocene top (~5.33 Ma; dark blue dotted line); H3=late Pliocene discontinuity (~3.5-3.0 Ma; light blue dotted line); H4=early Quaternary discontinuity (~2.5-2.1 Ma; green dotted line); H5=mid Pleistocene discontinuity (~0.9-0.7 Ma; orange dotted line); H6=late Quaternary discontinuity (~0.47 Ma; red dotted line).

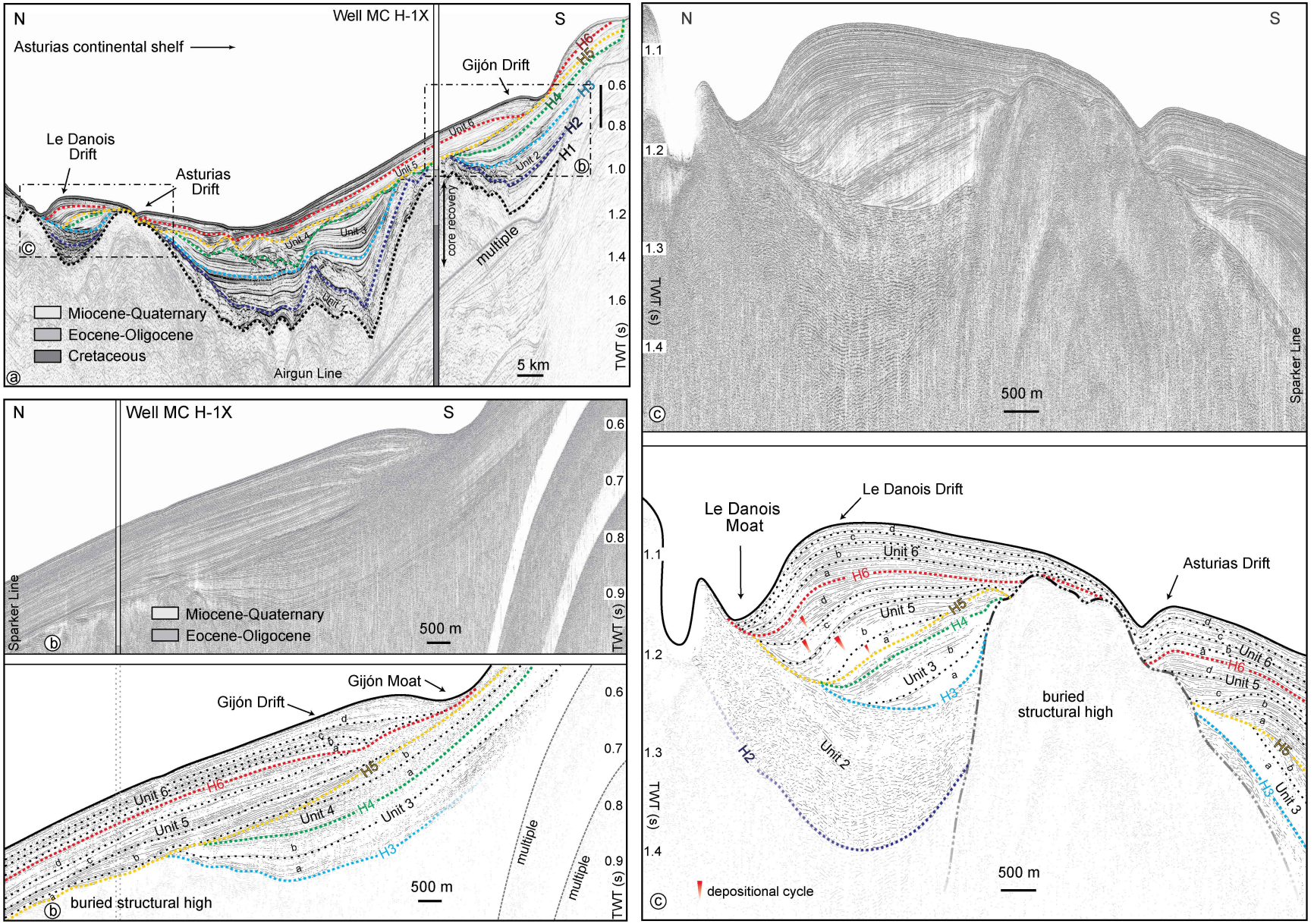
N
Well MC H-1X
S
Asturias continental shelf
Gijón Drift
Le Danois Drift
Asturias Drift
Unit 6
Unit 5
Unit 4
Unit 3
Unit 2
H6
H5
H4
H3
H2
H1
core recovery
multiple
Miocene-Quaternary
Eocene-Oligocene
Cretaceous
Airgun Line
5 km
TWT (s)
Sparker Line
500 m
Gijón Moat
buried structural high
Le Danois Moat
depositional cycle

5.4.1.3 Unit 3

Unit 3 is bound by H3 at its base. H3 is erosional unconformities with high amplitude reflections (Figures 5.3, 5.7). Onlap and downlap terminations have been observed onto H3, while toplap and truncations towards the top of the unit are recognized. Unit 3 displays distinctive geometries at different parts of the intraslope basin. Mounded features with upslope progradation are only identified along the southern foot of the Le Danois Bank, with a thickness of about 200 ms TWT and a width of 5 km (Figure 5.7). At the rest part of the intraslope basin, this unit mainly fills in the mini-basins with subparallel reflectors at the mini-basin centres and divergent features towards buried structural highs (Figure 5.6). At the top of a buried structural high, which is located at the central part of the northern boundary of the Le Danois intraslope basin, continuous subparallel reflections are partly disrupted by fault-like features (Figure 5.3).

Unit 3 consists of two subunits, 3a and 3b, from bottom to top. They are separated through a conformity boundary with a high amplitude reflection (Figure 5.3). Unit 3a is characterized by low-moderate amplitude, continuous subparallel-oblique reflection configurations (Figures 5.3, 5.5c). The thickness is about 70 ms TWT and decreases towards the buried structural highs and the Le Danois Bank. Compared with unit 3a, unit 3b has similar configurations, but higher (moderate-high) amplitude and larger thickness (90-110 ms TWT) (Figure 5.3). At the top of unit 3b, erosional features with truncated configurations are present at the northeast boundary of the intraslope basin (Figures 5.6, 5.8).

5.4.1.4 Unit 4

Unit 4 is bound by H4 at the base and consists of moderate-high amplitude and continuous oblique-subparallel configurations (Figures 5.2, 5.6). Low-angle downlap and onlap terminations are recognized onto H4 at the base, while high-angle truncated terminations are widely observed at the top of unit 4. Almost half of unit 4 is eroded in the intraslope basin (Figures 5.4, 5.6). The associated erosional surfaces are distributed along the southern foot of the Le Danois Bank and the uppermost continental slope, where the scale of the erosions is about 5-7.5 km wide, 68 km long and 7.5-10 km wide, 27 km long, respectively (Figure 5.9d). The total thickness of this unit, therefore, is difficult to calculate. The least eroded part, positioned at the centre of the basin, is about 20-100 ms TWT thick, where internal structures display moderate-high amplitude, semi-continuous wavy configurations (Figure 5.3). The individual wavelength is about 1.5-2 km and the wave height about 10-20 ms TWT. The wavy features migrate towards the upper continental slope. Along the easternmost boundary of the intraslope basin, unit 4, associated with the Lastres canyon, displays different internal structures. Low-moderate amplitude, continuous subparallel configurations and an elongated geometry are observed (Figures 5.6, 5.7). The thickness is larger (varies from 100-240 ms TWT) compared to the wavy section at the basin centre.

On the basis of internal erosive surfaces smaller erosional surfaces and reflection terminations, three subunits, being units 4a, 4b and 4c, are discerned from the bottom to the top of unit 4 (Figure 5.3). These subunits are distributed at the central part of the Le Danois intraslope basin. Unit 4a is less eroded and has a relatively larger thickness compared with units 4b and 4c (Figures 5.3, 5.4). In unit 4b, wavy features are better developed and show moderate amplitude at the centre of the intraslope basin (Figure 5.3). Unit 4c, characterized by high amplitude configurations, are widely eroded and is only present at the basin centre (Figures 5.3, 5.4). The average thickness of these subunits is about 30 ms TWT.

5.4.1.5 Unit 5

H5, marked as the base of unit 5, is the most pronounced erosional unconformity of the entire seismic sequence (Figures 5.4, 5.8, 5.9). Low-angle onlap and downlap onto H5 are observed at its bottom, while low-angle toplap terminations are recognized at the top of unit 5. Along the southeast foot of the Le Danois Bank (Figure 5.8) and the southern flank of a structural high (Figure 5.6c). The Le Danois and Asturias drifts within this unit shows mounded features with an upslope progradation. The thickness is about 100-150 ms TWT and has a lateral reduction towards the west. Whereas along the southwest boundary of the intraslope basin, the thickness is around 120-200 ms TWT and laterally decreases towards the east (Figure 5.9). Three moat-like features are respectively observed associated with a mounded geometry at these locations. They are about 1-2 km wide and 10-50 ms TWT deep. Along the southeast boundary of the intraslope basin, reflection configurations laterally change from subparallel to chaotic. Towards the centre of the basin, progradation and mounded features diminish. The thickness of unit 5 declines towards the E-W trending axis of the intraslope basin and partly drop to 5 ms TWT (Figure 5.4).

Four subunits (units 5a, 5b, 5c, 5d) are respectively present in unit 5 from the bottom to the top. These subunits display similar cyclic features, which consist of an acoustically transparent lower part, a moderate amplitude upper part and a high amplitude erosional surface at the top (Figures 5.3, 5.4). The scale of the cyclicity decreases from units 5a to 5d. The average thickness of unit 5a is around 40 ms TWT. From units 5b towards 5d, the thickness reduces from 50 to 10 ms TWT.

5.4.1.6 Unit 6

Unit 6 is bounded by H6 at the base and the seafloor at the top. H6 is an unconformity with strong high-amplitude reflections. Toplap terminations towards the seafloor, onlap and downlap terminations onto H6 are observed in unit 6. Along the entire southern foot of the Le Danois Bank (Figure 5.8) and the southern flank of a past structure high (Figure 5.6c), mounded features with upslope progradation are observed in unit 6. The thickness at these locations is around 50-100 ms TWT. Mounded geometries are identified along the entire southern boundary of the intraslope basin as well (Figure 5.5, 5.7), where the thickness is calculated as 100-150 ms TWT. Three moat-like features associated with the mounded seismic sequence could be respectively identified at these locations. They are around 1-2 km in width and 10-40 ms TWT in depth. Along the eastern boundary of the intraslope basin, the internal structure of unit 6 is characterized by acoustically transparent-subparallel interbedded configurations (Figure 5.7). These interbedded features extend towards the east and the thickness gradually declines from 150-190 to 50 ms TWT. Along the upper continental slope, the southern flank and the southeast foot of the Le Danois Bank, plastered features with a thickness of 10 ms TWT are identified. Unit 6 consists of four subunits, being units 6a, 6b, 6c, and 6d from the bottom to the top. The thickness of these subunits is constant (20 ms TWT) and the amplitude of reflection configurations has small variations (moderate-high amplitude) (Figure 5.5). Unlike unit 5, no cyclic features are shown in unit 6.

5.4.2 Contourite depositional and erosional features

The Le Danois Drift, encompassing an area of 242 km^2, displays a high mounded geometry, continuous parallel-stratified reflections and a sigmoidal progradational pattern (Figure 5.4). The mean thickness of this drift laterally decreases from 280 to 20 ms TWT towards the south (Figure 5.9). The sedimentary body of the Le Danois Drift consist of units 3, 5 and 6. Whereas the U-shaped profile of the associated Le Danois Moat started to show from unit 3b (Figure 5.6).

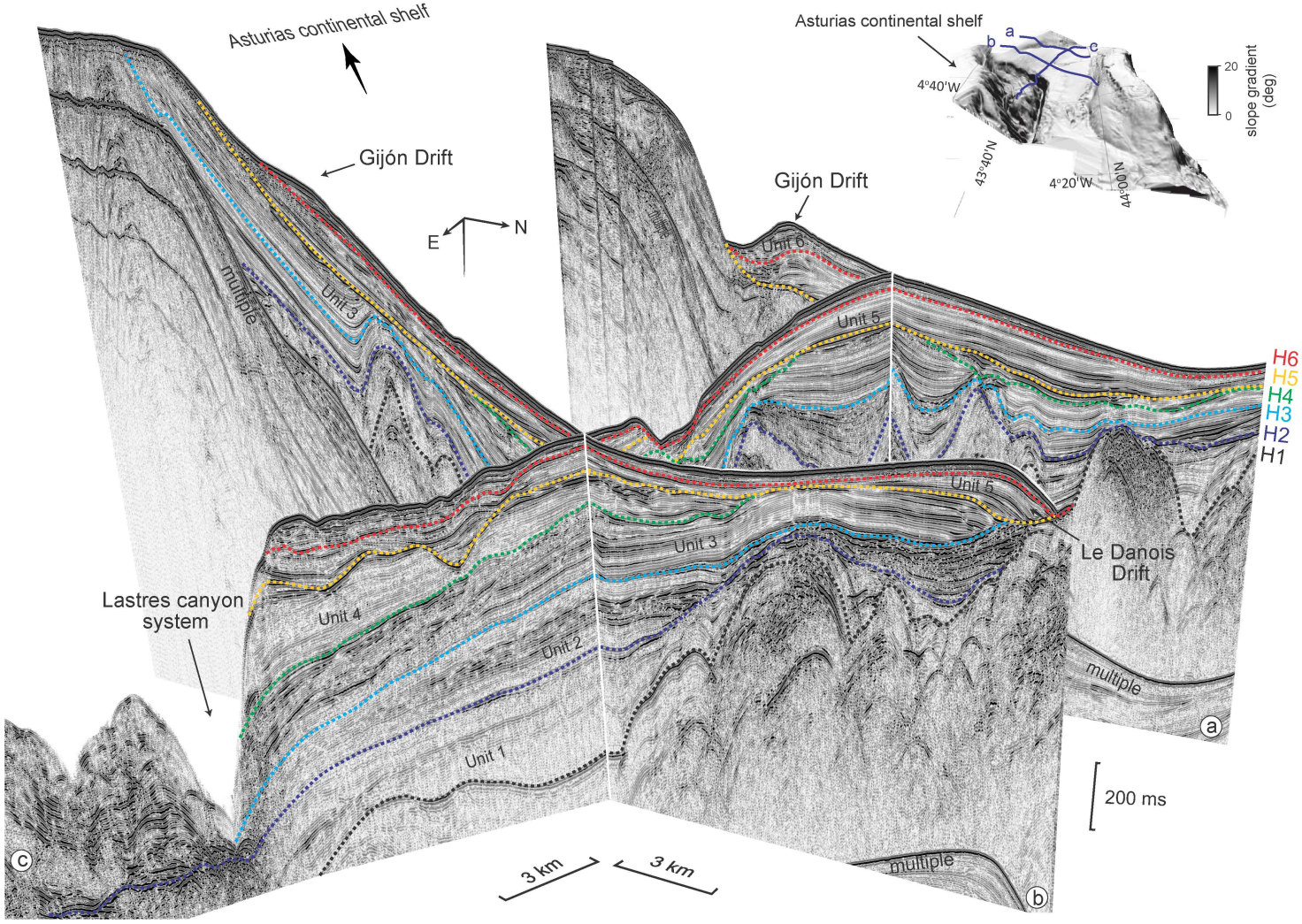

Figure 5.6: Pseudo-3D model of the Gijón and Le Danois Drifts using multi-channel airgun seismic profiles, showing 6 units (U1-U6) from the bottom to the top. Locations of these seismic data are indicated in the slope gradient map. H1= the Miocene base (black dotted line); H2=the Miocene top (~5.33 Ma; dark blue dotted line); H3=late Pliocene discontinuity (~3.5-3.0 Ma; light blue dotted line); H4=early Quaternary discontinuity (~2.5-2.1 Ma; green dotted line); H5=mid Pleistocene discontinuity (~0.9-0.7 Ma; orange dotted line); H6=late Quaternary discontinuity (~0.47 Ma; red dotted line).

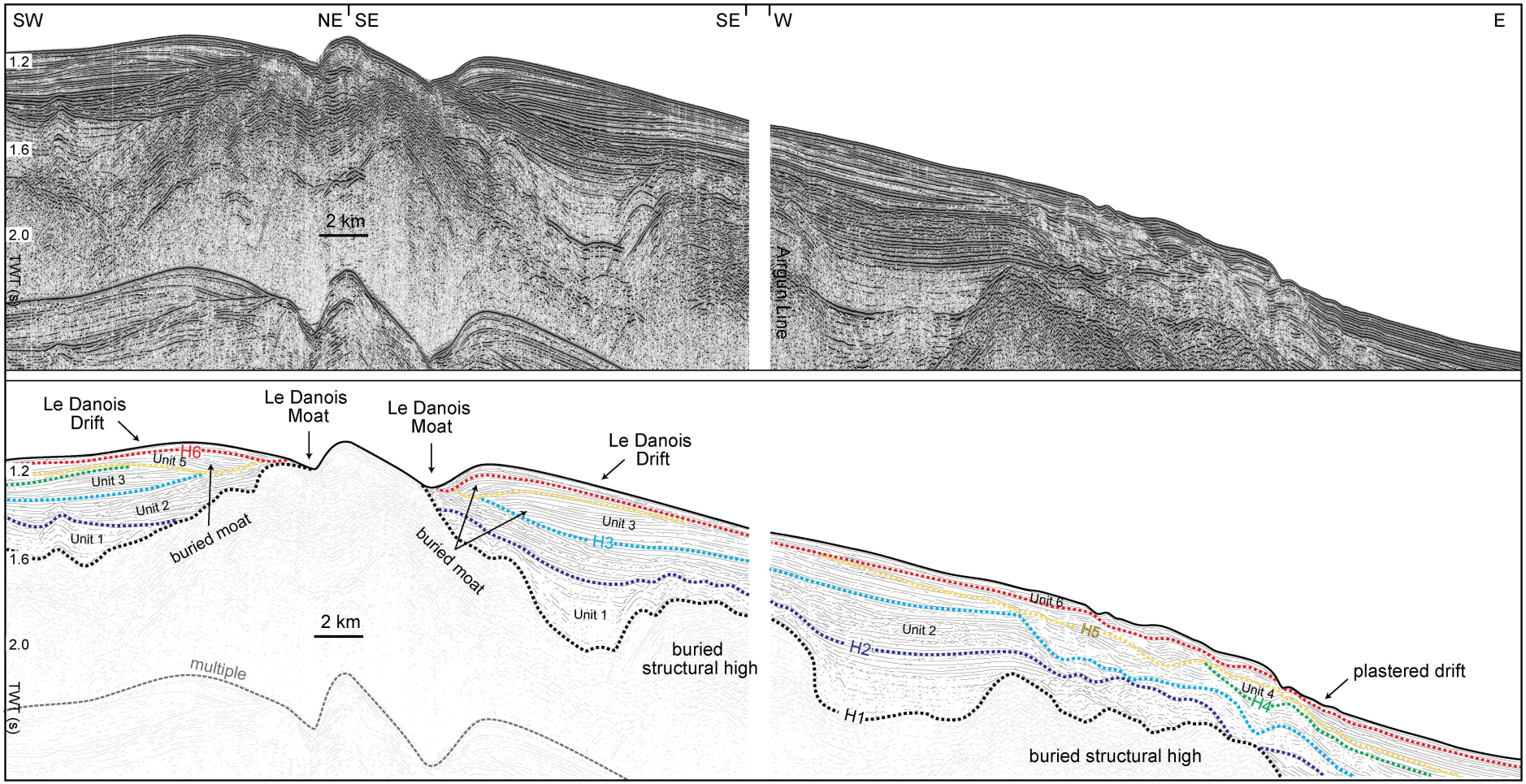

Figure 5.7: Multi-channel airgun seismic profile and the interpretation, showing 6 units (U1-U6) from the bottom to the top. The location of this seismic line is displayed in Figure 2a. H1= the Miocene base (black dotted line); H2=the Miocene top (~5.33 Ma; dark blue dotted line); H3=late Pliocene discontinuity (~3.5-3.0 Ma; light blue dotted line); H4=early Quaternary discontinuity (~2.5-2.1 Ma; green dotted line); H5=mid Pleistocene discontinuity (~0.9-0.7 Ma; orange dotted line); H6=late Quaternary discontinuity (~0.47 Ma; red dotted line).

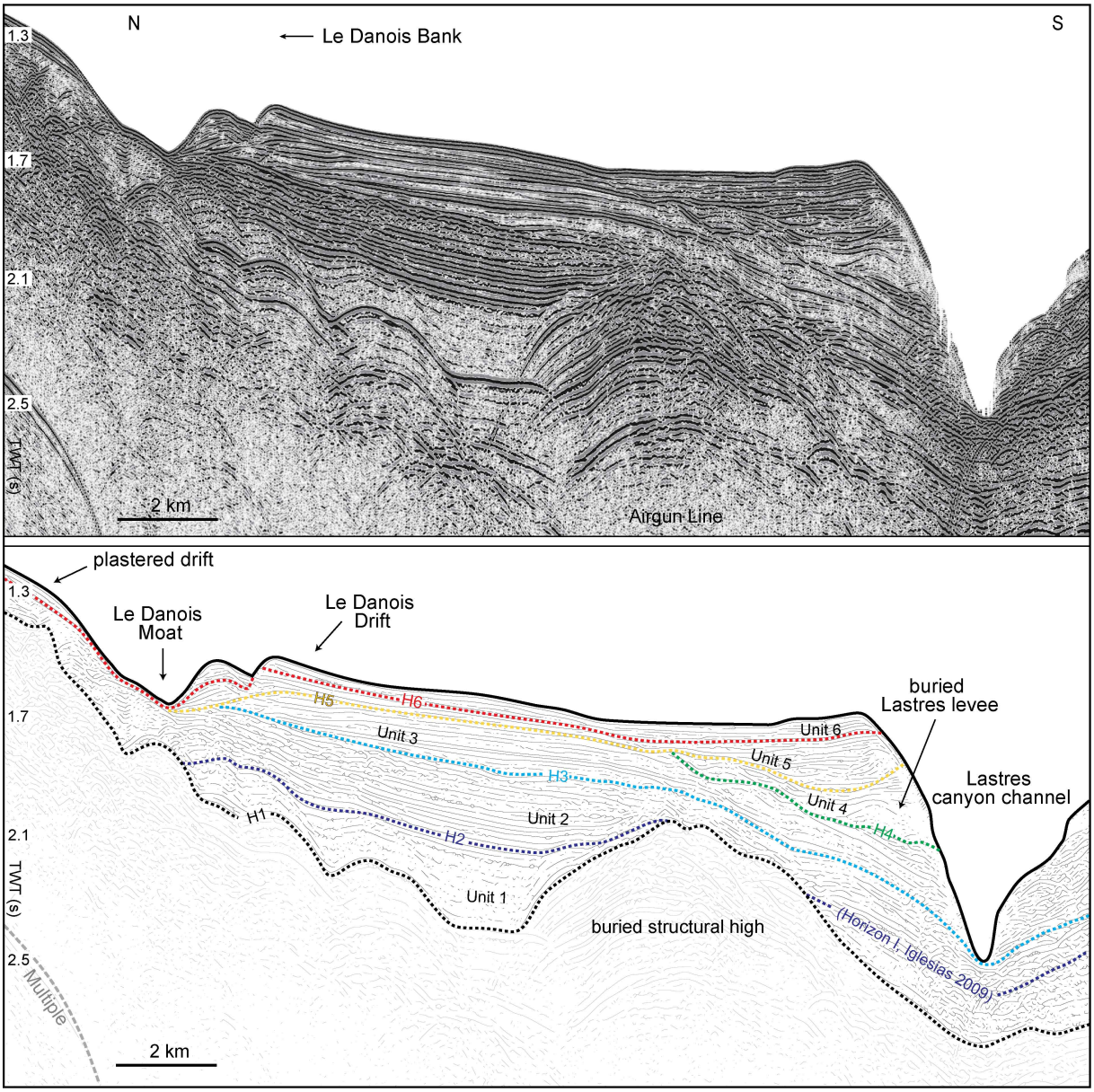

Figure 5.8: Three-channel airgun seismic profile and the interpretation, showing 6 units (U1-U6) from the bottom to the top. The location of this seismic line is displayed in Fig. 2a. H1= the Miocene base (black dotted line); H2=the Miocene top (~5.33 Ma; dark blue dotted line); H3=late Pliocene discontinuity (~3.5-3.0 Ma; light blue dotted line); H4=early Quaternary discontinuity (~2.5-2.1 Ma; green dotted line); H5=mid Pleistocene discontinuity (~0.9-0.7 Ma; orange dotted line); H6=late Quaternary discontinuity (~0.47 Ma; red dotted line).

The Gijón Drift is 34 km long and 2 to 13 km wide. It displays a broad mounded geometry and is composed of unit 5 and 6 (Figure 5.5). The Gijón Drift is characterized by stratified layers of continuous sigmoidal reflections interbedded with discontinuous low-amplitude chaotic reflections (Figure 5.7). Its thickness gradually decreases from 320 to 30 ms TWT towards the southeast (Figure 5.7). The associated Gijón Moat shows an asymmetric U-shape profile and it started to develop in unit 5 (Figure 5.5).

The Asturias Drift is smaller in size, which covers an area of 21 km^2. It displays a sigmoidal-oblique seismic stacking pattern and the maximum thickness is 90 ms TWT, decreasing towards the southwest (Figures 5.6, 5.10). The drift overlies on H5 and consists of units 5 and 6 (Figure 5.6).

All plastered drifts are characterized by sigmoidal reflections draped over the slope (Figures 5.5, 5.9). They overly on H6 and are composed by unit 6 (Figure 5.5).

5.5 Discussion

5.5.1 Chronostratigraphic framework

The tectonic and sedimentary evolution of the Cantabrian continental margin have been described by previous studies, which use borehole log and seismic reflection data to discuss chronostratigraphic framework (Ercilla et al., 2008; Iglesias 2009; Van Rooij et al., 2010; Cadenas and Fernandez-Viejo, 2017). Borehole MC H-1X, the only well located in the intraslope basin (Figure 2a), only recovered sediments with a Cretaceous-Eocene age (Cadenas and Fernandez-Viejo, 2017). The resolution of the borehole data will not allow identifying possible lag or lead with respect to the complete chronostratigraphy from the Cretaceous to the present day. The Pliocene-Quaternary seismic section of the Le Danois intraslope basin mainly consists of erosional and depositional contourite features which are shaped by the AMW (Ercilla et al., 2008; Iglesias 2009). Seismic architectures associated with these features, as well as the occurrence of major unconformities, are linked with the AMW variability since Pliocene times (Van Rooij et al., 2010). Similar variation of seismic characteristics are observed in contourite drifts, CDS or sediment waves in the Gulf of Cádiz (Hernández-Molina et al., 2016), along the SW Portuguese margin (Teixeira et al., 2019), in the Landes Plateau (Faugères et al., 2002), in Goban Spur (Delivet et al., 2016) and Porcupine Seabight (Van Rooij et al., 2007). These regions are namely located along the pathways of the MOW/AMW from the proximal to distal sites (Hernández-Molina et al., 2011). As such, the Pliocene-Quaternary chronostratigraphic framework of the Le Danois Bank region is tentatively correlated with established stratigraphic frameworks from these regions to mark major erosion events and/or changes in circulation patterns of the AMW (Figure 5.2).

5.5.1.1 Horizon 1: Lower Miocene

Based on offshore well logging and seismic reflection data, Cadenas and Fernandez-Viejo (2017) identified the Triassic-Quaternary seismic units. Their study has correlated the well MC H-1X with other boreholes on the continental shelf, indicating a regional late Miocene discontinuity, which is about 1.2 s TWT deep at the location of the well MC H-1x, in the intraslope basin (Cadenas and Fernandez-Viejo, 2017). This regional discontinuity from their study is tentatively correlated with horizon 1 from this study through connecting seismic profiles (Figures 5.6a, b). As such, horizon 1 could be considered as the late Miocene discontinuity.

5.5.1.2 Horizon 2: Upper Miocene

Ercilla et al. (2008) and Iglesias (2009) discussed the Oligocene-Quaternary seismic sequence of the Le Danois Bank region with a higher resolution, compared with studies on tectonic evolution (Gallastegui et al., 2002; Cadenas and Fernandez-Viejo, 2017). Horizon I from their studies is considered as a regional unconformity separating the underlying low-moderate amplitude unit and the overlying high reflective seismic unit. This significant change in seismic facies is related to the occurrence of high-energetic gravity flows and mass-movements at the end of the Miocene (Iglesias, 2009). A similar seismic feature is observed in units 1 and 2 of this study, suggesting similar time intervals (Figure 5.2). Indeed, horizon I is correlated with horizon 2 of this study through the correlation of seismic profiles (Figure 5.2). Therefore, unit 1 is attributed a Miocene age and horizon 2 could be marked as the top of the Miocene.

5.5.1.3 Horizon 3: Late Pliocene

In the intraslope basin, the formation of the Le Danois Drift initiated in unit 3, where the first seismic evidence of mounded features is observed. Previous studies demonstrated the association of the Le Danois Drift to the AMW (Van Rooij et al., 2010). Thus, seismic sections and associated unconformities resulting from the MOW/AMW could be correlated with the ones of the Le Danois Drift. The acoustic responses (low to high amplitude from the base to the top) in Pliocene units of the Cádiz CDS (Llave et al., 2011; Roque et al., 2012; Hernández-Molina et al., 2016; Lofi et al., 2016) and the Sines contourite drift (Teixeira et al., 2019) can be compared with the seismic facies of the Le Danois Drift in unit 3. The basal unconformity, being the LPD (late Pliocene discontinuity, 3.2-3.0 Ma; Hernández-Molina et al., 2016), marked the initiation of mounded contourite drifts in the Cádiz CDS. Additionally, cold-water corals (CWC), fed by food particles transported by the AMW, and associated contourite drifts started to grow and develop upon the RD-1 unconformity in Porcupine CDS during the late Pliocene (Van Rooij et al., 2007; Huvenne et al., 2009). The evidences of AMW enhancement during the late Pliocene are linked with the initiation of the Le Danois Drift. As such, horizon 3 could tentatively be associated with the LPD (Figure 5.3).

5.5.1.4 Horizon 4: Early Quaternary

Besides the LPD, another major erosional unconformity is observed in the Cádiz CDS and Goban Spur (Delivet et al., 2016; Hernández-Molina et al., 2016). Such unconformity, known as the EQD (the early Quaternary discontinuity; at ~2.4-2.0 Ma), was attributed to the second major intensification phase of the MOW/AMW (Llave et al., 2007; Lofi et al., 2016). This stage coincides with the final enhancement of the northern hemisphere glaciation (NHG) during the early Quaternary (Friedrich et al., 2013; Hernández-Molina et al., 2014). Consequently, erosive features are observed along the entire NE Atlantic margins during this time interval (Faugères et al., 2002; Van Rooij et al., 2007; Roque et al., 2012). Horizon 4 is a major erosional unconformity in the Le Danois intraslope basin and could be compared with the EQD due to high reflective seismic facies and associated termination configurations (Figures 5.5, 5.8). Thus, horizon 4 could be considered to have an early Quaternary age.

5.5.1.5 Horizon 5: Middle Pleistocene

In unit 5, contourite drifts with mounded features are widely generated in the intraslope basin. The basal unconformity, being the most pronounced erosional surface (Figure 5.7), could be compared with the ones in the Gulf of Cádiz and Porcupine Seabight (Van Rooij et al., 2007; Huvenne et al., 2009; Llave et al., 2011; Hernández-Molina et al., 2016). These erosional surfaces, resulting from the winnowing of the MOW/AMW, are marked as the MPD (Mid-Pleistocene discontinuity; 0.9-0.7 Ma), associated to the Early-Middle Pleistocene Climate Transition (MPT) (Llave et al., 2011; Huvenne et al., 2009). Since the MPT, changes of global climate cycles with long glaciations and short deglaciations significantly influenced the MOW/AMW regime in the NE Atlantic (Lisiecki and Raymo, 2005; Hernández-Molina et al., 2014). The related third major intensification of the MOW/AMW resulted in widely distributed erosional features, especially in areas adjacent to topographic obstacles and basement highs along the NE Atlantic margins (Van Rooij et al., 2007; Llave et al., 2011; Roque et al., 2012; Hernández-Molina et al., 2016). Similar erosional character is observed in the Le Danois intraslope basin as well (Figure 5.6). As such, horizon 5 could be linked to the MPD.

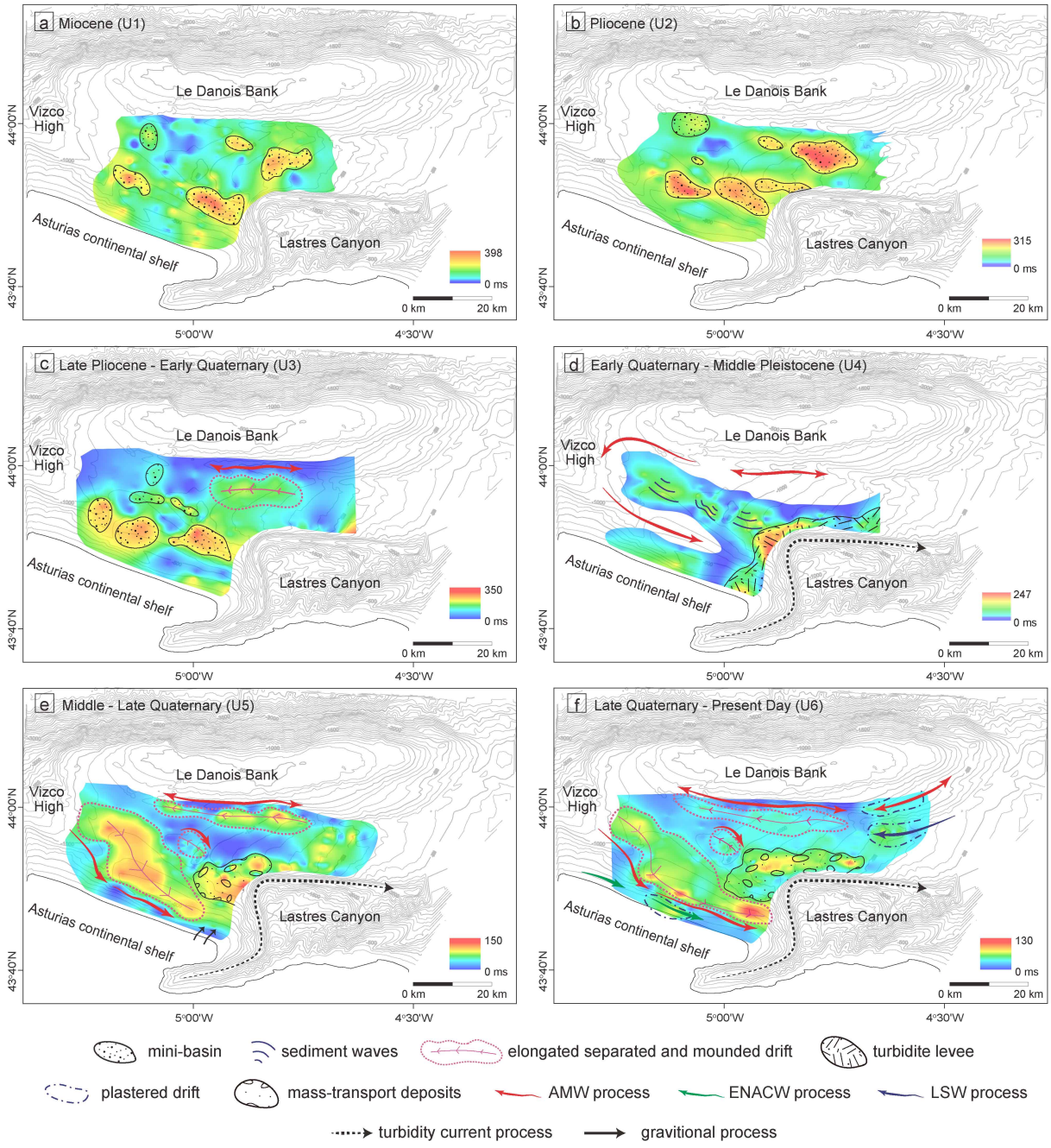

Figure 5.9: Isochore maps of units 1 to 6. The thicknesses are displayed in ms TWT (two-way travel time). Morpho-sedimentary interpretation on sedimentary deposition and associated processes are included.

5.5.1.6 Horizon 6: Late Quaternary

Horizon 6, the youngest major unconformity of this study, could be compared with the ones in the Gulf Cádiz and Porcupine Seabight as well. Where the latest major discontinuity, coinciding with the fourth strengthening stage of the MOW/AMW, is marked as the LQD (late Quaternary discontinuity) (Kano et al., 2007; Hernández-Molina et al., 2016; Lofi et al., 2016). During the late Quaternary, the coldest Pleistocene time interval have been recorded in the Mediterranean Sea at 474–427 ka (MIS 12) (Hughes et al., 2007), suggesting a denser MOW/AMW circulating along the NE Atlantic Ocean (Roque et al., 2012). This MOW/AMW circulation variability is recorded by the erosional unconformity, the LPD, in the Cádiz and Porcupine CDS (Van Rooij et al., 2007; Huvenne et al., 2009; Llave et al., 2011; Hernández-Molina et al., 2016), which display similar seismic facies

compared with horizon 6 (Figures 5.4, 5.5). As a result, horizon 6 could be tentatively correlated with the LQD.

5.5.2 Processes and depositional patterns

Isochore mapping and associated geological interpretation show distinctive depositional patterns and sedimentary processes within each unit (Figure 5.9). Four sedimentary stages of the Pliocene–Quaternary evolution of the Le Danois CDS are identified, regarding variations of the bottom-current circulation. They are respectively marked as pre-drift (units 1 and 2, ~5.3 to 3.5-3.0 Ma), onset (unit 3, 3.5-3.0 to 2.5-2.1 Ma), intermediate (unit 4, 2.5-2.1 to 0.9-0.7 Ma) and drift-growth (units 5 and 6, 0.9-0.7 Ma to present day) stages (Figure 5.10).

5.5.2.1 Pre-drift Stage (Miocene-late Pliocene)

In the Le Danois intraslope basin, the Miocene to late Pliocene deposits of units 1 and 2 mainly filled in mini-basins locating between buried structural highs (Figures 5.9a, b, 5.10a). Transparent acoustic features of these units are interpreted as pelagic or hemipelagic deposits. Muddy contourite drifts can show transparent seismic reflections as well (Stow et al., 2002). However, it is difficult to distinguish hemipelagic deposits from muddy contourites in seismic profiles. The buried structural highs and associated mini-basins were formed by compressional processes along the Cantabrian continental margin during the Eocene and Oligocene (Gallastegui et al., 2002; Zamora et al., 2017). Along the Celtic and Armorican margins in the Bay of Biscay, turbidite depositional systems intensively initiated since the early Miocene tectonic inversion (Bourillet et al., 2006). These turbidite systems were primarily fed by large rivers originated from northern Europe (Auffret et al., 2003; Droz et al., 2003). In the southern Bay of Biscay, however, turbidite systems, sourcing from the Cantabrian and Pyrenees mountains, started to generate only since the Pliocene (Bourillet et al., 2006; Gaudin et al., 2006; Rumín-Caparrós et al., 2016). No channel-levee features or turbidite fans are observed in the Miocene unit, indicating the absence of dominant turbidity currents. The lack of high-energy turbulent currents could lead to the predominant deposition of pelagic or hemipelagic sediments (Bowland, 1993; Soreghan et al., 1999), which possibly make up the sedimentary section of the Miocene unit of this study.

The Miocene-Pliocene transition (horizon 2) marks a significant shift in sedimentary stacking patterns, due to distinctive changes in seismic reflection architecture (Figure 5.7). This transition is coeval with the onset of the MOW at ~5.33 Ma (Llave et al., 2011). However, no mounded contourite features have been observed in unit 2 (Figure 5.5a). In the Gulf of Cádiz, sheeted contourite drifts were generated during the early Pliocene (Roque et al., 2012). One possibility to trigger the absence of contourite drifts in the Le Danois Bank region is the occurrence of active diapirism and uplift of structural highs in the Gulf of Cádiz during this time interval (García et al., 2016; Hernández-Molina et al., 2016), which could change circulation patterns of the AMW in the rest of the NE Atlantic. Additionally, in Goban Spur and Porcupine Seabight, there is no evidence of contourite drifts during this time interval as well (Van Rooij et al., 2007; Delivet et al., 2016). Margin-wide tectonic tilting and erosive processes associated with the enhanced North Atlantic Deep Water (NADW) dominated these regions during the early Pliocene (Stoker et al., 2005; Elliot et al., 2006). In addition, a distinct long-term rise of the MOW production in the NE Atlantic only occurred during the mid-Pliocene (at 3.5 Ma) (Khélifi et al., 2009). Therefore, the AMW may not be able to reach or was relatively weak in the Le Danois Bank region during this stage. Along the southern foot of the Le Danois Bank, the disrupted to semi-continuous chaotic internal structure

of this seismic section could be linked to mass-transport deposits (Figure 5.5c), resulting from regional gravity and debris flows documented by Bourillet et al. (2006).

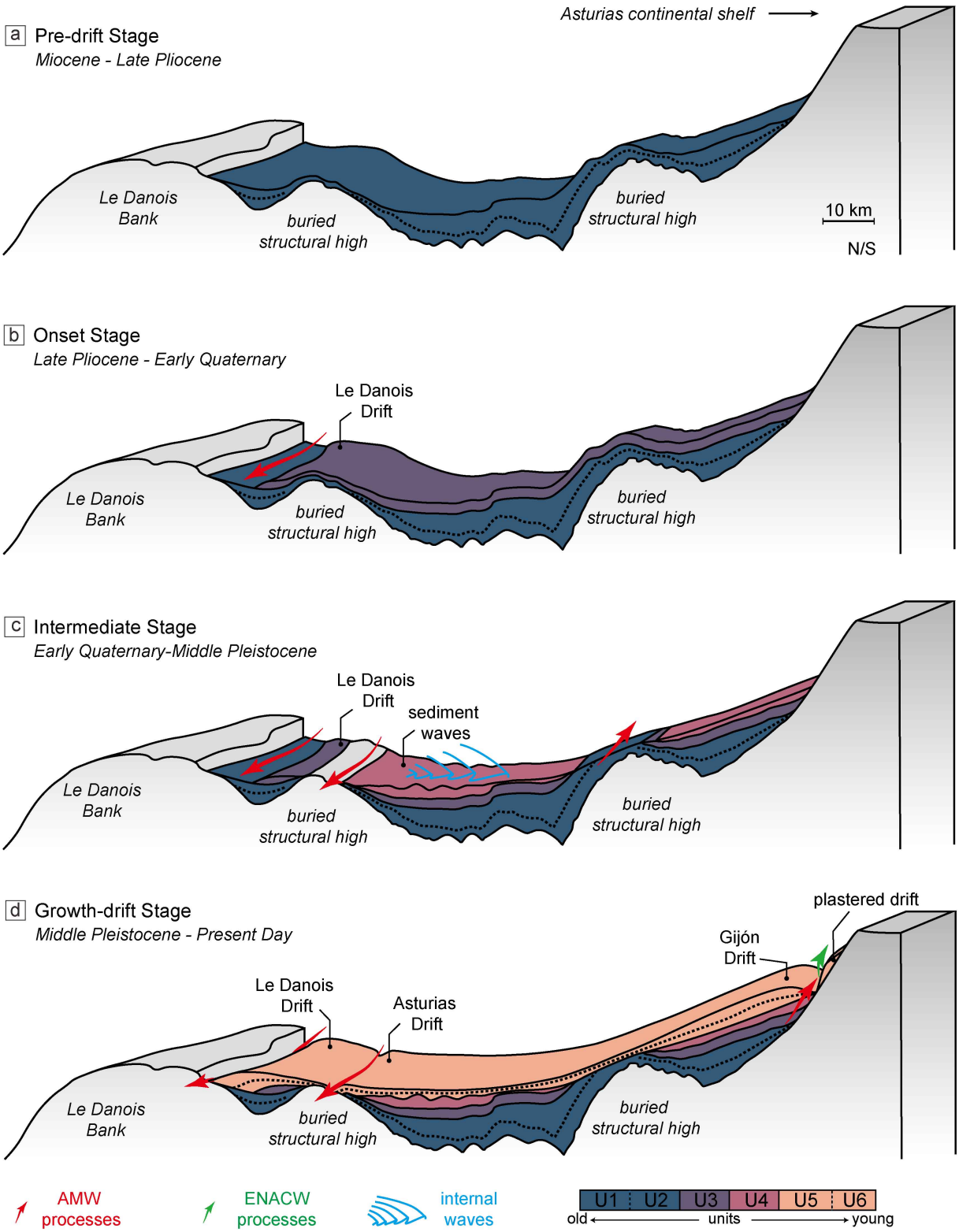

Figure 5.10: Sketch of the Pliocene-Quaternary evolution of the Le Danois CDS, including four stages: a) Pre-drift (~5.3 to 3.5-3.0 Ma); b) onset stage (3.5-3.0 to 2.5-2.1 Ma); c) intermediate stage (2.5-2.1 to 0.9-0.7 Ma); d) growth-drift stage (0.9-0.7 Ma to present day).

5.5.2.2 Onset Stage (late Pliocene-early Quaternary)

In the study area, the onset of the building up of the Le Danois Drift (Figures 5.9c, 5.10b) is coeval with the enhanced stage of the AMW (~3.2-3.0 Ma; Hernández-Molina et al., 2014), indicating effective interactions of the AMW and the Cantabrian continental margin since the late Pliocene. During the late Pliocene, the intensified AMW extended further after exiting the Gulf of Cádiz, whereas the earliest evidence of the AMW is dated at ~3.5-3.3 Ma in Goban Spur (Khélifi et al., 2009). Thus, compared with sediment records of the Gulf of Cádiz and Porcupine Seabight, the full domination of the AMW on the entire southwest European continental margin could be set at ~3.5-3.0 Ma.

In unit 3, a moat-like feature is observed associated with the Le Danois Drift along the southern foot of the Le Danois Bank (Figures 5.3, 5.9c), indicating more focused bottom-current dynamics during this stage. From units 3a to 3b, the mounded nature of the Le Danois Drift gradually increased from the base towards the top. Variation in the geometry of contourite drifts implies different bottom-current conditions, whereas mounded geometry of drifts is associated with bottom currents with higher velocities (Faugères and Stow, 2008; Stow et al., 2009). This temporal change of the geometry, together with the presence of a moat, displays a local enhancement of the AMW, which coincides with the late Pliocene dynamics of the MOW/AMW in the NE Atlantic (Rogerson et al., 2012; Hernández-Molina et al., 2014; Khélifi et al., 2014). During the onset of the widespread NHG, the southward advance of ice-sheets induced cold conditions in the Mediterranean and North Atlantic regions, favouring the formation of a denser MOW (Flesche Kleiven et al., 2002; Becker et al., 2006; Rohling et al., 2014). This variability of the MOW has been recorded by the Cádiz CDS with the presence of distinctive contourite channels and drifts, indicating the pathways of the MOW (Roque et al., 2012). At the distal site of the AMW, the enhanced circulation was accompanied by a flourishing CWC period in Porcupine Seabight (Huvenne et al., 2009). By comparing all these sites along the pathways of the MOW/AMW, the onset of the contourite stage, which is associated with the intermediate water mass, started from the late Pliocene along the southwest European continental margin.

5.5.2.3 Intermediate Stage (early Quaternary-middle Pleistocene)

Widely distributed wavy features in unit 4 indicate the generation of sediment waves (Figure 5.3). The occurrence of sediment waves is generally linked to high energetic current flows, such as turbidity currents, bottom currents or internal waves (Howe, 1996; Marani et al., 1993; Lee et al., 2002; Wynn and Stow, 2002; Ribó et al., 2016; 2018). In the Le Danois Bank region, channel-levee features are observed in unit 4 (Figures 5.6, 5.8), indicating the initiation of the Lastres canyon system and associated turbidity processes (Figure 5.9d). Concentrate turbidity currents (with a velocity of about 42-125 cm/s) could trigger the formation of sediment waves in canyon channels (Wynn et al., 2000; 2002; Mulder and Alexander, 2001). Due to high-energy overspill, sediments could overtop the levee crest and sediment waves may occur on the backslope of levees (Normark et al., 2002; Kane et al., 2010). However, sediment waves observed in the intraslope basin are not associated with the turbidite levee or positioned in canyon channels (Figure 5.3). These sediment waves are about 8-11 km away from the Lastres canyon system (Figure 5.9d). Therefore, other genetic mechanisms need to be suggested, as it is explained next.

Bottom currents are not likely responsible for the formation of these sediment waves as well. Along the southern foot of the Le Danois Bank, unit 4 has been eroded and the early Quaternary AMW pathway is unknown (Figure 5.3). However, the presence of a moat in unit 3 documented

the NW-SE trending pathway of the AMW during the previous stage (Figure 5.9c). Due to the alongslope flowing nature of bottom currents and the orientation of slope morphology, a NW-SE trending AMW flow is suggested. This orientation is parallel to wave crests (NW-SE to W-E orientations) of sediment waves (Figures 5.3, 5.9d), which does not fit with the oblique-perpendicular orientated relationship between flow directions and bottom-current induced sediment waves (Wynn and Masson, 2008).

As such, internal waves could be the only possibility for the occurrence of these sediment waves. During the early Quaternary glacial periods, the AMW core was varied around 1500 m and the MOW/AMW had less stratification, due to the intensive mixing with the North Atlantic water masses (Lebreiro et al., 2015). Mixing of different water masses could significantly trigger the occurrence of pycnoclines, where internal waves propagate along the layers between different densities (Pomar et al., 2012; Ribo et al., 2016). In the intraslope basin, sediment waves (positioned at 1500-1600 m) are located at the depth interval of the glacial AMW during the early Quaternary. The related internal wave processes, which are capable of transporting and depositing sediments (Pomar et al., 2012; Ribó et al., 2016), are possible to generate these sediment waves in the Le Danois intraslope basin. During interglacial periods of this stage, the AMW was well stratified and the core was too shallow (~1100 m; Lebreiro et al., 2015) to reach the seabed of the centre of the intraslope basin. The interface between the AMW and the LSW (1400-1700 m, Delivet et al., 2016), however, could provide a favourable environment for the occurrence of internal waves, in turn generating sediment waves. Similar features have been observed in Goban Spur, where the internal tide regime was promoted by bottom currents and internal waves locating at the AMW/LSW interface induced the formation of sediment waves (positioned at 1300-1600 m) (White, 2006; White and Dorschel, 2010; Delivet et al., 2016). The scales of wave height and length, vertical position and time ranges of these sediment waves are correlated with ones in the study area, suggesting a similar formation mechanism. Compared with the Cádiz CDS, where only mounded contourite drifts were formed during the early Quaternary (Hernández-Molina et al., 2016), the occurrence of sediment waves in the Bay of Biscay indicates regional mixing processes within the glacial AMW and at the interglacial AMW/LSW interface.

At the end of this stage, sediments within the intraslope basin were largely eroded during the middle Pleistocene (Figures 5.7, 5.8, 5.9d). Similar erosional surfaces have almost been observed in all CDS and contourite drifts along the southwest European margins (Van Rooij et al., 2007; Llave et al., 2011). The related extreme erosive activities were resulted from a denser, deeper and enhanced circulation of the MOW/AMW during the MPT (Rohling et al., 2014; Hernández-Molina et al., 2016; Bahr et al., 2018). The intensification of the MOW/AMW may be coeval with the global cooling, sea-level fall, and a particularly strong MOW production from the Mediterranean Sea (Roque et al., 2012; Lofi et al., 2016). Additionally, due to the vigorous AMW flow, previous slope irregularities around past structure highs were significantly eroded in the intraslope basin (Figure 11c). The resulted slope morphology, thus, provided a favourable condition for the wide distribution and growth of contourite drifts in the study area.

5.5.2.4 Growth-drift Stage (middle Pleistocene to present day)

During this stage, the Le Danois CDS exhibited the most pronounced phase for contourite deposition and drift development (Figures 5.9e, f). Besides the Le Danois Drift, the Gijón and the Asturias Drifts with elongated, mounded and separated features namely started to generate along the southern boundary and at the centre of the intraslope basin (Figures 5.5, 5.7). The associated

moats have a more distinctive morphology, indicating more focused bottom currents along the upper continental slope and the Le Danois Bank during this stage.

In units 5 and 6, the vertical position of the Le Danois Moats varied between 1.1-1.85 s TWT (900-1900 m). Based on the vertical glacial (1300-2000 m) and interglacial (600-1000 m) position of the AMW during this stage (Schönfeld and Zahn, 2000; Rogerson et al., 2005; Voelker et al., 2006), the Le Danois Drift was built up by the AMW in both interglacial and glacial periods. Whereas the Gijón and the Asturias Moats, locating at a shallower depth (400-1100 m), are beyond the reach of the glacial AMW and could only be generated during the interglacial climatic conditions. As such, due to the limited depth of the slope morphology, the denser glacial AMW, obstructing by the intraslope basin and failing to penetrate along the seafloor of the basin, only flowed along the southern and northern flank of the Le Danois Bank. During the interglacial intervals, however, the shallower AMW widely interacted with the entire intraslope basin.

In unit 6, a plastered drift (200-500 m), locating within the depth intervals of the ENACW, is identified along the upper continental slope (Figures 5.4, 5.9f). During the coldest Pleistocene time interval (MIS 12), the northward extension of the subtropical front resulted in the domination of the Iberian Poleward Current (IPC), promoting the ENACW along the western and northern Iberian margins (Lambert et al., 2008; Voelker et al., 2010). Eventually, the effective interaction between the ENACW and the Le Danois upper continental slope initiated and generated plastered drifts from the late Quaternary onwards.

Along the southern flank and the southeast foot of the Le Danois Bank, two plastered drifts (1400-1920 m) are observed in unit 6 within the depth range of the present-day LSW (Figures 5.7, 5.8, 5.9f). However, these two drifts are not possibly generated by the LSW. During the late Pleistocene, the polar front was located south of the Labrador Sea, providing an unfavourable condition for the formation of the LSW (Venz et al., 1999). The stable LSW was established only until the early Holocene (Hillaire-Marcel et al., 2001; 2011). As such, these two plastered drifts are most likely formed by the denser glacial AMW, which flowing between 1300-2000 m (Schönfeld and Zahn, 2000) during this stage.

5.5.3 Sedimentary cycles and accumulation rate

In the Le Danois Drift, the sedimentary section of unit 5 displays distinctive cyclic features. This cyclic pattern could be compared with the cyclicity observed in the upper sequences in the Cádiz CDS (Llave et al., 2001; Mestdagh et al., 2019) and the Porcupine CDS (Van Rooij et al., 2003). In the Gulf of Cadiz, the period of low-frequency sedimentary cycles is registered in the range of 95–105 ky, coinciding with the periodicity of glacial/interglacial cycles (100 ky) of the earth since the middle Pleistocene (Elderfield et al., 2012; Lofi et al., 2016). The acoustically transparent lower part and the moderate-high amplitude upper part respectively represent mud and sandy dominated sediments, indicating coarsening-upward sequences (Hernández-Molina et al., 2016; Lofi et al., 2016). This variation is linked to the intensity changes of the MOW/AMW during the interglacial to glacial periods (Rogerson et al., 2005; Voelker et al., 2015). However, no similar cyclic features are observed in the Gijón and the Asturias Drifts (Figures 5.4, 5.5b, c). The difference in the internal structure of the drifts further demonstrated that the Gijón and the Asturias Drifts are resulted from the interglacial-AMW. In unit 6 (after ~0.4 Ma), no cyclic features are shown in the entire Le Danois Bank region. Similar conditions are observed at IODP Site U1386 in the Cádiz CDS, where the upper MOW core was largely unaffected by glacial-interglacial climatic

conditions between ~0.47 and ~0.13 Ma (Kaboth et al., 2017). These features could be related to the interplay of renewed tectonic activity and bottom-current circulation in the Gulf of Cádiz between MIS 13 and 11 (Hernández-Molina et al., 2016).

Based on the thickness of each unit, the related velocity model of time-depth conversion (Figure 5.1b) and the tentative chronostratirgraphy, the accumulation rate of the Le Danois CDS has been calculated (Figure 5.2). During the intermediate stage, unit 3 (200-250 m thick) deposited within ~1 My. The accumulation rate is about 25 cm/ky. During the intermediate stage, the least eroded strata of unit 4 (380 m thick) at the centre of the intraslope basin deposited within ~1.4 My, indicating a rate of at least ~27 cm/ky. During the subsequent growth-drift stage, sedimentation rates of units 5 (50-75 m thick) and 6 (20-50 m thick) are namely within the range of 15-10 and 5-12.5 cm/ky. This characteristic of the Le Danois CDS is compatible with the one of the Cádiz CDS (Llave et al., 2001; Hernández-Molina et al., 2014), where accumulation rates significantly increased since late Pliocene times (~ 3.5-3.0Ma) (Llave et al., 2001; 2011; Hernández-Molina et al., 2016).

In the Cádiz CDS, increased sedimentation rate is coeval with the onset of the present-day contourite features, indicating higher volumes of MOW input into the Atlantic and a rise in sediment supply to offshore depocenters since the late Pliocene (Hernández-Molina et al., 2016). The NE Atlantic drifts, generated at the deeper water depth, developed since Miocene times and have the maximum sedimentation rate during the early Pliocene (Hunter et al., 2007; Knutz, 2008; Müller-Michaelis et al., 2013). Increased sediment supply from meltwater plumes along glacier margins, as well as high NADW production, yielded higher sedimentation rates of the NE Atlantic drifts during the warm Pliocene (Knutz, 2008). By comparing these areas, larger volumes of the intermediate water mass, instead of deep Atlantic water masses, highly influenced sediment transportation in the NE Atlantic from the late Pliocene onwards.

5.6 Conclusion

The Pliocene-Quaternary temporal variability of contourite features and depositional processes of the Le Danois CDS illustrate past bottom-current circulations along the Cantabrian continental margin. The effective interaction of the AMW and the Cantabrian continental margin initiated during the late Pliocene (3.5-3.0 Ma). During the early Quaternary (2.5-0.9 Ma), internal waves resulted from turbulent mixing of water masses induced the occurrence of sediment waves. After the regional winnowing of the AMW (0.9-0.7 Ma), previous topographic irregularities were eroded, providing a favourable condition for the wide distribution and growth of contourite drifts. During the middle Pleistocene (0.9-0.7 to ~0.47 Ma), The denser and deeper AMW only flowed along the flank of the Le Danois Bank and failed to penetrate along the seafloor of the intra-middle slope basin during glacial intervals. Whereas during the interglacial periods, the shallower AMW interacted with the whole intraslope basin. The ENACW started to be involved in generating plastered drifts from the late Quaternary (~0.47 Ma) onwards. By comparison with the Cádiz and Porcupine CDS, the full domination of the MOW/AMW along the entire southwest European continental margin is addressed at ~3.5-3.0 Ma. The major growth-drift stage of the Le Danois CDS is about ~1.0 Ma late compared with the Cádiz CDS. This temporal gap may be related to the vertical position of the Le Danois CDS and regional mixing processes in the Bay of Biscay.

The cyclic features within the Le Danois Drift are coeval with enhanced AMW processes during MIS 18, 16, 14 and 12 in the southern Bay of Biscay. However, these repeated depositional

structures lost their expression after the late Quaternary (~0.47 Ma). This change could be linked to the interplay of the MOW and renewed tectonic activity in the Gulf of Cádiz between MIS 13 and 11. In addition, the sedimentation rate of the Le Danois CDS reached its maximum during the mid-Pleistocene and decreased afterwards. This variation on sedimentation rates suggests the domination of the intermediate water mass on the sediment transportation along the NE Atlantic continental margins from the late Pliocene (3.5-3.0 Ma) onwards.

The CDS is generally individualized on the basis of their regional settings, sediment supply, slope morphology, local behaviour of bottom currents, etc. However, there are many similarities in those CDS which are generated by the same water mass. Tectonic activities occurred near the source area of a water mass could have far-reaching implications on the circulation patterns along its pathways, even at the distal sites. Seafloor morphological features of the CDS could be linked with the present-day oceanography. However, modern water mass may not be involved in the built-up of contourite drifts during the past. Therefore, past circulation patterns and settling depth of the water masses, as well as their responses to the paleoclimate variation, should be considered for the contourite studies.

Acknowledgements

This study was carried out within the framework of a Chinese Scholarship Council "CSC Grant" (201506410062). This study built on achievements of project ESF Euromargins MOUNDFORCE, EC FP5 RTN EURODOM and EC FP6 HERMES 626 (GOCE-CT-2005-511234-1). The research cruises namely framed within the ECOMARG (REN2002-624 00916/MAR) and MARCONI (REN2001-1734 C03-01/M) projects. Shiptime RV Belgica was provided by BELSPO and RBINS–OD Nature. This study was conducted in collaboration with "The Drifters Research Group" of the Royal Holloway University of London (UK) and it is related to the projects CTM 2012-39599-C03, CGL2016-80445-R, and CTM2016-75129-C3-1-R (REN2001-1734 C03-01/M). It was also carried out in collaboration with the Continental Margins Group-GMC from ICM-CSIC (Spain) and its related Spanish projects (CTM2008-06399-C04-04/MAR; CTM2012-39599-CO3-O3; CMT2015-65461-C2-R (MINEICO/FEDER).

References

Alvarez-Marrón, J., Pérez-Estaún, A., Danñobeitia, J.J., Pulgar, J.A., Martínez, Catalán, J.R., Marcos, A., Bastida, F., Ayarza, Arribas, P., Aller, J., Gallart, A., Gonzalez-Lodeiro, F., Banda, E., Comas, M.C., Córdoba, D., 1996. Seismic structure of the northern continental margin of Spain from ESCIN deep seismic profiles. Tectonophysics 264, 153-174.

Auffret, G.A., Le Suavé, R., Garlan, T., Bourillet, J.F., Henriet, J.P., Zaragosi, S., Voisset, M., Lucas, S., 2003. The Celtic and Armorican Margins — a New View, in: Mienert, J., Weaver, P. (Eds.), European Margin Sediment Dynamics: Side-Scan Sonar and Seismic Images. Springer Berlin Heidelberg, Berlin, Heidelberg, pp. 223-228.

Bahr, A., Kaboth, S., Hodell, D., Zeeden, C., Fiebig, J., Friedrich, O., 2018. Oceanic heat pulses fueling moisture transport towards continental Europe across the mid-Pleistocene transition. Quaternary Science Reviews 179, 48-58.

Bahr, A., Kaboth, S., Jiménez-Espejo, F.J., Sierro, F.J., Voelker, A.H.L., Lourens, L., Röhl, U., Reichart, G.J., Escutia, C., Hernández-Molina, F.J., Pross, J., Friedrich, O., 2015. Persistent monsoonal forcing of Mediterranean Outflow Water dynamics during the late Pleistocene. Geology 43, 951-954.

Bender, V.B., Hanebuth, T.J.J., Mena, A., Baumann, K.-H., Francés, G., von Dobeneck, T., 2012. Control of sediment supply, palaeoceanography and morphology on late Quaternary sediment dynamics at the Galician continental slope. Geo-Marine Letters 32, 313-335.

Boillot, G., Dupeuble, P.A., Malod, J., 1979. Subduction and tectonics on the continental margin off northern Spain. Marine Geology 32, 53-70.

Bourillet, J.F., Zaragosi, S., Mulder, T., 2006. The French Atlantic margin and deep-sea submarine systems Geo-Marine Letters 26, 311-315.

Bowland, C.L., 1993. Depositional history of the western Colombian Basin, Caribbean Sea, revealed by seismic stratigraphy. GSA Bulletin 105, 1321-1345.

Burton, K.W., Ling, H.-F., O'Nions, R.K., 1997. Closure of the Central American Isthmus and its effect on deep-water formation in the North Atlantic. Nature 386, 382.

Cadenas, P., Fernández-Viejo, G., 2017. The Asturian Basin within the North Iberian margin (Bay of Biscay): seismic characterisation of its geometry and its Mesozoic and Cenozoic cover. Basin Research 29, 521-541.

Catalán, J.R.M., Arenas, R., García, F.D., Cuadra, P.G., Gómez-Barreiro, J., Abati, J., Castiñeiras, P., Fernández-Suárez, J., Martínez, S.S., Andonaegui, P., Clavijo, E.G., Montes, A.D., Pascual, F.J.R., Aguado, B.V., 2007. Space and time in the tectonic evolution of the northwestern Iberian Massif: Implications for the Variscan belt. Geological Society of America Memoirs 200, 403-423.

Costa, S., Rey, P., 1995. Lower crustal rejuvenation and growth during post-thickening collapse: Insights from a crustal cross section through a Variscan metamorphic core complex. Geology 23, 905-908.

Delivet, S., Van Eetvelt, B., Monteys, X., Ribó, M., Van Rooij, D., 2016. Seismic geomorphological reconstructions of Plio-Pleistocene bottom current variability at Goban Spur. Marine Geology 378, 261-275.

Droz, L., Auffret, G.A., Savoye, B., 2003. The Celtic Deep-Sea Fan: Seismic Facies, Architecture and Stratigraphy, in: Mienert, J., Weaver, P. (Eds.), European Margin Sediment Dynamics: Side-Scan Sonar and Seismic Images. Springer Berlin Heidelberg, Berlin, Heidelberg, pp. 233-238.

Elderfield, H., Ferretti, P., Greaves, M., Crowhurst, S., McCave, I.N., Hodell, D., Piotrowski, A.M., 2012. Evolution of Ocean Temperature and Ice Volume Through the Mid-Pleistocene Climate Transition. Science 337, 704-709.

Elliott, G.M., Shannon, P.M., Haughton, P.D.W., Praeg, D., O'Reilly, B., 2006. Mid- to Late Cenozoic canyon development on the eastern margin of the Rockall Trough, offshore Ireland. Marine Geology 229, 113-132.

Ercilla, G., García-Gil, S., Estrada, F., Gràcia, E., Vizcaino, A., Váquez, J.T., Díaz, S., Vilas, F., Casas, D., Alonso, B., Dañobeitia, J., Farran, M., 2008. High-resolution seismic stratigraphy of the Galicia Bank Region and neighbouring abyssal plains (NW Iberian continental margin). Marine Geology 249, 108-127.

Faugères, J.-C., Gonthier, E., Mulder, T., Kenyon, N., Cirac, P., Griboulard, R., Berné, S., Lesuavé, R., 2002. Multi-process generated sediment waves on the Landes Plateau (Bay of Biscay, North Atlantic). Marine Geology 182, 279-302.

Faugères, J.C., Stow, D.A.V., 2008. Chapter 14 Contourite Drifts: Nature, Evolution and Controls, in: Rebesco, M., Camerlenghi, A. (Eds.), Developments in Sedimentology. Elsevier, pp. 257-288.

Flesche Kleiven, H., Jansen, E., Fronval, T., Smith, T.M., 2002. Intensification of Northern Hemisphere glaciations in the circum Atlantic region (3.5–2.4 Ma) – ice-rafted detritus evidence. Palaeogeography, Palaeoclimatology, Palaeoecology 184, 213-223.

Friedrich, O., Wilson, P.A., Bolton, C.T., Beer, C.J., Schiebel, R., 2013. Late Pliocene to early Pleistocene changes in the North Atlantic Current and suborbital-scale sea-surface temperature variability. Paleoceanography 28, 274-282.

Gallastegui, J., Pulgar, J.A., Gallart, J., 2002. Initiation of an active margin at the North Iberian continent-ocean transition. Tectonics 21, 15-11-15-14.

García, M., Hernández-Molina, F.J., Alonso, B., Vázquez, J.T., Ercilla, G., Llave, E., Casas, D., 2016. Erosive sub-circular depressions on the Guadalquivir Bank (Gulf of Cadiz): Interaction between bottom current, mass-wasting and tectonic processes. Marine Geology 378, 5-19.

Gaudin, M., Mulder, T., Cirac, P., Berne, S., Imbert, P., 2006. Past and present sedimentary activity in the Capbreton Canyon, southern Bay of Biscay. Geo-Marine Letters 26, 331-345.

González-Pola, C., Díaz del Río, G., Ruiz-Villarreal, M., Sánchez, R.F., Mohn, C., 2012. Circulation patterns at Le Danois Bank, an elongated shelf-adjacent seamount in the Bay of Biscay. Deep Sea Research Part I: Oceanographic Research Papers 60, 7-21.

Hayward, B.W., Sabaa, A.T., Kawagata, S., Grenfell, H.R., 2009. The Early Pliocene re-colonisation of the deep Mediterranean Sea by benthic foraminifera and their pulsed Late Pliocene–Middle Pleistocene decline. Marine Micropaleontology 71, 97-112.

Hernández-Molina, F.J., Llave, E., Preu, B., Ercilla, G., Fontan, A., Bruno, M., Serra, N., Gomiz, J.J., Brackenridge, R.E., Sierro, F.J., Stow, D.A.V., García, M., Juan, C., Sandoval, N., Arnaiz, A., 2014. Contourite processes associated with the Mediterranean Outflow Water after its exit from the Strait of Gibraltar: Global and conceptual implications. Geology 42, 227-230.

Hernández-Molina, F.J., Serra, N., Stow, D.A.V., Llave, E., Ercilla, G., Van Rooij, D., 2011. Along-slope oceanographic processes and sedimentary products around the Iberian margin. Geo-Marine Letters 31, 315-341.

Hernández-Molina, F.J., Sierro, F.J., Llave, E., Roque, C., Stow, D.A.V., Williams, T., Lofi, J., Van der Schee, M., Arnáiz, A., Ledesma, S., Rosales, C., Rodríguez-Tovar, F.J., Pardo-Igúzquiza, E., Brackenridge, R.E., 2016. Evolution of the gulf of Cadiz margin and southwest Portugal contourite depositional system: Tectonic, sedimentary and paleoceanographic implications from IODP expedition 339. Marine Geology 377, 7-39.

Hillaire-Marcel, C., Bilodeau, G., 2000. Instabilities in the Labrador Sea water mass structure during the last climatic cycle. Canadian Journal of Earth Sciences 37, 795-809.

Hillaire-Marcel, C., de Vernal, A., Bilodeau, G., Weaver, A.J., 2001. Absence of deep-water formation in the Labrador Sea during the last interglacial period. Nature 410, 1073.

Hillaire-Marcel, C., de Vernal, A., McKay, J., 2011. Foraminifer isotope study of the Pleistocene Labrador Sea, northwest North Atlantic (IODP Sites 1302/03 and 1305), with emphasis on paleoceanographical differences between its “inner” and “outer” basins. Marine Geology 279, 188-198.

Howe, J.A., 1996. Turbidite and contourite sediment waves in the northern Rockall Trough, North Atlantic Ocean. Sedimentology 43, 219-234.

Hughes, P.D., Woodward, J.C., Gibbard, P.L., 2007. Middle Pleistocene cold stage climates in the Mediterranean: New evidence from the glacial record. Earth and Planetary Science Letters 253, 50-56.

Hunter, S.E., Wilkinson, D., Stanford, J., Stow, D.A.V., Bacon, S., Akhmetzhanov, A.M., Kenyon, N.H., 2007. The Eirik Drift: a long-term barometer of North Atlantic deepwater flux south of Cape Farewell, Greenland. Geological Society, London, Special Publications 276, 245.

Huvenne, V.A.I., Van Rooij, D., De Mol, B., Thierens, M., O’Donnell, R., Foubert, A., 2009. Sediment dynamics and palaeo-environmental context at key stages in the Challenger cold-water coral mound

formation: Clues from sediment deposits at the mound base. Deep Sea Research Part I: Oceanographic Research Papers 56, 2263-2280.

Iglesias, J., 2009. Sedimentation on the cantabrian continental margin from late oligocene to quaternary. Universidade de Vigo, Vigo, p. 185.

Iorga, M.C., Lozier, M.S., 1999a. Signatures of the Mediterranean outflow from a North Atlantic climatology 1. Salinity and density fields. Journal of Geophysical Research-Oceans 104, 25985-26009.

Iorga, M.C., Lozier, M.S., 1999b. Signatures of the Mediterranean outflow from a North Atlantic climatology 2. Diagnostic velocity fields. Journal of Geophysical Research-Oceans 104, 26011-26029.

Jia, Y., Coward, A.C., de Cuevas, B.A., Webb, D.J., Drijfhout, S.S., 2007. A Model Analysis of the Behavior of the Mediterranean Water in the North Atlantic. Journal of Physical Oceanography 37, 764-786.

Kaboth, S., Bahr, A., Reichart, G.-J., Jacobs, B., Lourens, L.J., 2016. New insights into upper MOW variability over the last 150 kyr from IODP 339 Site U1386 in the Gulf of Cadiz. Marine Geology 377, 136-145.

Kaboth, S., de Boer, B., Bahr, A., Zeeden, C., Lourens, L.J., 2017. Mediterranean Outflow Water dynamics during the past ~570 kyr: Regional and global implications. Paleoceanography 32, 634-647.

Kane, I.A., McCaffrey, W.D., Peakall, J., Kneller, B.C., 2010. Submarine channel levee shape and sediment waves from physical experiments. Sedimentary Geology 223, 75-85.

Kano, A., Ferdelman, T.G., Williams, T., Henriet, J.-P., Ishikawa, T., Kawagoe, N., Takashima, C., Kakizaki, Y., Abe, K., Sakai, S., Browning, E.L., Li, X., 2007. Age constraints on the origin and growth history of a deep-water coral mound in the northeast Atlantic drilled during Integrated Ocean Drilling Program Expedition 307. Geology 35, 1051-1054.

Khélifi, N., Frank, M., 2014. A major change in North Atlantic deep water circulation 1.6 million years ago. Clim. Past 10, 1441-1451.

Khélifi, N., Sarnthein, M., Andersen, N., Blanz, T., Frank, M., Garbe-Schönberg, D., Haley, B.A., Stumpf, R., Weinelt, M., 2009. A major and long-term Pliocene intensification of the Mediterranean outflow, 3.5–3.3 Ma ago. Geology 37, 811-814.

Khélifi, N., Sarnthein, M., Frank, M., Andersen, N., Garbe-Schönberg, D., 2014. Late Pliocene variations of the Mediterranean outflow. Marine Geology 357, 182-194.

Knutz, P.C., 2008. Chapter 24 Palaeoceanographic Significance of Contourite Drifts, in: Rebesco, M., Camerlenghi, A. (Eds.), Developments in Sedimentology. Elsevier, pp. 511-535.

Lambert, F., Delmonte, B., Petit, J.R., Bigler, M., Kaufmann, P.R., Hutterli, M.A., Stocker, T.F., Ruth, U., Steffensen, J.P., Maggi, V., 2008. Dust-climate couplings over the past 800,000 years from the EPICA Dome C ice core. Nature 452, 616.

Lavín, A., Valdés, L., Sánchez, F., Abaunza, P., Forest, A., Boucher, J., Lazure, P., Jegou, A.M., 2006. The Bay of Biscay: the encountering of the ocean and the shelf, in: Brink, A.R.R.K.H. (Ed.), The Sea. the President and Fellows of Harvard College, pp. 933-999.

Lebreiro, S.M., Antón, L., Reguera, M.I., Fernández, M., Conde, E., Barrado, A.I., Yllera, A., 2015. Zooming into the Mediterranean outflow fossil moat during the 1.2–1.8millionyears period (Early-Pleistocene) — An approach by radiogenic and stable isotopes. Global and Planetary Change 135, 104-118.

Lee, H.J., Syvitski, J.P.M., Parker, G., Orange, D., Locat, J., Hutton, E.W.H., Imran, J., 2002. Distinguishing sediment waves from slope failure deposits: field examples, including the 'Humboldt slide', and modelling results. Marine Geology 192, 79-104.

Lisiecki, L.E., Raymo, M.E., 2005. A Pliocene-Pleistocene stack of 57 globally distributed benthic δ18O records. Paleoceanography 20.

Liu, S., Van Rooij, D., Vandorpe, T., González-Pola, C., Ercilla, G., Hernández-Molina, F.J., 2019. Morphological features and associated bottom-current dynamics in the Le Danois Bank region (southern Bay of Biscay, NE Atlantic): A model in a topographically constrained small basin. Deep Sea Research Part I: Oceanographic Research Papers 149, 103054.

Llave, E., Hernandez-Molina, F.J., Somoza, L., Diaz-del Rio, V., Stow, D.A.V., Maestro, A., Alveirinho Dias, J.M., 2001. Seismic stacking pattern of the Faro-Albufeira contourite system (Gulf of Cadiz): a Quaternary record of paleoceanographic and tectonic influences. Marine Geophysical Researches 22, 487-508.

Llave, E., Hernandez-Molina, F.J., Somoza, L., Stow, D.A.V., Diaz del Rio, G., 2007. Quaternary evolution of the contourite depositional system in the Gulf of Cadiz, in: Viana, A.R., Rebesco, M. (Eds.), Economic and Palaeoceanographic Significance of Contourite Deposits. Geological Society, London, pp. 49-79.

Llave, E., Matias, H., Hernandez-Molina, F.J., Ercilla, G., Stow, D.A.V., Medialdea, T., 2011. Pliocene-Quaternary contourites along the northern Gulf of Cadiz margin: sedimentary stacking pattern and regional distribution. Geo-Marine Letters 31, 377-390.

Lofi, J., Voelker, A.H.L., Ducassou, E., Hernández-Molina, F.J., Sierro, F.J., Bahr, A., Galvani, A., Lourens, L.J., Pardo-Igúzquiza, E., Pezard, P., Rodríguez-Tovar, F.J., Williams, T., 2016. Quaternary chronostratigraphic framework and sedimentary processes for the Gulf of Cadiz and Portuguese Contourite Depositional Systems derived from Natural Gamma Ray records. Marine Geology 377, 40-57.

Marani, M., Argnani, A., Roveri, M., Trincardi, F., 1993. Sediment drifts and erosional surfaces in the central Mediterranean: seismic evidence of bottom-current activity. Sedimentary Geology 82, 207-220.

Maslin, M.A., Ridgwell, A.J., 2005. Mid-Pleistocene revolution and the 'eccentricity myth'. Geological Society, London, Special Publications 247, 19-34.

Mena, A., Francés, G., Pérez-Arlucea, M., Hanebuth, T.J.J., Bender, V.B., Nombela, M.A., 2018. Evolution of the Galicia Interior Basin over the last 60 ka: sedimentary processes and palaeoceanographic implications. Journal of Quaternary Science 33, 536-549.

Mestdagh, T., Lobo, F.J., Llave, E., Hernández-Molina, F.J., Van Rooij, D., 2019. Review of the late Quaternary stratigraphy of the northern Gulf of Cadiz continental margin: New insights into controlling factors and global implications. Earth-Science Reviews 198, 102944.

Mulder, T., Alexander, J., 2001. The physical character of subaqueous sedimentary density flows and their deposits. Sedimentology 48, 269-299.

Müller-Michaelis, A., Uenzelmann-Neben, G., Stein, R., 2013. A revised Early Miocene age for the instigation of the Eirik Drift, offshore southern Greenland: Evidence from high-resolution seismic reflection data. Marine Geology 340, 1-15.

Normark, W.R., Piper, D.J.W., Posamentier, H., Pirmez, C., Migeon, S., 2002. Variability in form and growth of sediment waves on turbidite channel levees. Marine Geology 192, 23-58.

Pomar, L., Morsilli, M., Hallock, P., Bádenas, B., 2012. Internal waves, an under-explored source of turbulence events in the sedimentary record. Earth-Science Reviews 111, 56-81.

Raddatz, J., Rüggeberg, A., Margreth, S., Dullo, W.-C., 2011. Paleoenvironmental reconstruction of Challenger Mound initiation in the Porcupine Seabight, NE Atlantic. Marine Geology 282, 79-90.

Raymo, M.E., Oppo, D.W., Flower, B.P., Hodell, D.A., McManus, J.F., Venz, K.A., Kleiven, K.F., McIntyre, K., 2004. Stability of North Atlantic water masses in face of pronounced climate variability during the Pleistocene. Paleoceanography 19, PA2008.

Ribó, M., Durán, R., Puig, P., Van Rooij, D., Guillén, J., Masqué, P., 2018. Large sediment waves over the Gulf of Roses upper continental slope (NW Mediterranean). Marine Geology 399, 84-96.

Ribó, M., Puig, P., Muñoz, A., Lo Iacono, C., Masqué, P., Palanques, A., Acosta, J., Guillén, J., Gómez Ballesteros, M., 2016. Morphobathymetric analysis of the large fine-grained sediment waves over the Gulf of Valencia continental slope (NW Mediterranean). Geomorphology 253, 22-37.

Ries, A.C., 1978. The opening of the Bay of Biscay - a review. Earth-Science Reviews 14, 35-63.

Rogerson, M., Colmenero-Hidalgo, E., Levine, R.C., Rohling, E.J., Voelker, A.H.L., Bigg, G.R., Schönfeld, J., Cacho, I., Sierro, F.J., Löwemark, L., Reguera, M.I., de Abreu, L., Garrick, K., 2010. Enhanced Mediterranean-Atlantic exchange during Atlantic freshening phases. Geochemistry, Geophysics, Geosystems 11, Q08013.

Rogerson, M., Rohling, E.J., Bigg, G.R., Ramirez, J., 2012. Paleoceanography of the Atlantic-Mediterranean exchange: Overview and first quantitative assessment of climatic forcing. Reviews of Geophysics 50, RG2003.

Rogerson, M., Rohling, E.J., Weaver, P.P.E., Murray, J.W., 2005. Glacial to interglacial changes in the settling depth of the Mediterranean Outflow plume. Paleoceanography 20, PA3007.

Rohling, E.J., Foster, G.L., Grant, K.M., Marino, G., Roberts, A.P., Tamisiea, M.E., Williams, F., 2014. Sea-level and deep-sea-temperature variability over the past 5.3 million years. Nature 508, 477-482.

Roque, C., Duarte, H., Terrinha, P., Valadares, V., Noiva, J., Cachão, M., Ferreira, J., Legoinha, P., Zitellini, N., 2012. Pliocene and Quaternary depositional model of the Algarve margin contourite drifts (Gulf of Cadiz, SW Iberia): Seismic architecture, tectonic control and paleoceanographic insights. Marine Geology 303–306, 42-62.

Rumín-Caparrós, A., Sanchez-Vidal, A., González-Pola, C., Lastras, G., Calafat, A., Canals, M., 2016. Particle fluxes and their drivers in the Avilés submarine canyon and adjacent slope, central Cantabrian margin, Bay of Biscay. Progress in Oceanography 144, 39-61.

Schönfeld, J., Zahn, R., 2000. Late Glacial to Holocene history of the Mediterranean Outflow. Evidence from benthic foraminiferal assemblages and stable isotopes at the Portuguese margin. Palaeogeography, Palaeoclimatology, Palaeoecology 159, 85-111.

Soreghan, M.J., Scholz, C.A., Wells, J.T., 1999. Coarse-grained, deep-water sedimentation along a border fault margin of Lake Malawi, Africa; seismic stratigraphic analysis. Journal of Sedimentary research 69, 832-846.

Stoker, M.S., Praeg, D., Hjelstuen, B.O., Laberg, J.S., Nielsen, T., Shannon, P.M., 2005. Neogene stratigraphy and the sedimentary and oceanographic development of the NW European Atlantic margin. Marine and Petroleum Geology 22, 977-1005.

Stow, D.A.V., Javier Hernández-Molina, F., Llave, E., Sayago, M., 2009. Bedform-velocity matrix: The estimation of bottom current velocity from bedform observations. Geology 37, 327-330.

Teixeira, M., Terrinha, P., Roque, C., Rosa, M., Ercilla, G., Casas, D., 2019. Interaction of alongslope and downslope processes in the Alentejo Margin (SW Iberia) – Implications on slope stability. Marine Geology 410, 88-108.

van Aken, H.M., 2000a. The hydrography of the mid-latitude northeast Atlantic Ocean: I: The deep water masses. Deep Sea Research Part I: Oceanographic Research Papers 47, 757-788.

van Aken, H.M., 2000b. The hydrography of the mid-latitude Northeast Atlantic Ocean: II: The intermediate water masses. Deep Sea Research Part I: Oceanographic Research Papers 47, 789-824.

Van Rooij, D., Blamart, D., Kozachenko, M., Henriet, J.-P., 2007. Small mounded contourite drifts associated with deep-water coral banks, Porcupine Seabight, NE Atlantic Ocean. Geological Society, London, Special Publications 276, 225-244.

Van Rooij, D., De Mol, B., Huvenne, V., Ivanov, M., Henriet, J.P., 2003. Seismic evidence of current-controlled sedimentation in the Belgica mound province, upper Porcupine slope, southwest of Ireland. Marine Geology 195, 31-53.

Van Rooij, D., Iglesias, J., Hernández-Molina, F.J., Ercilla, G., Gomez-Ballesteros, M., Casas, D., Llave, E., De Hauwere, A., Garcia-Gil, S., Acosta, J., Henriet, J.P., 2010. The Le Danois Contourite Depositional System: Interactions between the Mediterranean Outflow Water and the upper Cantabrian slope (North Iberian margin)(Bay of Biscay). Marine Geology 274, 1-20.

Venz, K.A., Hodell, D.A., Stanton, C., Warnke, D.A., 1999. A 1.0 Myr Record of Glacial North Atlantic Intermediate Water Variability from ODP Site 982 in the Northeast Atlantic. Paleoceanography 14, 42-52.

Vissers, R.L.M., Meijer, P.T., 2012. Iberian plate kinematics and Alpine collision in the Pyrenees. Earth-Science Reviews 114, 61-83.

Voelker, A.H.L., Lebreiro, S.M., Schönfeld, J., Cacho, I., Erlenkeuser, H., Abrantes, F., 2006. Mediterranean outflow strengthening during northern hemisphere coolings: A salt source for the glacial Atlantic? Earth and Planetary Science Letters 245, 39-55.

Voelker, A.H.L., Rodrigues, T., Billups, K., Oppo, D., McManus, J., Stein, R., Hefter, J., Grimalt, J.O., 2010. Variations in mid-latitude North Atlantic surface water properties during the mid-Brunhes (MIS 9–14) and their implications for the thermohaline circulation. Clim. Past 6, 531-552.

Volkov, D.L., Fu, L.-L., 2010. On the Reasons for the Formation and Variability of the Azores Current. Journal of Physical Oceanography 40, 2197-2220.

White, M., 2006. Benthic dynamics at the carbonate mound regions of the Porcupine Sea Bight continental margin. International Journal of Earth Sciences 96, 1.

White, M., Dorschel, B., 2010. The importance of the permanent thermocline to the cold water coral carbonate mound distribution in the NE Atlantic. Earth and Planetary Science Letters 296, 395-402.

Wynn, R.B., Masson, D.G., 2008. Chapter 15 Sediment Waves and Bedforms, in: Rebesco, M., Camerlenghi, A. (Eds.), Developments in Sedimentology. Elsevier, pp. 289-300.

Wynn, R.B., Masson, D.G., Stow, D.A.v., Weaver, P.P.e., 2000. The Northwest African slope apron: a modern analogue for deep-water systems with complex seafloor topography. Marine and Petroleum Geology 17, 253-265.

Wynn, R.B., Stow, D.A.V., 2002. Classification and characterisation of deep-water sediment waves. Marine Geology 192, 7-22.

Y., F., B., L., S., S., B., B., S., D.S., 2007. A regional numerical ocean model of the circulation in the Bay of Biscay. Journal of Geophysical Research: Oceans 112, C09008.

Zamora, G., Fleming, M., Gallastegui, J., 2017. Chapter 16 - Salt Tectonics Within the Offshore Asturian Basin: North Iberian Margin, in: Soto, J.I., Flinch, J.F., Tari, G. (Eds.), Permo-Triassic Salt Provinces of Europe, North Africa and the Atlantic Margins. Elsevier, pp. 353-368.

Chapter 6

Salt tectonic control on past oceanographic circulation in the Le Danois intraslope basin (southern Bay of Biscay, NE Atlantic)

An edited version of this chapter will be submitted as:

Liu, S., Hernández-Molina, F. J., Van Rooij, D., in prep. Salt tectonic control on past oceanographic circulation in the Le Danois intraslope basin (southern Bay of Biscay, NE Atlantic). *Basin Research*.

Abstract: The Le Danois intraslope basin experienced four evolutionary stages; the extension, compression, interaction and contourite stages. The extension stage occurred during the late Cretaceous when the intraslope basin was much wider compared to the present-day constrained morphology. During the Paleocene-Oligocene compression stage, salt movements created several strike-slip faults with positive flower structures. The intraslope basin was narrowed and topographic highs were formed with significant expression on the paleo-seafloor. During the interaction stage, salt movements were still active. Bottom currents associated with the Atlantic Mediterranean Water (AMW) initiated to modify the paleo seafloor. Their interactions controlled the generation and the distribution of the Le Danois Drift from the late Pliocene to the middle Pleistocene. The contourite stage occurred from the middle Pleistocene to the present day, when all the tectonic activities ceased. The Le Danois depositional system (CDS) was widely generated in the entire intraslope basin. Salt tectonics significantly changed the past circulation patterns of the AMW. Variations in the MOW/AMW pathways further influenced the geometry and the morphology of the intraslope basin, providing new insights into the effects of salt tectonics on the paleoceanography and the margin evolution.

Keywords: salt tectonics, bottom currents; contourite drifts; confined basins.

Author contributions: Seismic data was provided by F. J. Hernández-Molina in collaboration with TGS-NOPEC. Data interpretation was performed by S. Liu and F. J. Hernández-Molina. Writing was performed by S. Liu under supervision and revision by D. Van Rooij.

6.1 Introduction

During the Jurassic, the Earth experienced a dramatic change, which marked the shaping of the modern continents and oceans (Lagabrielle and Cannat, 1990; Scotese, 1991). The subsequent plate convergences and seafloor spreading, induced by the breakup of supercontinent Pangea (Bartolini and Larson, 2001; Frizon de Lamotte et al., 2015), significantly controlled uplift events and had respective impacts on the opening and closure of oceanic gateways (Berggren and Hollister, 1977). The topography of gateways, which is an important motor for water exchange and heat transfer, widely contributed to global oceanic circulations (Smith and Pickering, 2003; Potter and Szatmari, 2009; De Schepper et al., 2015). The circulation of water masses and associated bottom-current processes persistently modified the physical shape of the seafloor and variously changed the geometry of the sedimentary basins in the deep sea (Nisancioglu et al., 2003; Meijer et al., 2004; Scher and Martin, 2006).

In the North Atlantic, plate tectonics between the African and Eurasian plates triggered the opening of the Strait of Gibraltar during the late Miocene (Krijgsman, 2002; Vergés and Fernàndez, 2012; Flecker et al., 2015). Water exchange between the Mediterranean Sea and the Atlantic Ocean initiated, generating one of the most distinctive modern water masses, the Mediterranean Outflow Water (MOW) (Hernández-Molina et al., 2014; Roveri et al., 2014). After passing through the Gulf of Cadiz, the MOW is defined as the Atlantic Mediterranean Water (AMW) due to the mixing between the Mediterranean outflow and the Atlantic ambient water (Rogerson et al., 2005). The AMW circulated along the SW European continental margin and associated bottom currents transported sediments along its pathways (Llave et al., 2007; Van Rooij et al., 2007; Hernández-Molina et al., 2011; Roque et al., 2012). Deep-sea sedimentary basins, including the Algarve basin (Brackenridge et al., 2013), the Galicia interior basin (Mena et al., 2018), the Le Danois intraslope basin (Liu et al., 2019) and the Porcupine basin (Van Rooij et al., 2007), were largely filled by extensive sediment bodies, also known as contourite drifts (Rebesco et al., 2008). Eventually, the MOW/AMW circulation leads to the development of the modern seafloor morphology along the SW European margins and has left its signature in sedimentary records in deep-sea basins (Ercilla et al., 2011; García et al., 2016; Capella et al., 2017).

A contourite depositional system (CDS), an association of depositional and erosional contourite features, provides valuable records of palaeoceanography and paleoclimate (Knutz, 2008; Llave et al., 2011; Lofi et al., 2016). Margin-scale plate tectonics and regional tectonic activities can be documented by the CDS as well (Pérez-Asensio et al., 2012; Hernández-Molina et al., 2016). Past oceanic seaways, such as the Rifian Corridor, could cause the morphological restriction, which favours the formation of bottom currents (Capella et al., 2017). Regional uplift events could induce profound changes in the distribution and sedimentary stacking patterns of contourite drifts (García et al., 2016; Vandorpe et al., 2016). Interactions between strike-slip fault systems and bottom currents may significantly influence the type of erosional features (Lobo et al., 2011). However, cause-and-effect relationships between basin-scale tectonics (i.e. salt movements) and the circulation of water masses, as well as their impacts on temporal changes of basin geometry, remain challenging to identify or study in sufficiently high resolution.

The Le Danois intraslope basin was influenced by both tectonic and bottom-current processes during the Neogene and Quaternary (Gallastegui et al., 2002; Iglesias, 2009). Previous studies also addressed the Cretaceous-Neogene tectonic evolution and Quaternary sedimentary processes of

the intraslope basin (Van Rooij et al., 2010; Fernández-Viejo et al., 2011; Cadenas and Fernández-Viejo, 2017). Salt movements and the associated salt-roof thrust deformed the overlying strata during the Paleogene and the Neogene (Zamora et al., 2017). Whereas the Neogene and Quaternary sedimentary sections, mainly consisting of contourite drifts, indicate the domination of the AMW-related bottom currents (Liu et al., 2019). However, little is known about the responses of the AMW to salt tectonics in the Le Danois intraslope basin during the Neogene.

This study describes the sedimentary evolution of the Le Danois intraslope basin and links the tectonic evolution and local paleoceanographic processes for the first time. Based on basin-level analysis derived from the interpretation on seismic reflection data, the main objectives of this study are: 1) to construct paleo-seafloor morphology; 2) to understand paleo-circulation dynamics resulted from intermediate water masses; 3) to evaluate the effects of salt tectonics on paleoceanography and margin evolution.

6.2 Geological Setting

6.2.1 Geology and tectonic evolution

The Le Danois intraslope basin is located at the northern Iberian continental margin, southern Bay of Biscay, in water depth ranging from 400 to 2000 m (Figure 6.1). During the early Cretaceous, progressive seafloor spreading led to the continuous northward propagation of the North Atlantic, resulting in the opening of the Bay of Biscay, which was accompanied by a ~35° counter-clockwise rotation of the Iberian plate (García-Mondéjar, 1996; Gong et al., 2008). Consequently, the Iberian plate was separated from the Eurasian and African plates (Vissers and Meijer, 2012). The Permo-Triassic evaporites became deformed and early-stage salt diapirism was triggered during this time interval (Zamora et al., 2017). Between the late Cretaceous and the Paleocene, the seafloor spreading along the former axis of the Bay of Biscay was hindered, resulting in a change in plate kinematics from extension to compression (Srivastava et al., 1990; Muñoz, 2002; Vergés et al., 2002; Fernández-Lozano et al., 2011). The subsequent compression orientated in N-S to NW-SE directions in the southern Bay of Biscay (Figure 6.1) (Andeweg et al., 1999; Somoza et al., 2019). As a result, salt diapirs were squeezed upwards along the northern Iberian margin during the Paleocene and the Oligocene (Zamora et al., 2017). During the Eocene and the Miocene, continuous salt movements resulted in the presence of mini-basins in the Le Danois Bank intraslope basin and most of salt diapirism stopped at the end of the Miocene (Zamora et al., 2017).

Unlike other basins in the Cantabrian continental margin, the sedimentary infill within the Le Danois intraslope basin is relatively thin and its maximum thickness is estimated at about 10 km (Boillot et al., 1979; Cadenas and Fernández-Viejo, 2017). Early oil exploration wells confirmed the presence of Triassic evaporites which were formed during the comparison stage between the Cantabrian and the Armorican margin. With the onset of seafloor spreading during the Cretaceous, a carbonate platform, containing limestones, was created (Boillot and Malod, 1988; Riaza Molina, 1996). The Eocene and Oligocene sediments originate from shallow marine settings, but an important presence of neritic limestones and calcareous sandstones has been observed (Cadenas and Fernández-Viejo, 2017). In the Miocene units, slumps and mass-wasting deposits have been recognized, suggesting downslope processes (Cadenas and Fernández-Viejo, 2017; Zamora et al., 2017). The observation of contourite drifts in the Pliocene unit suggests a shift from downslope to alongslope processes (Van Rooij et al., 2010). Two mounded and elongated drifts, being the Le

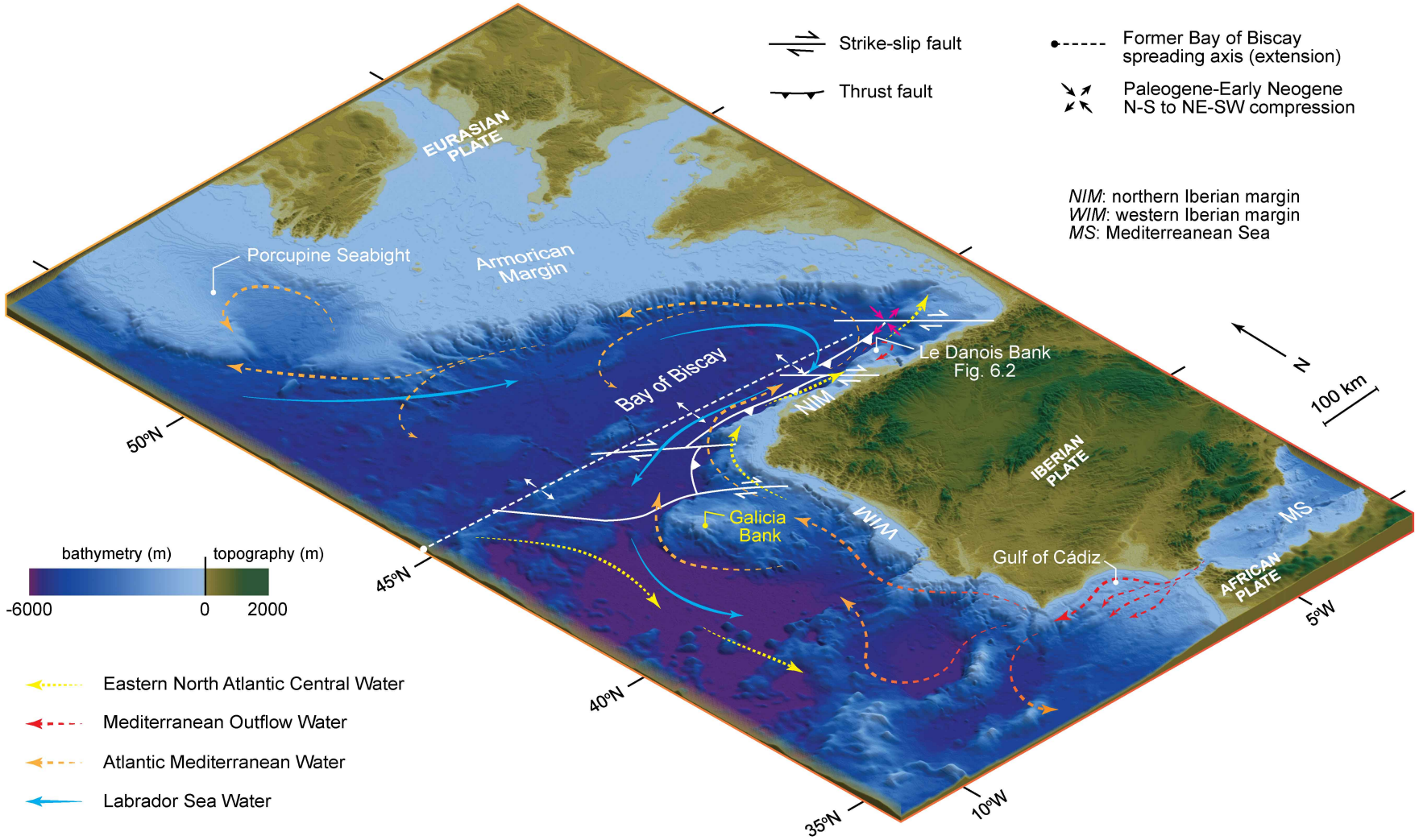

Figure 6.1: Map of the southwest European continental margins with the indication of: the morphological features; present-day pathways of the Eastern North Atlantic Central Water (ENACW), the Mediterranean Outflow Water (MOW)/ the Atlantic Mediterranean Water (AMW) and the Labrador Sea Water (LSW); tectonic structures of the southern Biscay margins (Somoza et al., 2019). The background bathymetric and topographic map is derived from the tangrams/heightmapper platform (https://tangrams.github.io/heightmapper/).

Danois and the Gijón Drifts, primarily make up the uppermost succession of the Le Danois intraslope basin (Figure 6.2a) (Liu et al., 2019).

6.2.2 Oceanography

The Le Danois intraslope basin is positioned within the depth intervals of three water masses: the Eastern North Atlantic Central Water (ENACW), the AMW and the Labrador Sea Water (LSW) (González-Pola et al., 2012). The ENACW, forming by winter mixing near the region between the northeast Azores and the European margins, comprise subpolar and subtropical branches (Pollard et al., 1996). The subtropical branch of the ENACW is regionally transported polewards by the Iberian Poleward Current (IPC) along the western and northern Iberian margins (Peliz et al., 2003; Lavín et al., 2006) (Figure 6.1). The ENACW has a minimum salinity of 35.53-35.58 and extends within the depth of 300-600 m with a core settling at ~350 m (Ríos et al., 1992; Pingree, 1993). Below the ENACW, the AMW penetrates between 600-1500 m water depth along the Iberian margins (Iorga and Lozier, 1999). The AMW is divided into two major cores after exiting the Gulf of Cadiz (Mazé et al., 1997; Sánchez-Leal et al., 2017). The upper core continues northward after passing through the Galicia Bank, while the lower core flows eastwards into the Bay of Biscay (Collart et al., 2018) (Figure 6.1). In the southern Bay of Biscay, the AMW is centred at depths of ~1000 m and has a maximum salinity and temperature of 35.8 and 10°C, respectively (Iorga and Lozier, 1999; van Aken, 2000b; González-Pola et al., 2012). The LSW, which is originated from the Labrador Sea, has been recognized below the AMW (Gascard and Clarke, 1983; van Aken, 2000b). It penetrates westwards in the southern Bay of Biscay at 1500-2000 m water depth (Talley and McCartney, 1982; Fiúza et al., 1998). The core of the LSW is positioned at 1800 m water depth with a minimum salinity of 35.05 (van Aken, 2000a; Lavín et al., 2006).

During the late Neogene and Quaternary, the Le Danois intraslope basin was prevailingly dominated by the AMW (Liu et al., 2019). Effective interactions between the AMW and the North Atlantic initiated after the opening of the Strait of Gibraltar during the early Pliocene (Hernández-Molina et al., 2014). From the late Pliocene onwards, the AMW dynamics exhibited clear responses to climatic variations and glacial/interglacial cyclicity (Schönfeld and Zahn, 2000; Rogerson et al., 2005; Voelker et al., 2006; Hayward et al., 2009; Raddatz et al., 2011; Khélifi et al., 2014). In the Gulf of Cadiz, renewed tectonic changes affected the bottom-current circulation of the MOW during the middle and late Pleistocene (Hernández-Molina et al., 2016).

6.3 Methodology

This study is based on multichannel reflection seismic data, which are obtained during the M/V Nanhai 502 cruise in 2001 within the framework of TGS-NOPEC seismic experiment CS-01 (Figure 6.2b). Sleeve guns were used as the seismic source and were toward 7 m below the water surface. The data were recorded by Syntrak 480 MSRS through a streamer with a length of 6000 m and 240 channels. The record length was 12 s TWT. Forty-three E-W and NNE-SSW orientated seismic lines were surveyed. The total survey length is 4080 km. The NNE-SSW orientated seismic lines extend from the continental shelf to the abyssal plain and covering the Le Danois intraslope basin. The seismic processing was performed by TGS-NOPEC, including a timing correction (-128 ms), datum statics, an amplitude recovery 10 dB/s and a butterworth filter (cut-off frequencies: 4–90 Hz).

The lithology and well log-based stratigraphy are derived from the data associated with the oil well MAR CANTÁBRICO H-1X (MC H-1X). This well was drilled in 1980 and located at 43°49'55.471" N, 5°3'40.168" W (Figure 6.2b). The depth of the well MC H-1X reached at 4658 m, where sediments are marked as a Jurassic age (Figure 6.3). By using the velocity model, depths of the well MC H-1X have been converted from metres to seconds two-way-travel time (Figure 6.3). Major discontinuities, identified from the seismic reflection data, are correlated with the well log-based stratigraphy.

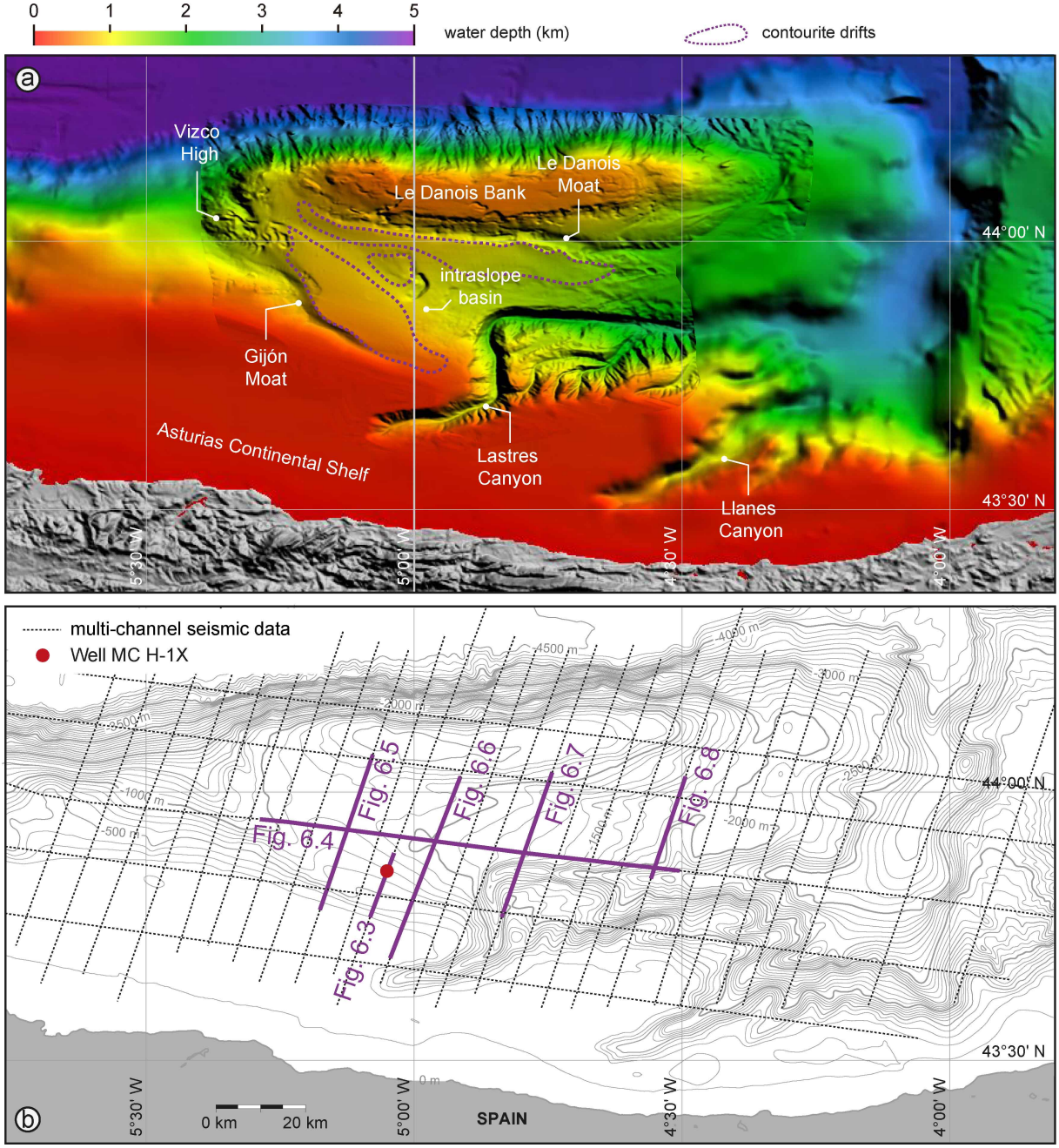

Figure 6.2: (a) Map of the Le Danois Bank area with the indication of the morphological domains and the location of contourite drifts (red box); (b) Dataset map (contour lines every 100 m) indicating locations of multi-channel seismic profiles. The ones used in this study are highlighted in purple colour. The position of Well MC H1-X is from Cadenas and Fernández-Viejo (2017).

6.4 Results

6.4.1 Seismic stratigraphy

Based on the interpretation of seismic reflection data, three major seismic units (units 1, 2 and 3), including eleven subunits (units 1a, 1b, 1c, 2a, 2b, 3a, 3b, 3c, 3d, 3e, 3f), have been identified from old to young (Figure 6.3). They are separated by major discontinuities (horizons a, b, c, d, e, f, g, h, i, j, k) from the bottom to the top. All these discontinuities display relatively high amplitude seismic reflections (Figure 6.3).

Horizons a, b, c, d and e are respectively correlated with the upper Aptian, the Aptian top, the Albian top, the intra-Paleocene and the Eocene top unconformities of the well MC H-1X (Figure 6.3) (Gallastegui et al., 2002; Cadenas and Fernández-Viejo, 2017). Horizons f, g, h, i, j and k are derived from the previous study through the correlation of seismic profiles (Liu et al., 2019). They are respectively marked as the middle Miocene, the Miocene top, the late Pliocene, the early Quaternary, the middle Pleistocene and the late Quaternary discontinuities (Liu et al., 2019) (Figure 6.3).

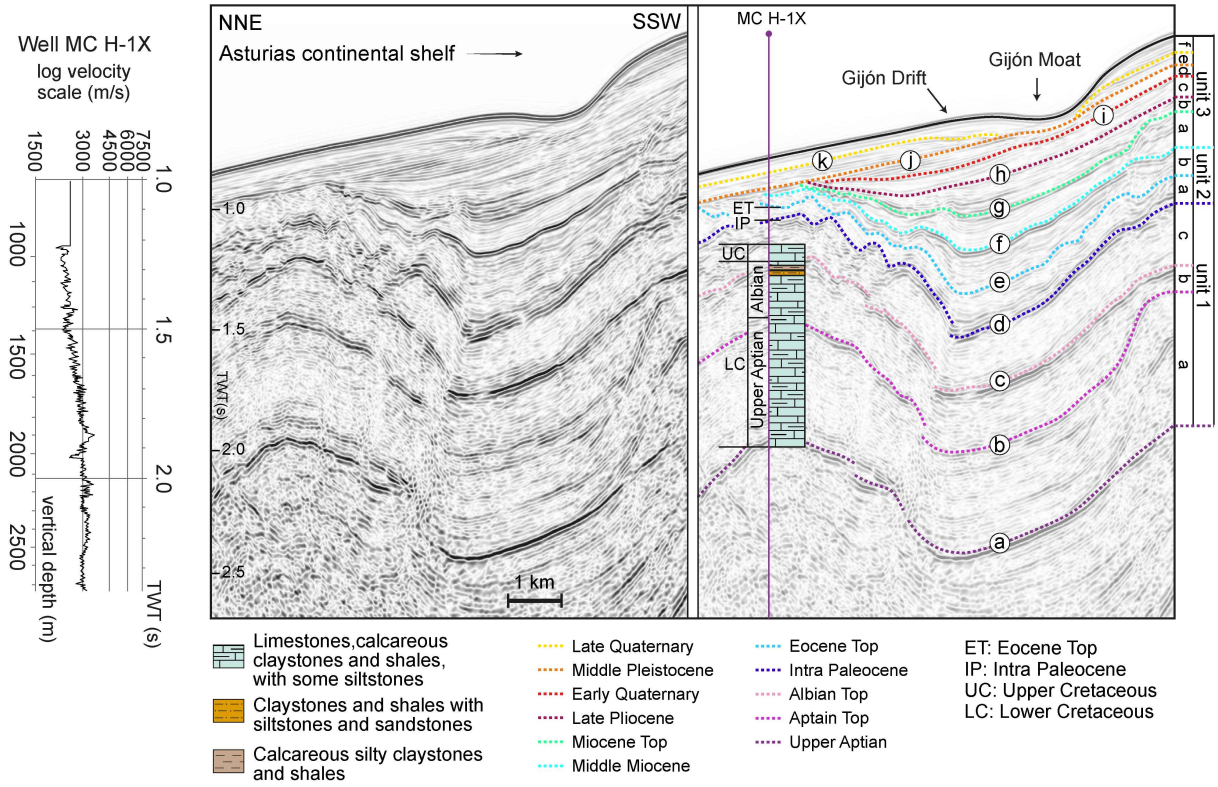

Figure 6.3: Time-depth velocity model and a seismic profile with the indication of seismic interpretation. Three major seismic units (units 1, 2 and 3), eleven subunits (units 1a, 1b, 1c, 2a, 2b, 3a, 3b, 3c, 3d, 3e, 3f) and major discontinuities (horizons a, b, c, d, e, f, g, h, i, j, k) have been identified. Among them, horizons a, b, c, d and e are namely correlated with the upper Aptain, the Aptain top, the Albian top, the intra Paleocene and the Eocene top unconformities of the well MC H-1X. Horizons f, g, h, i, j and k are derived from the previous study through the correlation of seismic profiles (Liu et al., 2019).

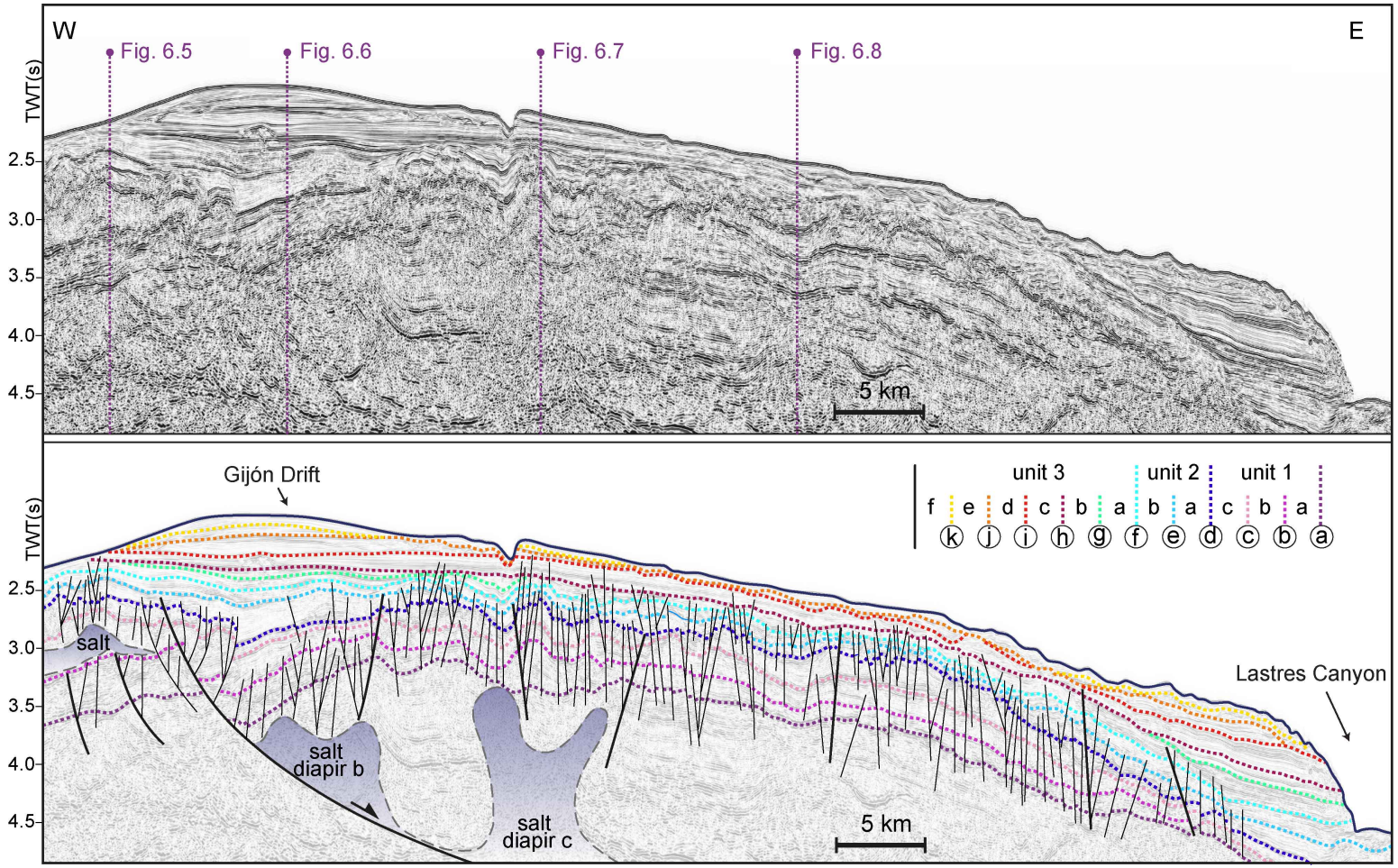

Figure 6.4: An interpreted seismic profile showing the Gijón Drift, salt diapirs b and c, and faults. The seismic stratigraphy is shown in the legend. The location of this seismic line is indicated in the dataset map. The junctions of seismic lines in Figures 6.5, 6.6, 6.7 and 6.8 (dotted purple lines) are indicated.

Below horizon a, seismic section displays moderate-high amplitude chaotic reflections (Figure 6.4). The related discontinuities could hardly be identified. By combining the seismic data and borehole MC H-1X, this base unit have a Jurassic age (Cadenas and Fernández-Viejo, 2017). Internal acoustic features are resulted from the rifting of the northern Iberian continental margin during the Jurassic and the early Cretaceous (Cadenas and Fernández-Viejo, 2017).

The late Cretaceous-Miocene section (from horizons a to f) is separated by the intra-Paleocene unconformity (horizon d) into two units (units 1 and 2) based on the correlation with the tectonic history of the Le Danois intraslope basin (Figure 6.3) (Cadenas and Fernández-Viejo, 2017; Zamora et al., 2017). Units 1 and 2 are namely compared with pre-tectonic and syn-tectonic units derived from the previous studies (Gallastegui et al., 2002; Fernández-Viejo et al., 2011). The overlying Neogene-Quaternary section (unit 3) records different contourite stages, driven by the past AMW variability (Liu et al., 2019). Subunits of unit 3 have been correlated with the respective oceanographic and bottom-current processes (Figure 6.3).

6.4.1.1 Unit 1 (pre-tectonic unit)

Unit 1, bounded by horizon a at the base and horizon d at the top, displays low-moderate amplitude, subparallel to discontinuous seismic reflections (Figures 6.4, 6.5). Downlap and onlap terminations are locally observed along the Asturias continental shelf (Figure 6.3). This unit is widely distributed in the entire intraslope basin (Figure 6.4). The thickness progressively decreases from the west (1000 ms TWT thick) towards the east (400-500 ms TWT thick) along the axis of the intraslope basin (Figure 6.4). From the continental shelf to the Le Danois Bank, the thickness of unit 1 reduces from 1000-1300 ms TWT to 300-500 ms TWT (Figure 6.5). Discontinuous internal structures and deformation features are shown in the central part of the intraslope basin (Figure 6.6). Three well-identified subunits (units 1a, 1b and1c), respectively separated by horizons b and c, can be recognized (Figure 6.3). Among them, unit 1a has the largest average thickness (400 ms TWT) compared with units 1b (250 ms TWT) and 1c (200 ms TWT).

6.4.1.2 Unit 2 (syn-tectonic unit)

Unit 2 is bounded by horizon d at the base and horizon f at the top (Figure 6.3). It displays low amplitude, transparent to chaotic reflections at the central part and along the northern boundary of the intraslope basin, while moderate to high amplitude, subparallel to discontinuous reflections are shown in the rest area (Figures 6.6, 6.7). This unit is widely distributed in the entire intraslope basin and displays infilling geometry at the central part of the basin (Figure 6.7). Discontinuous internal structure and deformed features are shown along the northern and southern boundaries of the intraslope basin (Figure 6.6). Onlap terminations and erosional truncations are observed at the central part of the basin (Figure 6.5) and along the southern flank of the Le Danois Bank (Fig 7). Unit 2 shows marked thickening (400-500 ms TWT thick) at the central part and northern boundary of the intraslope basin (Figure 6.7). Its thickness progressively decreases to 150-200 ms TWT towards the Le Danois Bank (Figure 6.6). Unit 2 is separated by horizon e into two subunits (units 2a and 2b) (Figure 6.3). The thickness of units 2a and 2b are uniform and have an average value of 150 ms TWT.

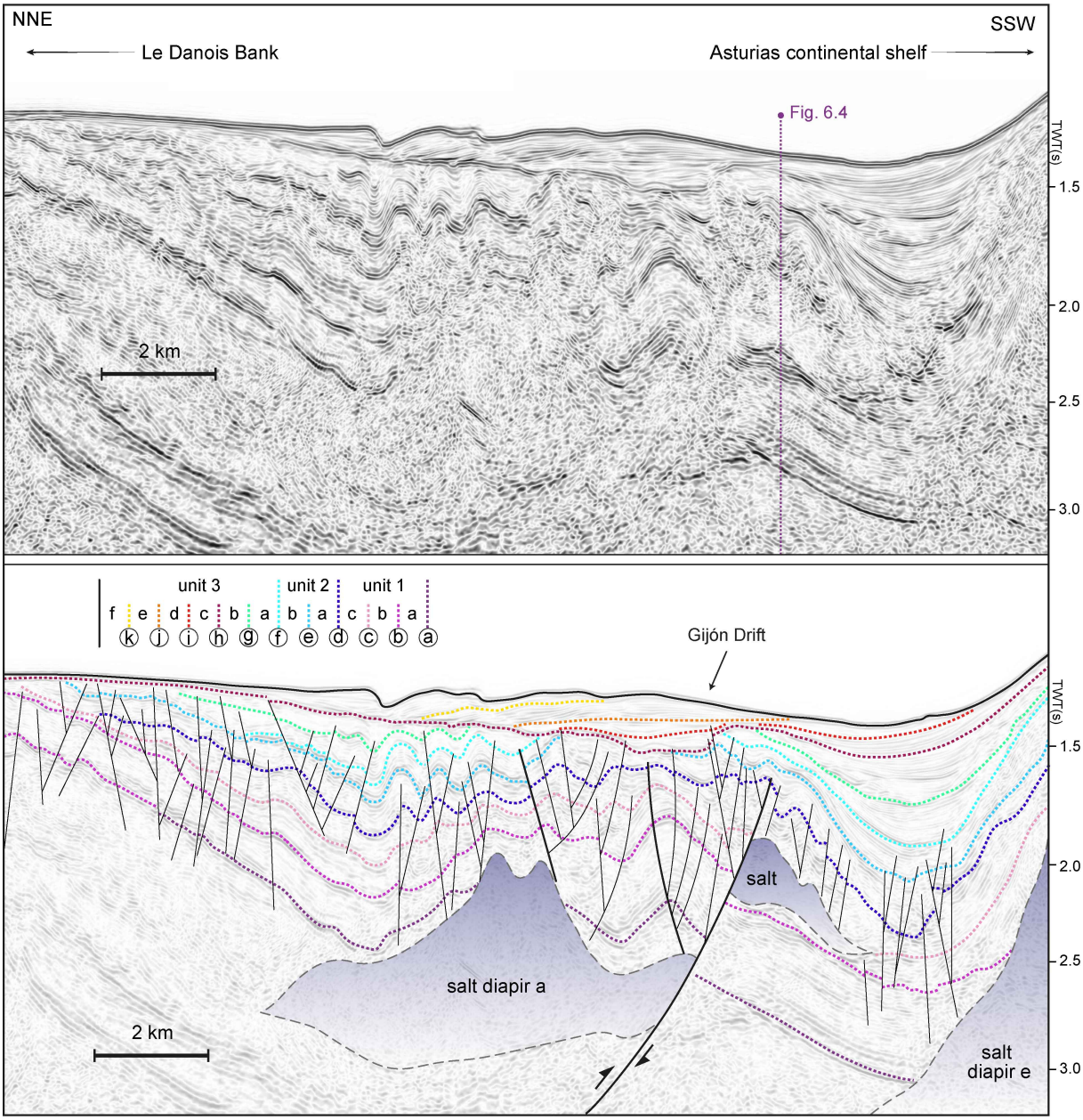

Figure 6.5: An interpreted seismic profile showing the Gijón Drift, salt diapirs a and e, and faults. The seismic stratigraphy is shown in the legend. The location of this seismic line is indicated in the dataset map. The junction of the seismic line in Figure 6.4 (dotted purple line) is indicated.

6.4.1.3 Unit 3 (contourite unit)

Unit 3, bounded by horizon f at the base and the present seafloor at the top, is separated by horizons g, h, i, j and k into six subunits (units 3a, 3b, 3c, 3d, 3e and 3f) (Figure 6.3). Units 3a and 3b are located at the central part and along the northern boundary of the intraslope basin, where infilling geometry with moderate to high amplitude, discontinuous to subparallel reflections are observed (Figure 6.6). The thickness of these two subunits is uniform and has an average value of 100 ms TWT (Figure 6.7). Truncation and toplap terminations are observed towards the western and central parts of the intraslope basin (Figure 6.3).

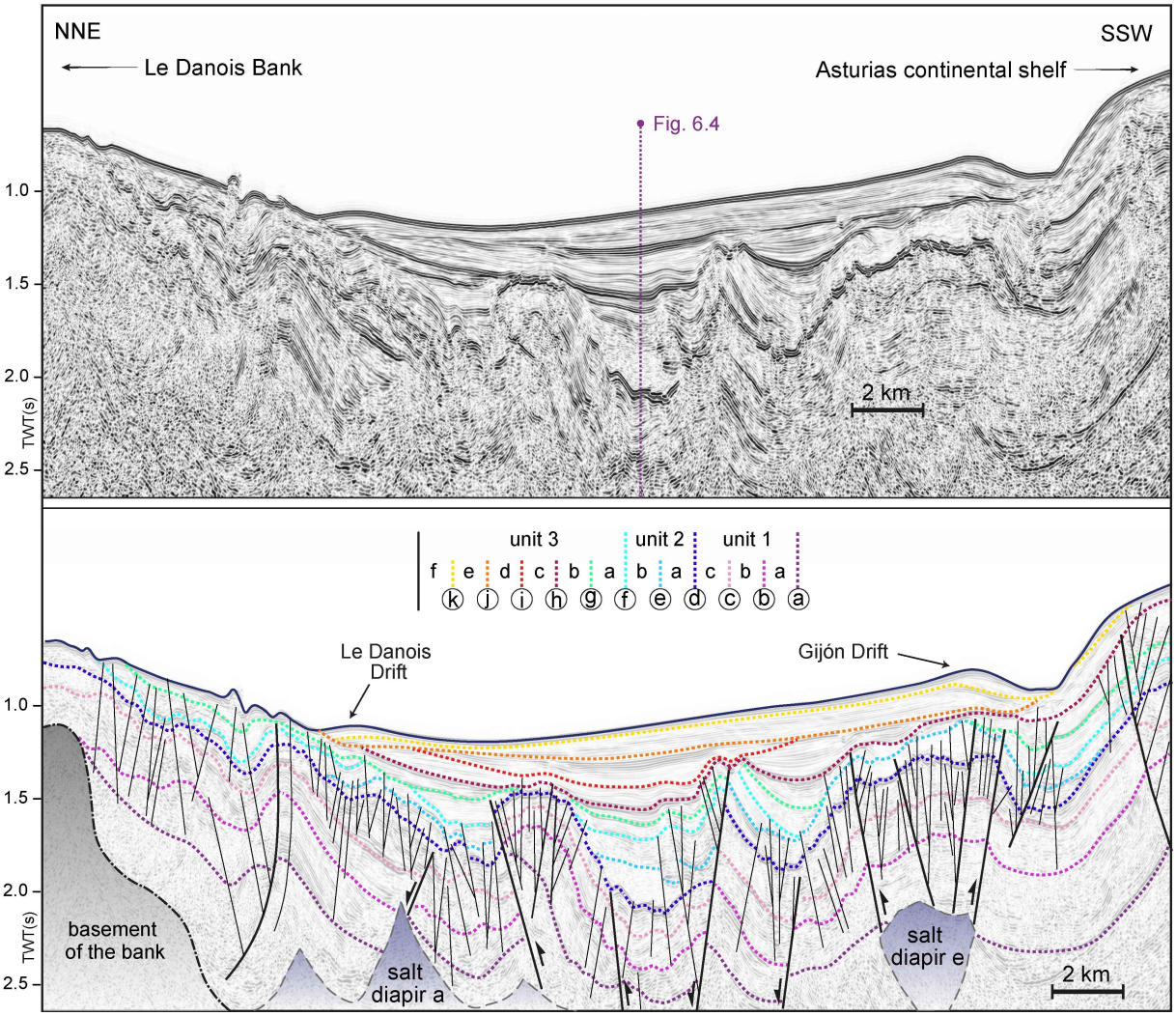

Figure 6.6: An interpreted seismic profile showing the Gijón and the Le Danois Drifts, salt diapirs a and e, and faults. The seismic stratigraphy is shown in the legend. The location of this seismic line is indicated in the dataset map. The junction of the seismic line in Figure 6.4 (dotted purple line) is indicated.

Unit 3c is characterized by moderate to high amplitude, continuous and subparallel reflections and displays mounded geometry along the northern boundary of the Le Danois intraslope basin, indicating the initiation of the Le Danois Drift (Figure 6.7). In contrast, discontinuous structure and deformation, instead of mounded features, are identified along the southern part of the intraslope basin (Figures 6.7). The thickness of this unit declines from the upper continental slope (200 ms TWT) towards the Le Danois Bank (70-100 ms TWT) (Figure 6.7).

Unit 3d has been widely eroded in the intraslope basin, especially along the northern and southern boundaries of the Le Danois intraslope basin (Figure 6.6). This unit displays moderate-high amplitude, subparallel to wavy reflections (Figure 6.7). The wavy features have an average wavelength of 1.5-2 km and a wave height of about 10-20 ms TWT, displaying upslope migration trend. The least eroded part of this unit, positioned at the centre of the basin, is about 20-100 ms TWT thick.

Units 3e and 3f are widely distributed in the entire intraslope basin (Figures 6, 7). Both units are characterized by moderate to high amplitude, continuous and subparallel reflections (Figure 6.4). Mounded features of the Le Danois and the Gijón Drifts are namely observed along the southern foot of the Le Danois Bank and the upper continental slope (Figure 6.7). Towards the Lastres

Canyon and the eastern boundary of the intraslope basin, mounded geometry of the Le Danois and the Gijón Drifts progressively lose the expression (Figure 6.8). The variation of the geometry is accompanied by a thickness change of units 3e and 3f, which declines from the basin centre (200-100 ms TWT) towards the eastern parts of the intraslope basin (30-70 ms TWT) (Figure 6.4).

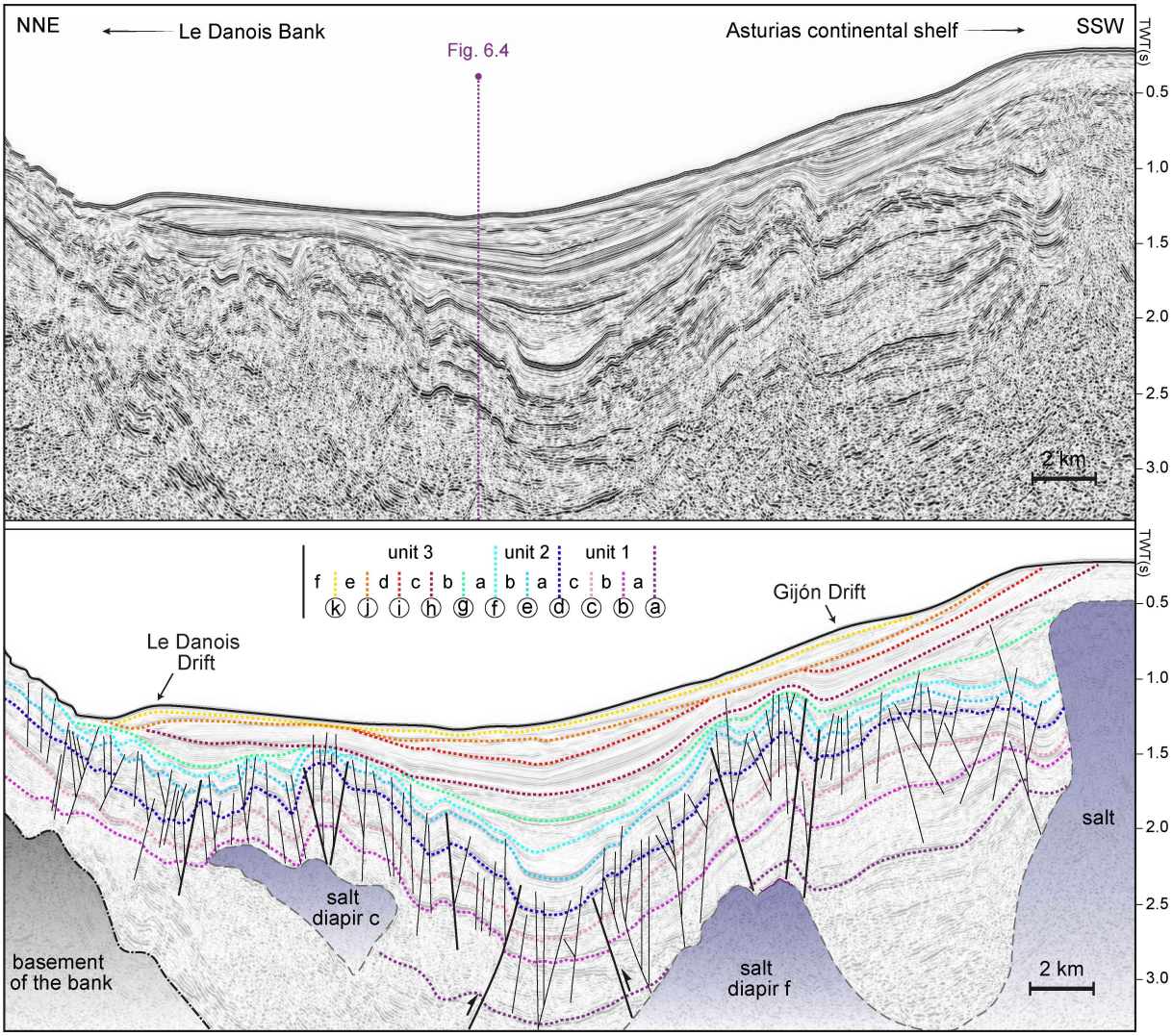

Figure 6.7: An interpreted seismic profile showing the Gijón and the Le Danois Drifts, salt diapirs c and f, and faults. The seismic stratigraphy is shown in the legend. The location of this seismic line is indicated in the dataset map. The junction of the seismic line in Figure 6.4 (dotted purple line) is indicated.

Figure 6.8: An interpreted seismic profile showing a plastered drift, the Le Danois Drifts, the Lastres Canyon, salt diapirs d and g, and faults. The seismic stratigraphy is shown in the legend. The location of this seismic line is indicated in the dataset map. The junction of the seismic line in Figure 6.4 (dotted purple line) is indicated.

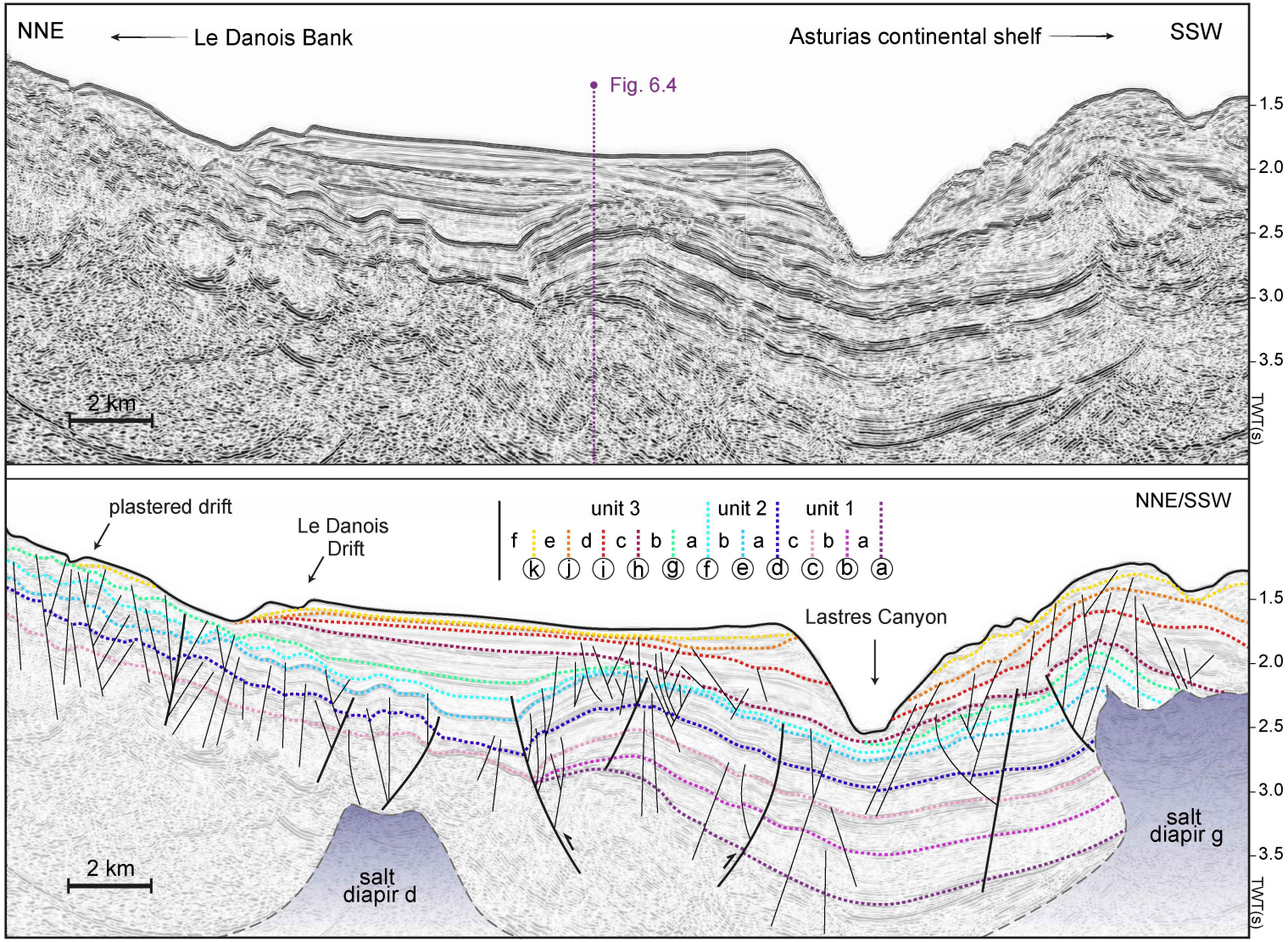
NNE
Le Danois Bank
Asturias continental shelf
SSW
Fig. 6.4
2 km
1.5
2.0
2.5
3.0
3.5
TWT(s)
plastered drift
Le Danois Drift
unit 3
unit 2
unit 1
f e d c b a b a c b a
k j i h g f e d c b a
NNE/SSW
Lastres Canyon
2 km
salt diapir d
salt diapir g
1.5
2.0
2.5
3.0
3.5
TWT(s)

6.4.2 Salt structures and faults

Based on the seismic interpretation, various salt-related structures, including salt diapirs a, b, c, d, e, f, g and detached faults, are identified (Figures 6.4, 6.5, 6.6, 6.7, 6.8). Among them, salt diapirs a, b, c, and d, characterized by chaotic to transparent seismic reflectors (Figures 6.4, 6.5, 6.8), are respectively located along the northern boundary of the Le Danois intraslope basin from the west to the east (Figure 6.9). The geometry of these salt diapirs varies from ellipse-elongated (salt diapirs a, c and d) to circular (salt diapir b) shapes. The ellipse-elongated ones are orientated in an E-W direction with a crestal length of 10-20 km and a width of 5-6 km, whereas the circular one has a diameter of 5-6 km (Figure 6.9).

Folded features with an anticlinal geometry are observed from units 1a to 3b above salt diapirs a, b, c and d (Figures 6.4, 6.5, 6.8). Abundant faults are associated with the deformation (Figure 6.6). In the northwest part of the intraslope basin, E-W orientated strike-slip faults with the positive flower structure are identified detaching into salt diapirs c and d (Figures 6.7, 6.8). Sedimentary layers from units 1a to 3b were strongly uplifted under the influence of the strike-slip faults. The deformed zone rose up to 05 s TWT above the paleo-seafloor and had a width of 2.5-4 km (Figure 6.6). From units 3c to 3f, only a few faults are recognized above these salt diapirs (Figure 6.7). Nearly subparallel seismic reflections and horizontal seismic strata indicate less affect of the faulting on the sedimentary deposition. Above horizon h, the Le Danois Drift with the mounded geometry makes up the late Pliocene to the present-day units (Figure 6.6).

Along the southern boundary of the Le Danois intraslope basin, salt diapirs e, f and g are namely distributed from the west to the east (Figure 6.9). They are characterized by chaotic-transparent seismic reflectors (Figures 6.6, 6.7, 6.8). Salt diapirs e and f have NW-SE orientated elongated shapes and are 17-19 km long, 5 km wide (Figure 6.9). Salt diapir g extends northwards from the Asturias continental shelf to the Lastres Canyon. The length could hardly be estimated since its southern part is beyond the reach of the seismic data, while the crestal width is about 12 km (Figure 6.8).

Salt diapirs e and f are buried by sediments from the Upper Cretaceous to the present day (Figures 7, 8). The overlying strata (units 1a to 3d) is folded and displays an anticline geometry (Figure 6.7). NW-SE orientated strike-slip faults with a positive flower structure are identified detaching into salt diapir e and f (Figures 6.6, 6.7). Consequently, sedimentary layers from units 1a to 3d rose 0.1 s TWT above the paleo-seafloor and the deformed zone is about 3.5 km wide (Figure 6.7). Above horizon j, seismic strata are horizontal and have a mounded geometry, indicating no motion of faults in the southern part of the intraslope basin since the mid-Pleistocene (Figure 6.7).

Due to the deformation and the strike-slip faulting above these salt diapirs, several mini-basins in the Le Danois intraslope basin (Figure 6.9). They show a NW-SE orientated elongated shape and have lengths and widths of about 13-18 km and 8-15 km. The depth varies between 150 to 350 ms TWT (Figure 6.9). These mini-basins are distributed along the W-E axis of the intraslope basin, whereas their width gradually increases (from 8 to 13 km) from the west to the east (Figure 6.9). The largest mini-basin is located at the centre of the intraslope basin with a width of about 15 km and a length of about 18 km. Seismic sections (from units 1a to 3d) infilling the mini-basins show syncline geometry at the central part of the intraslope basin. Discontinuous internal structures, which are disrupted by a large number of NW-SE to E-W orientated normal (Figure 6.6) and

reverse (Figures 6.7, 6.8) faults, are shown in these seismic units. In units 3e and 3f, seismic strata are horizontal and no faults are observed (Figure 6.7).

Besides strike-slip faults detached to salt diapirs, a north-dipping reverse fault, trending in an E-W direction, is observed at the central part of the Le Danois intraslope basin (Figure 6.5). The reverse displacement of the fault resulted in discontinuous seismic reflections from units 1a to 2a, indicating that the occurrence of the fault is later than the Paleocene. Sedimentary layers along the hanging wall (upper side) of the fault were widely folded (Figure 6.5). Whereas seismic strata were more horizontal at the footwall (lower side).

6.5 Discussion

6.5.1 Evolutionary model of the Le Danois intraslope basin

Base on the seismic interpretation, the past seafloor morphology of the Le Danois intraslope basin is reconstructed (Figure 6.10). Changes of morphological features are linked to the variation of the tectonic and bottom-current regime (Marchès et al., 2010; García et al., 2016; Rodriguez et al., 2016; Nugraha et al., 2018). As such, four major stages of the basin evolution, including extension, compression, interaction and contourite stages, are identified regarding their dominant processes (Figure 6.10). These evolution stages are respectively coeval with tectonic and paleoceanographic variations from the late Cretaceous to the present day in the southern Bay of Biscay.

6.5.1.1 Extension stage

The late Cretaceous unit (unit 1) displays NW-SE to E-W orientated normal faults at the central part of the Le Danois intraslope basin (Figure 6.6). These normal faults, which are parallel with the Cretaceous spreading axis of the Bay of Biscay (Vissers and Meijer, 2012; Somoza et al., 2019), are possibly triggered by extensional processes documented by the previous studies (Soto et al., 2007; Jammes et al., 2010). During the late Cretaceous, the extensional tectonic regime, resulting from the North Atlantic rifting, was prevalent in the southern Bay of Biscay (Fernández-Viejo et al., 2011). Numerous extensional faults are observed along the northern Iberian margin (Boillot et al., 1979; Boillot et al., 1987; Somoza et al., 2019). Along the Cantabrian continental margin, especially east of 6°W, the highly thinned continental crust widens the extension basins (Fernández-Viejo et al., 2011). As such, the Le Danois intraslope basin was controlled by the late Cretaceous extension and is suggested to have a wider size comparing with the present-day constrained morphology (Figure 6.10a). Among subunits of unit 1, unit 1a has the largest thickness. This feature may be linked with an increase of the sediment supply or a change in the accommodation space along the Cantabrian margin during the Aptian due to tectonically induced seabed tilting (Thinon et al., 2001; Roca et al., 2011; Zamora et al., 2017).

6.5.1.2 Compression stage

In unit 2, seismic sections are widely deformed by folding and faults (Figure 6.7). This is most likely resulted from the regional compression and salt movements along the Cantabrian continental margin (Roca et al., 2011; Zamora et al., 2017). During the Paleocene, a change in plate kinematics in the Bay of Biscay and the shortening of the northern Iberian margin hindered the former extension and induced the N-S trending compression (Boillot and Malod, 1988; García-

Mondéjar, 1996; Vázquez et al., 2008). The compression started to widely create paleo-seafloor morphologies, such as fault scarps and folds along the NW Iberian margin (Vázquez et al., 2008; Somoza et al., 2019). In the study area, the presence of E-W trending reverse faults, which are perpendicular to the orientation of the regional compression, created scarps, morphological highs and mini-basins on the paleo-seafloor (Figures 6.6, 6.10b).

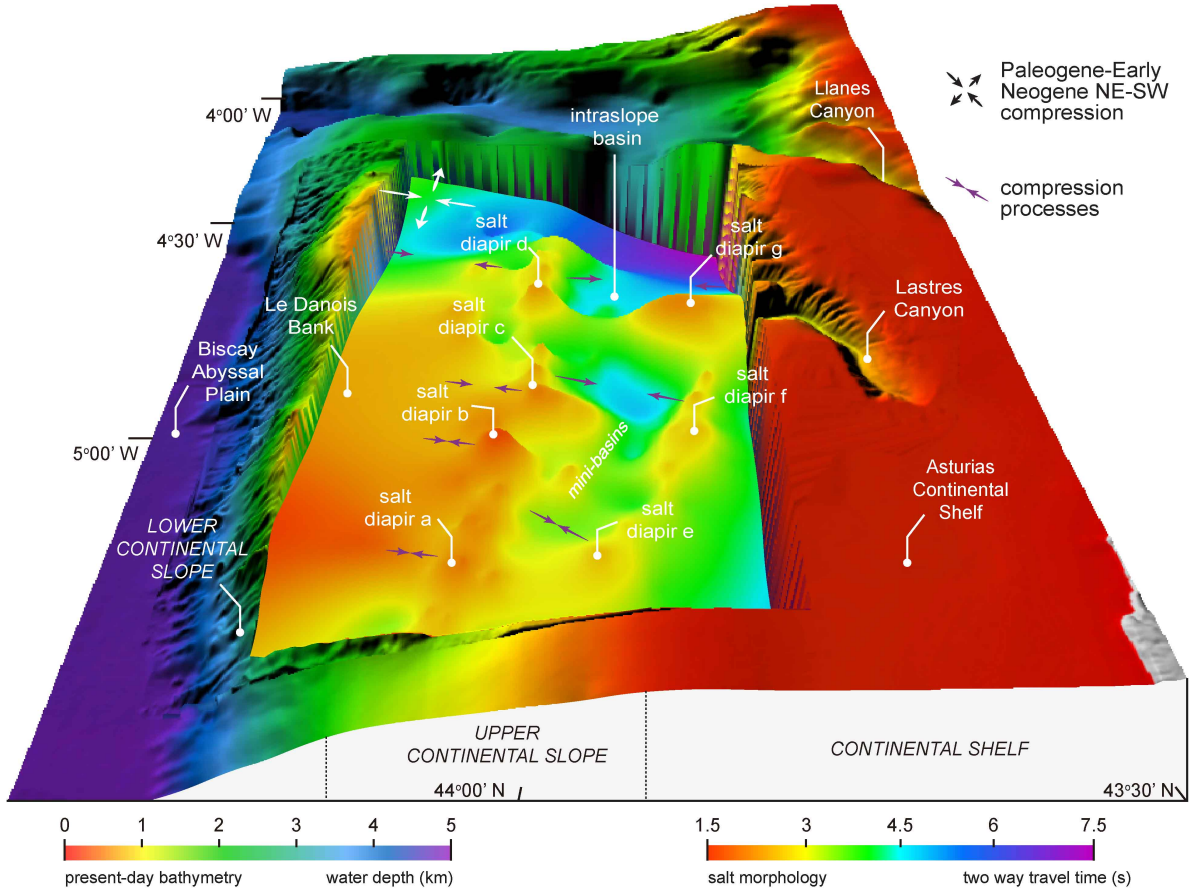

Figure 6.9: The morphology and location of salt diapirs a, b, c, d, e, f and g. The scale of the depth is two-way travel time (s). location and size of the resulted mini-basins are shown. Regional compression processes are displayed by purple arrows. The background map shows the location of morphological domains. The scale of the depth is in metres (m).

Figure 6.10: Sketch of the evolution of the Le Danois intraslope basin. Four major stages, including (a) extension; (b) compression; (c) interaction and (d) contourite stages, are identified regarding the dominant processes.

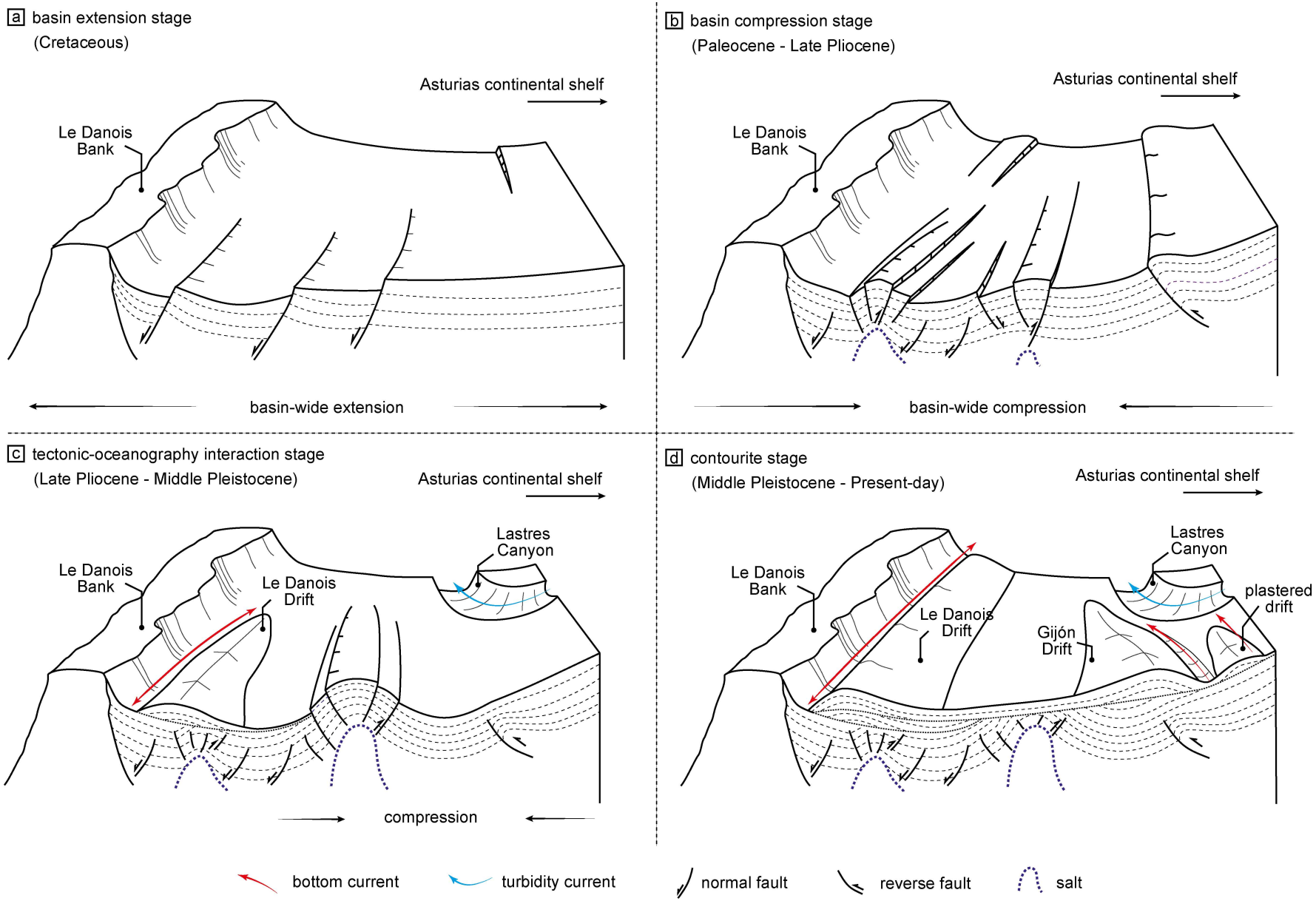
a basin extension stage
(Cretaceous)
Asturias continental shelf
Le Danois Bank
basin-wide extension
b basin compression stage
(Paleocene - Late Pliocene)
Asturias continental shelf
Le Danois Bank
basin-wide compression
c tectonic-oceanography interaction stage
(Late Pliocene - Middle Pleistocene)
Asturias continental shelf
Le Danois Bank
Le Danois Drift
Lastres Canyon
compression
d contourite stage
(Middle Pleistocene - Present-day)
Asturias continental shelf
Le Danois Bank
Le Danois Drift
Gijón Drift
Lastres Canyon
plastered drift
bottom current
turbidity current
normal fault
reverse fault
salt

NW-SE orientated strike-slip faults are detached into salt diapirs c, d, e and f (Figures 6.7, 6.8). The positive flower structure of these strike-slip faults, which are trigged in compression or uplift conditions (McClay and Bonora, 2001; Le Guerroué and Cobbold, 2006), indicates active salt movements in the intraslope basin during this stage. Indeed, the combined onshore and offshore seismic data show that the Cretaceous salt sheets were squeezed up during the Eocene and the Oligocene, in turn effectively folded the overlying strata along the Cantabrian margin (Zamora et al., 2017). The Le Danois intraslope basin, therefore, was significantly narrowed and deformed by the compression and salt movements during this stage.

6.5.1.3 Tectonic-oceanographic interaction stage

Previous studies suggest that most of the tectonic activities ceased along the Cantabrian continental margin since the end of the Miocene (Cadenas and Fernández-Viejo, 2017). However, folded strata and strike-slip faults, which are detached to salt diapir f are identified in the Pliocene and the early Quaternary units of the Le Danois intraslope basin (Figure 6.7, 6.8), pointing out active salt movements during this stage. Consequently, the southern part of the intraslope basin was strongly uplifted, forming bathymetric highs on the paleo-seafloor (Figure 6.6). The resulted topographic obstacles distributed along the southern boundary of the intraslope basin based on the identified location of salt diapirs (Figure 6.9).

Tectonic activities are not the only dominant process regime during this stage. The circulation of the MOW, resulting from the Atlantic-Mediterranean water exchange, initiated at the latest Miocene (~5.33 Ma) (Hernández-Molina et al., 2014; Roveri et al., 2014). At ~4.5 Ma, the MOW circulated into the Gulf of Cádiz and started to generate contourite features (Hernández-Molina et al., 2016). During the late Pliocene, the onset of the northern hemisphere glaciation (NHG) triggered cold climate conditions in the Mediterranean and North Atlantic regions (Flesche Kleiven et al., 2002; Becker et al., 2006; Rohling et al., 2014). The denser AMW started to effectively interact with the Le Danois intraslope basin from the late Pliocene (3.5-3.0 Ma) onwards (Liu et al., 2019).

The late Pliocene discontinuity (horizon h), a profound erosional unconformity, is widely observed in the intraslope basin (Figures 6.5, 6.6), suggesting significant erosive events during the late Pliocene. Folded strata overlying on salt diapirs a and c were eroded, providing a gentle slope for the generation of the Le Danois Drift (Figure 6.5). Interestingly, no contourite drifts were formed at the southern part of the intraslope basin during this stage (Figure 6.7). This feature is possibly related to the domination of salt movements at the southern part of the intraslope basin. Bathymetric highs, which were squeezed upwards by salt movements, possibly hindered the pathways of the AMW. Therefore, a topographically constrained morphology was created between the salt-related bathymetric highs and the Le Danois Bank, in turn influencing the distribution of contourite drifts on the paleo-seafloor (Figure 6.10c).

6.5.1.4 Contourite stage

During this stage, no deformation and faults are observed in units 3e and 3d (Figure 6.5), suggesting the end of the tectonic activities. The intraslope basin was dominated by alongslope and downslope processes. Extreme erosive events, which were represented by the wide distributed mid-Pleistocene discontinuity (horizon j), occurred in the Le Danois intraslope basin during the middle Pleistocene (Figure 6.7). This event is coeval with the profound enhancement

of the AMW, when the periodicity of climate cycles of the Earth switched to 100 ky during the Mid-Pleistocene Transition (MPT, ~1.25-0.7 Ma) (Maslin and Ridgwell, 2005; Elderfield et al., 2012; Rohling et al., 2014; Hernández-Molina et al., 2016; Bahr et al., 2018). As a result, previously existed seafloor irregularities were eroded away and contourite drifts, including the Le Danois Drift, the Gijón Drift and some small-scale contourite drifts (Figures 6.1, 6.6, 6.8), started to develop in the entire intraslope basin (Figure 6.10d).

6.5.2 Salt tectonic considerations

In the study area, salt diapirs located at northern (a, b, c, d) and southern (e, f, g) parts of the intraslope basin have different growth phases (Figure 6.7). This feature could be related to the variation of sedimentary input at different parts of the intraslope basin. Salt tectonics, which were primarily driven by differential loading, can create topographic irregularities or bathymetric highs on the (paleo-) seafloor (Jackson et al., 2015). The rising rate of salt structures highly depends on the sedimentary aggradation (Hudec and Jackson, 2007). Therefore, salt diapirs from the same region could grow in different time intervals and the resulted morphology are in various scales due to the localised sedimentary input (Harding and Huuse, 2015). In the Le Danois intraslope basin, the accommodation space is nearly the same during the extension stage (Figure 6.10a). However, the thickness of all seismic units reduces from the continental shelf towards the Le Danois Bank (Figures 6.6, 6.7, 6.8), indicating larger sedimentary supply at the southern part of the intraslope basin. Thick sedimentary layers can trigger down-building processes and cause the rise of the salts (Chemia et al., 2008; Jackson and Hudec, 2017). As such, due to differential sedimentary loading, salt movements respectively ceased during the late Pliocene and the middle Pleistocene along the northern and southern parts of the intraslope basin. Bottom currents interacted with the salt-related morphology during different times, resulting in the specific depositional pattern of the Le Danois CDS (Figures 6.10b, c).

Contourite features of a CDS are commonly generated at the same geological time (Hernández-Molina et al., 2008). However, the Le Danois and the Gijon Drifts namely started to develop during the late Pliocene and the middle Pleistocene, which are coeval with the growth phases of different salt diapirs. When a water mass passes through topographic obstacles, deflected bottom currents can be formed and the pathways of the water mass can significantly change (Wåhlin, 2004; Nugraha et al., 2019). The salt rise at different periods hindered or controlled the pathways of the AMW at the southern and northern parts of the intraslope basin (Figure 6.10). Consequently, a time gap (~2.4 Ma) of the formation of contourite drifts occurred in the Le Danois CDS. Therefore, interactions between salt tectonics and bottom currents play an important role in the evolution of contourite drifts.

6.6 Conclusion

In the Le Danois Bank region, previous studies suggested no major tectonic events after the end of the Miocene (Cadenas and Fernández-Viejo, 2017). However, the seismic interpretation of this study indicates that active salt movements stopped until the middle Pleistocene. Based on the dominant tectonic and bottom-current processes, the evolution of the intraslope basin is divided into four stages, including extension, compression, interaction and contourite stages. During the compression stage, the basin was significantly narrowed. The related salt movements and regional tectonics created various bathymetric highs on the paleo-seafloor. These past topographic

obstacles distributed along the northern and southern parts of the intraslope basin. They further interacted with AMW and efficiently accelerate the associated bottom currents. When the intraslope basin was dominated by alongslope processes, the Le Danois CDS was developed. The resulted contourite features significantly change the geometry of the intraslope basin.

Due to the influence of the salt movements, the Le Danois and the Gijón Drifts, which belong to one CDS, are respectively generated since the late Pliocene and the middle Pleistocene. The time gap (~2.4 Ma) between the built-up of the Le Danois and the Gijón Drifts is related to the growth phase of different salt diapirs. This feature differs from any well-known drift systems and provides new insights into their conceptual model. Contourite features of a CDS can be formed during different time intervals under the control of salt tectonics. Effects of tectonics, not only in the plate- and margin-scale, but also in basin-scale, should be considered in the future contourite studies.

6.7 Acknowledgements

This study was carried out within the framework of a Chinese Scholarship Council "CSC Grant" (201506410062). The research was conducted in collaboration with "The Drifters Research Group" of the Royal Holloway University of London (UK) and it is related to the projects CTM 2012-39599-C03, CGL2016-80445-R, and CTM2016-75129-C3-1-R. The authors wish to express our gratitude to the crews and scientific researchers of the ECOMARG (REN2002-00916/MAR) and M/V Nanhai 502 cruises. This study also builds upon achievements of project ESF Euromargins MOUNDFORCE, EC FP5 RTN EURODOM and EC FP6 HERMES (GOCE-CT-2005-511234-1).

References

Andeweg, B., De Vicente, G., Cloetingh, S., Giner, J., Muñoz Martin, A., 1999. Local stress fields and intraplate deformation of Iberia: variations in spatial and temporal interplay of regional stress sources. Tectonophysics 305, 153-164.

Bahr, A., Kaboth, S., Hodell, D., Zeeden, C., Fiebig, J., Friedrich, O., 2018. Oceanic heat pulses fueling moisture transport towards continental Europe across the mid-Pleistocene transition. Quaternary Science Reviews 179, 48-58.

Bartolini, A., Larson, R.L., 2001. Pacific microplate and the Pangea supercontinent in the Early to Middle Jurassic. Geology 29, 735-738.

Becker, J., Lourens, L.J., Raymo, M.E., 2006. High-frequency climate linkages between the North Atlantic and the Mediterranean during marine oxygen isotope stage 100 (MIS100). Paleoceanography 21.

Berggren, W.A., Hollister, C.D., 1977. Plate tectonics and paleocirculation — Commotion in the ocean. Tectonophysics 38, 11-48.

Boillot, G., Dupeuble, P.A., Malod, J., 1979. Subduction and tectonics on the continental margin off northern Spain. Marine Geology 32, 53-70.

Boillot, G., Malod, J., 1988. The north and north-west Spanish continental margin: a review. Rev. Soc. Geol. España 1, 295-316.

Boillot, G., Malod, J.A., Dupeuble, P.-A., Cybere Group, 1987. Mesozoic evolution of Ortegal spur, North Galicia margin: Comparison with adjacent margins. in Boillot, G., Winterer, E. L., Meyer, A. W., et al.,

Proceedings, Initial reports, Ocean Drilling Program, Volume 103, Part A: College Station, Texas, Ocean Drilling Program, p. 107–119.

Brackenridge, R.E., Hernández-Molina, F.J., Stow, D.A.V., Llave, E., 2013. A Pliocene mixed contourite–turbidite system offshore the Algarve Margin, Gulf of Cadiz: Seismic response, margin evolution and reservoir implications (Cadiz). Marine and Petroleum Geology 46, 36-50.

Cadenas, P., Fernández-Viejo, G., 2017. The Asturian Basin within the North Iberian margin (Bay of Biscay): seismic characterisation of its geometry and its Mesozoic and Cenozoic cover. Basin Research 29, 521-541.

Capella, W., Hernández-Molina, F.J., Flecker, R., Hilgen, F.J., Hssain, M., Kouwenhoven, T.J., van Oorschot, M., Sierro, F.J., Stow, D.A.V., Trabucho-Alexandre, J., Tulbure, M.A., de Weger, W., Yousfi, M.Z., Krijgsman, W., 2017. Sandy contourite drift in the late Miocene Rifian Corridor (Morocco): Reconstruction of depositional environments in a foreland-basin seaway. Sedimentary Geology 355, 31-57.

Chemia, Z., Koyi, H., Schmeling, H., 2008. Numerical modelling of rise and fall of a dense layer in salt diapirs. Geophysical Journal International 172, 798-816.

Collart, T., Verreydt, W., Hernandez-Molina, F.J., Llave, E., Leon, R., Gomez-Ballesteros, M., Pons-Branchu, E., Stewart, H., Van Rooij, D., 2018. Sedimentary processes and cold-water coral mini-mounds at the Ferrol canyon head, NW Iberian margin. Progress in Oceanography 169, 48-65.

De Schepper, S., Schreck, M., Beck, K.M., Matthiessen, J., Fahl, K., Mangerud, G., 2015. Early Pliocene onset of modern Nordic Seas circulation related to ocean gateway changes. Nature Communications 6, 8659.

Elderfield, H., Ferretti, P., Greaves, M., Crowhurst, S., McCave, I.N., Hodell, D., Piotrowski, A.M., 2012. Evolution of Ocean Temperature and Ice Volume Through the Mid-Pleistocene Climate Transition. Science 337, 704-709.

Ercilla, G., Casas, D., Vázquez, J.T., Iglesias, J., Somoza, L., Juan, C., Medialdea, T., León, R., Estrada, F., García-Gil, S., Farran, M.l., Bohoyo, F., García, M., Maestro, A., 2011. Imaging the recent sediment dynamics of the Galicia Bank region (Atlantic, NW Iberian Peninsula). Marine Geophysical Research 32, 99-126.

Fernández-Lozano, J., Sokoutis, D., Willingshofer, E., Cloetingh, S., De Vicente, G., 2011. Cenozoic deformation of Iberia: A model for intraplate mountain building and basin development based on analogue modeling. Tecctonics 30, TC1001.

Fernández-Viejo, G., Gallastegui, J., Pulgar, J.A., Gallart, J., 2011. The MARCONI reflection seismic data: A view into the eastern part of the Bay of Biscay. Tectonophysics 508, 34-41.

Fiúza, A.F.G., Hamann, M., Ambar, I., Díaz del Río, G., González, N., Cabanas, J.M., 1998. Water masses and their circulation off western Iberia during May 1993. Deep Sea Research Part I: Oceanographic Research Papers 45, 1127-1160.

Flecker, R., Krijgsman, W., Capella, W., de Castro Martíns, C., Dmitrieva, E., Mayser, J.P., Marzocchi, A., Modestou, S., Ochoa, D., Simon, D., Tulbure, M., van den Berg, B., van der Schee, M., de Lange, G., Ellam, R., Govers, R., Gutjahr, M., Hilgen, F., Kouwenhoven, T., Lofi, J., Meijer, P., Sierro, F.J., Bachiri, N., Barhoun, N., Alami, A.C., Chacon, B., Flores, J.A., Gregory, J., Howard, J., Lunt, D., Ochoa, M., Pancost, R., Vincent, S., Yousfi, M.Z., 2015. Evolution of the Late Miocene Mediterranean–Atlantic gateways and their impact on regional and global environmental change. Earth-Science Reviews 150, 365-392.

Flesche Kleiven, H., Jansen, E., Fronval, T., Smith, T.M., 2002. Intensification of Northern Hemisphere glaciations in the circum Atlantic region (3.5–2.4 Ma) – ice-rafted detritus evidence. Palaeogeography, Palaeoclimatology, Palaeoecology 184, 213-223.

Frizon de Lamotte, D., Fourdan, B., Leleu, S., Leparmentier, F., de Clarens, P., 2015. Style of rifting and the stages of Pangea breakup. Tectonics 34, 1009-1029.

Gabriela, F.-V., Carlos, L.-F., José, D.-C.M., Patricia, C., 2014. How much confidence can be conferred on tectonic maps of continental shelves? The Cantabrian-Fault case. Scientific Reports 4, 3661.

Gallastegui, J., Pulgar, J.A., Gallart, J., 2002. Initiation of an active margin at the North Iberian continent-ocean transition. Tectonics 21, 15-11-15-14.

García-Mondéjar, J., 1996. Plate reconstruction of the Bay of Biscay. Geology 24, 635-638.

García, M., Hernández-Molina, F.J., Alonso, B., Vázquez, J.T., Ercilla, G., Llave, E., Casas, D., 2016. Erosive sub-circular depressions on the Guadalquivir Bank (Gulf of Cadiz): Interaction between bottom current, mass-wasting and tectonic processes. Marine Geology 378, 5-19.

Gascard, J.-C., Clarke, R.A., 1983. The Formation of Labrador Sea Water. Part II. Mesoscale and Smaller-Scale Processes. Journal of Physical Oceanography 13, 1779-1797.

Gong, Z., Langereis, C.G., Mullender, T.A.T., 2008. The rotation of Iberia during the Aptian and the opening of the Bay of Biscay. Earth and Planetary Science Letters 273, 80-93.

González-Pola, C., Díaz del Río, G., Ruiz-Villarreal, M., Sánchez, R.F., Mohn, C., 2012. Circulation patterns at Le Danois Bank, an elongated shelf-adjacent seamount in the Bay of Biscay. Deep Sea Research Part I: Oceanographic Research Papers 60, 7-21.

Hayward, B.W., Sabaa, A.T., Kawagata, S., Grenfell, H.R., 2009. The Early Pliocene re-colonisation of the deep Mediterranean Sea by benthic foraminifera and their pulsed Late Pliocene–Middle Pleistocene decline. Marine Micropaleontology 71, 97-112.

Hernández-Molina, F.J., Serra, N., Stow, D.A.V., Llave, E., Ercilla, G., Van Rooij, D., 2011. Along-slope oceanographic processes and sedimentary products around the Iberian margin. Geo-Marine Letters 31, 315-341.

Hernández-Molina, F.J., Sierro, F.J., Llave, E., Roque, C., Stow, D.A.V., Williams, T., Lofi, J., Van der Schee, M., Arnáiz, A., Ledesma, S., Rosales, C., Rodríguez-Tovar, F.J., Pardo-Igúzquiza, E., Brackenridge, R.E., 2016. Evolution of the gulf of Cadiz margin and southwest Portugal contourite depositional system: Tectonic, sedimentary and paleoceanographic implications from IODP expedition 339. Marine Geology 377, 7-39.

Hernández-Molina, F.J., Stow, D.A.V., Alvarez-Zarikian, C.A., Acton, G., Bahr, A., Balestra, B., Ducassou, E., Flood, R., Flores, J.-A., Furota, S., Grunert, P., Hodell, D., Jimenez-Espejo, F., Kim, J.K., Krissek, L., Kuroda, J., Li, B., Llave, E., Lofi, J., Lourens, L., Miller, M., Nanayama, F., Nishida, N., Richter, C., Roque, C., Pereira, H., Sanchez Goñi, M.F., Sierro, F.J., Singh, A.D., Sloss, C., Takashimizu, Y., Tzanova, A., Voelker, A., Williams, T., Xuan, C., 2014. Onset of Mediterranean outflow into the North Atlantic. Science 344, 1244-1250.

Hudec, M.R., Jackson, M.P.A., 2007. Terra infirma: Understanding salt tectonics. Earth-Science Reviews 82, 1-28.

Iglesias, J., 2009. Sedimentation on the cantabrian continental margin from late oligocene to quaternary. Universidade de Vigo, Vigo, p. 185.

Iorga, M.C., Lozier, M.S., 1999. Signatures of the Mediterranean outflow from a North Atlantic climatology 1. Salinity and density fields. Journal of Geophysical Research-Oceans 104, 25985-26009.

Jackson, C.A.L., Jackson, M.P.A., Hudec, M.R., Rodriguez, C.R., 2015. Enigmatic structures within salt walls of the Santos Basin—Part 1: Geometry and kinematics from 3D seismic reflection and well data. Journal of Structural Geology 75, 135-162.

Jackson, M.P.A., Hudec, M.R., 2017. Salt Stocks and Salt Walls, in: Jackson, M.P.A., Hudec, M.R. (Eds.), Salt Tectonics: Principles and Practice. Cambridge University Press, Cambridge, pp. 76-118.

Jammes, S., Lavier, L., Manatschal, G., 2010. Extreme crustal thinning in the Bay of Biscay and the Western Pyrenees: From observations to modeling. Geochemistry, Geophysics, Geosystems 11, n/a-n/a.

Khélifi, N., Sarnthein, M., Frank, M., Andersen, N., Garbe-Schönberg, D., 2014. Late Pliocene variations of the Mediterranean outflow. Marine Geology 357, 182-194.

Knutz, P.C., 2008. Chapter 24 Palaeoceanographic Significance of Contourite Drifts, in: Rebesco, M., Camerlenghi, A. (Eds.), Developments in Sedimentology. Elsevier, pp. 511-535.

Krijgsman, W., 2002. The Mediterranean: Mare Nostrum of Earth sciences. Earth and Planetary Science Letters 205, 1-12.

Lagabrielle, Y., Cannat, M., 1990. Alpine Jurassic ophiolites resemble the modern central Atlantic basement. Geology 18, 319-322.

Lavín, A., Valdés, L., Sánchez, F., Abaunza, P., Forest, A., Boucher, J., Lazure, P., Jegou, A.M., 2006. The Bay of Biscay: the encountering of the ocean and the shelf, in: Brink, A.R.R.K.H. (Ed.), The Sea. the President and Fellows of Harvard College, pp. 933-999.

Le Guerroué, E., Cobbold, P.R., 2006. Influence of erosion and sedimentation on strike-slip fault systems: insights from analogue models. Journal of Structural Geology 28, 421-430.

Llave, E., Hernández-Molina, F.J., Stow, D.A.V., Fernández-Puga, M.C., García, M., Vázquez, J.T., Maestro, A., Somoza, L., Díaz del Río, V., 2007. Reconstructions of the Mediterranean Outflow Water during the quaternary based on the study of changes in buried mounded drift stacking pattern in the Gulf of Cadiz. Marine Geophysical Researches 28, 379-394.

Llave, E., Matias, H., Hernandez-Molina, F.J., Ercilla, G., Stow, D.A.V., Medialdea, T., 2011. Pliocene-Quaternary contourites along the northern Gulf of Cadiz margin: sedimentary stacking pattern and regional distribution. Geo-Marine Letters 31, 377-390.

Lobo, F.J., Hernández-Molina, F.J., Bohoyo, F., Galindo-Zaldívar, J., Maldonado, A., Martos, Y., Rodríguez-Fernández, J., Somoza, L., Vázquez, J.T., 2011. Furrows in the southern Scan Basin, Antarctica: interplay between tectonic and oceanographic influences. Geo-Marine Letters 31, 451-464.

Lofi, J., Voelker, A.H.L., Ducassou, E., Hernández-Molina, F.J., Sierro, F.J., Bahr, A., Galvani, A., Lourens, L.J., Pardo-Igúzquiza, E., Pezard, P., Rodríguez-Tovar, F.J., Williams, T., 2016. Quaternary chronostratigraphic framework and sedimentary processes for the Gulf of Cadiz and Portuguese Contourite Depositional Systems derived from Natural Gamma Ray records. Marine Geology 377, 40-57.

Marchès, E., Mulder, T., Gonthier, E., Cremer, M., Hanquiez, V., Garlan, T., Lecroart, P., 2010. Perched lobe formation in the Gulf of Cadiz: Interactions between gravity processes and contour currents (Algarve Margin, Southern Portugal). Sedimentary Geology 229, 81-94.

Maslin, M.A., Ridgwell, A.J., 2005. Mid-Pleistocene revolution and the 'eccentricity myth'. Geological Society, London, Special Publications 247, 19-34.

Mazé, J.P., Arhan, M., Mercier, H., 1997. Volume budget of the eastern boundary layer off the Iberian Peninsula. Deep Sea Research Part I: Oceanographic Research Papers 44, 1543-1574.

McClay, K., Bonora, M., 2001. Analog Models of Restraining Stepovers in Strike-Slip Fault Systems. AAPG Bulletin 85, 233-260.

Meijer, P.T., Slingerland, R., Wortel, M.J.R., 2004. Tectonic control on past circulation of the Mediterranean Sea: A model study of the Late Miocene. Paleoceanography 19, PA1026.

Mena, A., Francés, G., Pérez-Arlucea, M., Hanebuth, T.J.J., Bender, V.B., Nombela, M.A., 2018. Evolution of the Galicia Interior Basin over the last 60 ka: sedimentary processes and palaeoceanographic implications. Journal of Quaternary Science 33, 536-549.

Muñoz, J., 2002. The pyrenees. The geology of Spain, 370-385.

Nisancioglu, K.H., Raymo, M.E., Stone, P.H., 2003. Reorganization of Miocene deep water circulation in response to the shoaling of the Central American Seaway. Paleoceanography 18, 1006.

Nugraha, H.D., Jackson, C.A.L., Johnson, H.D., Hodgson, D.M., Reeve, M.T., 2018. Tectonic and oceanographic process interactions archived in Late Cretaceous to Present deep-marine stratigraphy on the Exmouth Plateau, offshore NW Australia. Basin Research 31, 405-430.

Peliz, Á., Dubert, J., Haidvogel, D.B., Cann, B.L., 2003. Generation and unstable evolution of a density-driven Eastern Poleward Current: The Iberian Poleward Current. Journal of Geophysical Research: Oceans 108, 3268.

Pérez-Asensio, J.N., Aguirre, J., Schmiedl, G., Civis, J., 2012. Impact of restriction of the Atlantic-Mediterranean gateway on the Mediterranean Outflow Water and eastern Atlantic circulation during the Messinian. Paleoceanography 27, PA3222.

Pingree, R.D., 1993. Flow of surface waters to the west of the British Isles and in the Bay of Biscay. Deep Sea Research Part II: Topical Studies in Oceanography 40, 369-388.

Pollard, R.T., Grifftths, M.J., Cunningham, S.A., Read, J.F., Pérez, F.F., Ríos, A.F., 1996. Vivaldi 1991 - A study of the formation, circulation and ventilation of Eastern North Atlantic Central Water. Progress in Oceanography 37, 167-192.

Potter, P.E., Szatmari, P., 2009. Global Miocene tectonics and the modern world. Earth-Science Reviews 96, 279-295.

Raddatz, J., Rüggeberg, A., Margreth, S., Dullo, W.-C., 2011. Paleoenvironmental reconstruction of Challenger Mound initiation in the Porcupine Seabight, NE Atlantic. Marine Geology 282, 79-90.

Rebesco, M., Camerlenghi, A., Van Loon, A.J., 2008. Chapter 1 Contourite Research: A Field in Full Development, in: Rebesco, M., Camerlenghi, A. (Eds.), Developments in Sedimentology. Elsevier, pp. 1-10.

Riaza Molina, C., 1996. Inversión estructural en la cuenca mesozoica del off-shore asturiano. Revisión de un modelo exploratorio Geogaceta. Geogaceta 20, 169–171.

Ríos, A.F., Pérez, F.F., Fraga, F., 1992. Water masses in the upper and middle North Atlantic Ocean east of the Azores. Deep Sea Research Part A. Oceanographic Research Papers 39, 645-658.

Roca, E., Muñoz, J.A., Ferrer, O., Ellouz, N., 2011. The role of the Bay of Biscay Mesozoic extensional structure in the configuration of the Pyrenean orogen: Constraints from the MARCONI deep seismic reflection survey. Tectonics 30, TC2001.

Rodriguez, M., Bourget, J., Chamot-Rooke, N., Huchon, P., Fournier, M., Delescluse, M., Zaragosi, S., 2016. The Sawqirah contourite drift system in the Arabian Sea (NW Indian Ocean): A case study of interactions between margin reactivation and contouritic processes. Marine Geology 381, 1-16.

Rogerson, M., Rohling, E.J., Weaver, P.P.E., Murray, J.W., 2005. Glacial to interglacial changes in the settling depth of the Mediterranean Outflow plume. Paleoceanography 20, PA3007.

Rohling, E.J., Foster, G.L., Grant, K.M., Marino, G., Roberts, A.P., Tamisiea, M.E., Williams, F., 2014. Sea-level and deep-sea-temperature variability over the past 5.3 million years. Nature 508, 477-482.

Roque, C., Duarte, H., Terrinha, P., Valadares, V., Noiva, J., Cachão, M., Ferreira, J., Legoinha, P., Zitellini, N., 2012. Pliocene and Quaternary depositional model of the Algarve margin contourite drifts (Gulf of Cadiz, SW Iberia): Seismic architecture, tectonic control and paleoceanographic insights. Marine Geology 303–306, 42-62.

Roveri, M., Flecker, R., Krijgsman, W., Lofi, J., Lugli, S., Manzi, V., Sierro, F.J., Bertini, A., Camerlenghi, A., De Lange, G., Govers, R., Hilgen, F.J., Hübscher, C., Meijer, P.T., Stoica, M., 2014. The Messinian Salinity Crisis: Past and future of a great challenge for marine sciences. Marine Geology 352, 25-58.

Sánchez-Leal, R.F., Bellanco, M.J., Fernández-Salas, L.M., García-Lafuente, J., Gasser-Rubinat, M., González-Pola, C., Hernández-Molina, F.J., Pelegrí, J.L., Peliz, A., Relvas, P., Roque, D., Ruiz-Villarreal, M., Sammartino, S., Sánchez-Garrido, J.C., 2017. The Mediterranean Overflow in the Gulf of Cadiz: A rugged journey. Science Advances 3, eaao0609.

Scher, H.D., Martin, E.E., 2006. Timing and Climatic Consequences of the Opening of Drake Passage. Science 312, 428.

Schönfeld, J., Zahn, R., 2000. Late Glacial to Holocene history of the Mediterranean Outflow. Evidence from benthic foraminiferal assemblages and stable isotopes at the Portuguese margin. Palaeogeography, Palaeoclimatology, Palaeoecology 159, 85-111.

Scotese, C.R., 1991. Jurassic and cretaceous plate tectonic reconstructions. Palaeogeography, Palaeoclimatology, Palaeoecology 87, 493-501.

Smith, A.G., Pickering, K.T., 2003. Oceanic gateways as a critical factor to initiate icehouse Earth. Journal of the Geological Society 160, 337-340.

Somoza, L., Medialdea, T., González, F.J., León, R., Palomino, D., Rengel, J., Fernández-Salas, L.M., Vázquez, J.T., 2019. Morphostructure of the Galicia continental margin and adjacent deep ocean floor: From hyperextended rifted to convergent margin styles. Marine Geology 407, 299-315.

Soto, R., Casas-Sainz, A.M., Villalaín, J.J., Oliva-Urcia, B., 2007. Mesozoic extension in the Basque–Cantabrian basin (N Spain): Contributions from AMS and brittle mesostructures. Tectonophysics 445, 373-394.

Srivastava, S.P., Roest, W.R., Kovacs, L.C., Oakey, G., Lévesque, S., Verhoef, J., Macnab, R., 1990. Motion of Iberia since the Late Jurassic: Results from detailed aeromagnetic measurements in the Newfoundland Basin. Tectonophysics 184, 229-260.

Talley, L.D., McCartney, M.S., 1982. Distribution and Circulation of Labrador Sea Water. Journal of Physical Oceanography 12, 1189-1205.

Thinon, I., Fidalgo-González, L., Réhault, J.-P., Olivet, J.-L., 2001. Déformations pyrénéennes dans le golfe de Gascogne. Comptes Rendus de l'Académie des Sciences - Series IIA - Earth and Planetary Science 332, 561-568.

van Aken, H.M., 2000a. The hydrography of the mid-latitude northeast Atlantic Ocean: I: The deep water masses. Deep Sea Research Part I: Oceanographic Research Papers 47, 757-788.

van Aken, H.M., 2000b. The hydrography of the mid-latitude Northeast Atlantic Ocean: II: The intermediate water masses. Deep Sea Research Part I: Oceanographic Research Papers 47, 789-824.

Van Rooij, D., Blamart, D., Kozachenko, M., Henriet, J.-P., 2007. Small mounded contourite drifts associated with deep-water coral banks, Porcupine Seabight, NE Atlantic Ocean. Geological Society, London, Special Publications 276, 225-244.

Van Rooij, D., Iglesias, J., Hernández-Molina, F.J., Ercilla, G., Gomez-Ballesteros, M., Casas, D., Llave, E., De Hauwere, A., Garcia-Gil, S., Acosta, J., Henriet, J.P., 2010. The Le Danois Contourite Depositional System: Interactions between the Mediterranean Outflow Water and the upper Cantabrian slope (North Iberian margin)(Bay of Biscay). Marine Geology 274, 1-20.

Vandorpe, T., Martins, I., Vitorino, J., Hebbeln, D., García, M., Van Rooij, D., 2016. Bottom currents and their influence on the sedimentation pattern in the El Arraiche mud volcano province, southern Gulf of Cadiz. Marine Geology 378, 114-126.

Vázquez, J.T., Medialdea, T., Ercilla, G., Somoza, L., Estrada, F., Fernández Puga, M.C., Gallart, J., Gràcia, E., Maestro, A., Sayago, M., 2008. Cenozoic deformational structures on the Galicia Bank Region (NW Iberian continental margin). Marine Geology 249, 128-149.

Vergés, J., Fernàndez, M., 2012. Tethys–Atlantic interaction along the Iberia–Africa plate boundary: The Betic–Rif orogenic system. Tectonophysics 579, 144-172.

Vergés, J., Fernàndez, M., Martìnez, A., 2002. The Pyrenean orogen: pre-, syn-, and post-collisional evolution. Journal of the Virtual Explorer 8, 55-74.

Vissers, R.L.M., Meijer, P.T., 2012. Iberian plate kinematics and Alpine collision in the Pyrenees. Earth-Science Reviews 114, 61-83.

Voelker, A.H.L., Lebreiro, S.M., Schönfeld, J., Cacho, I., Erlenkeuser, H., Abrantes, F., 2006. Mediterranean outflow strengthening during northern hemisphere coolings: A salt source for the glacial Atlantic? Earth and Planetary Science Letters 245, 39-55.

Wåhlin, A.K., 2004. Topographic advection of dense bottom water. Journal of Fluid Mechanics 510, 95-104.

Zamora, G., Fleming, M., Gallastegui, J., 2017. Chapter 16 - Salt Tectonics Within the Offshore Asturian Basin: North Iberian Margin, in: Soto, J.I., Flinch, J.F., Tari, G. (Eds.), Permo-Triassic Salt Provinces of Europe, North Africa and the Atlantic Margins. Elsevier, pp. 353-368.

Chapter 7

The late Miocene circulation pattern of the Mediterranean overflow

---

An edited version of this chapter will be submitted as:

Liu, S., Hernández-Molina, F. J., Van Rooij, D., in prep. The late Miocene circulation pattern of the Mediterranean overflow. *Geology*.

Abstract: The late Miocene contouritic features in the Le Danois Bank region (Cantabrian margin) are presented for the first time. Elongated and mounded contourite drifts, overlying on the mid-Miocene discontinuity (~9 Ma), are generated by an early Mediterranean overflow water mass. A paleo-moat is associated with one contourite drift, indicating focused bottom currents in the study area. Acoustically semi-transparent features of contourite drifts are compared with other late Miocene deposits along the SW European continental margin. These features suggest a specific sedimentary depositional pattern resulting from Mediterranean overflow waters. By combining all these contourite examples, the pathway of the late Miocene Mediterranean overflow is reconstructed. During the Tortonian, the Atlantic-Mediterranean water exchange created an intermediate water mass, which flowed into the NE Atlantic after its exiting the Betic and Rifian corridors. This early Mediterranean overflow had sufficient energy to circulate further and reached the southern Bay of Biscay. This understanding of the late Miocene Mediterranean overflow has far-reaching implications for the paleoceanography in the NE Atlantic and may significantly contribute to the late Miocene global cooling.

Keywords: Mediterranean overflow; NE Atlantic; contourite drifts; late Miocene.

Author contributions: Seismic and borehole data was provided by F. J. Hernández-Molina in collaboration with TGS-NOPEC and Shell. Data interpretation was performed by S. Liu. Writing was performed by S. Liu and supervised/revised by D. Van Rooij.

7.1 Introduction

The Mediterranean Outflow Water (MOW), one of the most significant modern water masses, plays an essential role in shaping the seafloor morphology and changing the global climate (Sánchez-Leal et al., 2017; Llave et al., 2019). This dense and saline intermediate water mass is generated as a consequence of the strong evaporation during the Messinian Salinity Crisis (MSC) (5.97 to 5.33 Ma) and flowed into the NE Atlantic after the opening of the Strait of Gibraltar (at ~5.33 Ma) (Roveri et al., 2014). Recent discoveries demonstrate an earlier Atlantic-Mediterranean water exchange through several deep seaways during the late Tortonian (~11.6 to 7.2 Ma) (de la Vara et al., 2015; Flecker et al., 2015). Those restricted seaways favoured the formation of the proto-MOW, producing contourite drifts at the exit of the Mediterranean Sea (Capella et al., 2018). However, there is no evidence that shows the pathways of this late Miocene proto-Mediterranean overflow after its exit from the source area, further along the European margin. By comparing this with the "modern" MOW, which took ~1.8 My to accelerate to finally reach its distal site (Khélifi et al., 2009), the existence of this "first" late Miocene Mediterranean overflow in the rest of the NE Atlantic is argued. In this work, the late Miocene contourite features, which are located in the Le Danois Bank region (the southern Bay of Biscay), are presented for the first time. This paper provides a description of the late Miocene contourite drifts and compares with similar bottom-current controlled depositions in the NE Atlantic, aiming to reconstruct the pathways of the Mediterranean overflow during the late Miocene. By establishing the circulation pattern of the proto-MOW, the linkage between the onset of this water mass and the late Miocene global cooling is addressed.

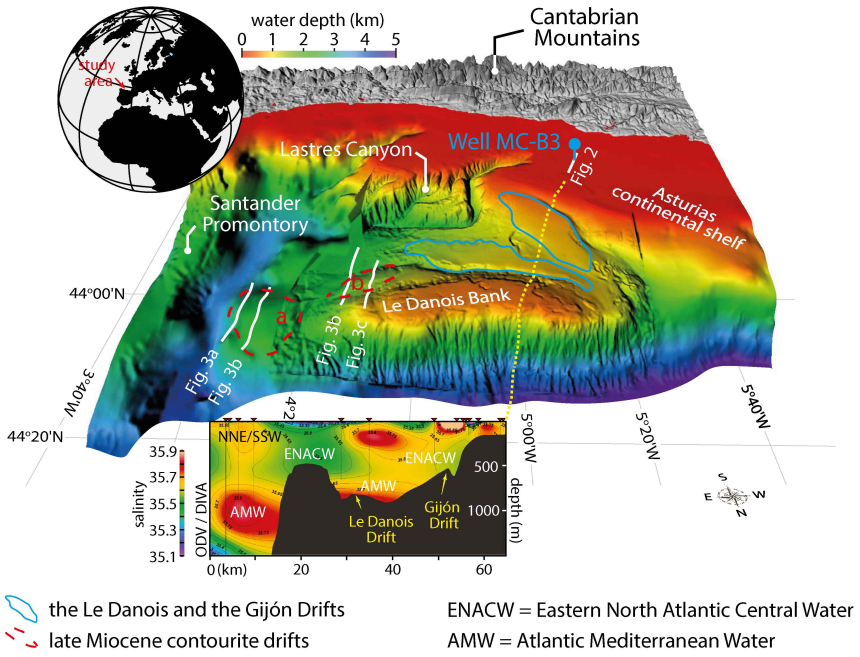

Figure 7.1: The location of the Le Danois Bank region with the indication of the high-resolution bathymetric map (ECOMARG project, IEO), positions of the borehole well (well MC-B3) and seismic profiles (RV Nanhai 502, TGS-NOPEC) and the present-day oceanography (World Ocean Database, 2013). Locations of the modern and the late Miocene contourite drifts are respectively represented by blue and red outlines. Letters (a, b) respectively denote the late Miocene elongated and mounded drifts.

7.2 Methods

This study is based on the regional database comprising bathymetry (ECOMARG Project), a petroleum exploration borehole (Well MC-B3) and multi-channel seismic reflection data (TGS-NOPEC seismic experiment CS-01) (Figures 7.1). The multibeam bathymetry and multi-channel seismic reflection data are respectively obtained during the RV Vizconde de Eza in 2003 and during the RV Nanhai 502 cruise in 2001. The lithology, well log-based stratigraphy, time-depth velocity model and logging data are derived from the oil well MAR CANTÁBRICO B-3 (MC-B3) from Shell España (Figure 7.2). The MC-B3 is located at 43°42'13.94" N, 5°16'29.89" W and the sediment recovery has a middle Miocene-Jurassic age (Figure 7.2).

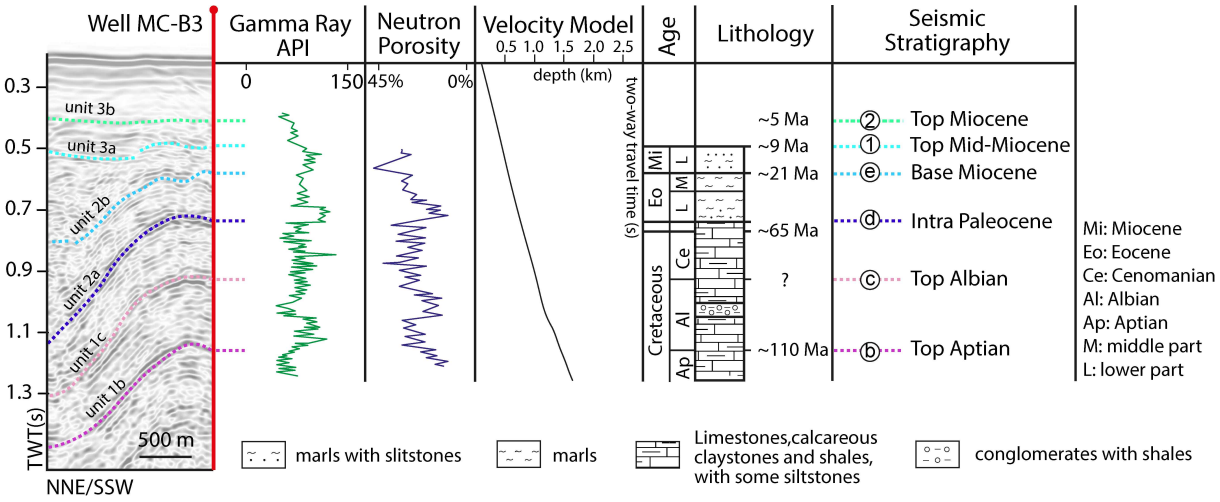

Figure 7.2: Seismic reflection data with the indication of the seismic stratigraphy and major discontinuities. They are correlated with the unconformities and the lithology of Well MC-B3. Ages of each unconformity are derived from Gallastegui (2002). Natural Gamma Ray, Neutron Porosity and the velocity model are shown. The depth scale of the logging data is converted from metre to two-way travel time (TWT).

7.3 Results: Late Miocene contourite features

Previous study has identified and described the modern contourite drifts, which are generated by the AMW and the Eastern North Atlantic Central Water (ENACW) from the late Pliocene (~3.3-3.5 Ma) to the present-day in the study area (Liu et al., 2019). Among them, the largest two contourite drifts, the Le Danois and the Gijon Drifts, are located in the intraslope basin between the Le Danois Bank and the continental shelf (Figure 7.1). Several plastered drifts are located at the southern flank of the bank (Liu et al., 2019). Beneath the modern contourite features, buried elongated and mounded drifts a and b are respectively recognized at the eastern part and along the southeast flank of the Le Danois Bank based on new reflection seismic data and the correlated seismic stratigraphy. Both of them are bound by horizon 1 (at ~9 Ma) at the base and horizon 2 (~5 Ma) at the top, suggesting a late Miocene age (Figures 7.2, 7.3). These drifts display semi-transparent to low amplitude seismic reflections, which differ from the modern contourite drifts with moderate-high amplitude reflections (Figure 7.3d). Onlap terminations are observed onto horizon 1 in both buried elongated and mounded drifts.

Elongated and mounded drift a encompasses an area of 125 km^2 and is about 16 km long and 14 km wide (Figures 7.3a, b). The mounded geometry gradually loses its expression from the east to

the west. A reduction in thickness (from 4 s to 1.5s TWT) is accompanied by this geometry change towards the east. Internally, the continuous subparallel-stratified reflections are locally disrupted (Figure 7.3b). A sigmoidal-oblique progradational pattern towards the Le Danois Bank is observed. This drift is located between 1920 m and 2200 m water depth based on the velocity model of Well MC-B3.

Elongated and mounded drift b, having a length of 16 km and a width of 4 km, covers an area of 95 km^2 (Figures 7.3 c, d). The thickness decreases from the west (1.5 s TWT) to the east (0.9 s TWT). The seismic facies of this drift is characterized by stratified layers of semi-continuous sigmoidal reflections. A paleo-moat, 1.5 km wide and 14 km long, is observed associating with the elongated and mounded drift b, indicating focused bottom currents along the southeast flank of the Le Danois Bank (Figures 7.3c, d). This paleo-moat is located at 1330-1520 m water depth by using time-depth conversion.

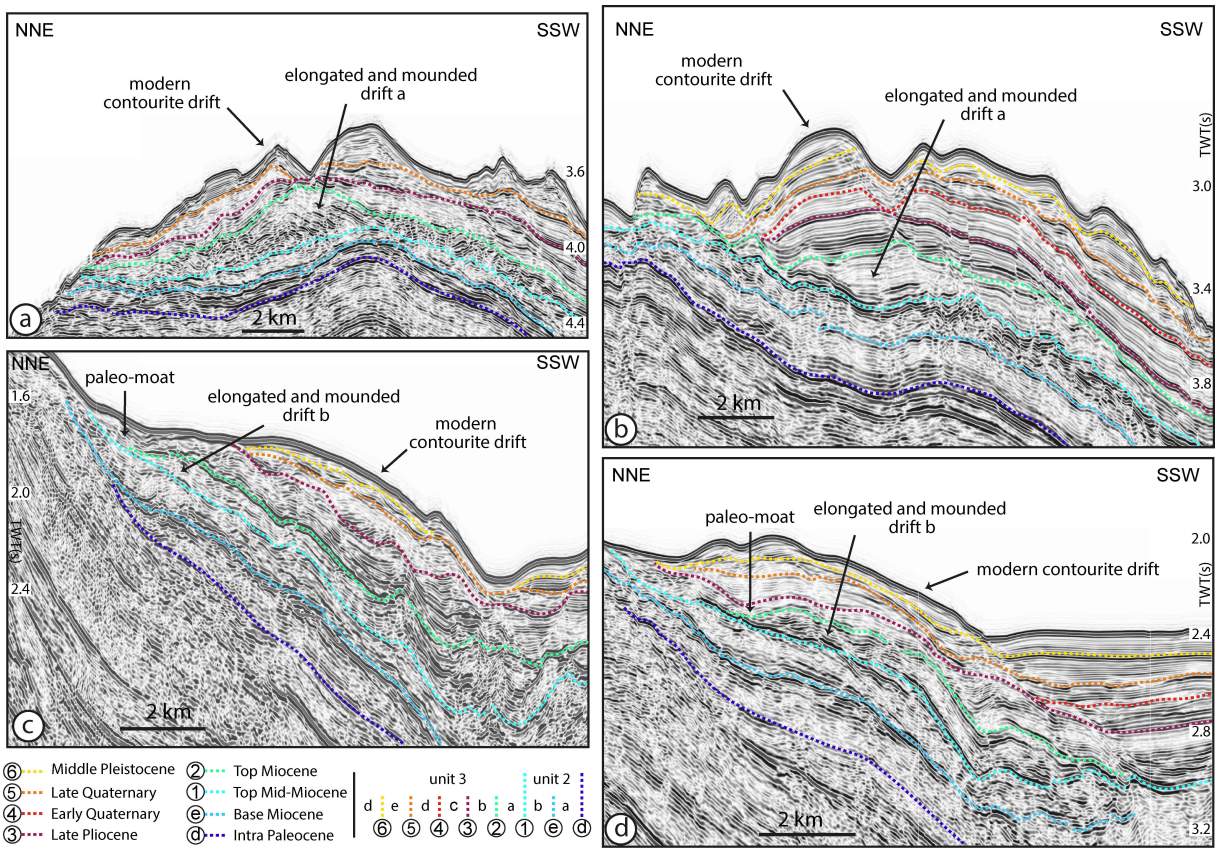

Figure 7.3: Multi-channel reflection seismic profiles and their interpretation, showing units 2 and 3, as well as associated subunits from the bottom to the top. Major discontinuities are correlated to Well MC-B3 and are displayed in Figure 7.2. Locations of these seismic lines are shown in Figure 7.1.

7.4 Discussion

In the Le Danois Bank region, elongated and mounded drift a, generated at a greater depth without considering the basin subsidence and tectonic events, could have been located within the depth range of the North Atlantic Deep Water (NADW). Further north to the Norwegian-Greenland margins, large-scale mounded (500-1000 km^2) drifts, which are resulted from the NADW, are developed during the middle-late Miocene (Laberg et al., 2005; Stoker et al., 2005; Müller-Michaelis et al., 2013). The drift-growth phase was coeval with an enhancement in Atlantic-Arctic

water exchange (van Weering et al., 2008; Knutz et al., 2015). However, the NADW supply was low and less stratified at 2000-3000 m water depth in the Bay of Biscay during the middle-late Miocene (Miller et al., 1987). In addition, the NADW production is suggested to significantly reduce between 8 Ma and 6 Ma (Poore et al., 2006). Weak bottom currents associated with water masses are commonly not capable of creating depositional and erosional features (Stow et al., 2009). As such, deep water masses are most likely not involved in the generation of elongated and mounded drifts in this region.

Discrete acoustic reflections of elongated and mounded drift a, which are interpreted as normal faults, extend from horizon e to horizon 5 (Figures 7.3a, b), indicating the occurrence of faulting and subsidence at the eastern part of the Le Danois Bank during the Quaternary. In addition, major tectonic activities, which could trigger large-scale uplift events, significantly ceased in the southeast Bay of Biscay during the Miocene (Fernández-Viejo et al., 2011). Small-scale uplifts and deformation, triggered by active salt diapirism, are only observed in the intraslope basin in the study area (Zamora et al., 2017). Therefore, elongated and mounded drift a must be located at a shallower depth and out of the range of the NADW during the late Miocene. Elongated and mounded drift b was less influenced by tectonics due to the absence of faults (Figures 7.3c, d). As such, the buried contourite features of the Le Danois Bank region were shaped by an intermediate water mass during the late Miocene.

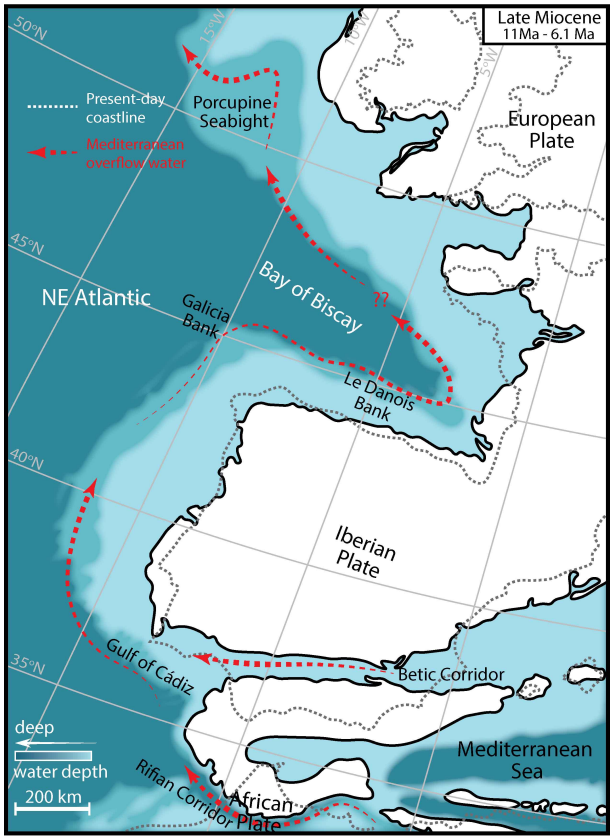

Figure 7.4: Sketch of the possible pathways of the early Mediterranean overflow during the late Miocene. Paleogeography of the NE Atlantic and the Mediterranean Sea presented here is based on Popov (2004).

At the Betic and Rifian corridors, bedforms and grain size of the late Miocene contourite drifts indicate possible moderately strong velocities (0.5-1 m/s) of the related Mediterranean overflow (Capella et al., 2018). By comparing this with the modern MOW, which has a velocity of 0.3-1.2 m/s after its exit from the Strait of Gibraltar (Sánchez-Leal et al., 2017), the scale of the late

Miocene Atlantic-Mediterranean water exchange was comparable. The production of the Mediterranean overflow was large enough for this water mass to circulate further towards the Bay of Biscay. The identification of late Miocene contourite drifts in the Galicia Bank (González et al., 2016) and the Le Danois Bank regions evidently support this hypothesis. At the southeast foot of the Galicia Bank, a contourite drift, located at 1125 to 1570 m water depth, overlies a late Miocene discontinuity (~9.5 Ma), also characterized by semi-transparent seismic reflections (González et al., 2016). Its vertical position and the internal structure can be compared with the ones of the elongated and mounded drift b in the study area (Figure 7.3c). Unlike the contourite drift in the Galicia Bank, a paleo-moat is associated with elongated and mounded drift b (Figures 7.3c, d). Erosional or non-depositional contourite features, such as contourite channels, moats and furrows, require a velocity of >0.3 m/s of bottom currents (Stow et al., 2009). The vigorous Mediterranean overflow at this location could be resulted from the restricted morphology between the Le Danois Bank and the continental shelf (Figure 7.1). At a more distal site of the proto-MOW, an acoustically transparent late Miocene unit is presented in Porcupine Seabight (Van Rooij et al., 2003). This unit has been widely eroded and the internal structure can hardly be observed (Van Rooij et al., 2007; Huvenne et al., 2009). Therefore, the late Miocene Atlantic-Mediterranean water exchange resulted in an intermediate water mass, which at least had reached the southern Bay of Biscay (Figure 7.4).

At the most proximal site of the proto-MOW (the Gulf of Cadiz), where a large modern contourite deposition system is presented, no ancient contourite drifts have been observed in the late Miocene units up to now (Hernández-Molina et al., 2016). The absence of contourite features may be linked to the past settling depth of the Mediterranean overflow. The present-day vertical position of Miocene contourite drifts along the Galicia Bank (González et al., 2016) and the Le Danois Bank point out possible depth (1100-1500 m) of the proto-Mediterranean overflow. As such, the interaction between the proto-MOW and the middle slope (500-1000 m; Llave et al., 2011) of the Gulf of Cadiz, where modern Cadiz CDS is located, could hardly occurred However, deep-sea basin subsidence can reach several hundreds of metres every million year, due to tectonic events and the sea-level change (Xie and Heller, 2009). More evidence is needed to demonstrate the flowing depth of the Mediterranean overflow. Another possibility is the active tectonics in the Gulf of Cadiz. During the late Miocene (~11 Ma), fault movements started to change the morphology of the past seafloor (Duarte et al., 2011). These changes possibly controlled the circulation of the Mediterranean overflow and disrupted the deposition of contourite drifts in the Gulf of Cadiz.

Interestingly, late Miocene units of the above examples all display semi-transparent seismic reflections, suggesting a specific sedimentary depositional pattern along the proto-MOW pathways. Similar features are identified in the late Miocene units in the Gulf of Cadiz as well (Roque et al., 2012). The semi-transparent seismic reflections correspond to mud to fine sand dominated succession, which was deposited in a hemipelagic setting and shows subtle parallel lamination and pervasive bioturbation (Hernández-Molina et al., 2016). Those sedimentary textures are observed in some muddy contourite drifts, which deposited by settling of hemipelagic sediments through bottom currents (Stow et al., 2008). Therefore, the proto-MOW may be transported and deposited sediments along its pathways and resulted in semi-transparent acoustic features in some late Miocene layers.

More importantly, the establishment of this water mass may significantly contribute to the late Miocene global cooling. During the warm Miocene, a decline in atmospheric CO_2 levels occurs

during ~8-6 Ma, which is the key element to trigger a long-term global cooling during Tortonian and Messinian stages (Andersson and Jansen, 2003; Herbert et al., 2016). The onset of the proto-MOW is coeval with these late Miocene climate events. Evidences show that the circulation of the modern MOW causes a drawdown of CO_2 content in the Earth's ocean-air system and profoundly reduces the surface sea temperature (Reid, 1979; Álvarez et al., 2005; Carracedo et al., 2018). The proto-MOW, penetrating along the SW European margins, had similar pathway in the NE Atlantic by comparing with the modern one, which may play an important role in changing the global CO_2 cycle and contribute to the late Miocene global cooling.

7.5 Conclusion

Evidence of ancient contourite features in the Le Danois Bank region strongly suggest the presence of a proto-Mediterranean overflow in the NE Atlantic before the MSC during the late Miocene. The velocity of resulted bottom currents along the southeast flank of the bank is estimated as >0.3 m/s. By comparing with other similar contourite examples, this old Mediterranean overflow moved along the past continental slopes after exiting the Betic and Rifian corridors. It at least had reached the southern Bay of Biscay. Sediments were transported by a proto Mediterranean overflow and deposited along the SW European margins, showing semi-transparent acoustic features. The settling depth of the proto Mediterranean overflow is suggested at 1100-1500 m, which could be one possibility to cause the absence of late Miocene contourite features in the Gulf of Cadiz. The circulation of the Mediterranean overflow in the NE Atlantic may influence the global CO_2 cycle and contribute to the late Miocene global cooling.

Acknowledgments

This study was carried out within the framework of a Chinese Scholarship Council "CSC Grant" (201506410062). The research was conducted in collaboration with "The Drifters Research Group" of the Royal Holloway University of London (UK) and it is related to the projects CTM 2012-39599-C03, CGL2016-80445-R, and CTM2016-75129-C3-1-R. The authors wish to express our gratitude to the crews and scientific researchers of the ECOMARG (REN2002-00916/MAR) and M/V Nanhai 502 cruises. This study also builds upon achievements of project ESF Euromargins MOUNDFORCE, EC FP5 RTN EURODOM and EC FP6 HERMES (GOCE-CT-2005-511234-1).

References

Álvarez, M., Pérez, F. F., Shoosmith, D. R., and Bryden, H. L. 2005, Unaccounted role of Mediterranean Water in the drawdown of anthropogenic carbon. Journal of Geophysical Research: Ocean 110, C09S03.

Andersson, C., Jansen, E., 2003. A Miocene (8–12 Ma) intermediate water benthic stable isotope record from the northeastern Atlantic, ODP Site 982. Paleoceanography 18.

Carracedo, L.I., Pérez, F.F., Gilcoto, M., Velo, A., Padín, A., Rosón, G., 2018. Role of the circulation on the anthropogenic CO2 inventory in the North-East Atlantic: A climatological analysis. Progress in Oceanography 161, 78-86.

Capella, W., Barhoun, N., Flecker, R., Hilgen, F.J., Kouwenhoven, T., Matenco, L.C., Sierro, F.J., Tulbure, M.A., Yousfi, M.Z., Krijgsman, W., 2018. Palaeogeographic evolution of the late Miocene Rifian Corridor (Morocco): Reconstructions from surface and subsurface data. Earth-Science Reviews 180, 37-59.

de la Vara, A., Topper, R.P.M., Meijer, P.T., Kouwenhoven, T.J., 2015. Water exchange through the Betic and Rifian corridors prior to the Messinian Salinity Crisis: A model study. Paleoceanography 30, 548-557.

Duarte, J.C., Rosas, F.M., Terrinha, P., Gutscher, M.-A., Malavieille, J., Silva, S., Matias, L., 2011. Thrust–wrench interference tectonics in the Gulf of Cadiz (Africa–Iberia plate boundary in the North-East Atlantic): Insights from analog models. Marine Geology 289, 135-149.

Fernández-Viejo, G., Gallastegui, J., Pulgar, J.A., Gallart, J., 2011. The MARCONI reflection seismic data: A view into the eastern part of the Bay of Biscay. Tectonophysics 508, 34-41.

Flecker, R., Krijgsman, W., Capella, W., de Castro Martíns, C., Dmitrieva, E., Mayser, J.P., Marzocchi, A., Modestou, S., Ochoa, D., Simon, D., Tulbure, M., van den Berg, B., van der Schee, M., de Lange, G., Ellam, R., Govers, R., Gutjahr, M., Hilgen, F., Kouwenhoven, T., Lofi, J., Meijer, P., Sierro, F.J., Bachiri, N., Barhoun, N., Alami, A.C., Chacon, B., Flores, J.A., Gregory, J., Howard, J., Lunt, D., Ochoa, M., Pancost, R., Vincent, S., Yousfi, M.Z., 2015. Evolution of the Late Miocene Mediterranean–Atlantic gateways and their impact on regional and global environmental change. Earth-Science Reviews 150, 365-392.

Gallastegui, J., 2000. Estructura cortical de la cordillera y margen continental cantábricos: perfiles ESCI-N. Trabajos de Geología 22, 3-234.

González, F.J., Somoza, L., Hein, J.R., Medialdea, T., León, R., Urgorri, V., Reyes, J., Martín-Rubí, J.A., 2016. Phosphorites, Co-rich Mn nodules, and Fe-Mn crusts from Galicia Bank, NE Atlantic: Reflections of Cenozoic tectonics and paleoceanography. Geochemistry, Geophysics, Geosystems 17, 346-374.

Hernández-Molina, F.J., Stow, D.A.V., Alvarez-Zarikian, C.A., Acton, G., Bahr, A., Balestra, B., Ducassou, E., Flood, R., Flores, J.-A., Furota, S., Grunert, P., Hodell, D., Jimenez-Espejo, F., Kim, J.K., Krissek, L., Kuroda, J., Li, B., Llave, E., Lofi, J., Lourens, L., Miller, M., Nanayama, F., Nishida, N., Richter, C., Roque, C., Pereira, H., Sanchez Goñi, M.F., Sierro, F.J., Singh, A.D., Sloss, C., Takashimizu, Y., Tzanova, A., Voelker, A., Williams, T., Xuan, C., 2014. Onset of Mediterranean outflow into the North Atlantic. Science 344, 1244-1250.

Hernández-Molina, F.J., Sierro, F.J., Llave, E., Roque, C., Stow, D.A.V., Williams, T., Lofi, J., Van der Schee, M., Arnáiz, A., Ledesma, S., Rosales, C., Rodríguez-Tovar, F.J., Pardo-Igúzquiza, E., Brackenridge, R.E., 2016. Evolution of the gulf of Cadiz margin and southwest Portugal contourite depositional system: Tectonic, sedimentary and paleoceanographic implications from IODP expedition 339. Marine Geology 377, 7-39.

Khélifi, N., Sarnthein, M., Andersen, N., Blanz, T., Frank, M., Garbe-Schönberg, D., Haley, B.A., Stumpf, R., Weinelt, M., 2009. A major and long-term Pliocene intensification of the Mediterranean outflow, 3.5–3.3 Ma ago. Geology 37, 811-814.

Laberg, J.S., Stoker, M.S., Dahlgren, K.I.T., Haas, H.d., Haflidason, H., Hjelstuen, B.O., Nielsen, T., Shannon, P.M., Vorren, T.O., van Weering, T.C.E., Ceramicola, S., 2005. Cenozoic alongslope processes and sedimentation on the NW European Atlantic margin. Marine and Petroleum Geology 22, 1069-1088.

Llave, E., Matias, H., Hernandez-Molina, F.J., Ercilla, G., Stow, D.A.V., Medialdea, T., 2011. Pliocene-Quaternary contourites along the northern Gulf of Cadiz margin: sedimentary stacking pattern and regional distribution. Geo-Marine Letters 31, 377-390.

Llave, E., Hernández-Molina, F.J., García, M., Ercilla, G., Roque, C., Juan, C., Mena, A., Preu, B., Van Rooij, D., Rebesco, M., Brackenridge, R., Jané, G., Gómez-Ballesteros, M., Stow, D., 2019. Contourites along the Iberian continental margins: conceptual and economic implications. Geological Society, London, Special Publications 476, SP476-2017-2046.

Miller, K.G., Fairbanks, R.G., Thomas, E., 1987. Benthic foraminiferal carbon isotopic records and the development of abyssal circulation in the eastern North Atlantic. U.S. Govt. Printing Office, Washington.

Müller-Michaelis, A., Uenzelmann-Neben, G., Stein, R., 2013. A revised Early Miocene age for the instigation of the Eirik Drift, offshore southern Greenland: Evidence from high-resolution seismic reflection data. Marine Geology 340, 1-15.

Poore, H.R., Samworth, R., White, N.J., Jones, S.M., McCave, I.N., 2006. Neogene overflow of Northern Component Water at the Greenland-Scotland Ridge. Geochemistry, Geophysics, Geosystems 7, Q06010.

Roque, C., Duarte, H., Terrinha, P., Valadares, V., Noiva, J., Cachão, M., Ferreira, J., Legoinha, P., Zitellini, N., 2012. Pliocene and Quaternary depositional model of the Algarve margin contourite drifts (Gulf of Cadiz, SW Iberia): Seismic architecture, tectonic control and paleoceanographic insights. Marine Geology 303–306, 42-62.

Roveri, M., Flecker, R., Krijgsman, W., Lofi, J., Lugli, S., Manzi, V., Sierro, F.J., Bertini, A., Camerlenghi, A., De Lange, G., Govers, R., Hilgen, F.J., Hübscher, C., Meijer, P.T., Stoica, M., 2014. The Messinian Salinity Crisis: Past and future of a great challenge for marine sciences. Marine Geology 352, 25-58.

Sánchez-Leal, R.F., Bellanco, M.J., Fernández-Salas, L.M., García-Lafuente, J., Gasser-Rubinat, M., González-Pola, C., Hernández-Molina, F.J., Pelegrí, J.L., Peliz, A., Relvas, P., Roque, D., Ruiz-Villarreal, M., Sammartino, S., Sánchez-Garrido, J.C., 2017. The Mediterranean Overflow in the Gulf of Cadiz: A rugged journey. Science Advances 3, eaao0609.

Stoker, M.S., Praeg, D., Hjelstuen, B.O., Laberg, J.S., Nielsen, T., Shannon, P.M., 2005. Neogene stratigraphy and the sedimentary and oceanographic development of the NW European Atlantic margin. Marine and Petroleum Geology 22, 977-1005.

Stow, D.A.V., Hunter, S., Wilkinson, D., Hernández-Molina, F.J., 2008. Chapter 9 The Nature of Contourite Deposition, in: Rebesco, M., Camerlenghi, A. (Eds.), Developments in Sedimentology. Elsevier, pp. 143-156.

Stow, D.A.V., Javier Hernández-Molina, F., Llave, E., Sayago, M., 2009. Bedform-velocity matrix: The estimation of bottom current velocity from bedform observations. Geology 37, 327-330.

Van Rooij, D., De Mol, B., Huvenne, V., Ivanov, M., Henriet, J.P., 2003. Seismic evidence of current-controlled sedimentation in the Belgica mound province, upper Porcupine slope, southwest of Ireland. Marine Geology 195, 31-53.

van Weering, T., Stoker, M., Rebesco, M., 2008. Chapter 22 High-Latitude Contourites, in: Rebesco, M., Camerlenghi, A. (Eds.), Developments in Sedimentology. Elsevier, pp. 457-489.

Xie, X., Heller, P.L., 2009. Plate tectonics and basin subsidence historyBasin subsidence. GSA Bulletin 121, 55-64.

Zamora, G., Fleming, M., Gallastegui, J., 2017. Chapter 16 - Salt Tectonics Within the Offshore Asturian Basin: North Iberian Margin, in: Soto, J.I., Flinch, J.F., Tari, G. (Eds.), Permo-Triassic Salt Provinces of Europe, North Africa and the Atlantic Margins. Elsevier, pp. 353-368.

Chapter 8

Conclusion and outlook

This dissertation has looked at the morphology and the evolution of the Le Danois contourite depositional systems (CDS) with the objective to:

1) Improve the seismic diagnostic criteria of contourite drifts from large to small scales.

2) Document the interaction between bottom currents, other oceanographic processes and the slope morphology in small basin settings.

3) Investigate the relationship between the past circulation of the Atlantic Mediterranean Water (AMW; the Atlantic Mediterranean water at its intermediate and distal sites) and the temporal and spatial evolution of the Le Danois CDS.

4) Estimate the effect of basin-scale tectonics on the past dynamic of the AMW.

5) Unravel possible pathways of the Mediterranean overflow water before the opening of the Strait of Gibraltar during the late Miocene.

The identification and seismic facies of the Le Danois CDS were addressed by using multi-resolution seismic data in **chapter 3**, while the interaction between bottom currents, other oceanographic processes and the slope morphology of the Le Danois Bank region was documented in **chapter 4**. The evolution history the Le Danois CDS from the late Pliocene to the present day and the related bottom-current processes were discussed in **chapter 5**. Salt tectonic controls on the distribution and the development of contourite drifts were described in **chapter 6**. Finally, possible circulation patterns of the late Miocene Mediterranean overflow water were reconstructed by geophysical mapping of contourite drifts in the Le Danois Bank region in **chapter 7**. However, some aspects are still outstanding and an outlook is presented for future research.

8.1 Conclusions

8.1.1 Seismic criteria of contourite drifts

Based on the multi-resolution seismic imaging method, the seismic expression and characteristic of contourite drifts have been detected (in **chapter** 3). Nearly overlapping reflection seismic datasets are used to identify contourite drifts, provides new insights into the seismic criteria of contourite drifts. The multi-channel airgun seismic data are suitable to document the external mounded geometry, pre-drift sections and the overall seismic stratigraphy, allowing a broader view on large-scale seismic features of contourite drifts. Single-channel sparker seismic profiles are preferable for the recognition of stratigraphic details, progradation/aggradation patterns and

onlap/downlap terminations of contourite drifts. ParaSound seismic lines are favourable to display wavy or scar-shaped morphology at the surface of contourite drifts. This full scale interpretational method is relevant to investigate the current-controlled depositional environment of contourite drifts. Stratigraphic details and the mounded geometry, shown in medium-high penetration seismic systems, are suggested to be linked to tectonic, oceanographic, and paleoclimate variations. Whereas surficial morphology, which is displayed by high to ultra-high resolution seismic systems, can be related to sub-recent sedimentary processes.

Seismic source and acquisition methods play a significant role in the identification of contourite features (Faugères et al., 1999; Nielsen et al., 2008). A full-scale seismic interpretation method, therefore, are suggested to recognize contourite drifts and to investigate related bottom-current processes for future studies. Furthermore, there is a need to link this multi-resolution seismic method to sediment cores, in order to correlate the seismic resolution with sedimentary facies of contourite deposits in different scales.

8.1.2 Present-day bottom currents associated with the Le Danois CDS

The present-day morphology of the Le Danois Bank region was investigated based on bathymetric and high to ultra-high resolution seismic reflection data (**chapter 4**). The Eastern North Atlantic Central Water (ENACW), the AMW and the Labrador Sea Water (LSW) are involved in shaping the seafloor morphology. Bottom currents associated with the ENACW, the AMW and the LSW are more focused and strongly intensified (estimated acceleration up to 25 cm/s) due to the morphological constraint of the Le Danois Bank and the Vizco High. Lateral variations in drift geometry and internal structure of the Gijón Drift indicate changes of flow dynamics of bottom currents. Additionally, scouring of active bottom currents and rapid sedimentation rate of contourite drifts may trigger slope instability events, forming slide scars in the Le Danois Bank region. Besides contourite drifts, internal waves may have induced the formation of sediment waves.

Contourite models have been proposed by previous studies (Ercilla et al, 2016, Preu et al., 2013; Hernández-Molina et al., 2017). However, new conceptual models are still needed depending on the regional setting, bottom-current properties and the sediment supply (Rebesco et al., 2014). In the Le Danois intraslope basin, bottom currents strongly interacted with internal waves and slope instability events. The interplay between bottom currents and the constrained morphology plays an import role as well. Consequently, the model of the Le Danois CDS, which is located at a relatively small basin setting, display complex morphology and the associated sedimentary features have more frequent lateral variations. This model differs from any other contourite depositional systems along the open continental slopes. The Le Danois CDS, in turn, will improve the further refining of CDS models, which involve the morphological features, processes, seismic facies and architectures, for comparable topographic and oceanographic settings all over the world.

8.1.3 The evolution of the Le Danois CDS

The Pliocene-Quaternary evolution of the Le Danois CDS was investigated based on the airgun and sparker seismic reflection data (**chapter 5**). From old to young, six seismic units (U1 to U6) bounded by major discontinuities (H1 to H6) were identified. Regarding variations of the bottom-current circulation, four evolution stages, including pre-drift (~5.3 to 3.5-3.0 Ma), onset (3.5-3.0

to 2.5-2.1 Ma), intermediate (2.5-2.1 to 0.9-0.7 Ma) and drift-growth (0.9-0.7 Ma to present day) stages, of the Le Danois CDS were recognized. The effective interaction of the AMW and the Cantabrian continental margin initiated during the initiation stage (3.5-3.0 Ma). During the intermediate stage (2.5-0.9 Ma), regional mixing processes within the glacial AMW and at the interglacial AMW/LSW interface resulted in the occurrence of sediment waves. At the end of this stage, sediments within the intraslope basin were largely eroded due to the regional winnowing of the AMW. During the drift-growth stage (0.9-0.7 to present-day), the Le Danois CDS exhibited the most pronounced phase for contourite deposition and drift development. The CDS associated with the was widely generated after the Mid-Pleistocene Transition (MPT; 0.9-07 Ma).

Repeated internal structures of the Le Danois Drift in unit 5, consisting of acoustically transparent lower parts, moderate amplitude upper parts and high amplitude erosional surfaces at the top, are compared with glacial/interglacial cycles between Marine Isotope Stage (MIS) 18 to 12. Renewed tectonic activity in the Gulf of Cádiz between MIS 13 and 11 may significantly change the circulation of the AMW. No cyclic features have been observed in the later units. In addition, the sedimentation rate of the Le Danois CDS reached its maximum during the mid-Pleistocene and decreased afterwards.

In the NE Atlantic, the circulation of the MOW/AMW initiated at different times along the different continental margins (Khélifi et al., 2009; Hernández-Molina et al., 2016), making it difficult to define the dominated period of the MOW/AMW. The evolution of the Le Danois CDS have demonstrated that the efficient interaction between the AMW and the continental slopes only occurred after the late Pliocene (3.5-3.0 Ma). Prior to this time interval, the AMW was relatively weak. Furthermore, the Le Danois CDS resemble other MOW/AMW resulted CDS in the stacking pattern, erosional discontinuities and drift-growth stages. This similarity provides an overarching view on the growth mechanisms of the CDS created by the action of the same water mass, which could be applied by similar contourite examples along other continental margins in the world's ocean.

8.1.4 Basin-scale tectonic considerations for contourite studies

The late Cretaceous to the mid-Pleistocene seafloor morphology of the Le Danois intraslope basin was reconstructed base on the multi-channel seismic data (**chapter 6**). Changes of morphological features were linked to the variation of the dominant tectonic and bottom-current regimes. Four major stages of the basin evolution, including extension (the Cretaceous), compression (the Paleocene to the late Pliocene), interaction (the late Pliocene to the middle Pleistocene) and contourite (the middle Pleistocene to the present day) stages, were identified regarding their dominant tectonic and bottom-current processes. The extension stage occurred during the late Cretaceous when the intraslope basin was much wider compared to the present-day constrained morphology. The Le Danois intraslope basin was significantly narrowed and deformed by the compression and salt movements during the Paleocene-Oligocene compression stage. The related salt tectonics created various bathymetric highs on the paleo-seafloor. During the interaction stage, due to differential sedimentary loading, salt movements respectively ceased along the northern and southern parts of the intraslope basin during the late Pliocene and the middle Pleistocene. Bottom currents interacted with the salt-related morphology during those time intervals, resulting in the specific depositional pattern of the Le Danois CDS. The contourite stage

occurred from the middle Pleistocene to the present day, when all the tectonic activities ceased. Since then the Le Danois CDS was widely generated in the entire intraslope basin.

Previous assumptions on the evolution of the Le Danois CDS (**chapter 5**) did not consider the influence of tectonics due to limited penetration of the seismic data. The different evolution periods of the Le Danois and the Gijón Drifts were argued (**chapter 5**). However, the Le Danois and the Gijon Drifts namely started to develop during the late Pliocene and the middle Pleistocene, which are coeval with the growth phases of different salt diapirs (**chapter 6**). A time gap (~2.4 Ma) for the formation of these two contourite drifts, therefore occurred, indicates significant control of salt tectonics on the evolution of the Le Danois CDS. Our general knowledge of the CDS is that sedimentary features of a CDS are commonly generated at the same geological time (Hernández-Molina et al., 2008; Rebesco et al., 2014). In the Le Danois intraslope basin, contourite features of the same CDS were formed during different time intervals under the control of salt tectonics. Therefore, effects of tectonics, not only in the plate- and margin-scales, but also in basin-scale, should be considered when elucidating the conceptual model of the CDS.

8.1.5 Past Mediterranean overflow in the NE Atlantic during the late Miocene

The late Miocene contourite features in the Le Danois Bank region were presented, indicating the existence of an earlier Mediterranean overflow in the NE Atlantic before Messinian Salinity Crisis (MSC) (**chapter 7**). Elongated and mounded contourite drifts are generated on the mid-Miocene discontinuity (~9 Ma). A paleo-moat is associated with one contourite drift, showing focused bottom currents in the study area. The velocity of related bottom currents along the southeast flank of the bank is estimated as >0.3 m/s. These fast bottom currents were resulted from the restricted slope morphology of the Le Danois Bank region. Acoustically semi-transparent features of contourite drifts were compared with other late Miocene deposits along the SW European continental margin. These features suggest a specific sedimentary depositional pattern which was influenced by the earlier Mediterranean overflow water.

By combining all these contourite examples, the pathway of the late Miocene Mediterranean overflow was reconstructed. During the Tortonian, Atlantic-Mediterranean water exchange created an intermediate water mass, which flew into the NE Atlantic after its exiting the Betic and Rifian corridors. The Mediterranean overflow water circulated further and had reached the southern Bay of Biscay. The proto-MOW had similar pathway in the NE Atlantic by comparing with the modern one, which may play an important role in changing the global CO_2 cycle and contribute to the late Miocene global cooling.

8.1.6 Final considerations

This work strongly contributes to both fundamental aspects and challenges of the contourite paradigm by studying the Le Danois CDS. The multi-resolution seismic method enables a more detailed seismic interpretation of the encountered morphological features, as well as the stratigraphic details of the Le Danois CDS. The present-day complex morphology of the CDS evidenced the significant interactions between topographic obstacles and bottom currents. The knowledge on local oceanographic processes that interplay with bottom currents has been improved. A conceptual CDS model for topographically constrained small basin settings, thus, is provide. Temporally and spatially variable sedimentary architectures of the Le Danois CDS are

derived on the basis of the seismic stratigraphic framework and have been linked to the AMW palaeoceanography from the late Pliocene to the present day. Basin-scale salt tectonics are tied to the evolution of the Le Danois CDS as well. Moreover, buried contourite drifts, which have a late Miocene age (Tortonian), are discovered and have been linked to the past Mediterranean overflow.

The study on the Le Danois CDS not only improves the acoustically diagnostic criteria, but also contributes to the conceptual model of contourite drifts and CDS. Some sedimentary features, such as a wide lateral variation and a time gap for the built-up of two connected drifts are rarely known in any other contourite examples in the world's ocean. Furthermore, the evolution of the Le Danois CDS has a clear response to either the long-term tectonic/oceanographic variations, or short-term global climate changes. The key location of the Le Danois CDS allows a comprehensive comparison between the MOW/AMW related products, in turn unravelling the circulation pattern of the MOW/AMW from the onset of this intermediate water mass in the NE Atlantic. However, there is still an urgent need to classify the associated oceanographic processes, the detailed sedimentary texture and the chronostratigraphy of the Le Danois CDS.

8.2 Outlook

8.2.1 The definition of the contourite depositional system

A contourite depositional system (CDS) is associated with one water mass and is generally located at the same water depth (Hernández-Molina et al., 2008). Some studies have previously show that only one CDS can be observed along the same continental margin or in the same basin (Llave et al., 2001; 2007; Preu et al. 2013). However, three CDS which are namely associated with different water masses are generated in the Le Danois intraslope basin (in **chapter 4**). These CDS are generated during different time intervals due to the paleoceanography and tectonic control in the study area (in **chapters 5** and **6**). As such, the Le Danois CDS is the combination of three contourite depositional systems which are respectively associated with the Eastern North Atlantic Central Water (ENACW), the Atlantic Mediterranean Water (AMW) and the Labrador Sea Water (LSW). This feature of the Le Danois CDS can hardly be defined by the present concept of the CDS. Therefore, the definition of the CDS is suggested to be reconsidered. From a future perspective, It may be necessary to take a step back to check the involvement of different water masses in the development of contourite drifts or CDS in the same region, especially in small basin settings.

8.2.2 The implications of paleo-oceanic gateways in global ocean circulation

The existence of an earlier Mediterranean overflow water in the NE Atlantic indicates the significant impacts of paleo-oceanic gateways in global climate change and the ocean circulation (Chapter 7). However, there is more to investigate and discuss. The Le Danois Bank and the intraslope basin was in deep marine settings (>200 m water depth) since the Cretaceous (Cadenas and Fernández-Viejo, 2017). The southern Biscay margins, acted as the northern boundary of the Iberian micro-plate, was subsequently influenced by plate tectonics (García-Mondéjar, 1996; Gong et al., 2008). During the mid-Cretaceous, tropical and Norwegian seaways opened and the proto-North Atlantic and the Tethys were connected through several narrow pathways, including the proto-Bay of Biscay (Figure 8.1c) (Jarvis et al., 2011; Advokaat et al., 2014). If compared with the present-day oceanographic condition, those pathways favour the formation of the global ocean circulation (Thran et al., 2018). Indeed, the westward-flowing North Atlantic-Tethyan waters, centred at 500 m water depth, circulated from the Tethys Ocean towards the Demerara Rise

(Figure 8.1) (Jiménez Berrocoso et al., 2010; Zheng et al., 2016). However, their circulation pattern is still lack of knowledge.

The Le Danois Bank region is possible to be influenced by the North Atlantic-Tethyan waters during the mid-Cretaceous. To confirm or improve this hypothesis, seismic data with a higher penetration are needed to examine the deeper sections of the sedimentary infill in the Le Danois Bank region. If mounded sedimentary bodies were observed in seismic profiles, their geometry, internal structures and associated bottom-current or oceanographic processes should be discussed. These mounded contourite drifts could be compared with present-day ones to investigate their differences in related bottom-current processes. Additionally, the mid-Cretaceous was marked as a period of optimum global warmth and high sea surface temperatures (SST) (Jarvis et al., 2011). The global ocean circulation, a key factor for the Earth's heat transfer, may widely contribute to the climate change (Smith and Pickering, 2003; Potter and Szatmari, 2009; De Schepper et al., 2015). The evolution of the mid-Cretaceous contourite drifts may point out the duration of the influence of the water masses from Tethys to the North Atlantic. The temporal variation of the North Atlantic-Tethyan waters, in turn, could be linked to global climate events. If contourite drifts were not shown, an investigation as to why contourite features were absent would be valuable as well.

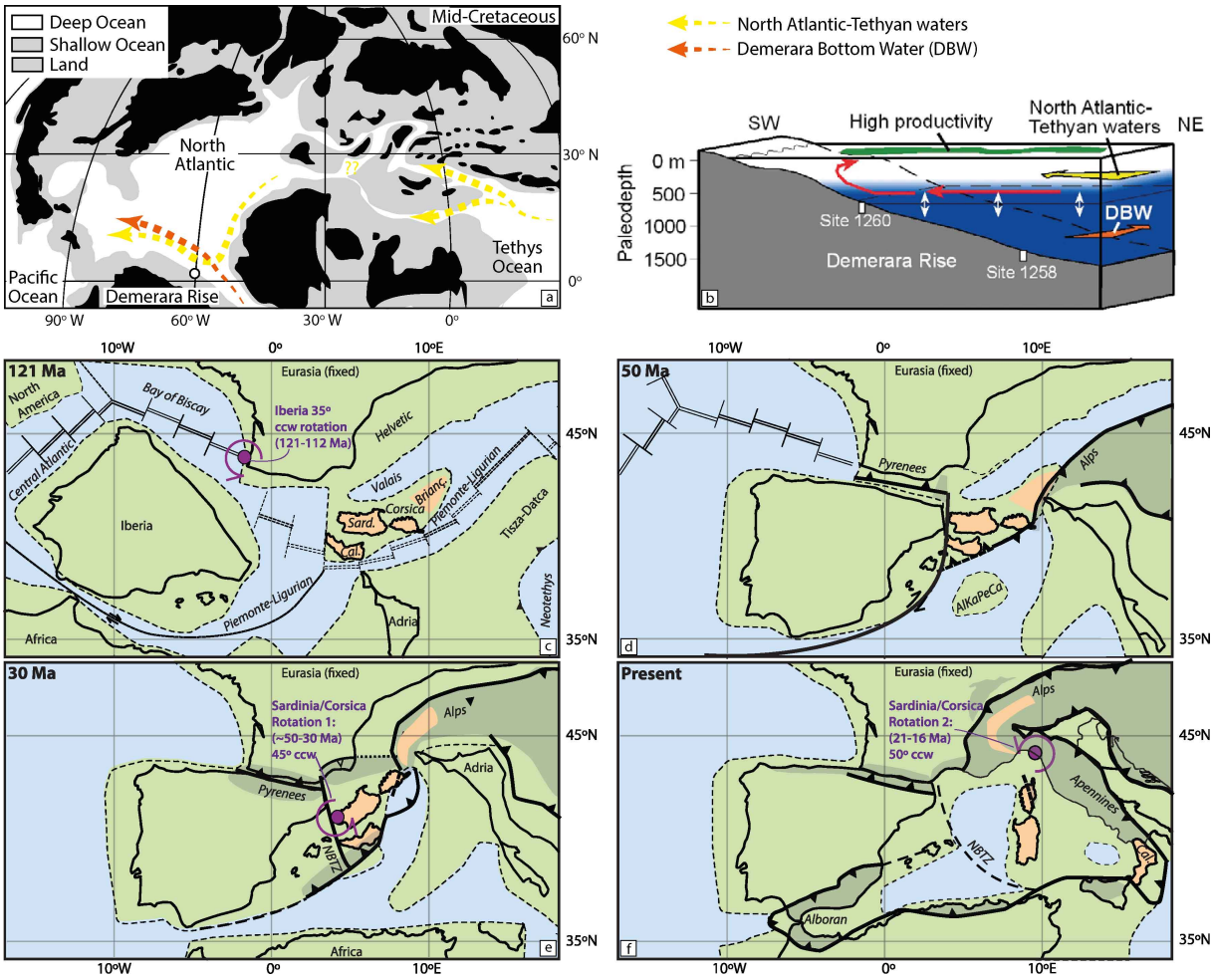

Figure 8.1: (a) The mid-Cretaceous paleogeographic map showing the general ocean circulation pattern (yellow and red arrows) (Zheng et al., 2016); (b) Diagram with Demerara Bottom Water (DBW), North Atlantic–Tethyan waters and their circulation patterns over Demerara Rise. The settling depth and flowing directions are indicated

as well (Jiménez Berrocoso et al., 2010); (c, d, e, f) Tectonic reconstructions of the Iberian micro-plate from the mid-Cretaceous (121 Ma) to the present day (Advokaat et al., 2014).

8.2.3 Recommended actions for the Le Danois CDS

The seismic stratigraphy of the Le Danois bank region and the evolution of the Le Danois CDS were discussed in **chapters 5** and **6**. The relationship between sedimentary stacking patterns of contourite drifts and the Quaternary climate cycles, however, are annotated with a question mark. This issue could be addressed with the acquirement of some core samples. Additionally, the Gijón Drift is positioned within two different water masses, being the AMW and the ENACW, at the present-day oceanographic condition (Figure 4.7). The presence of sediment waves in the Le Danois intraslope basin points out possible processes at interfaces of water masses as well (Chapter 4). Nevertheless, the oceanographic data used in this work, which were extracted from the World Ocean Database (2013) (https://www.nodc.noaa.gov/OC5/WOD13/), are not able to display greater details in those positions. More oceanographic observations are needed to quantify present-day bottom-current and oceanographic processes associated with the Le Danois CDS. As such, another scientific cruise is suggested for a more detailed study of the Le Danois CDS.

8.2.3.1 Sediment coring

Site ID	Longitude	Latitude	Seafloor Depth (m)
M1	5°00'04''W	43°59'17''N	822
M2	5°04'01''W	43°47'36''N	452
M3	4°29'47''W	44°02'16''N	1442
S1	4°44'00''W	43°39'05''N	1270
S2	4°47'16''W	43°58'33''N	1057
S3	5°11'34''W	43°51'46''N	762
S4	5°08'24''W	43°50'38''N	561
S5	5°07'09''W	44°02'32''N	722
S6	4°52'00''W	44°00'43''N	843
S7	5°10'31''W	43°48'39''N	273

Table 8.1: List of locations for MeBo (M1, M2, M3) and vibrocoring, gravity corer or piston (S1, S2, S3, S4, S5, S6, S7) cores.

In order to determine a more precise seismic stratigraphy of the Le Danois CDS, several long sediment cores have to be obtained in order to penetrate the lower initiation horizons of contourite drifts. The new MeBo (acronym for Meeresboden-Bohrgerät, German for seafloor drill rig) corer, which is able to drill to a maximum depth of 280 m (Freudenthal and Wefer, 2013), can contribute to achieving this goal. The first MeBo drilling point (M1) is suggested to set at 822 m (Table 8.1, Figure 8.2), where the basal horizon (the late Pliocene discontinuity; at 1020 m) of the Le Danois Drift is located. Subsequently, the entire seismic stratigraphic framework can be covered by M1. The second MeBo drilling point (M2), which can be located at 452 m water depth, can cover the whole sedimentary section of the Gijón Drift from the basal discontinuity (the mid-Pleistocene discontinuity; at 577 m) to the seafloor (452 m) (Table 8.1, Figure 8.2). The third MeBo drilling point (M3) could be set at 1442 m (Table 8.1, Figure 8.2), where the late Miocene contourite drifts are located (152 m below the seafloor). Such long sediment cores allow to assess the sedimentation rate, the sediment source and sedimentary facies of contourite drifts, as well as and the chronostratigraphy of the Le Danois CDS in the study area. They can help to reconstruct

the climate/oceanographic conditions in the Le Danois Bank region from the late Miocene (~9 Ma) until the present-day.

In addition, contourite drifts and the associated moats display distinct acoustic structures (Chapters 5 and 6). These differences are linked to the change of the bottom-current velocity and the associated sediment transportation. To investigate spatial changes of bottom currents, some sediment cores should be acquired by using vibrocoring, gravity corer or piston corer systems. Seven sites are suggested for the acquirement of sediment core samples. Four are respectively located at 1270 m (S1), at 1057 m (S2), at 762 m (S3) and at 561 m (S4) (Table 8.1). These sites will namely cover the Le Danois Moat (S1) and the Drift (S2), the Gijón Moat (S3) and the Drift (S4). Another three sites will target plastered drifts, which are still poorly understood at present. They are suggested to be located at 722 m (S5), 843 m (S6) and at 273 m (S7). Textural characteristics and facies of different types of contourite drifts can be illustrated by using computed tomography (CT), smear slide analysis and grain-size measurement. The sediment cores can illustrate the depositional cycles and their relationship with the paleoclimate changes as well. The results may highlight the importance of bottom current velocity, sediment supply and bioturbation mixing in controlling erosional and depositional contourite facies.

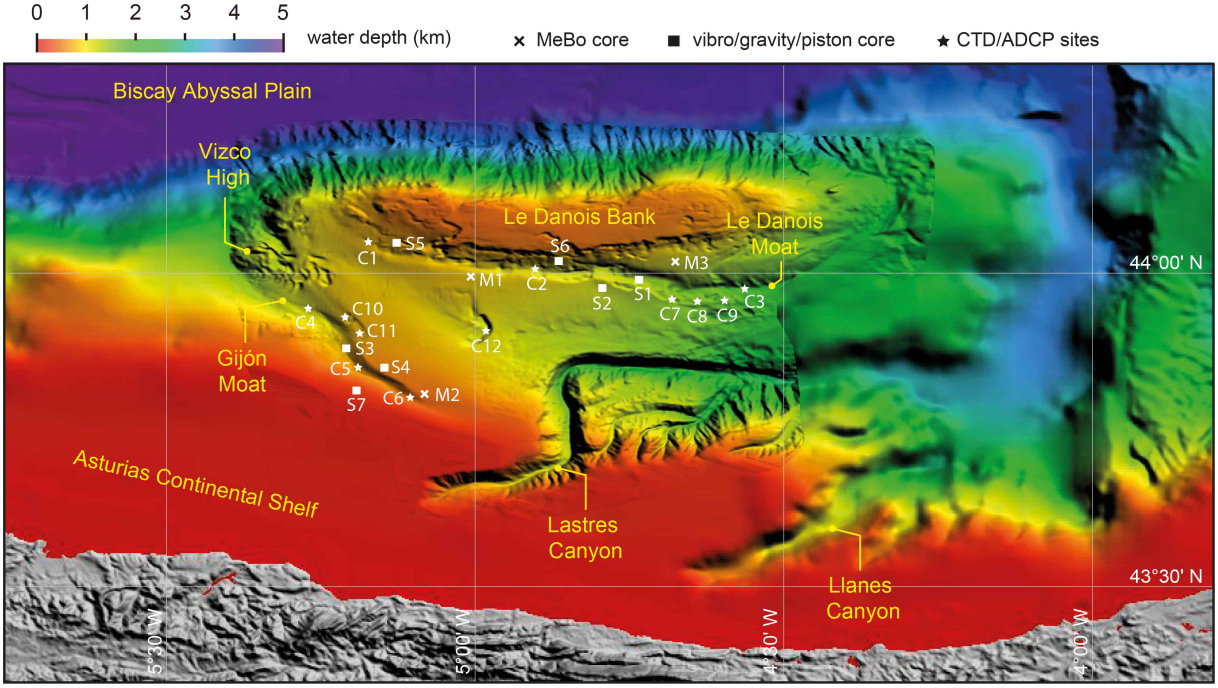

Figure 8.2: Bathymetry map of the Le Danois Bank region with the targets for core, CTD and ADCP acquisition.

8.2.3.2 CTD/ADCP measurements

Conductivity, Temperature, Depth (CTD) measurements and Acoustic Doppler Current Profiler (ADCP) should be applied to investigate the seawater properties, the direction and intensities of currents around contourite moats and sediment waves. The synchronous acquisition of both CTD and ADCP data could be an option by attaching two systems. Locations for the CTD/ADCP sites are listed in Table 8.2 and Figure 8.2. Among them, oceanographic data from stations C1, C2 and C3 may indicate the present-day direction and the velocity of the AMW within the Le Danois Moat. The acceleration of bottom currents, which are resulted from the interaction between the Le Danois Bank and the AMW (Chapter 4), in turn, can be evaluated.

Site ID	Longitude	Latitude	Seafloor Depth (m)
C1	5°09'55''W	44°02'58''N	787
C2	4°53'48''W	44°00'12''N	979
C3	4°34'18''W	43°58'22''N	1733
C4	5°15'26''W	43°56'27''N	1030
C5	5°10'54''W	43°50'24''N	673
C6	5°05'24''W	43°47'38''N	478
C7	4°41'09''W	43°57'25''N	1351
C8	4°38'32''W	43°57'32''N	1468
C9	4°35'57''W	43°57'07''N	1520
C10	5°11'49''W	43°55'15''N	817
C11	5°10'11''W	43°53'35''N	725
C12	4°58'35''W	43°54'07''N	1088

Table 8.2: List of locations for CTD and ACDP acquisition. CTD=Conductivity, Temperature, Depth; ADCP=Acoustic Doppler Current Profiler.

Oceanographic data from sites C4, C5 and C6 can exam bottom-current dynamics within the Gijón Moat. Furthermore, these data will solve outstanding questions, e.g. does the AMW upwell due to the morphological control of the upper continental slope? How strong are the currents associated with the ENACW? Does the deflection of the Gijón Moat accelerate bottom currents?

At sites C7, C8, C9, C10, C11, where interactions between the seafloor and the water masses interface occur (Chapter 4), mixing processes between the ENAW, the AMW and the LSW should be analysed. By combining these data and the morphology of sediments waves, such as their wavelength and the migration direction, our understanding regarding processes at water masses interface and how they affect the ocean floor will improve significantly.

To better understand the effect of bottom currents on the slope instability, it would be interesting to investigate a CTD/ADCP site which is located over a slide scar and at the pathway of a water mass. At site C12, the seafloor displays an ear-shaped slide scar, which is resulted from the active scouring of bottom currents (Chapter 4) (Figure 8.2). By combining the value of the slope angle and the scale of the scar, the oceanographic observation will help to exam the action of bottom currents at this location.

8.2.3.3 Mooring data and numerical modelling

The strength and structure of the water masses can be identified by using long-time series moored instruments (Rebesco et al., 2013). In order to better identify oceanographic processes and to correlate these processes with seafloor morphology, there is an urgent need for the mooring operations. Several comprehensive studies, using the combined long-term oceanographic measurements, numerical modelling, geophysical and sedimentological datasets, have carried out to study the behaviour of bottom current and the related internal waves (Rebesco et al., 2013; Ribó et al., 2016; Zhang et al., 2016). A similar approach can be applied in the Le Danois bank region to specifically study the relationship between contourites, sediment wave fields and slide scars. Three mooring profiles are suggested to be at the same location of stations C7, C11, C12, where sediment waves are positioned (Table 8.2, Figure 8.2). After acquiring the mooring data, Taylor–Goldstein equation, a 3-D morphodynamical numerical model (Zhang et al., 2014; 2016) and a nested grid operation should be applied to investigate the impact of internal waves on the Le Danois.

Finally, the Le Danois CDS represents a wealthy field laboratory to improve the aspect of contourite drifts and leaves imprints on other drift systems located in similar geological/oceanographic settings. However, past or present-day processes associated with the Le Danois CDS are not as simple as initially thought. This work is not yet finished and there are still scientific questions needed to be answered and addressed. Additional research should be prioritized to improve the knowledge on bottom currents and the resulted seafloor morphology, which could bridge gaps between physical oceanography and geology in contourite studies.

References

Advokaat, E.L., van Hinsbergen, D.J.J., Maffione, M., Langereis, C.G., Vissers, R.L.M., Cherchi, A., Schroeder, R., Madani, H., Columbu, S., 2014. Eocene rotation of Sardinia, and the paleogeography of the western Mediterranean region. Earth and Planetary Science Letters 401, 183-195.

Cadenas, P., Fernández-Viejo, G., 2017. The Asturian Basin within the North Iberian margin (Bay of Biscay): seismic characterisation of its geometry and its Mesozoic and Cenozoic cover. Basin Research 29, 521-541.

De Schepper, S., Schreck, M., Beck, K.M., Matthiessen, J., Fahl, K., Mangerud, G., 2015. Early Pliocene onset of modern Nordic Seas circulation related to ocean gateway changes. Nature Communications 6, 8659.

Ercilla, G., Juan, C., Hernández-Molina, F.J., Bruno, M., Estrada, F., Alonso, B., Casas, D., Farran, M.l., Llave, E., García, M., Vázquez, J.T., D'Acremont, E., Gorini, C., Palomino, D., Valencia, J., El Moumni, B., Ammar, A., 2016. Significance of bottom currents in deep-sea morphodynamics: An example from the Alboran Sea. Marine Geology 378, 157-170.

Faugères, J.-C., Stow, D.A.V., Imbert, P., Viana, A., 1999. Seismic features diagnostic of contourite drifts. Marine Geology 162, 1-38.

Freudenthal, T., Wefer, G., 2013. Drilling cores on the sea floor with the remote-controlled sea floor drilling rig MeBo. Geosci. Instrum. Method. Data Syst. 2, 329-337.

García-Mondéjar, J., 1996. Plate reconstruction of the Bay of Biscay. Geology 24, 635-638.

Gong, Z., Langereis, C.G., Mullender, T.A.T., 2008. The rotation of Iberia during the Aptian and the opening of the Bay of Biscay. Earth and Planetary Science Letters 273, 80-93.

Hernández-Molina, F.J., Llave, E., Stow, D.A.V., 2008. Chapter 19 Continental Slope Contourites, in: Rebesco, M., Camerlenghi, A. (Eds.), Developments in Sedimentology. Elsevier, pp. 379-408.

Hernández-Molina, F.J., Sierro, F.J., Llave, E., Roque, C., Stow, D.A.V., Williams, T., Lofi, J., Van der Schee, M., Arnáiz, A., Ledesma, S., Rosales, C., Rodríguez-Tovar, F.J., Pardo-Igúzquiza, E., Brackenridge, R.E., 2016. Evolution of the gulf of Cadiz margin and southwest Portugal contourite depositional system: Tectonic, sedimentary and paleoceanographic implications from IODP expedition 339. Marine Geology 377, 7-39.

Hernández-Molina, F.J., Campbell, S., Badalini, G., Thompson, P., Walker, R., Soto, M., Conti, B., Preu, B., Thieblemont, A., Hyslop, L., Miramontes, E., Morales, E., 2017. Large bedforms on contourite terraces: Sedimentary and conceptual implications. Geology 46, 27-30.

Jarvis, I., Lignum, J.S., Gröcke, D.R., Jenkyns, H.C., Pearce, M.A., 2011. Black shale deposition, atmospheric CO2 drawdown, and cooling during the Cenomanian-Turonian Oceanic Anoxic Event. Paleoceanography 26.

Jiménez Berrocoso, Á., MacLeod, K.G., Martin, E.E., Bourbon, E., Londoño, C.I., Basak, C., 2010. Nutrient trap for Late Cretaceous organic-rich black shales in the tropical North Atlantic. Geology 38, 1111-1114.

Khélifi, N., Sarnthein, M., Andersen, N., Blanz, T., Frank, M., Garbe-Schönberg, D., Haley, B.A., Stumpf, R., Weinelt, M., 2009. A major and long-term Pliocene intensification of the Mediterranean outflow, 3.5–3.3 Ma ago. Geology 37, 811-814.

Llave, E., Hernandez-Molina, F.J., Somoza, L., Diaz-del Rio, V., Stow, D.A.V., Maestro, A., Alveirinho Dias, J.M., 2001. Seismic stacking pattern of the Faro-Albufeira contourite system (Gulf of Cadiz): a Quaternary record of paleoceanographic and tectonic influences. Marine Geophysical Researches 22, 487-508.

Llave, E., Hernandez-Molina, F.J., Somoza, L., Stow, D.A.V., Diaz del Rio, G., 2007. Quaternary evolution of the contourite depositional system in the Gulf of Cadiz, in: Viana, A.R., Rebesco, M. (Eds.), Economic and Palaeoceanographic Significance of Contourite Deposits. Geological Society, London, pp. 49-79.

Nielsen, T., Knutz, P.C., Kuijpers, A., 2008. Chapter 16 Seismic Expression of Contourite Depositional Systems, in: Rebesco, M., Camerlenghi, A. (Eds.), Developments in Sedimentology. Elsevier, pp. 301-321.

Potter, P.E., Szatmari, P., 2009. Global Miocene tectonics and the modern world. Earth-Science Reviews 96, 279-295.

Preu, B., Hernández-Molina, F.J., Violante, R., Piola, A.R., Paterlini, C.M., Schwenk, T., Voigt, I., Krastel, S., Spiess, V., 2013. Morphosedimentary and hydrographic features of the northern Argentine margin: The interplay between erosive, depositional and gravitational processes and its conceptual implications. Deep Sea Research Part I: Oceanographic Research Papers 75, 157-174.

Rebesco, M., Wåhlin, A., Laberg, J.S., Schauer, U., Beszczynska-Möller, A., Lucchi, R.G., Noormets, R., Accettella, D., Zarayskaya, Y., Diviacco, P., 2013. Quaternary contourite drifts of the Western Spitsbergen margin. Deep Sea Research Part I: Oceanographic Research Papers 79, 156-168.

Rebesco, M., Hernández-Molina, F.J., Van Rooij, D., Wåhlin, A., 2014. Contourites and associated sediments controlled by deep-water circulation processes: State-of-the-art and future considerations. Marine Geology 352, 111-154.

Ribó, M., Puig, P., Muñoz, A., Lo Iacono, C., Masqué, P., Palanques, A., Acosta, J., Guillén, J., Gómez Ballesteros, M., 2016. Morphobathymetric analysis of the large fine-grained sediment waves over the Gulf of Valencia continental slope (NW Mediterranean). Geomorphology 253, 22-37.

Smith, A.G., Pickering, K.T., 2003. Oceanic gateways as a critical factor to initiate icehouse Earth. Journal of the Geological Society 160, 337-340.

Thran, A.C., Dutkiewicz, A., Spence, P., Müller, R.D., 2018. Controls on the global distribution of contourite drifts: Insights from an eddy-resolving ocean model. Earth and Planetary Science Letters 489, 228-240.

Zhang, Z., Wang, W., Qiu, B., 2014. Oceanic mass transport by mesoscale eddies. Science 345, 322.

Zheng, X.-Y., Jenkyns, H.C., Gale, A.S., Ward, D.J., Henderson, G.M., 2016. A climatic control on reorganization of ocean circulation during the mid-Cenomanian event and Cenomanian-Turonian oceanic anoxic event (OAE 2): Nd isotope evidence. Geology 44, 151-154.

Chapter 8 Conclusion and outlook

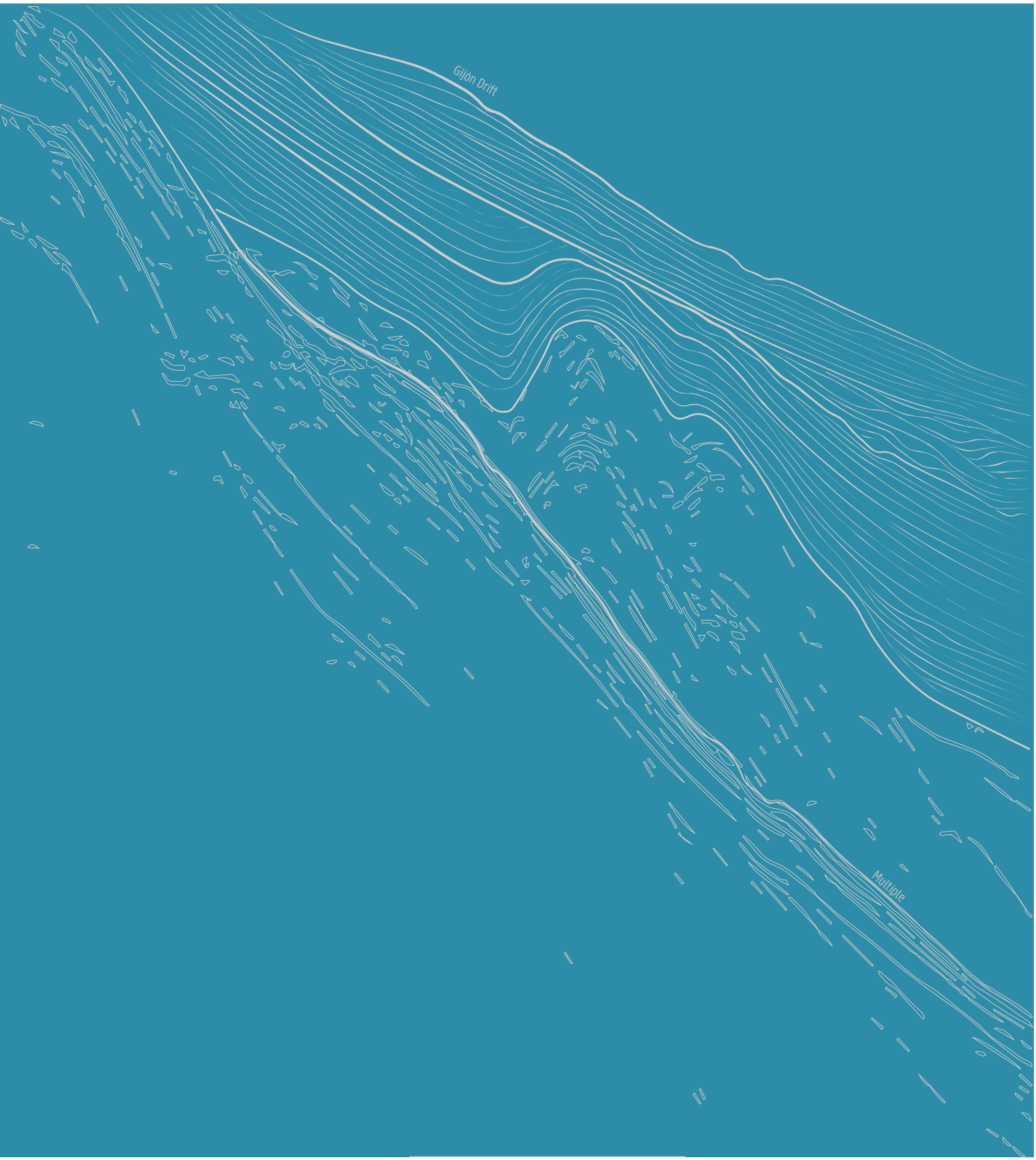

GHENT
UNIVERSITY